INSTITUTO DE AGROQUÍMICA Y TECNOLOGÍA DE ALIMENTOS (IATA-CSIC)
Grupo de Nuevos Materiales y Nanotecnología

UNIVERSIDAD POLITÉCNICA DE VALENCIA (UPV)

MICRO- Y NANOENCAPSULACIÓN MEDIANTE PROCESADO ELECTROHIDRODINÁMICO DE INTERÉS EN APLICACIONES ALIMENTARIAS

MICRO- AND NANOENCAPSULATION VIA ELECTRO-HYDRODYNAMIC PROCESSING OF INTEREST IN FOOD APPLICATIONS

TESIS DOCTORAL

Rocío Pérez Masiá

Valencia, 2014

Dirigida por:
Dr. Jose M. Lagarón Cabello
Dra. Amparo López Rubio

Dr. José María Lagarón Cabello, investigador científico del Consejo Superior de Investigaciones Científicas (CSIC) en el Instituto de Agroquímica y Tecnología de Alimentos (IATA) y Dra. Amparo López Rubio, científica titular del mismo instituto

CERTIFICAN: que la presente memoria titulada MICRO- Y NANOENCAPSULACIÓN MEDIANTE PROCESADO ELECTROHIDRODINÁMICO DE INTERÉS EN APLICACIONES ALIMENTARIAS constituye la tesis doctoral de Rocío Pérez Masiá. Asimismo, certifican haber dirigido y supervisado el trabajo realizado y autorizan su presentación.

Y para que conste a los efectos oportunos, firmamos la presente en Valencia a 11 de Julio de 2014

Fdo. Jose M. Lagarón

Fdo. Amparo López Rubio

AGRADECIMIENTOS

Me gustaría dar las gracias a todas las personas que han compartido conmigo estos casi 4 años de tesis.

En primer lugar, gracias a mis directores. Gracias a Chema por haberme dado la oportunidad de empezar a trabajar en su grupo y aprender muchísimas cosas. Muchas gracias a Amparo (Ampi) porque me has enseñado un montón, porque has confiado en mí y porque me has ayudado a sacar adelante esta mezcla de trabajos que al final han formado mi tesis.

Muchísimas gracias a toda la gente que ha pasado por el laboratorio 502 del IATA porque hacéis que venir a trabajar sea hasta divertido. Gracias a Maria José, Antonio, Marta, Jesús, Pablo, Gloria, Wilson, Lorena y Laura porque sois un grupo genial y siempre habéis estado ahí para apoyarme, para ayudarme y sobre todo para desahogarme en esos momentos de nervios y crisis que también he pasado. Antonio con sus agitaciones, Marta con su Bob esponja, Jesús que tiene ideas para todo y si no con su móvil siempre te aclara cualquier duda (mil gracias por el diseño de la portada!!) y Maria José que siempre está ahí dispuesta a escucharme, ayudarme y enseñarme. Por supuesto también quiero agredecer a toda la gente que ha venido de prácticas o estancia y me ha ayudado con el experimental de esta tesis. Y muchísimas gracias también a todos los técnicos de microscopía de la UV que siempre están dispuestos a ayudar.

Me gustaría dar las gracias también al proyecto Frisbee por la financiación y en especial muchas gracias a la coordinadora Graciela Álvarez por tratarme tan bien y cuidarme tanto en todos los viajes del proyecto.

También GRACIAS A TODA MI FAMILIA. Gracias porque a lo largo de esta tesis han pasado muchas cosas y vosotros siempre me habéis apoyado. Gracias por hacer lo imposible por ayudarme siempre. Y gracias por hacerme creer que soy un poquito mejor de lo que yo me pienso.

Y ya para terminar muchas gracias a Sergio por aguantar lo pesada que soy y aun así querer estar siempre a mi lado.

ABSTRACT

Micro- and nanoencapsulation have generated great interest over the last years in multiple fields. Particularly in the food industry, this technology presents potential applications for the development of smart packaging structures, as well as for the protection of sensitive ingredients and the production of novel healthy foods. Therefore, in this thesis, the development of different encapsulation structures of interest in the food area was carried out. Specifically, capsules were obtained through electro-hydrodynamic processing, since this technology presents several advantages over other well-established and even more innovative encapsulation technologies. For instance, it does not require the use of high temperature, it allows for controlled morphology, size and size distribution and encapsulation can occur from aqueous solutions.

Initially, microencapsulation for smart packaging applications was investigated. In this area novel heat management packaging structures were obtained through the encapsulation of phase change materials (PCMs) within different polymeric matrices. The morphology, thermal properties, molecular organization and thermal energy storage ability of these capsules were evaluated.

Afterwards, the encapsulation of bioactive ingredients for functional food applications was studied. In this field, novel micro- and nanoencapsulation structures were initially obtained through electrospraying from food contact materials. Finally, a vitamin and an antioxidant were encapsulated within different hydrocolloid matrices through electrospraying. Capsules attained were characterized and compared to those obtained through other encapsulation techniques. Moreover, stability of the encapsulated bioactives was studied under adverse conditions.

RESUMEN

En los últimos años, las tecnologías de micro- y nanoencapsulación han despertado un gran interés en diferentes áreas. Concretamente en la industria alimentaria, estas técnicas presentan aplicaciones muy interesantes para el desarrollo de envases inteligentes, así como para la protección de ingredientes sensibles a las condiciones de producción, almacenamiento y comercialización de alimentos. Así, el principal objetivo de esta tesis, consiste en el desarrollo de diferentes estructuras de encapsulación de interés en el área de alimentaria. Las cápsulas se obtuvieron a través del procesado electrohidrodinámico, ya que esta tecnología presenta varias ventajas sobre otras técnicas de encapsulación tradicionalmente utilizadas. Por ejemplo, el procesado electrohidrodinámico no requiere el uso de altas temperaturas y se pueden obtener cápsulas a partir de algunos biopolímeros mediante el uso de disoluciones acuosas.

Inicialmente, se desarrollaron micro- y nanocápsulas para aplicaciones de envasado inteligente. Así, se obtuvieron varias estructuras con capacidad de gestión de temperatura mediante la encapsulación de materiales de cambio de fase en diferentes matrices poliméricas. La morfología, las propiedades térmicas, la organización molecular y la capacidad de almacenamiento de energía de estas cápsulas fueron evaluadas.

Posteriormente, se estudió la encapsulación de ingredientes bioactivos para el desarrollo de nuevos alimentos funcionales. En este campo, nuevas micro- y nanocápsulas fueron obtenidas mediante electrospraying a partir de materiales de contacto alimentario. Por último, una vitamina y un antioxidante se encapsularon en diferentes matrices de hidrocoloides mediante electroesprayado. Las cápsulas obtenidas se caracterizaron y se compararon con otras obtenidas a través de técnicas de encapsulación más utilizadas actualmente. Además, la estabilidad de los bioactivos encapsulados se estudió bajo diferentes condiciones adversas (calor y humedad).

RESUM

En els últims anys, les tecnologies de micro- i nanoencapsulació han generat un gran interès en diferents àrees. Concretament a la indústria alimentària, aquestes tècniques presenten aplicacions molt interessants per al desenvolupament d'envasos intel·ligents, i per a la protecció d'ingredients sensibles a les condicions de producció, emmagatzematge i comercialització d'aliments. Així, el principal objectiu d'aquesta tesi, consisteix en el desenvolupament de diferents estructures d'encapsulació d'interès en l'àrea alimentària. Les càpsules es van obtenir a través del processat electrohidrodinámic, ja que aquesta tecnologia presenta diversos avantatges sobre altres tècniques d'encapsulació tradicionalment utilitzades. Per exemple, el processat electrohidrodinámic no requereix l'ús d'altes temperatures i es poden obtenir càpsules a partir d'alguns biopolímers mitjançant l'ús de dissolucions aquoses.

Inicialment, es van obtenir micro- i nanocàpsules per a aplicacions d'envasament intel·ligent. Així, es van obtenir diverses estructures amb capacitat de gestió de temperatura mitjançant l'encapsulació de materials de canvi de fase en diferents matrius polimèriques. La morfologia, les propietats tèrmiques, l'organització molecular i la capacitat d'emmagatzematge d'energia d'aquestes càpsules van ser avaluades.

Posteriorment, es va estudiar l'encapsulació d'ingredients bioactius per al desenvolupament de nous aliments funcionals. En aquest camp, noves micro- i nanocàpsules van ser obtingudes mitjançant electrosprayat a partir de materials de contacte alimentari. Finalment, una vitamina i un antioxidant es van encapsular en diferents matrius de hidrocoloides mitjançant electroesprayado. Les càpsules obtingudes es van caracteritzar i es van comparar amb altres obtingudes mitjançant tècniques d'encapsulació més utilitzades actualment. A més, l'estabilitat dels bioactius encapsulats es va estudiar sota diferents condicions adverses (calor i humitat).

INDEX

I. INTRODUCTION

1. MICRO- AND NANOENCAPSULATION

Encapsulation is a technique by which a core particle (solid, liquid or gaseous) is packaged within a solid wall (shell or matrix) which is made of another material for the purpose of shielding the core ingredient from the surrounding environment. The process is referred to as microencapsulation when the capsules attained range in size from one micron to few millimeters. When capsule's diameters are under one micron, the process is called nanoencapsulation (Dubey et al. 2009), even though strictly speaking, "nano" refers to sizes of less than 100 nm. This technique can be applied in multiple fields, such as agricultural, pharmaceuticals, food, cosmetics, textiles or printing. For this reason, widespread interest has been paid to research and development of micro/nanoencapsulation systems in recent years. Generally, the main reasons for the encapsulation of materials can be summarized as follows (Kuang et al. 2010):

- Protection of unstable, sensitive materials from adverse conditions
- Controlled, sustained, or timed release of materials
- Targeted release of materials
- Odor or taste masking
- Promote easier handling of materials (to facilitate the handling of toxic materials or liquids)
- Better processability of materials (improving solubility, dispersibility, flowability)

Several of these properties can be attained through the obtention of macrocapsules; however micro- and nanoencapsulation provide particles with very high surface to volume ratios and this fact improves the incorporation, adaptation and functionality of these capsules in the surrounding environment where they are applied (Bansode et al. 2010). Specifically, micro- and nanoencapsulation have the potential to enhance bioavailability, improve controlled release, and enable precision targeting of the core compounds (Ezhilarasi et al. 2013).

1.1. Most commonly used micro- and nanoencapsulation technologies.

In recent years, multiple technologies have been developed and successfully applied to generate microencapsulated materials. These techniques are classified in chemical, physical-chemical and physical/mechanical methods according to the methodology employed for the capsule's formation. Appropriate combination of starting materials and synthesis methods can be chosen to produce micro/nanoencapsulated products with a wide variety of compositional and morphological characteristics (Dubey et al. 2009). Some of the most important and most common microencapsulation techniques are briefly explained below.

1.1.1. Chemical methods

Chemical methodologies include those methods in which the starting materials are monomers or pre-polymers and thus, chemical reactions take place along with capsules formation. These techniques have been employed for different applications, mainly in textiles and agriculture, and there are several patent

applications and commercial products which use these technologies. The main drawback of these methods is the requirement of aggressive conditions of temperature, pressure or pH in order to begin the polymerization. These requirements could affect to the stability of some sensitive core materials.

Emulsion/Suspension Polymerization

For encapsulation using the emulsion/suspension polymerization technique, the monomer is added to the stirred aqueous polymerization medium containing the core material to be encapsulated and a suitable emulsifier. When the polymerization begins, the initially produced polymer molecules precipitate in the aqueous medium to form primary nuclei. As the polymerization proceeds, these nuclei gradually grow and simultaneously entrap the core material to form the final microcapsules. Generally, alkyl acrylates have been used as shell materials and lipophilic materials are more suitable to be encapsulated by this technique (Tiarks et al. 2001).

Interfacial Polycondensation

This technique involves the polycondensation of two complementary monomers at the interface of a two phase system (Janssen et al. 1992). For the preparation of capsules, this two-phase system is mixed under controlled conditions to form small droplets of one phase (dispersed phase) in the other one (continuous phase/suspension medium). The material to be encapsulated must be dissolved or dispersed in the droplets. It is also necessary to use a small amount of a suitable stabilizer to prevent droplet coalescence or particle coagulation during the process and capsule formation. This technique is applicable to a large number of polymers and can be adopted to produce micrometer or nanometer size capsules.

1.1.2. Physico-Chemical Methods

In the physico-chemical methods the starting materials are polymers, but some chemical reactions are also involved in the process. These techniques use softer conditions than chemical methods, and moreover they can use biopolymers as matrix components, such as proteins, polysaccharides or biodegradable polyesters. However organic solvents are usually required, which could lead to toxicity problems in case of food or nutraceutical applications.

Suspension Crosslinking

Microcapsule formation by this technique involves dispersion of the polymer aqueous solution containing the core material in an immiscible organic solvent (suspension/dispersion medium) in the form of small droplets. The suspension medium contains a suitable stabilizer to maintain the individuality of the droplet/microcapsules. The droplets are subsequently hardened by covalent crosslinking. The crosslinking process is accomplished either thermally (at T>500ºC) or by the use of a crosslinking agent. Suspension crosslinking is usually employed for the preparation of protein and polysaccharide-based capsules. It can be used for the production of both micro and nanocapsules (Arshady, 1989) and it has been employed for the development of drug delivery systems.

Solvent Evaporation/Solvent Extraction

In this case the shell material (the polymer) is dissolved in an organic solvent, where the core material is also dissolved or dispersed. The resulting solution is added dropwise to a stirring aqueous solution having a suitable stabilizer to

form small polymer droplets containing the encapsulated material. With time, the droplets are hardened to produce the corresponding polymer capsules. This hardening process is accomplished by the removal of the solvent either by solvent evaporation (by heat or reduced pressure), or by solvent extraction (with a third liquid which is a precipitant for the polymer and miscible with both water and the organic solvent) (Arshady, 1990a). Solvent evaporation/extraction processes are suitable for the preparation of drug loaded microcapsules based on biodegradable polyesters.

Coacervation/Phase Separation

Phase separation processes are divided into simple and complex coacervation. Simple coacervation involves the use of a single polymer, while complex coacervation involves the use of two oppositely charged polymeric materials. In both cases, the process consists on the gradual desolvation of the fully solvated polymer molecules (Arshady, 1990b). Microencapsulation by coacervation is carried out by preparing an aqueous polymer solution into which the core material (hydrophobic) is also dispersed. A suitable stabilizer may also be added to the mixture to maintain the individuality of the final microcapsules. A suitable desolvating agent (coacervating agent) is gradually incorporated into the mixture, which leads to the formation of partially desolvated polymer molecules and, hence, induce their precipitation on the surface of the core particles. The coacervation mixture is cooled down, followed by the addition of a crosslinking agent to harden the microcapsule wall. It is widely employed for the preparation of gelatin, cellulose-based products and synthetic polymer microcapsules.

1.1.3. Physical/Mechanical methods

The physical/mechanical techniques consist of those methods in which starting materials are polymers and do not involve chemical reactions. Most of them are easily scalable and thus, micro- and nanocapsules obtained through these methods are commercially available. However, they usually need high temperature conditions, which could affect to the stability of the core material.

Spray Drying

Spray drying is nowadays the most common and the cheapest technology in the food industry to produce microencapsulated additives/compounds (Gharsallaoui et al. 2007). The active material to be encapsulated using the spray drying technique is dispersed in a carrier polymer solution which is atomized into small droplets. The solvent is evaporated using a warmed gas and the resulting solid capsules are collected as dried powder (Gibbs et al., 1999; Gharsallaoui et al., 2007). Capsules size is usually in the micron range and can be modified by changing the spraying head membrane porosity.

Fluidized bed coating

This technique is used for encapsulation of solid core materials. Solid particles to be encapsulated are suspended in a jet of air and then covered by a spray of liquid coating material. The capsules are then moved to an area where their shells are solidified by cooling or solvent vaporization. The process of suspending, spraying and cooling is repeated until the capsule walls are of the desired thickness (Dewettinck & Huyghebaert, 1999). This technology is used extensively to encapsulate pharmaceuticals for drug delivery systems, since

the controlled-release behavior can be easily modulated by varying the coating thickness and the coating formulations (Kuang et al. 2010).

Extrusion-spheronization

The process begins with a granulation step whereby a polymer, bioactive agent, stabilizers, and other ingredients are mixed with a liquid binder, usually water, to form a wet mass or paste. The next step involves screw extrusion of the wet mass through a die to form cylindrical strands of uniform length and diameter. These strands are then made into spheres by first chopping them into equal lengths before rounding into pellets of spherical shape on a plate. Alternatively, the wet mass may be extruded through the screen of an oscillating granulator and the resulting jagged cylinders formed into spheres by rotation in a conventional coating pan under forced-air drying conditions. The final step involves collecting the wet spheres and drying them in either a fluidized bed or tray drier prior to use. Capsules size is usually in the micron range. This technique is widely used in pharmaceutical industry to make controlled release dosage forms (Bajaj et al. 2010; Berner et al. 1992).

Supercritical Fluids

Microencapsulation has also been carried out by supercritical fluids (Krober & Teipel, 2005; Chiou et al. 2006). Supercritical fluids are highly compressed gases that possess several advantageous properties of both liquids and gases. Most widely used ones are supercritical CO_2, alkanes (C2 to C4) and nitrous oxide (N_2O). In this process, supercritical fluid containing the active ingredient and the shell material are maintained at high pressure and then released at atmospheric pressure through a small nozzle. The sudden drop in pressure causes desolvation of the shell material, which is then deposited around the

active ingredient and forms a coating layer. This process do not required temperature nor organic solvents, however, the costs of equipment and operation are too high and the technological parameters need further research optimization (Guo et al. 2012).

Layer-by-Layer Deposition

In this process polyelectrolyte multilayers are prepared by sequentially immersing a substrate in positively and negatively charged polyelectrolyte solutions in a cyclic procedure. Core-shell particles with tailored size and properties are prepared using colloidal particles as the core material that serves as a template onto which multilayers are fabricated (Trau & Renneberg, 2003; Caruso et al. 2000). This technique also presents scalability difficulties.

1.2. Micro- and nanoencapsulation applications

Micro- and nanoencapsulation technologies are employed in a diverse range of fields. Although microcapsules were first obtained in 1950s for printing applications (Green & Schleicher, 1957; Green, 1957), it was in the mid of 1970s when microencapsulation became increasingly popular in biomedical and pharmaceutical applications, mainly for drug delivery systems (Dubey et al. 2009). Recently, in addition to the health sector, the cosmetic, textile, agricultural and food industries are also using the encapsulation technology for multiple purposes.

1.2.1. Biomedical and pharmaceutical applications

In this field, micro- and nanocapsules have been used for immobilized enzymes and catalysts (Wang & Hsieh, 2004; Wu et al. 2005), for artificial blood vessels (Ma et al. 2005) and as vehicles for sustained and targeted drug delivery (Sill & Von Recum, 2008; Meinel et al. 2012). Especially in the controlled delivery area, microencapsulation could potentially overcome the limitations of other delivery systems and has drawn much research attention in the last decades, particularly in the fields of cancer therapies, hormonal treatments, asthma, and tissue engineering, for which tailored and multiple-molecule delivery is necessary for therapeutic effect (Chen et al. 2010; Bock et al. 2012). Specifically, biodegradable polyesters and their copolymers have demonstrated their potential as effective carriers for drug delivery applications (Langer, 1990; Youxin et al. 1994).

1.2.2. Cosmetic applications

Recently, cosmetic products are focused on antiaging, whitening and brightening skin effects (Nakai et al. 2013). Besides, these products usually employed multiple fragrance chemicals in order to enhance and improve their aroma (Tekin et al. 2013). Therefore, different active ingredients, as well as aroma compounds are used in cosmetic formulations. However, most of these substances are very sensitive to ambient conditions, such as light or moisture, thus losing their beneficial properties. Moreover, some of them often present a poor biodisponibility mainly due to low water solubility (Munin et al. 2011). Micro- and nanoencapsulation can avoid these drawbacks and nowadays different technologies have been used to obtain microcapsules in this field. For example, fragrances, volatile oils (Tekin et al. 2013), polyphenols (Munin et al.

2011) and natural plant extracts (Kim et al. 2010) have been already microencapsulated for cosmetic applications through different techniques. Particularly, lipid-based and biodegradable-based systems have been used as shell materials in this area (Kim et al. 2010).

1.2.3. Textile applications

Microencapsulation has been used in fabrics since 1980s, specifically in military applications, in which special fabrics were designed in order to enhance their chemical protection against chemical warfare. In particular, these military fabrics incorporated microcapsules with chemical decontaminants microcapsules (Cowsar, 1980). Nevertheless, in recent years, the most important applications of microcapsules in the textile industry are thermoregulating fibers and cosmetotextiles. Thermoregulating textiles are based on the incorporation of phase change materials (PCMs) into the textile structures. PCMs can store and release latent heat during their phase transition within a defined temperature range. Therefore, they can buffer thermal variations and keep thermal human comfort. Particularly, these textiles have been mainly used in sport and professional clothing, medical applications, bedding and automotive textiles (Mondal, 2008). Cosmetotextiles are textiles which contain bioactive substances with cosmetic effects that release these active molecules in contact with the human body (Ripoll et al. 2010). For this aim, bioactive ingredients, such as vitamins, anti-cellulite or antioxidants are microencapsulated and incorporated into the textiles. These compounds are released by friction with skin or biodegradation of the matrices. Nowadays there are different commercial cosmetotextiles for various applications (Singh et al. 2011).

1.2.4. Agricultural applications

The increasing awareness of the environmental and toxicity problems related to the fertilizers, pesticides and insect sprays used in the agricultural industry has promoted the use of novel natural products which do not bring this kind of issues. Therefore, in order to substitute the traditional chemicals, immobilization and encapsulation of microorganisms, micronutrients and pheromones have been widely used in the agricultural industry. Specifically, bacterial cells have been microencapsulated in natural and synthetic polymers and then inoculated in plants for inducing their growth and development (Schoebitz et al. 2013; Herrmann & Lesueur, 2013). Moreover, the microencapsulation and release of female pheromones in order to extinguish insect plagues in crops, has been successfully achieved and is currently used in the plant protection area (Bansal et al. 2012; Kong et al. 2009). Traditional pesticides are also microencapsulated to be released over time, allowing farmers to apply the chemicals less often rather than requiring very highly concentrated and toxic initial applications. Besides, some soluble fertilizers incorporated into the soil react with soil components forming insoluble products, which are not efficiently taken up by plants. Thus, the encapsulation and controlled release of these fertilizers can avoid this problem and improve the fertilizers absorbance (Pilar-Izquierdo et al. 2013).

1.2.5. Food applications

The development of functional foods containing bioactive ingredients is an area of increasing interest. These bioactive ingredients are expected to impart a health benefit to consumers in addition to the nutrition that the food itself offers. However, functional substances are known to lose effectiveness either

during processing, storage or in the gastrointestinal tract. The development of micro- and nanocapsules which are able to protect the active ingredients and to act as carriers and delivery vehicles for controlled release is undoubtedly a plausible option to preserve the bioactivity of these ingredients. For the encapsulation of food bioactives, biopolymers are the preferred choice because they may be nontoxic, edible and digestible. Specifically, various components have been already microencapsulated in this area, such as enzymes, probiotic bacteria, antimicrobials, flavors, antioxidants or omega-3 fatty acids. Furthermore, in this field micro- and nanocapsules can also be also incorporated within the packaging structures in order to obtain active and smart packaging systems. For instance, antimicrobial compounds have been microencapsulated and incorporated in packaging films and results suggest that this technique could be an effective approach to control food pathogens without compromising the basic physico-chemical attributes of the packaging structures (Guarda et al. 2011; Imran et al. 2012; Brasil et al. 2012).

On a different line, micro- and nanoencapsulated phase change materials (PCMs) can also be incorporated within the packaging films in order to keep the cold chain and protect thermo-sensitive foodstuffs. It is estimated that 15% of the electricity consumed is used for refrigeration, especially in food refrigeration (retail, commercial, chilling, freezing and warehouse storage) (Market Transformation Program - http://www.mtprog.com). Thus, encapsulation of PCMs presents a high potential for smart packaging with thermal buffering ability to improve the quality and safety of food products. Moreover, PCM capsules could be also used in transport systems and refrigeration cabinets in order to better keep the correct temperature along the whole cold chain, which would reduce energy consumption.

2. ELECTRO-HYDRODYNAMIC PROCESS FOR ENCAPSULATION APPLICATIONS

As it was seen before, the available micro- and nanoencapsulation techniques often require a large amount of organic solvents, which can lead to emission of volatile organic compounds, raise waste elimination problems, and potentially leave toxic residues in the finished products. Moreover, some of them also require temperature or pH conditions which could limit their application for the encapsulation of sensitive ingredients. Another restrictive condition is the possibility of scaling up the production to industrial scale. As an alternative, electro-hydrodynamic processing techniques have been recently suggested to be simple and straightforward methods to generate submicron encapsulation structures for a wide variety of molecules (Xie et al. 2008; Lopez-Rubio & Lagaron 2012; Bock et al. 2012; Pérez-Masiá et al. 2013a). Furthermore, these techniques do not require the use of aggressive conditions, such as high temperatures, and, thus, sensitive ingredients can be encapsulated without any activity loss. Moreover, organic solvents are not required, since capsules can be attained from aqueous-solutions through electro-hydrodynamic processing.

2.1. Generalities about the electro-hydrodynamic process

The electro-hydrodynamic process consists on the use of high electrostatic potentials for the fabrication of ultrathin polymer structures. Although this process was firstly described in 1902 (Morton, 1902), it was not until the 1990s when widespread interest in the use of this technology emerged. In recent years, much attention has been paid to the use of electro-hydrodynamic processing in the field of nanoscience and nanotechnology and, thus, many

investigations in the production of nanofiber morphologies have been carried out. The process uses high voltage electric fields to produce electrically charged “jets” from viscoelastic polymer solutions which, on drying by means of the evaporation of the solvent, produce diverse ultrathin structures (Li & Xia, 2004). Generally, the basic setup for electro-hydrodynamic process consists of four components: a high-voltage power supply, a syringe pump to pull out the solution, a spinneret (a metallic needle) and a collector surface (a single piece of conductive substrate). An example of the typical setup of a lab-scale apparatus for electro-hydrodynamic processing is depicted in Figure 1.

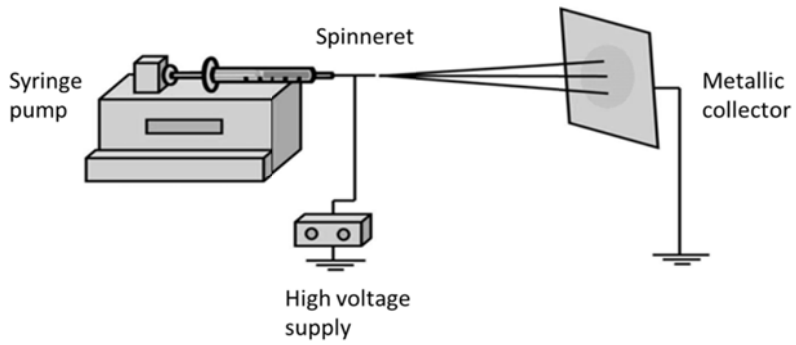

Figure 1. Schematic representation of the electro-hydrodynamic process.

The structures morphology and diameter obtained are affected by different processing conditions. The most relevant factors can be divided in two categories: (I) those dependent on the intrinsic properties of the solution, such as the kind of polymer, the viscosity, the electrical conductivity, the polarity and the surface tension; and (II) those related to the operational conditions of the equipment, such as the applied electric field, the distance between the spinneret and the collector and the feeding rate of the polymer solution (Reneker & Chun, 1996). Therefore, by changing these parameters, multiple

morphologies can be attained and continuous polymeric fibers and/or capsules (beads) with diameters ranging from a few nanometers to a few microns can be obtained. When continuous fibers are obtained, the process is called “electrospinning”. When size-reduced capsules are attained, the process is normally referred to as “electrospraying” due to the non-continuous nature of the structures obtained. As an example, several morphologies obtained through electrospinning and electrospraying are shown in Figure 2.

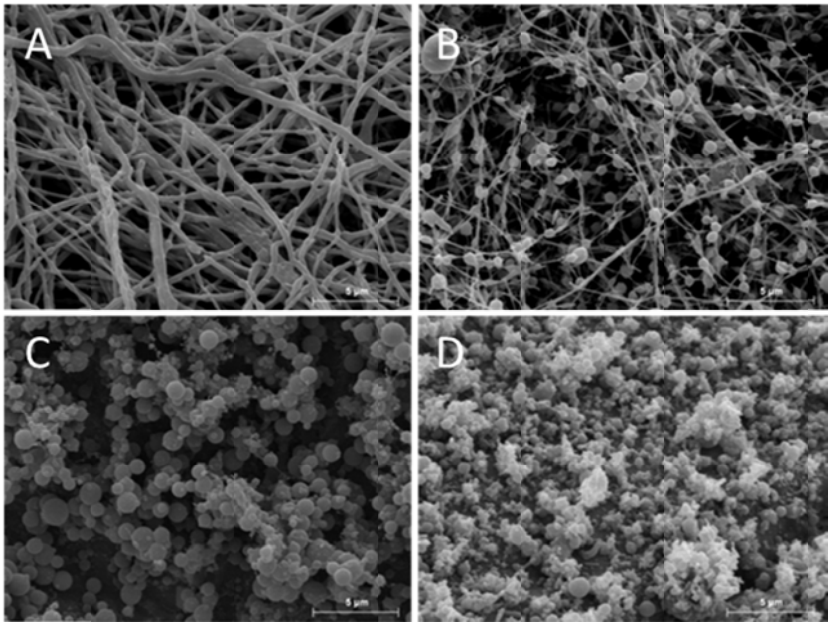

Figure 2. Examples of different encapsulation morphologies attained from zein (A), polyethylene oxide (PEO) (B), dextran (C) and soy protein (D) through electrospinning and electrospraying.

Because of their high specific surface areas and small pore size in comparison with commercial textiles, the electrospun and electrosprayed materials are excellent candidates for many applications. For instance, they can be used in

filtration or separation membranes, since the submicrometer-size fibers produce a layer that has high porosity but very small pore size (Gibson et al. 1999). Due to the ultrathin size of these materials, they can also be used as reinforcement in composite materials, since they can provide superior structural properties which generally cannot be achieved by microfibers of the same material (Lagaron et al. 2005). Besides, the biomedical field is probably one of the most important application areas for the electrospinning technique, as the topographical similarity of electrospun matrices with the extracellular matrix was realized as favorable for tissue engineering purposes and medical implants (Meinel et al. 2012). Finally, the electro-hydrodynamic process can be used as encapsulation technique creating small droplets of solid or liquid particles (core material) which are packed into a matrix (wall material) designed to protect the core or release it under desired conditions.

2.2. Advantages of electro-hydrodynamic processing for encapsulation

Electro-hydrodynamic process has a number of advantages over other well-established encapsulation technologies. For instance, it does not require the use of high temperatures and, thus, temperature-sensitive ingredients may be encapsulated using this processing technique without suffering from any activity loss. Moreover, although many polymers require to be dissolved in organic solvents for a stable electrospinning/electrospraying process, one can also produce electrospun structures from some biopolymers using aqueous solutions, mainly by adjusting the process parameters and/or changing the solution properties through the addition of proper additives. This has special interest in food and nutraceutical applications, where the use of organic

solvents for the development of edible ingredients can pose reasonable concerns regarding the toxic effects due to the presence of remaining solvents in the structures.

Another advantage of the electro-hydrodynamic process is that the morphology and size of the encapsulation structures obtained can be controlled by adjusting the process parameters. Therefore, for a certain material, fibers or beads can be obtained by lowering the polymer concentration or increasing the tip-to-collector distance. Moreover, this technology can generate structures with diameters between 10 and more than 1000 nm depending on the solution and the processing conditions. The key advantage of producing capsules with very small diameters is their large surface to volume ratio, high porosity and superior mechanical performance, which improve controlled release and enable precision targeting of the bioactive compounds (Frenot & Chronakis, 2003; Kim & Reneker, 1999; Mozafari et al. 2006).

Furthermore, there is no limitation in terms of the substance to encapsulate, independently of the chemical nature of the encapsulating matrix, as emulsion or coaxial electrospinning/electrospraying might be employed. In the emulsion process, an immiscible liquid phase which contains the core material is dispersed into a polymer solution until a stable emulsion is formed. The coaxial configuration consists of two concentrically arranged needles connected to two reservoirs which contain different solutions, one with the polymer matrix and one with the core material. This configuration presents the possibility of including with the core material a favorable fluid medium for the functional component to encapsulate, which does not have to be spinnable as it becomes entrained by the outer polymeric shell (Greiner et al. 2006).

Another advantage is that, the properties of the electrospun/electrosprayed polymeric structures can be modified, either by tailoring the fiber or capsule surface morphology, or by using polymer blends to create composite materials for encapsulation that may be able to better fulfill specific industrial requirements. Recently, investigations have focused on the inclusion of other nanoscale structures within the nanofibers in order to produce structures with added functionalities. For instance, silver nanoparticles have been included in synthetic polymer fibers to produce potent antimicrobially active materials (Son et al. 2006). Likewise, a combination of nanofibers and self-assembled structures such as micelles, liposomes and microemulsions, could also create novel delivery systems with superior properties for encapsulation properties (Kriegel et al. 2008).

Electro-hydrodynamic process as an encapsulation technique is still in an exploratory phase and most of the equipment used is lab-scale. However, there are a number of companies that are already commercializing pilot plant scale and even industrial scale equipments, which can be tailor-made to match the specific requirements for a certain application.

2.3. Use of electro-hydrodynamic process for encapsulation in the food area.

As it was commented before, the use of micro- and nanoencapsulation in the food area have a broad variety of potential applications, both to be directly applied in foods and for the development of novel and functional packaging materials. Microencapsulation is well established in the food industry, but nanoencapsulation can offer a number of advantages. The use of electro-hydrodynamic processing in this field allows the production of nanometric

particles which may have increased bioavailability and controlled release properties and present better dispersion of the capsules (Chaudhry et al. 2008; Mozafari et al. 2006). Some examples of recent studies using electro-hydrodynamic processing to generate structures of interest in the food area are outlined below.

2.3.1. Encapsulation of bioactive ingredients

Enzyme encapsulation

Enzymes have multiple applications in the food area, not only for food processing, but also used as antioxidant or antimicrobial additives and for food quality control. It is widely recognized that enzyme immobilization can stabilize enzymes, enable better control of the enzymatic reaction and allow their repeated use. Encapsulation for the immobilization of enzymes might, thus, improve their properties (Betancor & Luckarift, 2008). The use of electrospinning for incorporation of diverse enzymes has gained increasing attention. Electrospun nanofibers are excellent candidates for hosting enzymes for several reasons: (I) their small size confers a large surface area and makes possible the creation of materials with high enzyme concentrations; (II) the porosity of the fibers can be tailored and, thus, the movement of molecules into and out of the fibers can be controlled according to specific requirements; (III) the use of non-soluble fibrous mats in aqueous medium provides the ability to recover the mat for reuse; and (IV) multiple enzymes from diverse sources can be encapsulated together (Dror et al. 2008).

Probiotics encapsulation

Probiotics are defined as living microorganisms which, when administered in adequate amounts, confer health benefits to the host (Havenaar & Huis in't Veld, 1992). However, probiotics must be alive, metabolically active and abundant in the product to guarantee their efficacy. Microencapsulation has been suggested to increase their survival during product storage and marketing and electro-hydrodynamic processing is an ideal tool for this purpose. This technology does not involve severe conditions, both in terms of temperature and solvents used, can incorporate the probiotics in a favorable medium (through the coaxial configuration) and give rise to small capsule sizes. Indeed, different encapsulation structures have demonstrated the ability to prolong bifidobacterial survival during storage at various temperature and relative humidity conditions (López-Rubio et al. 2009 and 2012).

Antioxidant encapsulation

In foods, antioxidants are added to minimize changes in flavor, aroma, color or nutritional value. But, moreover, antioxidants can protect the body against damages caused by free radicals and degenerative diseases and, thus, are increasingly studied to be included in functional foods. However, due to their intrinsic sensitivity to several factors, such as light, oxygen or temperature, natural antioxidants should be protected from the surrounding medium or the processing conditions during food production. Thus, the electro-hydrodynamic technique has been evaluated for the encapsulation of antioxidants, as no temperature is required in the process and, therefore, the antioxidant activity of the molecules is thought to remain unchanged during encapsulation. Recently, β-carotene and epigallocatechin-gallate have been encapsulated

through electrospinning/electrospraying demonstrating an increased stability of the antioxidant within the encapsulation matrices in comparison with the non-encapsulated compound (Fernandez et al. 2009; Lopez-Rubio & Lagaron, 2012; Singh et al. 2011).

Omega-3 Fatty Acids

Omega-3 fatty acids (ω-3), have become popular as food supplements due to the beneficial health effects including a reduction in blood pressure, modulation of the response to endogenous and exogenous thrombolytic agents, antiarrhythmic actions, inhibition of platelet activation, modulation of inflammation, triglycerides reduction, and decrease of cardiovascular diseases (Horrocks & Yeo, 1999). Docosahexaenoic acid (DHA), a long chain polyunsaturated fatty acid of the ω-3 group, was encapsulated in zein ultrathin capsules produced by electrospraying (Torres-Giner et al. 2010). Encapsulated DHA was observed to be more efficient against degradation under both ambient conditions and in a confined space (so-called headspace experiment). Moreover, the ultrathin zein-DHA capsules resulted to be more stable across relative humidity and temperature and released much less off-flavors (Torres-Giner et al. 2010).

Flavors encapsulation

Flavors are very valuable ingredients in any food formula. Even small amounts of some aroma substances can be expensive, and because they are usually delicate and volatile, preserving them is often a top concern of food manufacturers. Encapsulation of flavors has been carried out using many different methods such as spray drying, spray chilling, extrusion, coacervation and molecular inclusion (Madene et al. 2006). Cyclodextrin inclusion

complexes (CD-IC) have also been used to improve flavor stability (Marques, 2010). The encapsulation of these CD-IC within electrospun fibers has also proved to enhance the durability and provide high temperature stability of flavors and, specifically, of vanillin (Kayaci & Uyar, 2012).

2.3.2. Encapsulation for food packaging applications

Generally, electrospun nanofibers have been incorporated as reinforcement in the packaging matrices in order to enhance their mechanical and barrier properties. However, in recent years, new functions are claimed to the packaging and there is a greater interest in the design of active and smart packaging systems. Therefore, electro-hydrodynamic technology has been recently used to produce nanostructures with functional properties, which are later on incorporated in the packaging matrices. Particularly, the electro-hydrodynamic technology enables the incorporation of multiple functional substances into the structures. Moreover, electrospun nanocapsules lead to a better dispersion of the particles into the packaging matrix. Some examples of the use of electrospinning/electrospraying in the food packaging area are described below.

Antimicrobial food packaging

The growth of microorganisms is the major problem of food spoilage leading to degradation of quality, shortened shelf-life and changes in microflora that could induce pathogenic problems. Volatile substances with antimicrobial features, such as natural essential oils, essences, extracts, resins, infusions, etc. are of great interest for the active packaging industry. The efficient encapsulation and release of these ingredients represent a major challenge, considering their high volatility and the fact that they are very sensitive to

heat, oxygen and light. Most of the active packaging studies reported in the literature are based on the active agents dispersed in carriers with limited surface areas, such as polymer films and layers which present negligible delivery profiles (Appendini & Hotchkiss, 2002; Guillard et al., 2009). However, electro-hydrodynamic processing allows the production of nanocapsules which offer a number of additional advantages compared to film and sheet carriers, as they are more responsive to changes in the surrounding atmosphere (e.g., relative humidity and temperature changes), which enable a tunable release of the entrapped compounds (Vega Lugo & Lim, 2009). Recently, essential oils, antifungals and bacteriophage have been encapsulated through electrospinning technique showing suitable release mechanisms for food packaging applications (Mascheroni et al. 2013; Ai-Tang et al. 2013; Korehei & Kadla, 2014).

Heat management packaging structures

It is well-known that refrigeration temperatures have preservative effects on perishable products and thus, by controlling the temperature along the different stages of the food production and commercialization, a great number of deteriorative processes could be avoided and the shelf life of products could be increased. However, temperature fluctuations during storage and commercialization of foods often occur. A possible approach to control thermal variations during storage and distribution of food, maintaining the preservation temperature constant and, thus, preventing food quality loss is through packaging structures with thermal energy storage capacity. This can be attained through the incorporation of phase change materials (PCMs) into the packaging structures. PCMs are able to absorb or release a great amount of energy during their melting/crystallization process and, as a consequence,

they are able to buffer the thermal variations of the environment, and thus, they could provide thermal protection to the packaged food.

Nevertheless, the use of PCMs for food refrigeration applications presents some drawbacks. On one hand, some PCMs have a low thermal conductivity, which limits the energy that can be extracted from them. Another problem is their handling, since they are liquid at ambient temperature and, what is more important, they need to undergo a phase change (i.e. from liquid to solid and viceversa) at the target temperature to exert the desired functionality. Electro-hydrodynamic technology is a suitable tool for produce PCM nanocapsules, since this technique is able to produce capsules with very high specific area, which increase the heat-transfer area thus, increasing the velocity of heat transmision (Alkan et al. 2011), and the encapsulation of these particles in a solid matrix can solve the handling problems of the PCMs. Therefore, this technology shows a tremendous potential for developing novel packaging structures with thermal buffering ability to improve the quality and safety of food products.

References

Ai-Tang, R., Utarak, H., Yoovidhya, T., Intasanta, V., Wongsasulak, S. (2013). Fabrication and antifungal activity of cellulose acetate-based fibers encapsulating natural neem seed oil. Advanced Materials Research 747, pp. 166-169.

Alkan, C., Sari, A., & Karaipekli, A. (2011). Preparation, thermal properties and thermal reliability of microencapsulated n-eicosane as novel phase change material for thermal energy storage. Energy Conversion and Management, 52(1), 687-692.

Appendini, P. & Hotchkiss, J.H. (2002). Review of antimicrobial food packaging. Innovative Food Science and Emerging Technologies, 3 pp. 113–126.

Arshady, R. (1989). Microspheres and microcapsules: A Survey of manufacturing techniques Part I Suspension crosslinking. Polymer Engineering & Science, 29(24), 1746-58.

Arshady, R. (1990a). Microspheres and microcapsules: A Survey of manufacturing techniques Part III Solvent evaporation. Polymer Engineering & Science, 30, 915-24.

Arshady, R. (1990b). Microspheres and microcapsules: A survey of manufacturing techniques Part II Coacervation. Polymer Engineering & Science, 30(15), 905-14.

Bajaj, P.R., Survase, S.A., Bule, M.V., Singhal, R.S. (2010). Studies on Viability of Lactobacillus fermentum by Microencapsulation Using Extrusion Spheronization. Food Biotechnology, 24:2, 150-164.

Bansal, P., Bubel, K., Agarwal, S., Greiner, A. (2012). Water-stable all-biodegradable microparticles in nanofi bers by electrospinning of aqueous dispersions for biotechnical plant protection. Biomacromolecules 13:439–444.

Bansode, S.S., Banarjee, S.K., Gaikwad, D.D., Jadhav, S.L., Thorat, R.M. (2010). Microencapsulation: A review. International Journal of Pharmaceutical Sciences Review and Research 1 (2), pp. 38-43.

Berner, B., Dinh, S. (1992). Fundamental concepts in controlled-release. In: Kydonieus, A., ed. Treatise on Controlled Drug Delivery. Dekker, NY, pp. 155–195.

Betancor, L., & Luckarift, H.R. (2008). Bioinspired enzyme encapsulation for biocatalysis. Trends in Biotechnology 26(10), 566-572.

Bock, N., Dargaville, T.R. & Woodruff, M.A. (2012). Electrospraying of polymers with therapeutic molecules: State of the art. Progress in Polymer Science 37, 1510-1551.

Brasil, I.M., Gomes, C., Puerta-Gomez, A., Castell-Perez, M.E., Moreira, R.G. (2012). Polysaccharide-based multilayered antimicrobial edible coating enhances quality of fresh-cut papaya. LWT - Food Science and Technology 47 (1), pp. 39-45.

Caruso, F., Yang, W., Trau, D. Renneberg, R. (2000). Microencapsulation of uncharged low molecular weight organic materials by polyelectrolyte multilayer self-assembly. Langmuir, 16(23), 8932-936.

Chaudhry, Q., Scotter, M., Blackburn, J., Ross, B., Boxall, A., Castle, L., Aitken, R., & Watkins, R. (2008). Applications and implications of nanotechnologies for the food sector. Food Additives & Contaminants 25, 241-258.

Chen FM, Zhang M, Wu ZF. (2010). Toward delivery of multiple growth factors in tissue engineering. Biomaterials. 31:6279–308.

Chiou, A. H., Cheng, H. C., Wang, D. P. (2006). Micronization and microencapsulation of felodipine by supercritical CO2. Journal of Microencapsulation, 23(3) 265-76.

Cowsar, D. R. The United States of America as represented by the Secretary of the Army, Washington, D. C. (1980). Novel Fabric containing microcapsules of chemical decontaminants encapsulated within semipermeable polymers. US Patent 4,201,822. 6 May 1980. 6.

Dewettinck, K. & Huyghebaert, A. (1999). Fluidized bed coating in food technology. Trends in Food Science and Technology, 10, 163-68.

Dror, Y., Kuhn, J., Avrahami, R., & Zussman, E. (2008). Encapsulation of enzymes in biodegradable tubular structures. Macromolecules 41, 4187-4192.

Dubey, R., Shami, T.C., Bhasker Rao, K.U. (2009). Microencapsulation technology and applications. Defence Science Journal 59 (1), pp. 82-95.

Ezhilarasi, P.N., Karthik, P., Chhanwal, N., Anandharamakrishnan, C. (2013). Nanoencapsulation Techniques for Food Bioactive Components: A Review. Food and Bioprocess Technology 6 (3), pp. 628-647.

Fernandez, A., Torres-Giner, S., & Lagaron, J.M. (2009). Novel route to stabilization of bioactive antioxidants by encapsulation in electrospun fibers of zein prolamine. Food Hydrocolloids 23, 1427-1432.

Frenot, A. & Chronakis, I.S. (2003). Polymer nanofibers assembled by electrospinning. Current Opinion in Colloid & Interface Science 8, 64-75.

Gharsallaoui, A., Roudaut, G., Chambin, O., Voilley, A., Saurel, R. (2007). Applications of spray-drying in microencapsulation of food ingredients: An overview. Food Research International 40 (9), pp. 1107-1121.

Gibbs, F., Selim, A., Catherine, N., & Mulligan, B. (1999). Encapsulation in the food industry: a review. International Journal of Food Sciences and Nutrition, 50 (3), 213-224.

Gibson, P.W., Schreuder-Gibson, H.L., Rivin, D. (1999). Electrospun fiber mats: Transport properties. AIChE Journal, 45, 190-195.

Green, B. K. & Schleicher, L. (1957). The National Cash Register Company, Dayton, Ohio. Oil containing microscopic capsules and method of making them. US Patent 2,800,457. 23 July 1957, 11.

Green, B.K. (1957). The National Cash Register Company, Dayton, Ohio. Oil containing microscopic capsules and method of making them. US Patent 2,800,458. 23 July 1957, 7.

Greiner, A., Wendorff, J.H., Yarin, A.L., Zussman, E. (2006). Biohybrid nanosystems with polymer nanofibers and nanotubes. Applied Microbiology and Biotechnology 71, 387–393.

Guarda, A., Rubilar, J.F., Miltz, J., Galotto, M.J. (2011). The antimicrobial activity of microencapsulated thymol and carvacrol. International Journal of Food Microbiology 146 (2), pp. 144-150.

Guillard, V., Issoupov, V., Redl, A., Gontard, N. (2009). Food preservative content reduction by controlling sorbic acid release from a superficial coating. Innovative Food Science and Emerging Technologies, 10, pp. 108–115.

Guo, H., Huang, Y., Qian, J.-q., Gong, Q.-y., Tang, Y. (2012). Optimization of technological parameters for preparation of lycopene microcapsules. Journal of Food Science and Technology, DOI 10.1007/s13197-011-0600-0.

Havenaar, R., & Huis in't Veld, J.H.J. (1992). The lactic acid bacteria in health and disease. InWood, B. J. B. (Ed.). (1992). The lactic acid bacteria, Vol. 1 (pp. 209-224). London: Chapman & Hall.

Herrmann, L. & Lesueur, D. (2013). Challenges of formulation and quality of biofertilizers for successful inoculation. Applied Microbiology and Biotechnology 97 (20) , pp. 8859-8873.

Horrocks, L.A. & Yeo, Y.K. (1999). Health benefits of docosahexaenoic acid (DHA). Pharmacological Research 40, 211–225.

Imran, M., Revol-Junelles, A.-M., René, N., Jamshidian, M., Akhtar, M.J., Arab-Tehrany, E., Jacquot, M., Desobry, S. (2012). Microstructure and physico-chemical evaluation of nano-emulsion-based antimicrobial peptides embedded in bioactive packaging films. Food Hydrocolloids 29 (2) , pp. 407-419.

Janssen, J. M. & Nijenhuis, K. (1992). Encapsulation by interfacial polymerization I. The capsule production and a model for wall growth. Journal of Membrane Science, 65, 59-68.

Kayaci, F. & Uyar, T. (2012). Encapsulation of vanillin/cyclodextrin inclusión complex in electrospun polyvinyl alcohol (PVA) nanowebs: Prolonged shelf-life and high temperatura stability of vanillin. Food Chemistry 133, 641-649.

Kim, J.S. & Reneker, D.H. (1999). Mechanical properties of composites using ultrafine electrospun fibers. Polymer Composites 20, 124-131.

Kim, H.-J., Kim, T.-H., Kang, K.-C., Pyo, H.-B., Jeong, H.-H. (2010). Microencapsulation of rosmarinic acid using polycaprolactone and various surfactants. International Journal of Cosmetic Science 32 (3), pp. 185-191.

Kong, X.Z., Gu, X., Zhu, X., Zhang, Z. (2009). Spreadable dispersion of insect sex pheromone capsules, preparation via complex coacervation and release control of the encapsulated pheromone component molecule. Biomedical Microdevices 11 (1), pp. 275-285.

Korehei, R., Kadla, J.F. (2014). Encapsulation of T4 bacteriophage in electrospun poly(ethylene oxide)/cellulose diacetate fibers. Carbohydrate Polymers 100, pp. 150-157.

Kriegel, C., Arrechi, A., Kit, K., McClements, D.J., & Weiss, J. (2008). Fabrication, functionalization, and application of electrospun biopolymer nanofibers. Critical Reviews in Food Science and Nutrition 48, 775-797.

Krober, H. & Teipel, U. (2005). Microencapsulation of particles using supercritical CO2. Chemical Engineering Processing, 44(2), 215-19.

Kuang, S.S., Oliveira, J.C., Crean, A.M. (2010). Microencapsulation as a tool for incorporating bioactive ingredients into food. Critical Reviews in Food Science and Nutrition 50 (10) , pp. 951-968.

Lagaron, J.M., Cabedo, L., Cava, D., Feijoo, J.L., Gavara, R., Gimenez, E. (2005). Improving packaged food quality and safety. Part 2: Nanocomposites. Food Additives and Contaminants, 22, 994-998.

Langer, R. (1990). New methods of drug delivery. Science 249 (4976): 1527–1533.

Li, D., & Xia, Y. (2004). Electrospinning of nanofibers: Reinventing the wheel? Advanced Materials, 16, 1151-1170.

López-Rubio, A. & Lagaron, J.M. (2012). Whey protein capsules obtained through electrospraying for the encapsulation of bioactives. Innovative Food Science and Emerging Technologies 13, 200-206.

López-Rubio, A., Sanchez, E., Sanz, Y., & Lagaron, J.M. (2009). Encapsulation of living bifidobacteria in ultrathin PVOH electrospun fibers. Biomacromolecules, 10, 2823-2829.

López-Rubio, A., Sanchez, E., Wilkanowicz, S., Sanz, Y., & Lagaron, J.M. (2012). Electrospinning as a useful technique for the encapsulation of living bifidobacteria in food hydrocolloids. Food Hydrocolloids 28, 159-167.

Ma, Z., Kotaki, M., Yong, T., He, W., Ramakrishna, S. (2005). Surface engineering of electrospun polyethylene terephthalate (PET) nanofi bers towards development of a new material for blood vessel engineering. Biomaterials 26:2527–2536.

Madene, A., Jacquot, M., Scher, J., & Desobry, S. (2006). Flavour encapsulation and controlled release – a review. International Journal of Food Science & Technology 41, 1-21.

Marques, H.M.C. (2010). A review on cyclodextrin encapsulation of essential oils and volatiles. Flavour and Fragrance Journal, 25, 313–326.

Mascheroni, E., Fuenmayor, C.A., Cosio, M.S., Silvestro, G.D., Piergiovanni, L., Mannino, S., Schiraldi, A. (2013). Encapsulation of volatiles in nanofibrous polysaccharide membranes for humidity-triggered release. Carbohydrate Polymers 98 (1), pp. 17-25

Meinel, A.J., Germershaus, O., Luhmann, T., Merkle, H.P., Meinel, L. (2012). Electrospun matrices for localized drug delivery: Current technologies and selected biomedical applications. European Journal of Pharmaceutics and Biopharmaceutics 81, 1–13.

Mondal, S. (2008). Phase change materials for smart textiles - An overview. Applied Thermal Engineering 28 (11-12), pp. 1536-1550.

Morton, W.J. (1902). Method of dispersing fluids. US Patent. 705, 691.

Mozafari, M. R., Flanagan, J., Matia-Merino, L., Awati, A., Omri, A., Suntres, Z. E., Singh, H. (2006). Recent trends in the lipidbased nanoencapsulation of antioxidants and their role in foods. Journal of the Science of Food and Agriculture, 86(13), 2038–2045.

Munin, A., Edwards-Lévy, F. (2011). Encapsulation of natural polyphenolic compounds; a review. Pharmaceutics 3 (4), pp. 793-829.

Nakai, S., Akiyoshi, M., Okubo, M. (2013). Preparation of micrometer-sized, multifunctional capsule particles for cosmetic by microsuspension polymerization utilizing the self-assembling of phase separated polymer method. Journal of Applied Polymer Science 127 (4), pp. 2407-2413.

Pilar-Izquierdo, M.C., Busto, M.D., Ortega, N., Perez-Mateos, M. (2013). Barley seeds encapsulated in calcium-alginate gels with phosphatase and humate-phosphatase complexes for improving phosphorus bioavailability. Agronomy Journal 105 (6), pp. 1565-1570.

Reneker, D. H., & Chun, I. (1996). Nanometre diameter fibers of polymer, produced by electrospinning. Nanotechnology, 7, 216-223.

Ripoll, L., Bordes, C., Etheve, S., Elaissari, A., Fessi, H. (2010). Cosmeto-textile from formulation to characterization: An overview. E-Polymers , art. no. 40.

Schoebitz, M., López, M.D., Roldán, A. (2013). Bioencapsulation of microbial inoculants for better soil-plant fertilization. A review. Agronomy for Sustainable Development 33 (4), pp. 751-765.

Sill, T.J. & Von Recum, H.A. (2008). Electrospinning: Applications in drug delivery and tissue engineering. Biomaterials 29:1989–2006.

Singh, B.N., Shankar, S., & Srivastava, R.K. (2011). Green tea catechin, epigallocatechin-3-gallate (EGCG): Mechanisms, perspectives and clinical applications. Biochemical Pharmacology 82, 1807-1821.

Singh, M.K., Varun, V.K., Behera, B.K. (2011). Cosmetotextiles: State of art. Fibres and Textiles in Eastern Europe 87 (4), pp. 27-33.

Son, W.K., Youk, J.H., & Park, W.H. (2006). Antimicrobial cellulose acetate nanofibers containing silver nanoparticles. Carbohydrate Polymers 65, 430-434.

Tekin, R., Bac, N., Erdogmus, H. (2013). Microencapsulation of fragrance and natural volatile oils for application in cosmetics, and household cleaning products. Macromolecular Symposia 333 (1), pp. 35-40.

Tiarks, F., Landfester, K., Antonietti, M. (2001). Preparation of Polymeric Nanocapsules by Miniemulsion Polymerization. Langmuir, 2001, 17, 908-18.

Torres-Giner, S., Martinez-Abad, A., Ocio, M.J., Lagaron, J.M. (2010). Stabilization of a nutraceutical omega-3 fatty acid by encapsulation in ultrathin electrosprayed zein prolamine. Journal of Food Science 75, N69-N79.

Trau, D. & Renneberg, R. (2003). Encapsulation of glucose oxidase microparticles within a nanoscale layer by layer film: immobilization and biosensor applications. Biosensors & Bioelectronics, 18, 1491-499.

Vega Lugo, A.C. & Lim, L.T. (2009). Controlled release of allyl isothiocyanate using soy protein and poly(lactic acid) electrospun fibers. Food Research International, 42, pp. 933–940.

Wang, Y. & Hsieh, Y.-L. (2004). Enzyme immobilization to ultra-fi ne cellulose fibers via amphiphilic polyethylene glycol spacers. Journal of Polymer Science. Part A, Polymer Chemistry 42:4289–4299.

Wu, L., Yuan, X. & Sheng, J. (2005). Immobilization of cellulose in nanofi brous PVA membranes by electrospinning. Journal of Membrane Science 250:167–173.

Xie, J., Li, X. & Xia, Y (2008). Putting electrospun nanofibers to work for biomedical research. Macromolecular Rapid Communications 29, 1775-1792.

Youxin, L., Volland, C. & Kissel, T. (1994). In vitro degradation and bovine serum albumin release of the ABA triblock copolymers consisting of poly(L(+) lactic acid) or poly(L(+) lactic acid-co-glycolic acid) A-blocks attached to central polyoxyethylene B-blocks. Journal of Controlled Release 32:121–128.

II. OBJECTIVES

1. GENERAL AND SPECIFIC OBJECTIVES

As previously outlined in the introduction section, the development of micro- and nanoencapsulation structures have a great potential in various food-related applications. Moreover, electro-hydrodynamic processing is a simple methodology for micro- and nanocapsules production, which presents numerous advantages in this field. In this context, the general objective of this work was **the use of the electro-hydrodynamic technology for the development of micro/nanoencapsulation structures of interest in the food area.**

Specifically, two topic areas were tackled: micro/nanoencapsulation for smart packaging applications and micro/nanoencapsulation for bioactive compounds protection.

In the area of smart packaging, the aim was to develop novel heat management packaging structures through the encapsulation of phase change materials (PCMs). For this purpose, several specific objectives were planned. Initially, a selection of different PCMs was done in order to find suitable materials with phase change temperatures of interest in food preservation.

The first objective was to encapsulate the selected PCMs in a polymeric matrix. To this aim, zein (a prolamine) was initially selected as the shell material, since apart from being a food-derived renewable resource, this protein has the ability to form both fibers and capsules using electro-hydrodynamic processing, and it has good thermal and stability properties. Later on, to increase the thermal buffering capacity of the structures developed, biopolyesters were evaluated as shell matrices for encapsulation of PCMs

through electrospinning, due to the better affinity between the PCMs and these kinds of polymers.

The second topic of great interest within the food area that was addressed was the encapsulation of bioactive ingredients for functional food applications. An initial objective in this field was to optimize the development of novel micro/nanoencapsulation structures through electrospraying from food contact materials.

The next step was the encapsulation of different bioactives in selected food hydrocolloid-based matrices. Specifically a vitamin and an antioxidant were the chosen bioactives and their stability during the encapsulation process was evaluated.

Finally, a further objective was to study the stability of the bioactive-containing micro/nanocapsules against adverse conditions.

III. RESULTS AND DISCUSSION

CHAPTER I

Development of zein-based heat-management structures for smart food packaging

CHAPTER I: Development of zein-based heat-management structures for smart food packaging

ABSTRACT

In this work, novel materials with heat management properties have been developed by means of the encapsulation of a phase changing material (PCM) in a biopolymeric matrix using the electrospinning technique. This study optimizes the methodology to obtain micro-, submicro- and nanoencapsulation structures based on zein (a maize protein) and dodecane (a PCM paraffin which has a transition temperature at -10 ºC). The results demonstrate that dodecane can be properly encapsulated in the zein matrix under different conditions, although the efficiency and, thus, the heat management properties of the structures developed, change according to the encapsulation morphology and the electrospinning parameters/configuration employed. These encapsulation technologies can be of interest in the food industry in order to develop new smart packaging materials with the ability to maintain temperature control, e.g. to preserve the cold chain.

Keywords: Phase changing material (PCM), electrospinning, encapsulation, zein, paraffins, dodecane

1. INTRODUCTION

Nowadays, food industries market many products under refrigerating, chilling or freezing conditions, since low temperatures improve quality and microbial safety of foodstuffs. The preservation of the cold chain along the whole marketing period is vital to prevent the spoilage of the food products and to extend their shelf-life. Despite the efforts made by manufacturers and logistic providers, unwanted expositions to warm temperatures of the products often occur during their storage and transport from the industry to the consumers. These alterations in the cold chain can lead to detrimental changes in the food products such as crystal ice growth, acceleration of chemical reactions and/or microorganism growth. The development of energy storage systems in general and, specifically, phase changing materials (PCMs) included in the food packaging materials, could be a solution to buffer the temperature variations of the environment. PCMs are able to absorb or release energy during their melting/crystallization process and, as a consequence, they are able to increase the thermal energy storage capacity of the containers (Rentas et al. 2004).

A large number of organic and inorganic materials can be identified as PCMs from their melting temperature. However, they should also present suitable physical, chemical and kinetic properties. Paraffin compounds fulfil most of the requirements for being used as PCMs, as they are reliable, predictable and chemically inert and stable below 500ºC. They also show little volume changes on melting and have low vapor pressure in the melt form (Sharma et al. 2009). Nevertheless, PCMs, in general, present a number of drawbacks for direct practical applications, such as weak thermal stability, low thermal conductivity and the fact that some of them are liquid at ambient temperature and, thus,

are not easy to handle or to be directly incorporated into packaging structures (Fang et al. 2009). The encapsulation of the PCM in a shell material is a plausible solution to avoid all these problems. By means of encapsulation, the PCM is protected against the influences of the outside environment by a shell that increases the heat-transfer area and withstands changes in volume when phase change occurs (Alkan et al. 2011), thus increasing the potential applications of these materials. Moreover, micro-, ultrathin- (submicro-) and nanoencapsulation enhance the efficiency of this technique because these methods prevent volatile losses, allow a greater dispersion and minimize the amount of non-encapsulated product (Abhat, 1982; Jafari et al. 2008; Soottitantawat et al. 2005). Furthermore, due to their very high surface-to-volume ratio, ultrathin and nanoencapsulation structures have less impact in texture, morphology, viscosity and other physical properties of the material where they are included (Shefer & Shefer, 2003).

The electrospinning technique has proven to be a very suitable method for encapsulation and various compounds, including biomedical substances or functional food ingredients have been encapsulated in polymeric matrices by means of this versatile method (Goldberg et al. 2007; López-Rubio & Lagaron, 2012). Electrospinning makes use of high voltage electric fields to produce electrically charged jets from viscoelastic polymer solutions which on drying, by the evaporation of the solvent, produce ultrathin polymeric structures (Li & Xia, 2004). Some authors have already explored the electrospinning technique for the encapsulation of paraffins in various polymeric matrices. For instance, Arecchi et al. (2010) encapsulated up to 15% n-hexadecane in polyvinylalcohol (PVA) and McCann and coworkers (2006) combined melt electrospinning with coaxial electrospinning to encapsulate n-hexadecane, n-octadecane and n-

eicosane in a composite matrix which consisted on titanium dioxide and polyvinylpyrrolidone (TiO2-PVP). Nevertheless, it is worth mentioning that, to the best of our knowledge, there is no report on the encapsulation of a paraffin with a phase transition below 0 ºC using electrospinning.

Another important drawback for the practical application of PCMs is what is called the "supercooling effect" which produces a delay in the crystallization temperature of the material, causing a difference between the melting and the crystallization temperatures. One of the strategies devised to reduce this supercooling phenomenon, consists on the addition of a nucleating agent which facilitates crystallization of the PCM and, therefore, brings it closer to the melting temperature. Some authors have already studied this effect and, for instance, Yamagishi et al. (1996) selected tetradecanol for preventing the supercooling of microencapsulated n-tetradecane; Kishimoto et al. (1995) found that 1-pentadecanol was able to prevent the supercooling of microencapsulated n-pentadecane and Huang et al. (2010) selected a paraffin with a higher freezing point than those of the target paraffin to limit the supercooling effect in PCM emulsions. The aim of this work was to develop, optimize and characterize zein-based encapsulation structures containing a paraffin as novel PCM material for food packaging applications. A patent application has been recently filed on the method for obtaining such encapsulation and composite structures (P201131063 Patent Application, 2011). Zein is a prolamine, the major storage protein of corn, which comprises about 45-50% of its protein content. Zein was selected as the shell material because, apart from being a food-derived renewable resource, this protein has the ability to form both fibers and capsules using electrospinning, and it has good thermal and stability properties (Torres-Giner et al. 2008). The paraffin

selected in this work was dodecane ($C_{12}H_{26}$), since it has a melting point around -10 ºC which could be useful to keep the temperature constant in frozen food during storage and transport. No toxicity is expected, since paraffins are allowed to be used in contact with foodstuffs. Nevertheless, as this material is going to be encapsulated inside zein, it will not be in direct contact with food. Moreover, for optimization of the zein/dodecane micro-, submicro- and nanostructures and with the aim of reducing the supercooling of the encapsulated PCM, different substances such as nanoclays, other paraffins or fatty alcohols were added to the formulation for optimal encapsulation efficiency.

2. MATERIALS AND METHODS

2.1 Materials

Zein from corn (grade Z3625, 22–24 kDa), n-dodecane, n-tetracosane, dodecanol, Tween-20, Tween-80 and Span-20 were purchased from Sigma-Aldrich (Madrid, Spain). Ethanol of 96% v/v purity was purchased from Panreac (Barcelona, Spain). All products were used as received without further purification. A food contact compliant commercial laminar phyllosilicate grade termed O2block AC11 (from now on nanoclay AC11) based on modified mica was kindly supplied in powder form by NanoBioMatters S.L. (Paterna, Spain).

2.2 Electrospinning

Electrospun zein micro-, submicro- and nanostructures (fibers and capsules) were prepared based on previous results from the group (Torres-Giner, et al. 2008). Briefly, zein was dissolved in an 85 wt.-% aqueous-ethanol solution at room temperature to produce a 33 wt.-% zein solution to form fibers or a 12 wt.-% zein solution to obtain capsules or beads. The solutions were introduced in a glass syringe and were electrospun under a steady flow-rate using a stainless-steel needle. The needle was connected through a PTFE wire to the syringe. The syringe was lying on a digitally controlled syringe pump while the needle was in horizontal towards an aluminum-covered copper grid used as a collector. The electrospinning apparatus was equipped with a variable high voltage 0–30 kV power supply and the electrospinning conditions were the following: 0.30 mL/h flow-rate, 15 kV voltage and 10 cm tip-to-collector distance. Taking these initial parameters as standard, different conditions were tested to generate an optimum heat management material.

Initially, uniaxial electrospinning was assayed. In this case, dodecane was added to the standard zein solutions in different weight concentrations to optimize the amount of dodecane which remained retained in the final encapsulated system. The zein:dodecane mass percentages tested were: 90:10, 70:30, 50:50 and 30:70. Moreover, a 10% of different emulsifiers (Tween-20, Tween-80 or Span-20) with respect to the PCM were added to the system to try to improve the dispersion of the paraffin in the polymeric solution.

Coaxial electrospinning was also investigated. In this case, two separated systems were prepared: (I) 33% zein standard solution and (II) n-dodecane. They were introduced in different syringes and connected to different needles which were placed concentrically. The zein solution was pumped through the outer needle to form the shell material, while n-dodecane was circulated through the inner needle to form the core material. In order to facilitate the encapsulation of the PCM, the electrospinning conditions were changed to get thicker fibers. Specifically, a tip-to-collector distance of 5 cm was used. The power voltage used was kept at 15 kV, the zein flow-rate was increased up to 0.9 mL/h and 3 different n-dodecane flow rates were studied (0.15, 0.3 and 0.45 mL/h).

Once the optimum heat management system was selected, a 5 wt.-% of a nucleating agent (AC11, tetracosane or dodecanol) with respect to the total amount of n-dodecane was included in the electrospinning solutions.

2.3 Characterization of the solution properties

The viscosity and surface tension of the various zein/dodecane solutions were characterized before the electrospinning process. The viscosity of the solutions

was measured using a rotational viscosity meter Visco Basic Plus L from Fungilab S.A. (San Feliu de Llobregat, Spain) using a Low Viscosity Adapter (spindle LCP). The surface tension was measured using the Wilhemy plate method in a EasyDyne K20 tensiometer (Krüss GmbH, Hamburg, Germany). Both measurements were done at 25ºC.

2.4 Scanning electron microscopy (SEM)

The morphology of the electrospun structures was examined using scanning electron microscopy (SEM) on a Hitachi microscope (Hitachi S-4100) after sputtering the encapsulation structures with a gold–palladium mixture under vacuum. All SEM experiments were carried out at an accelerating voltage of 10 kV. The diameters of the electrospun materials were measured by means of the Adobe Photoshop CS4 software from the SEM micrographs in their original magnification. Specifically, 250-300 capsule diameters were measured and the size distribution is given.

2.5 Differential scanning calorimetry (DSC)

DSC analyses of the materials were performed on a Perkin Elmer DSC 7 applying various heating-cooling cycles from -40ºC to 10ºC in a nitrogen atmosphere using a refrigerating cooling accessory (Intracooler 2, Perkin Elmer, US). Pure dodecane and the obtained electrospun materials were analysed without any previous treatment. Scanning rates of 2, 5 and 10ºC/min were tested in order to observe the influence of this parameter in the thermal properties. The amount of material used for the DSC experiments was adjusted so as to have a theoretical dodecane content of, approximately, 2 mg. The enthalpy results obtained were, thus, corrected according to this PCM content.

2.6 Attenuated total reflectance infrared spectroscopy

ATR-FTIR spectra were collected at different temperatures coupling the low temperature Golden Gate Diamond ATR system (Specac, UK) to a FTIR Tensor 37 equipment (Bruker, Germany). The temperature was controlled by the 4000 Series High Stability Temperature Controller accessory (Specac, UK) and the spectra were collected in the different materials by averaging 7 scans at 4 cm^{-1} resolution.

3. RESULTS AND DISCUSSION

3.1 Characterization of uniaxial electrospun structures

3.1.1 Solution properties and morphology of the obtained structures

Initially, both zein fibers and capsules (beads) were developed through uniaxial electrospinning containing different amounts of n-dodecane. As the paraffin was dispersed in the solvent used for electrospinning the maize protein, dispersions containing both components were prepared and characterized before electrospinning. It should be noted that when high amounts of dodecane were added to the solutions, it was not possible to obtain a homogeneous dispersion of the paraffin even when emulsifying agents such as Tween-20, Tween-80 or Span-20, were added to the solution (data not shown), fact that could compromise the proper encapsulation of the PCM. The viscosity and surface tension of the various dispersions studied are compiled in Table 1.

Table 1. Viscosity (μ) and surface tension (σ) of the different solutions used for electrospinning.

Fibers[1]			**Beads**[2]		
Zein:Dodecane	μ (cP)	σ (mN/m)	Zein:Dodecane	μ (cP)	σ (mN/m)
100:0	239.48 ± 7.50	25.97 ± 0.06	100:0	8.41 ± 0.01	24.97 ± 0.15
90:10	264.01 ± 4.84	25.77 ± 0.06	90:10	8.77 ± 0.08	24.87 ± 0.06
70:30	366.86 ± 12.88	26.10 ± 0.10	70:30	10.06 ± 0.09	25.03 ± 0.15
50:50	452.24 ± 10.71	26.53 ± 0.15	50:50	11.70 ± 0.11	25.43 ± 0.05
30:70	476.87 ± 6.96	26.67 ± 0.06	30:70	18.54 ± 0.07	25.70 ± 0.17
0:100	1	24.7 ± 0.00	0:100	1	24.7 ± 0.00
Solvent	1	24.47 ± 0.06	Solvent	1	24.47 ± 0.06

[1]: structures obtained from a solution containing 33% of zein in weight; [2]: structures obtained from a solution containing 12% of zein in weight.

As expected, lower viscosity values were obtained when the zein concentration was reduced to 12 wt.-% in the formulations. From Table 1, it can be observed that the viscosity of the emulsions increases with the PCM content, as this parameter depends on the solid concentration which rises with the addition of the paraffin. As lower solution viscosity favors the formation of thinner fibers (Torres-Giner et al. 2008) and also to the formation of beads (Fong et al. 1999), the average size of the encapsulation structures was expected to increase with augmented dodecane contents. However, from Figure 1 it is seen that, generally, thinner fibers were attained when 30 or 50% of PCM was added. Taking into account that the surface tension was not significantly altered in the different systems, the reduced diameter of the fibers (especially in the solution with 70:30 zein:dodecane) must be due to changes in the conductivity of the systems (Tong et al. 2012). This effect was not observed for the fibers obtained from solutions containing 70 wt.-% of dodecane, probably because for such dodecane content, the solution components were not totally mixed and part of the paraffin was phase separated and, thus, was not effectively incorporated in the fibers (as confirmed later by DSC). Moreover, higher solution concentration and highly viscous systems have been previously correlated with thicker structures and formation of thin branches (Reneker & Yarin, 2008). Both effects can be observed in the structures obtained from the solutions with 50 wt.-% or more of dodecane, which have significantly higher viscosity (cf. Figure 1 and Table 1).

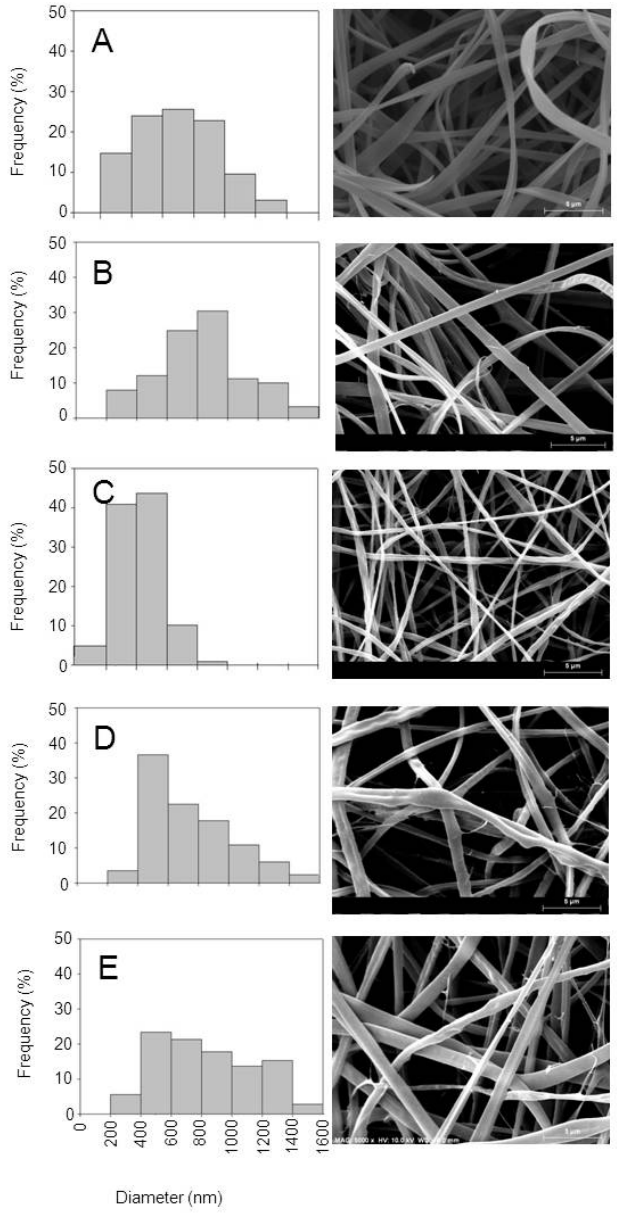

Figure 1. Selected SEM images and size distribution for fibers of zein:dodecane: a) 0:100; b) 90:10; c) 70:30 d) 50:50 and e) 30:70.

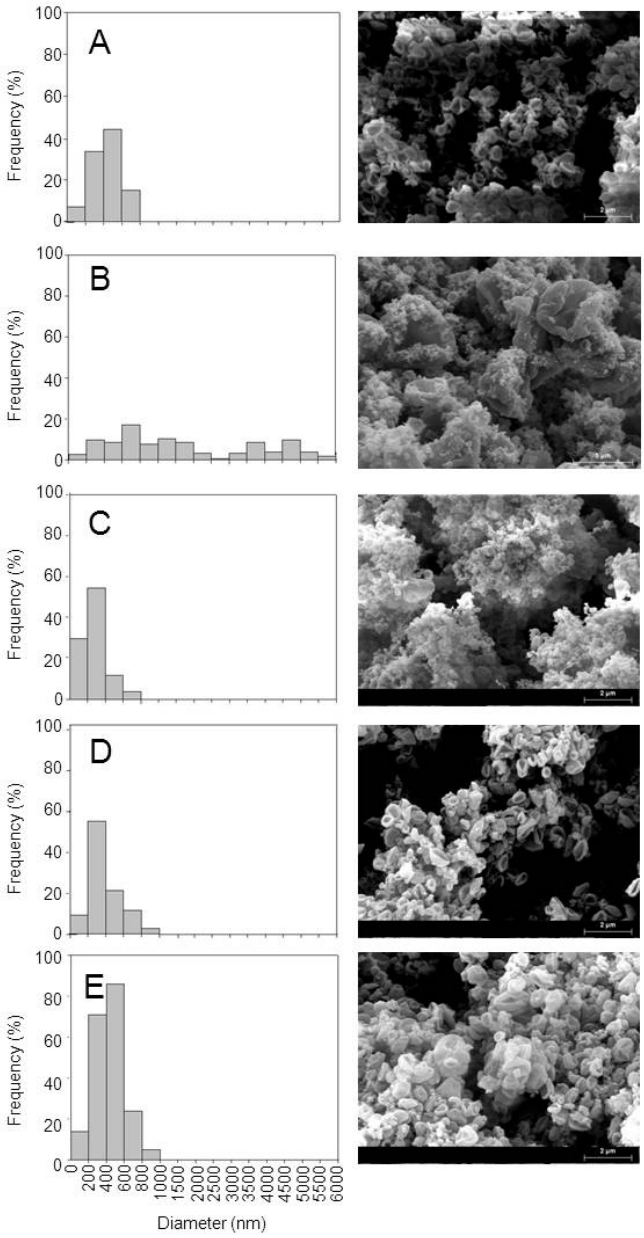

Figure 2. Selected SEM images and size distribution for fibers of zein:dodecane: a) 0:100; b) 90:10; c) 70:30 d) 50:50 and e) 30:70.

From Figures 1 and 2 it is confirmed that ribbon-like fiber networks are attained when the initial zein concentration is 33 wt.-%, while capsules or beads were produced for the 12 wt.-% zein solutions. For the lower zein concentration, which results in the formation of beads, it was observed that the structures containing more than 30 wt.-% dodecane have the same morphology as the pure zein structures, suggesting that from this concentration, the paraffin is not effectively incorporated into the structures. In this case, both components were mainly electrospun separated, as the PCM was observed to directly land on the collector. From the micrographs, it can be observed that only in the case of 10 wt.-% of n-dodecane, this PCM was effectively retained inside the zein beads, since the electrospun capsules showed significantly larger diameter in comparison with the pure zein structures.

As deduced from the morphology results, it appears that fiber-like structures are more adequate for the optimum encapsulation of large quantities of n-dodecane. DSC experiments were carried out to confirm these preliminary results.

3.1.2 Thermal properties and molecular changes of uniaxial electrospun hybrid structures

DSC and temperature scanned ATR-FTIR experiments were carried out to study the thermal behavior and potential molecular changes of the heat management structures developed. DSC was also used to ascertain the degree of PCM incorporation.

Initially, the DSC heating rate was optimized for the study of the structures. Pure n-dodecane was analyzed at the scanning rates of 2, 5 and 10 ºC/min.

From Figure 3, it is clearly seen that the supercooling effect was reduced when the sample was analyzed at 2 ºC/min, and, thus, the electrospun materials were also analyzed at this rate. However, it is worth noting that the melting and crystallization enthalpies obtained were almost unchanged with scanning rate.

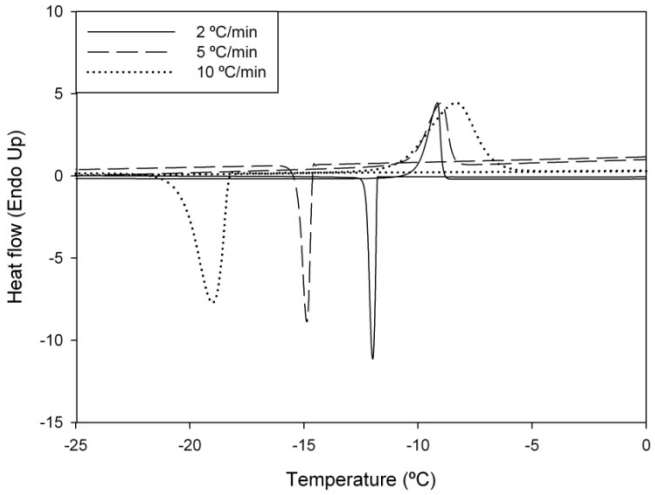

Figure 3. DSC thermograms of pure dodecane at (a) 2 ºC/min; (b) 5 ºC/min and (c) 10 ºC/min.

Table 2 shows the DSC results corresponding to the thermal characteristics of the materials obtained through uniaxial electrospinning. This table compiles the enthalpy values obtained for each scan, which have been corrected for the n-dodecane content in the polymer solution, the melting and crystallization temperatures and the peak widths. From the results, it is observed that pure dodecane melts at -9 ºC and crystallizes at -11.9 ºC in a relatively narrow temperature range having an enthalpy of 196.9 J/g.

Table 2. Thermal data collected at 2 ºC/min of the electrospun material obtained by the uniaxial technique.

Zein: Dodecane	ΔHm_1(J/g)	ΔHm_2(J/g)	Tm_1 (ºC)	Tm_2 (ºC)	ΔHc_1(J/g)	Tc_1 (ºC)	Tc_2 (ºC)	Tc_3 (ºC)	Supercooling(ºC)	
									1	2
0:100	196.88	196.88	-9	-8.9	196.88	-11.98	-	-	2.98	3.08
F-30:70	15.41 ± 1.6	14.79 ± 1.1	- 11.05 ± 0.1	-10.93 ± 0.1	-10.50 ± 2.2	-22.75 ± 0.7	- 28.24 ± 0.5	-	12.70 ± 0.7	12.83 ± 0.7
F-50:50	59.92 ± 1.7	58.78± 1.8	-9.55 ± 0.3	-9.45 ± 0.3	-53.42 ± 3.3	-16.29 ± 0.6	-20.15 ± 0.3	-27.51 ± 0.3	7.74 ± 0.4	7.84 ± 0.6
F-70:30	69.32 ± 5.5	69.13 ± 6.4	-10.16 ± 0.8	-10.29 ± 0.9	-64.53 ± 5.2	-17.81 ± 1.2	-22.08 ± 3.2	-28.55 ± 0.5	8.69 ± 1.7	8.55 ± 1.8
F-90:10	89.39 ± 2.8	87.3 ± 2.2	-11.33 ± 0.8	-11.21 ± 0.7	-84.12 ± 2.5	-21.71 ± 2.7	-25.69 ± 2.9	-31.19 ± 2.9	11.38 ± 2.2	11.50 ± 2.2
B-30:70	12.4 ± 4.0	11.27 ± 3.4	-10.22 ± 0.2	-10.12 ± 0.1	-10.60 ± 4.4	-21.02 ± 1.1	-24.41 ± 2.0	-	11.79 ± 0.9	11.89 ± 1.1
B-50:50	10.86 ± 2.4	10.78 ± 0.7	-9.78 ± 0.6	-9.73 ± 0.6	-10.63 ± 2.0	-21.92 ± 2.8	-25.16 ± 0.1	-	11.16 ± 0.2	11.22 ± 0.2
B-70:30	17.32 ± 0.7	15.28 ± 0.4	-10.56 ± 0.1	-10.37 ± 0.1	-12.44 ± 1.5	-21.40 ± 0.6	-26.77 ± 0.1	-	11.84 ± 0.5	12.03 ± 0.5
B-90:10	30.06 ± 21.9	27.32 ± 21.17	-10.70 ± 0.8	-10.68 ± 0.6	-25.27 ± 15.7	-24.25 ± 4.8	-26.35 ± 0.8	-32.73 ± 2.8	12.24 ± 1.0	12.18 ± 1.0

ΔHm1: melting enthalpy during the first heating scan; ΔHm2: melting enthalpy during the second heating scan; Tm1 and Tm2: melting temperatures during the first and the second heating scans respectively; ΔHc: crystallization enthalpy; Tc1, Tc2, Tc3: crystallization temperatures.

The melting and crystallization of pure dodecane can also be followed using ATR-FTIR, as there are specific spectral changes which correlate with conformational changes of the paraffins during the phase transitions (Gnatyuk, et al. 2007). Dodecane crystallization is mainly characterized by factor group splitting at 2957 cm^{-1} and by the appearance of a new band at 716 cm^{-1}. ATR-FTIR experiments as a function of temperature were carried out in pure dodecane to follow these conformational changes. Comparing DSC data with the results obtained using ATR-FTIR spectroscopy, it was observed that the melting temperature obtained by both techniques match (results not shown). During the heating scan, the doublet formed in the solid state of the paraffin turned into a single band at -9 ºC. Moreover, the intensity of the band observed at 716 cm^{-1} decreased continuously, as the melting of the paraffin occurred. However, the crystallization temperatures were slightly different. While through DSC the onset of crystallization was seen at -11.77 ºC, through FTIR, the splitting of the band at 2957 cm^{-1} into two components, at 2952 and 2959 cm^{-1} (factor group splitting), as well as the appearance of the band at 716 cm^{-1}, which suggests that the onset of crystallization takes place at -7ºC (cf. Figure 4). Discrepancies between DSC data and FTIR results can be explained because the spectroscopic technique is able to identify conformational changes associated to the crystallization process which are not as easily detectable by DSC. The existence of a unique band at 716 cm^{-1} for crystalline dodecane indicates that the solid paraffin presents the triclinic structure typical of even numbered n-paraffins with $n \leq 26$ (Gnatyuk et al., 2007).

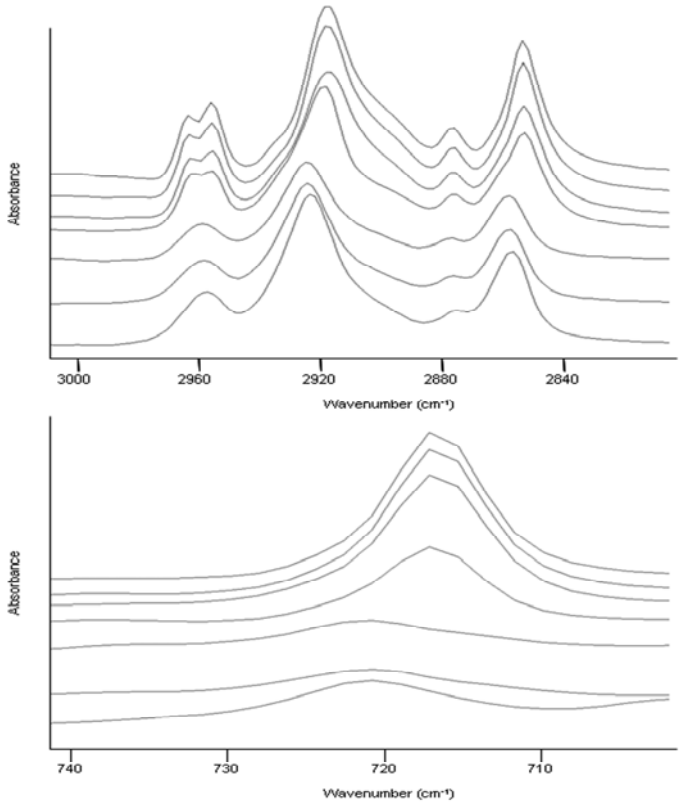

Figure 4. Crystallization spectra of pure dodecane obtained at various temperatures: From bottom to top: to top are 10, 5, 0, -7, -10, -15 and -20 ºC.

In the case of the encapsulated material, Table 2 also shows that when the PCM was incorporated into the different electrospun zein structures, lower melting points were observed and the melting and crystallization peaks of the hybrid structures became broader. Lower melting temperatures can be due to smaller or more imperfect crystals formed within the zein matrix. Both situations can take place in the developed materials as the small size of the encapsulation structures can either

lead to smaller crystals or somehow hinder the proper crystallization of the paraffin, creating more defective crystals (Nichols & Robertson, 1992). The lower melting temperature derived from smaller crystals has also been observed for paraffin miniemulsions (Gülseren & Coupland, 2007; Montenegro et al. 2003; Montenegro & Landfester, 2003).

The encapsulation efficiency of dodecane in the different electrospun zein structures was defined as the experimental melting enthalpy obtained for each of the hybrid materials divided by the DSC enthalpy value of the pure dodecane existing in the polymer solution. In accordance with the morphological results, Table 3 shows that the yield was considerably better in fibers than in beads and it was also better when the initial amount of the PCM was lower, probably because it was easier to generate the encapsulation structures when the biopolymer concentration was higher. From the results it can be concluded that the greatest encapsulation efficiency was obtained for the 90:10 and 70:30 zein:dodecane fibers which contained ~5 wt% and 10 wt% of PCM, respectively.

Table 3. Encapsulation efficiency and percentage of encapsulated dodecane in the various electrospun structures.

	Zein: Dodecane	**Efficiency (%)**	**Dodecane (%)**
Dodecane	0:100	100	100
Fibers	F-30:70	7.78 ± 1.15	4.64 ± 6.25
	F-50:50	30.42 ± 1.19	14.62 ± 15.81
	F-70:30	35.10 ± 3.92	9.35 ± 11.71
	F-90:10	45.38 ± 2.03	4.33 ± 4.74
Beads	B-30:70	5.96 ± 2.89	2.15 ± 6.19
	B-50:50	5.38 ± 1.72	1.83 ± 3.55
	B-70:30	8.79 ± 0.49	2.49 ± 2.78
	B-90:10	10.45 ± 15.74	1.45 ± 2.61

In order to have better sensitivity to detect the conformational changes occurring during the phase transition, the 70:30 zein:dodecane fibers were selected to carry out the temperature scanned ATR-FTIR experiments. As it was seen using DSC, the FTIR results also showed that the melting process started at a lower temperature than in the bulk PCM (results not shown). It was observed that the doublet at 2954 and 2960 cm^{-1} disappeared at -11 ºC while the band at 716 cm^{-1} continuously reduced its intensity until it disappeared.

Regarding the crystallization, from Table 2 it can be observed that the supercooling effect is more severe in the encapsulated material than in the pure dodecane. For the hybrid materials, supercooling exceeded 10 ºC, whereas for non-encapsulated dodecane, the difference between the melting and crystallization temperatures was just around 3 ºC. The increased supercooling degree of encapsulated dodecane could be

attributed to the smaller particle size of PCM inside the zein matrices, since the crystallization is known to be impeded when the particle diameter decreases. It has been reported that the number of nuclei for the crystallization of paraffins is reduced when the PCM drop size decreases (Yamagishi et al., 1996). Yamagishi et al. (1996) studied the melting and crystallization processes of microencapsulated n-tetradecane and n-dodecane with a melamine-formaldehyde and gelatin shell and they observed that the degree of supercooling increased when the diameter was lower than 100 μm which is the case of the fibers and beads obtained in the present work. Besides, in some cases, a multiple crystallization process was observed and up to three different crystallization temperatures were clearly present in the thermograms (Tc1, Tc2 and Tc3). This fact has been attributed to what is called the rotator phase transition. A rotator phase is defined as lamellar crystals which exhibit long-range order in the molecular axis orientation and center-of-mass position, but lack rotational degrees of freedom of the molecules about their long axis (Ungar & Masic, 1985; Kraack et al. 2000). All the odd n-alkanes between C9 and C45 undergo the rotator phase and, although it is difficult to detect in even n-alkanes below C20, it has been observed in n-octadecane and n-eicosane when these paraffins were microencapsulated (Zhang et al. 2005; Zhang et al. 2004). For all the encapsulation structures developed through uniaxial electrospinning (both fibers and beads), two or three peaks were observed on the DSC cooling curves. These peaks can be attributed to the heterogeneously nucleated liquid-rotator transition, the rotator-crystal transition and the homogeneously nucleated liquid-crystal transition, respectively. When there are two peaks, the second and the

third transitions are included in only one peak with a shoulder (Kraack et al. 2000). Conformational changes which can be related to these rotator crystalline states were also apparent in the ATR-FTIR spectra of the 70:30 zein:dodecane fibers. From Figure 5 it can be observed that, before factor group splitting, the band at 2954 cm^{-1} becomes broader at around -18 ºC, which can be related with the first crystallization peak observed through DSC (see Table 2). Furthermore, at this temperature, the band at 716 cm^{-1}, which is characteristic of triclinic crystals also appears, indicating that the PCM keeps its structure in the encapsulated systems. The absorbance of this band continuously increases along the crystallization process. The factor group splitting is observed at -27 ºC, which is an intermediate temperature between the other two rotator states identified by DSC. However, it should be emphasized that at this specific wavenumber where the factor group splitting occurs, there is some contribution from the encapsulating material, which could mask the follow up of the conformational changes taking place. At this point, it should be stressed that multiple crystallization points can also have advantages, since heat storage can take place over a broader temperature range, hence allowing the tailoring of the heat management process.

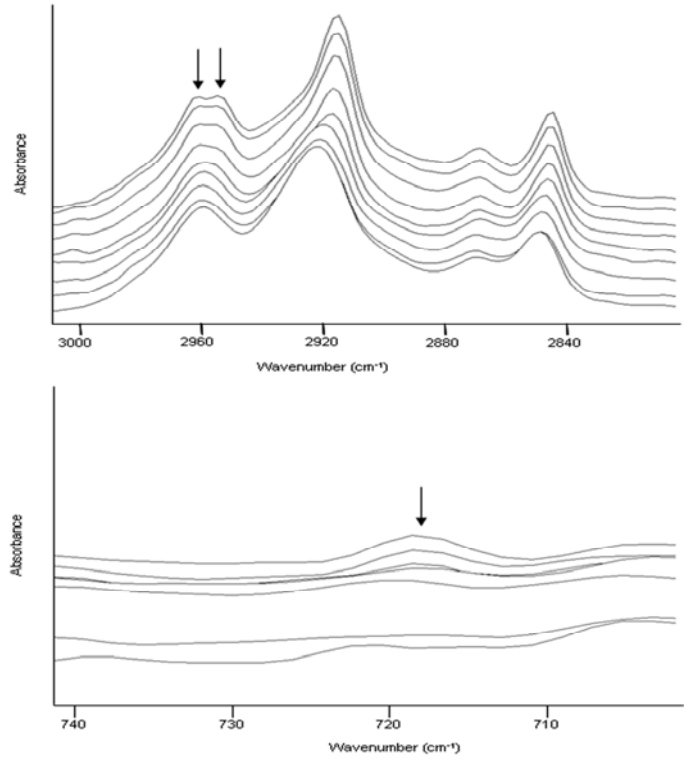

Figure 5. Crystallization spectra of zein-dodecane fibers obtained by uniaxial technique. Corresponding temperatures from bottom to top are 10, 0, -10, -15, -18, -23, -27, -35 and -40 ºC.

3.2 Incorporation of n-dodecane through coaxial electrospinning

Due to the difficult dispersion of the PCM in the biopolymeric solution and to try to alter the multiple crystallization behavior of the samples obtained by uniaxial electrospinning, the coaxial methodology was assayed. With the coaxial technique, both components were pumped through two independent circuits and they flew through two

concentrically mounted needles. The paraffin was incorporated as core material through the inner needle, whereas the biopolymer was introduced as shell material through the outer one. Thus, the problem with the poor dispersion of the dodecane in the zein solution observed in the uniaxial structures should be avoided. The optimum electrospinning conditions in terms of PCM encapsulation were initially investigated. Different tip-to-collector distances and different zein flow rates were studied and it was found that the greatest encapsulation efficiency was attained at a tip-to-collector distance of 5 cm and with 0.9 mL/h for the zein flow rate. Keeping fixed these parameters, different dodecane flow rates were examined as explained below.

3.2.1 Morphology of coaxially electrospun zein-dodecane fibers

For coaxial electrospinning, zein and dodecane were introduced separately in the equipment. In this case there were more noticeable differences between pure zein and zein-dodecane composite fibers, since for the latter the average diameter exceeded 1 μm probably because in these cases the tip-to-collector distance was reduced. Figure 6 shows selected SEM images of coaxially electrospun fibers. It was seen that uniform structures were attained when the flow rate of zein was six or three times that of n-dodecane. When the PCM flow rate was increased to 0.45 mL/h, the size distribution of the fibers was more irregular and, thus, very thick fibers most likely containing more of the encapsulated paraffin coexisted with thinner zein fibers.

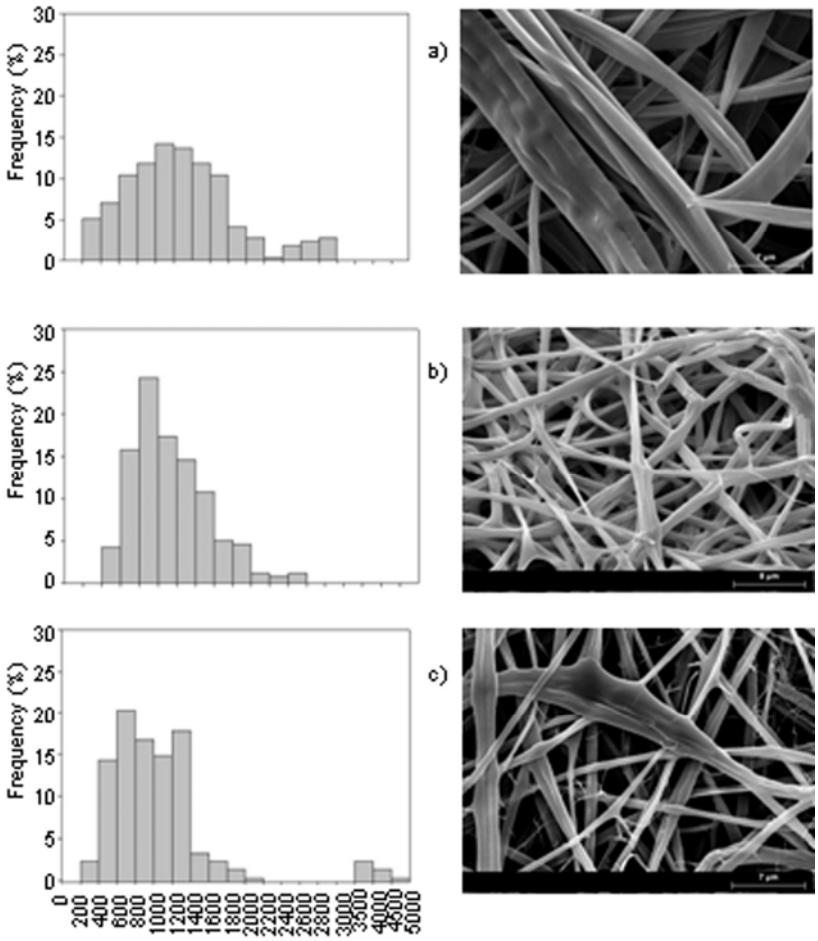

Figure 6. Selected SEM images and size distribution for coaxial fibres of zein:dodecane rates: a) 6:1; b) 3:1 c) 2:1.

3.2.2 Thermal properties of coaxially electrospun zein-dodecane fibres

Table 4 presents the thermal properties of the coaxially electrospun hybrid fibres obtained by DSC. From the results, it can be observed that only the structures obtained with a flow-rate of zein:dodecane of 3:1 were able to encapsulate a considerable amount of PCM. An

encapsulation efficiency of approximately 55% was observed for these structures, which corresponds to around 14 wt.-% of dodecane encapsulated that was able to storage 27.55 J/g. Other authors who have encapsulated paraffins in polymeric compounds have obtained similar results, i.e. between 5 and 15% of hexadecane was introduced inside poly(vinyl alcohol) (PVA) nanofibers (Arecchi et al. 2010). For the zein:dodecane structures obtained with a flow rate of 6:1, the enthalpy was almost negligible, probably because the PCM flow rate was too low compared to that of the biopolymer solution. In the case of the structures obtained with a flow rate zein:dodecane of 2:1, the PCM was irregularly encapsulated, as it was suggested by the SEM micrographs. In this latter case, the enthalpy of the structures was uneven amongst the DSC experiments. Nevertheless, for the various tested conditions, the thermal data showed that the crystallization process occurred in only one peak, that is, the rotator phase transition did not take place in these structures. This could be explained by the fact that the sizes of the coaxial fibres were bigger than those of the uniaxial electrospun fibres and moreover, in this case the paraffin was not incorporated in an emulsion, but it was introduced from the bulk product, so that the crystallization behavior was more similar to that of pure dodecane.

Table 4. Thermal data collected at 2 ºC/min of the electrospun materials obtained by the coaxial technique

Zein:Dodecane mass rates	ΔHm_1(J/g)	ΔHm_2(J/g)	Tm_1 (ºC)	Tm_2 (ºC)	ΔHc_1(J/g)	Tc (ºC)	Supercooling (ºC)	
							1	2
6:1	0.262 ± 0.28	0.230 ± 0.22	-9.80 ± 0.46	-9.77 ± 0.41	-0.238 ± 0.31	-18.96 ± 6.52	10.61 ± 1.65	10.66 ± 1.72
3:1	107.718 ± 2.62	107.942 ± 2.48	-8.17 ± 0.71	-8.19 ± 0.76	-103.628 ± 0.63	-14.48 ± 0.88	6.31 ± 0.18	6.29 ± 0.12
2:1	60.501 ± 45.13	61.198 ± 44.88	-9.05 ± 0.92	-9.0 ± 0.93	-58.299 ± 43.97	-16.47 ± 4.83	7.56 ± 0.94	7.60 ± 0.93

ΔHm1: melting enthalpy during the first heating scan; ΔHm2: melting enthalpy during the second heating scan; Tm1 and Tm2: melting temperatures during the first and the second heating scans respectively; ΔHc: crystallization enthalpy; Tc: crystallization temperature.

In comparison with the most efficient uniaxial structures, it was observed that the encapsulation efficiency of the process, as well as the total amount of PCM encapsulated increased when the coaxial methodology was used. Moreover, in the coaxial structures, the supercooling effect was reduced to ca. 6 ºC and the crystallization occurred in a single peak, whereas the more efficient uniaxial encapsulation structures had a supercooling effect of around 10 ºC and presented multiple crystallization peaks (compare Table 2 and 4). Hence, for the development of a heat-management structure through electrospinning using a zein matrix, the coaxial technique seems more suitable for the encapsulation of an organic PCM.

3.3 Incorporation of nucleating agents in the coaxial structures

In order to further reduce the supercooling effect in the optimized structures, several nucleating agents were added to the paraffin. Specifically, the nucleating effect of the nanoclay AC11, tetracosane, and dodecanol was studied. These substances are solid at the crystallization temperature of dodecane and, thus, they are able to act as first nuclei for the crystallization. Figure 7, shows the supercooling degree of the pure PCM and the PCM-nucleating agents assayed. It is observed that all substances caused a decrease of the supercooling, although the most effective compounds were the paraffin and the fatty alcohol.

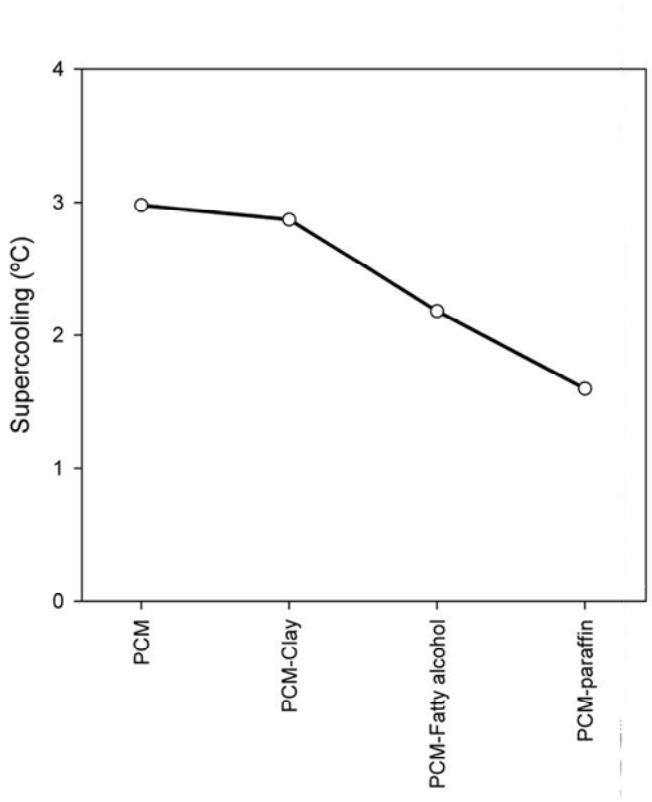

Figure 7. Supercooling degree in the pure PCM as a function of the nucleating agent used.

The different nucleating agents were also studied in the encapsulated systems. They were incorporated within the electrospun fibres using the uniaxial configuration with the mass rate 70:30 zein:dodecane and the coaxial configuration at a flow rate zein:dodecane of 3:1, since it was seen that, amongst all the tested conditions and compositions, these structures were the most suitable in terms of encapsulation efficiency and total amount of encapsulated dodecane. Regarding the uniaxial

structures, from Table 5 it can be observed that the rotator phase was also present in the additivated structures and that the most efficient nucleating agent for the encapsulated systems was the paraffin, as it was for the pure dodecane. In this case, the supercooling effect was reduced up to approximately 4ºC, whereas the fibres without nucleating agents showed a supercooling effect of around 9ºC. For the coaxial structures it was observed that, again, tetracosane was the most effective agent, reducing the supecooling to less than 3ºC, which is the value that presented the non-encapsulated dodecane (2.98ºC). It was also observed that addition of dodecanol caused a two-step crystallization of the paraffin. The first exothermic peak probably corresponded to the heterogeneous crystallization as a consequence of the addition of the nucleating agent, while the second peak corresponded to the homogeneous crystallization and it matched with the crystallization temperature of the coaxial structures without dodecanol. During the first transition, almost 10% of the total heat of the material was released with little supercooling. Finally, the nanoclay did not cause any improvement of the supercooling and, thus, it was not an efficient nucleating agent for these systems. From these results, it can be concluded that the coaxial fibers generated at a flow rate zein:dodecane of 3:1 and with the addition of a 5% of tetracosane into the PCM were the optimum structures, since they were able to encapsulate dodecane and to reduce the supercooling effect to the same value of the non-encapsulated PCM.

Table 5. Thermal data of the hybrid electrospun materials with nucleating agents

Fiber	Nucleating Agent	Tm (ºC)	Tc (ºC)	Tc2 (ºC)	Tc3 (ºC)	Supercooling (ºC)
Uniaxial electrospun fibers Zein:dodecane 70:30	-	-10.16 ± 0.8	-17.81 ± 1.2	-22.08 ± 3.2	-28.55 ± 0.5	8.69 ± 1.7
	AC11	-9.45 ± 0.3	-15.41 ± 1.0	-21.72 ± 0.2	-28.57 ± 0.2	5.96 ± 1.2
	Tetracosane	-10.37 ± 0.1	-14.42 ± 0.3	-28.31 ± 1.1	-34.22 ± 0.1	4.06 ± 0.4
	Dodecanol	-10.54 ± 0.1	-18.97 ± 0.6	-23.37 ± 0.1	-28.63 ± 0.5	8.44 ± 0.5
Coaxial electrospun fibers zein:dodecane mass rate 3:1	-	-8.17 ± 0.7	-14.48 ± 0.9	-	-	6.31 ± 0.2
	AC11	-9.44 ± 1.3	-19.28 ± 3.4	-	-	9.84 ± 4.7
	Tetracosane	-9.38 ± 0.1	-12.31 ± 0.3	-	-	2.93 ± 0.2
	Dodecanol	-9.59 ± 0.6	-13.02 ± 1.4	-15.23 ± 0.4	-	3.43 ± 0.8

Tm: melting temperature; Tc1, Tc2, Tc3: crystallization temperatures.

3.4 Stability of the optimized structures

The thermal stability of the optimized encapsulation zein:dodecane structures containing tetracosane was studied along repeating DSC thermal cycles. Figure 8 shows the DSC curves of the structures during 20 heating-cooling cycles. It is observed that both transition temperatures were unmodified after 20 thermal cycles and the enthalpies of the material were almost unchanged, i.e. for the first scan the melting enthalpy was 34.48 kJ/kg and for the 20th cycle, it was 30.67 kJ/kg. Thus, it can be concluded that the thermal reliability of the structures after thermal cycling is appropriate for energy storage applications.

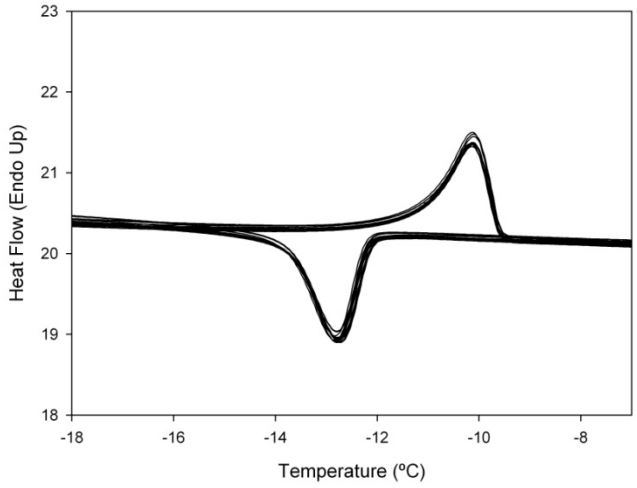

Figure 8. DSC thermogram of thermal cycled coaxial fibres of zein:dodecane obtained at a mass rate of 3:1 with tetracosane.

4. CONCLUSIONS

In this study, the encapsulation of dodecane inside zein micro-, submicro and nanostructures in order to obtain heat management materials with potential application in food biopackaging was developed and optimized by means of the electrospinning technique. For the uniaxial systems, different morphologies were obtained by modifying the polymer concentration, although the fibres seemed to be more appropriate for encapsulation applications, since the encapsulation efficiency, as well as the total amount of PCM encapsulated, were higher than for the capsule-like morphologies. DSC and FTIR results confirmed the proper encapsulation of the PCM within the zein electrospun structures. In all cases, a rotator phase transition was observed and, thus, a multiple crystallization process was detected in the uniaxially electrospun structures. However, when the coaxial methodology was used, the efficiency increased by up to ca. 55 wt.-% and the crystallization behaviour of the PCM was more similar to the bulk product. Moreover, when a nucleating agent (tetracosane) was added to the PCM, there was a decrease in the supercooling effect of the encapsulates, which became similar to that exhibited by the pure dodecane. Based on the results, it can be concluded that it is difficult to encapsulate great amounts of a paraffin PCM inside zein structures through uniaxial electrospinning, probably because of their different polarity and lack of affinity. Nevertheless, the coaxial electrospinning configuration allows better efficiencies and materials which can storage around 25 J/g were obtained.

5. REFERENCES

Abhat, A. (1982). Low temperature latent heat thermal energy storage system: heat storage materials. Solar Energy, 30 313-332.

Alkan, C., Sari, A., & Karaipekli, A. (2011). Preparation, thermal properties and thermal reliability of microencapsulated n-eicosane as novel phase change material for thermal energy storage. Energy Conversion and Management, 52(1), 687-692.

Arecchi, A., Mannino, S., & Weiss, J. (2010). Electrospinning of poly(vinyl alcohol) nanofibres loaded with hexadecane nanodroplets. Journal of Food Science, 75(6), N80-N88.

Fang, G., Li, H., Yang, F., Liu, X., & Wu, S. (2009). Preparation and characterization of nano-encapsulated n-tetradecane as phase change material for thermal energy storage. Chemical Engineering Journal, 153(1-3), 217-221.

Fong, H., Chun, I., & Reneker, D. H. (1999). Beaded nanofibres formed during electrospinning. Polymer, 40(16), 4585-4592.

Gnatyuk, I. I., Platonova, N. V., Puchkovskaya, G. A., Kotelnikova, E. N., Filatov, S. K., Baran, J., & Drozd, M. (2007). Polymorphic transformations of C26H54 and C 28H58 n-paraffins as typical rotator substances. Journal of Structural Chemistry, 48(4), 654-665.

Goldberg, M., Langer, R., & Jia, X. (2007). Nanostructured materials for applications in drug delivery and tissue engineering. Journal of Biomaterials Science, Polymer Edition, 18(3), 241-268.

Gülseren, I., & Coupland, J. N. (2007). The effect of emulsifier type and droplet size on phase transitions in emulsified even-numbered n-alkanes. JAOCS, Journal of the American Oil Chemists' Society, 84(7), 621-629.

Huang, L., Günther, E, Doetsch, C., & Mehling, H. (2010). Subcooling in PCM emulsions-Part 1: Experimental. Thermochimica Acta 509(2010) 93-99.

Jafari, S. M., Assadpoor, E., He, Y., & Bhandari, B. (2008). Re-coalescence of emulsion droplets during high-energy emulsification. Food Hydrocolloids, 22(7), 1191-1202.

Kishimoto, A., Setoguchi, T., Yoshikawa, M., & Nakahira, T. (1995) Proceedings of 16th Japan Symposium on Thermophysical Properties (pp. 223). Japan.

Kraack, H., Sirota, E. B., & Deutsch, M. (2000). Measurements of homogeneous nucleation in normal-alkanes. Journal of Chemical Physics, 112(15), 6873-6885.

Li, D., & Xia, Y. (2004). Electrospinning of nanofibres: Reinventing the wheel? Advanced Materials, 16(14), 1151-1170.

López-Rubio, A., & Lagaron, J. M. (2012) Whey protein capsules obtained through electrospraying for the encapsulation of bioactives. Innovative Food Science and Emerging Technologies. In press. DOI 10.1016

McCann, J. T., Marquez, M., & Xia, Y. (2006). Melt coaxial electrospinning: A versatile method for the encapsulation of solid materials and fabrication of phase change nanofibres. Nano Letters, 6(12), 2868-2872.

Montenegro, R., Antonietti, M., Mastai, Y., & Landfester, K. (2003). Crystallization in miniemulsion droplets. Journal of Physical Chemistry B, 107(21), 5088-5094.

Montenegro, R., & Landfester, K. (2003). Metastable and stable morphologies during crystallization of alkanes in miniemulsion droplets. Langmuir, 19(15), 5996-6003.

Nichols, M.E. & Robertson,, R.E. (1992). The origin of multiple melting endotherms in the thermal analysis of polymers. Journal of Polymer Science. Part B: Polymer Physics, 30(3), 305-307.

P201131063 Patent Application (2011). Procedimiento de encapsulación de PCMs. Inventors: Lagaron, J. M., Perez-Masia, R., & Lopez-Rubio, A. Holder entity: CSIC.

Reneker, D. H., & Yarin, A. L. (2008). Electrospinning jets and polymer nanofibres. Polymer, 49(10), 2387-2425.

Rentas, F. J., Macdonald, V. W., Houchens, D. M., Hmel, P. J., & Reid, T. J. (2004). New insulation technology provides next-generation containers for "iceless" and lightweight transport of RBCs at 1 to 10°C in extreme temperatures for over 78 hours. Transfusion, 44(2), 210-216.

Sharma, A., Tyagi, V. V., Chen, C. R., & Buddhi, D. (2009). Review on thermal energy storage with phase change materials and applications. Renewable and Sustainable Energy Reviews, 13(2), 318-345.

Shefer, A., & Shefer, S. (2003). Novel encapsulation system provides controlled release of ingredients. Food Technology, 57(11), 40-42.

Soottitantawat, A., Bigeard, F., Yoshii, H., Furuta, T., Ohkawara, M., & Linko, P. (2005). Influence of emulsion and powder size on the stability of encapsulated D-limonene by spray drying. Innovative Food Science and Emerging Technologies, 6(1), 107-114.

Tong, H-W., Zhang, X., Wang, M. (2012). A new nanofibre fabrication technique based on coaxial electrospinning. Material letters, 66(1), 257-260.

Torres-Giner, S., Gimenez, E., & Lagaron, J. M. (2008). Characterization of the morphology and thermal properties of Zein Prolamine nanostructures obtained by electrospinning. Food Hydrocolloids, 22(4), 601-614.

Ungar, G. & Masic, N. (1985). Order in the rotator phase of n.alkanes. Journal of Physical Chemistry, 89(6), 1036-1042.

Yamagishi, Y., Sugeno, T., Ishige, T., Takeuchi, H., & Pyatenko, A. T. (1996). An evaluation of microencapsulated PCM for use in cold energy transportation medium In Energy Conversion Engineering Conference. Proceedings of the 31st Intersociety (Vol. 3, pp. 2077-2083).

Zhang, X. X., Fan, Y. F., Tao, X. M., & Yick, K. L. (2005). Crystallization and prevention of supercooling of microencapsulated n-alkanes. Journal of Colloid and Interface Science, 281(2), 299-306.

Zhang, X. X., Tao, X. M., Yick, K. L., & Wang, X. C. (2004). Structure and thermal stability of microencapsulated phase-change materials. Colloid and Polymer Science, 282(4), 330-336.

CHAPTER II

Biodegradable polyester-based heat management materials of interest in refrigeration and smart packaging coatings

CHAPTER II: Biodegradable polyester-based heat management materials of interest in refrigeration and smart packaging coatings

ABSTRACT

In this study, two biodegradable matrices, polycaprolactone (PCL) and polylactide (PLA) were used to encapsulate for the first time a phase changing material (PCM), specifically dodecane (a paraffin which has a transition temperature at -10 ºC), through the use of the electrospinning technique with the aim of developing coating materials with energy storage capacity for thermal insulation applications. The encapsulation efficiency obtained using both matrices has been studied and the different morphology, thermal properties, and molecular structure of the materials developed were characterized. Results showed that dodecane can be properly encapsulated inside both biopolymers with a submicron drop size, albeit PCL provides better encapsulation performance. A temperature mismatch between melting and crystallization phenomena (the so-called supercooling effect) was observed in the encapsulated paraffin, mainly ascribed to the reduced PCM drop size inside the fibers. Addition of dodecanol was seen to best act as a nucleating agent for the PCL/PCM and PLA/PCM structures, allowing a significant amount of heat storage capacity for these systems without supercooling. These innovative ultrathin structured biomaterials are of interest as energy storage systems to advantageously coat or wrap temperature sensitive products in refrigeration equipment and constitute smart food or medical/pharmaceutical packaging.

Keywords: Electrospinning, PLA, PCL, dodecane, phase changing material (PCM), encapsulation, heat management.

1. INTRODUCTION

The development of sustainable energy technologies has been intensified over the last years due to the continuous environmental and economic problems related to the energy sources used nowadays. In this field, phase changing materials (PCMs) can be used as energy storage materials, since they are able to absorb or release energy during their melting/crystallization processes. A large number of organic and inorganic materials can be identified as PCMs from their melting temperature. However, they should also present suitable physical, chemical and kinetic properties. Paraffin compounds fulfill most of these requirements, as they are reliable, predictable and chemically inert and stable below 500ºC. They also show little volume changes on melting and have low vapor pressure in the melt form (Sharma et al. 2009). Nevertheless, the latent thermal energy storage systems based on PCMs present some drawbacks such as their low thermal conductivity, which limits the energy that can be extracted from them. Another hurdle is their handling, since some PCMs are liquid at ambient temperature and, what is more important, they need to undergo a phase change (i.e. from liquid to solid and vice versa) at the target temperature to exert the desired functionality. Nevertheless, there are some strategies to overcome these difficulties. On the one hand, the PCMs particles' diameter can be reduced to achieve a very high ratio of surface area to volume and, hence, to increase their thermal conductivity (Alkan et al. 2011). On the other hand, the encapsulation of these particles in a solid matrix allows an easier handling of liquid PCMs.

One innovative approach to encapsulate PCMs, reducing their drop size and controlling the morphology to a submicron scale is by the electrospinning process. This technique uses high voltage electric fields to produce electrically

charged jets from viscoelastic polymer solutions. The solutions are dried, by the rapid evaporation of the solvent, producing ultrathin droplets of solid or liquid particles (core material, i.e. the PCM) which are packed into a polymeric matrix (shell material) (Li & Xia, 2004). Thus, ultrathin structures of polymers containing PCMs can be developed to obtain novel thermal storage materials with suitable thermal performances.

Another important parameter which must be controlled during PCMs performance is the so-called supercooling effect, i.e. the lag between the melting and crystallization of the PCM. Generally, supercooling involves a reduction in the crystallization temperature and, as a result, the latent heat is released at lower temperatures or over a wider temperature range than expected. A more pronounced supercooling has been observed upon micro- and/or nanoencapsulation of the energy storage materials (Yamagishi et al. 1996), fact that limits their application. Some strategies have been developed to prevent supercooling, such as addition of nucleating agents together with the PCM.

Regarding the matrices for encapsulation, different polymers and biopolymers are currently being tested. Initially, zein, the major storage protein of corn, was researched in our group as a shell material, since it is readily soluble, renewable and biodegradable and can be electrospun quite easily (Miyoshi et al. 2005; Chen et al. 2007; Jiang et al. 2007; Torres-Giner et al. 2008). Additionally, this biopolymer is a food-derived renewable resource that has the ability to form fibers and capsules with enhanced thermal stability properties using electrospinning (Fernández et al. 2009; Torres-Giner et al. 2010). For this reason, in a previous work (Perez-Masia et al. 2013), zein was chosen as the matrix to incorporate a PCM into fibers and capsules. Dodecane

($C_{12}H_{26}$) was selected as a PCM because of its advantageous properties as a paraffin and its melting point around -10 ºC, which could be useful to keep temperature constant in freezing, chilling, storage and/or transportation systems in different ambits such as food or biomedical, where products are perishable and could be deteriorated if a specific temperature is not kept. Even when only few products may have specific interest at this refrigeration temperature, these studies also serve to demonstrate the potential of the technology for other liquid PCM systems. However, due to the lack of affinity between the polymer and the PCM, one of the main conclusions of this work was that only the coaxial electrospinning configuration was suitable for this system. Additionally, zein is not currently used as a packaging material and has many proccessability issues. As alternative materials, biopolyesters have lately attracted great industrial interest because of their characteristics. They present good physical properties (when compared to other biodegradable and renewable polymers), processability, water resistance, excellent biocompatibility and commercial availability (Pamula & Menaszek, 2008; Cohn & Hotovely Salomon, 2005; Huang et al. 2004; Garkhal et al. 2007). Biopolyester-based fibrous mats obtained by electrospinning have been developed for a wide number of applications, mainly in the biomedical field for tissue engineering applications or as drug delivery systems (Haroosh et al. 2012; Wang et al. 2012; Buschle-Diller et al. 2007; Zahedi et al 2012). However, to the best of our knowledge, the use of biodegradable polyesters to develop energy storage materials has not been reported.

The aim of this study was to overcome all of the previously mentioned issues encountered when using zein as a matrix, by making use of apolar solvents, more easily processable biopolyesters and of the uniaxial electrospinning

method. Specifically, polylactic acid (PLA) and polycaprolactone (PCL) were chosen in this study as shell matrices to carry out uniaxial electrospinning encapsulation of dodecane as PCM material (Lagaron et al. 2011). The encapsulation structures developed may be introduced in packaging structures or in refrigeration equipments, in order to obtain smart packaging materials with heat management properties, able to counteract temperature fluctuations and to increase the energetic efficiency of the devices, respectively.

The morphology, the encapsulation efficiency and the thermal properties of the developed energy storage materials were studied. Moreover, in order to reduce the supercooling of the encapsulated PCM, several nucleating components were introduced in the encapsulated systems. These materials are able to act as first nuclei for dodecane crystallization and thus, facilitate this process. In particular, a nanoclay, a paraffin with a higher melting point than dodecane and a fatty alcohol were studied. Out of these, the fatty alcohol (dodecanol) was seen the most effective substance to diminish the supercooling effect in these systems, in accordance with the work carried out by other authors (Kishimoto et al. 1995; Senador et al. 2001). Additionally, a temperature-resolved ATR-FTIR methodology has been put forward to compare the behavior of the phase changes at the molecular scale with the bulk calorimetric results during the first order thermal transitions.

2. MATERIALS AND METHODS

2.1. Materials

A semicrystalline extrusion grade of polylactid acid (PLA) (Natureworks) with a D-isomer content of approximately 2% was used in this study. This biopolymer had a weight average molecular weight (Mw) of 150,000 g/mol and a number average molecular weight (Mn) of ca. 130,000 g/mol. The polycaprolactone (PCL) grade FB100 was kindly supplied in pellet form by Solvay Chemicals (Belgium). This grade had a density of 1.1 g/cm3 and a mean molecular weight of 100,000 g/mol. Dodecane and N,N-dimethylformamide (DMF) with 99% purity were purchased from Sigma-Aldrich (Spain). Trichloromethane was purchased from Panreac Quimica S.A. (Spain). Regarding the nucleating agents, a food contact compliant organomodified bentonite clay commercially marketed as O2Block from Nanobiomatters S.L. (Paterna, Spain), tetracosane ($C_{24}H_{50}$) from Sigma-Aldrich (Spain) and dodecanol from Sigma-Aldrich (Spain) were used.

2.2. Preparation of biopolyesters-PCM solutions

The electrospinning solutions were prepared by dissolving the required amount of PLA and PCL, under magnetic stirring, in a solvent prepared with a mixture of trichloromethane:N,N-dimethylformamide (85:15 w/w) in order to reach a 5% or 15% in weight (wt.-%) of PLA or PCL, respectively. Afterwards, 20 wt.-% or 45 wt.-% of PCM (dodecane) with respect to the polymer weight was added to the PLA or PCL solutions, respectively and stirred at room temperature until it was completely dissolved. For the biopolymer/PCM solutions prepared with a nucleating agent, this was firstly dissolved in the PCM under magnetic stirring before being added to the PLA or PCL solution.

2.3. Characterization of biopolyesters-PCM solutions.

The viscosity and surface tension of all the biopolymeric solutions were characterized before the electrospinning process. The viscosity was determined by a rotational viscosity meter VISCO BASIC PLUS L with a Low Viscosity Adapter (spindle LCP) from Fungilab S.A. (Spain). The surface tension was measured with a tensiometer "EasyDyne" from Krüss (Germany) using the Wilhelmy Plate method. Both measurements were done, in triplicate, at 25ºC.

2.4. Preparation of the biopolyesters-PCM fibers through electrospinning

The electrospinning apparatus, equipped with a variable high-voltage 0-30 kV power supply, was a Fluidnatek® basic setup assembled and supplied by BioInicia S.L. (Valencia, Spain). PCL/PCM or PLA/PCM solutions were introduced in a 5 mL glass syringe and were electrospun under a steady flow-rate using a stainless-steel needle. The needle was connected through a PTFE wire to the syringe. The syringe was lying on a digitally controlled syringe pump while the needle was in horizontal towards a copper grid used as collector. The electrospinning conditions for obtaining both PCM-containing biopolymer structures were optimized and fixed at 1 mL/h of flow-rate, 12.5 kV of voltage and a tip-to-collector distance of 10 cm.

2.5. Scanning Electron Microscopy (SEM)

The morphology of the electrospun fibers was examined using SEM on a Hitachi microscope (Hitachi S-4800) after having been sputtered with a gold-palladium mixture in vacuum. All SEM experiments were carried out at 5 kV. Fiber diameters were measured by means of the Adobe Photoshop CS4 software from the SEM micrographs in their original magnification.

2.6. Differential Scanning Calorimetry (DSC)

Thermal analysis of electrospun fibers were carried out on a DSC analyzer (Perkin Elmer DSC 7, US) from -40 to 10ºC in a nitrogen atmosphere using a refrigerating cooling accessory (Intracooler 2, Perkin Elmer, US). The scanning rate was 2ºC/min in order to minimize the influence of this parameter in the thermal properties. The amount of material used for the DSC experiments was adjusted so as to have a theoretical dodecane content of 1-2 mg approximately. The enthalpy results obtained were, thus, corrected according to this PCM content. Measurements were done in triplicate.

2.7. Attenuated Total Reflectance Infrared Spectroscopy (ATR-FTIR)

ATR-FTIR spectra of biopolyester fibers, pure dodecane and electrospun biopolyesters-dodecane structures were collected at different temperatures coupling the low temperature Golden Gate Diamond ATR system accessory (Specac, UK) to FTIR Tensor 37 (Bruker, Germany) equipment. Temperature was controlled by the 4000 Series High Stability Temperature Controller accessory (Specac, UK). The spectra were collected in the pressed materials from -35 to 10ºC by averaging 7 scans at 4 cm-1 resolution. The spectra obtained at room temperature (20 ºC) were collected by averaging 20 scans at 4 cm-1 resolution. The experiments were repeated twice to verify that the spectra were consistent between individual samples.

2.8. Nuclear Magnetic Resonance (NMR)

NMR analyses were done, in triplicate, in order to estimate the PCM loading in the biopolymeric fibers. Initially, a calibration curve was obtained by recording the NMR data of the pure polymeric fibers, pure dodecane and different mixtures of polymeric fibers/dodecane. Specifically, the polymer fibers:PCM

mass range of the mixtures were 90:10, 70:30 and 50:50. The materials were dissolved in deuterated chloroform (CDCl3) and subjected to the NMR analyses. The spectra were collected at 300.13 MHz (1H) in a DPX 300 equipment (Bruker, Germany) with controlled temperature (25ºC) and 128 scans. The ratio of the polymers to the paraffin was calculated from the ratio of the integration of resonance peaks which represent the polymer chains (δ of 2.40-2.25 ppm of the adjacent protons to the carbonyl group for PCL and δ of 5.30-5.00 ppm of the –CH groups for PLA) and those for dodecane (δ of 1.40-1.15 ppm of the –CH2 groups of dodecane). The calibration curves obtained were:

$$y = -11.5 \bullet \ln(x) + 24.9 \text{ (for PCL materials)} \qquad \text{Eq. (1)}$$

$$y = -12.6 \bullet \ln(x) + 14.9 \text{ (for PLA materials)} \qquad \text{Eq. (2)}$$

Where “y” was the concentration of PCM included in the fibers and “x” was the calculated ratio of the integration of resonance peaks. Then, the hybrid electrospun biopolyesters-dodecane structures were analysed using the same conditions and the dodecane loading of the fibers was estimated from the calibration curves.

2.9. Thermogravimetric analysis (TGA)

Compositional analysis of the fibers was also carried out according to the method proposed by Desai et al. (2008) using a TA Instruments model Q500 TGA. The pure polymers (PLA and PCL) and the hybrid electrospun mats were weigthed (ca. 20 mg) and heated from 20ºC to 600 ºC with a heating rate of 10 ºC/min under nitrogen atmosphere. The weight loss for the polymers and the

paraffin in the hybrid fibers was evaluated by taking the first-order derivative of the weight loss thermograms. The area under the respective degradation temperature peaks is related to the polymer/pcm content in the blends.

2.10. Statistical analysis

Statistical analysis of the data was performed through analysis of variance (ANOVA) using Statgraphics Plus for Windows 5.1 (Manugistics Corp., Rockville, Md.). Fisher's least significant difference (LSD) procedure was used at the 95% confidence level.

3. RESULTS AND DISCUSSION

3.1. Solution properties and morphology of the electrospun structures

Based on screening studies on the electrospinning of the biopolyesters, the concentrations of PCL and PLA were optimized to obtain stable hybrid fibers containing dodecane (PCM). The optimum concentrations of the biopolymers in the solutions were found out to be 15 wt.-% for PCL and 5 wt.-% for PLA. Regarding the PCM concentration incorporated in the solutions, a screening study was also done in order to optimize this parameter, and it was observed that PLA structures were not able to encapsulate large amounts of dodecane and thus, only 20 wt.-% of PCM respect to the polymer could be incorporated. On the other hand, PCL structures facilitated the encapsulation of greater amount of PCM and, thus, 45 wt.-% of dodecane respect to the polymer could be incorporated in the fibers. Higher fractions tended to destabilize the encapsulation process for the selected polymer/PCM systems. Both the viscosity and surface tension of PCL/PCM and PLA/PCM solutions play an important role in determining the range of concentrations from which continuous fibers can be obtained. Generally, at low viscosities, surface tension is the dominant factor and just beads or beaded fibers are formed, while above a critical concentration, continuous fibrous structures can be obtained, being their morphology affected by the polymer concentration in the solution (Li & Xia, 2004; Senador et al. 2001). Table 1 shows the viscosity and surface tension values of PLA/PCM and PCL/PCM solutions and for pure PCM. The viscosity of the PCL solution was over 20 times higher than the PLA one, as this physical parameter is directly related with the total solids concentration in the final solution, which was greater for the PCL solution. However, the type and the concentration of biopolymer did not significantly

affect the surface tension values. The viscosity and surface tension values of the PCM were significantly lower than those obtained for PLA and PCL solutions.

Table 1. Viscosity and surface tension values of the hybrid biopolymeric solutions and pure dodecane

Sample	Surface Tension (mN m^{-1})	Viscosity (cP)
PCL/PCM	27.6 ± 0.4^{a}	876.4 ± 20.9^{a}
PLA/PCM	28.4 ± 0.5^{a}	42.8 ± 1.3^{b}
PCM	24.7 ± 0.0^{b}	1.0 ± 0.0^{c}

a-c: Different superscripts within a column indicate significant differences among dodecane and hybrid structures ($p < 0.05$)

The morphology of the fibers was analyzed through scanning electron microscopy (SEM). Figure 1 shows SEM images of the various hybrid fibers obtained. The fibers obtained from the PCL solution were thicker (up to 1 µm) while PLA solutions generated thin beaded fibers with an average diameter under 200 nm. These differences in fiber diameter can be explained by the greater viscosity of PCL solutions.

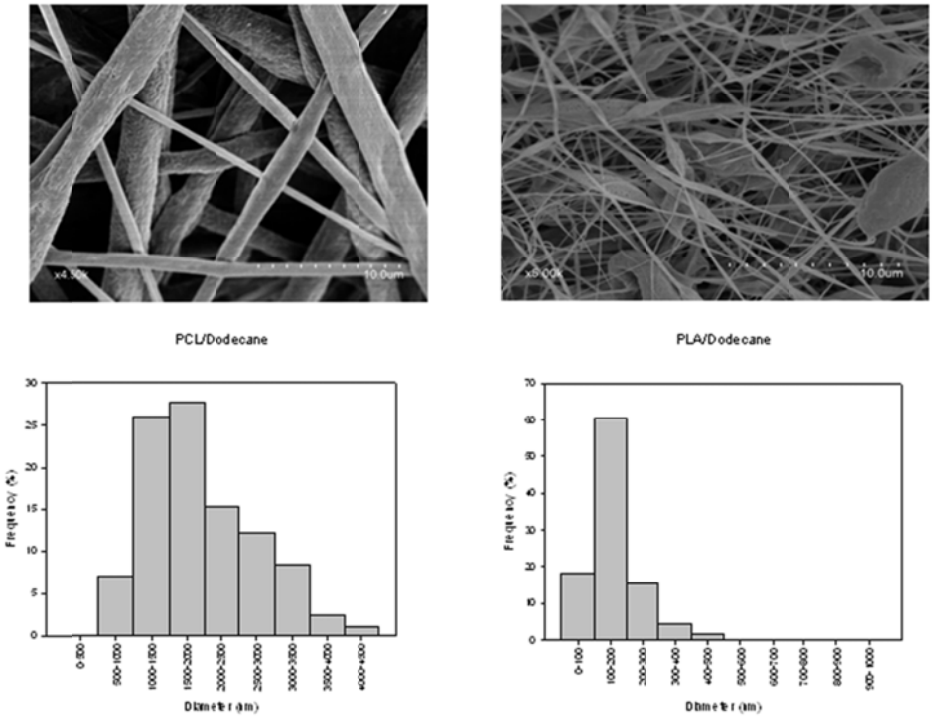

Figure 1. Selected SEM images and size distribution of PCL/PCM (left) and PLA/PCM (right) fibers.

Figure 2 shows the cross-sections of pure PCL and PCL/dodecane cryofractured fibers. From these images it can be observed that the pure PCL fiber is solid and without shafts. However, the incorporation of dodecane led to the formation of multiple channels (indicated with arrows) inside the fibrillar structures where the PCM was supposed to be allocated. For the PLA/dodecane fibers, it was not feasible to obtain detailed SEM images of the cross-sections due to the smaller size. Nevertheless, it could be assumed that the distribution of the PCM along the structures occurred in a similar way as in the PCL-based electrospun structures.

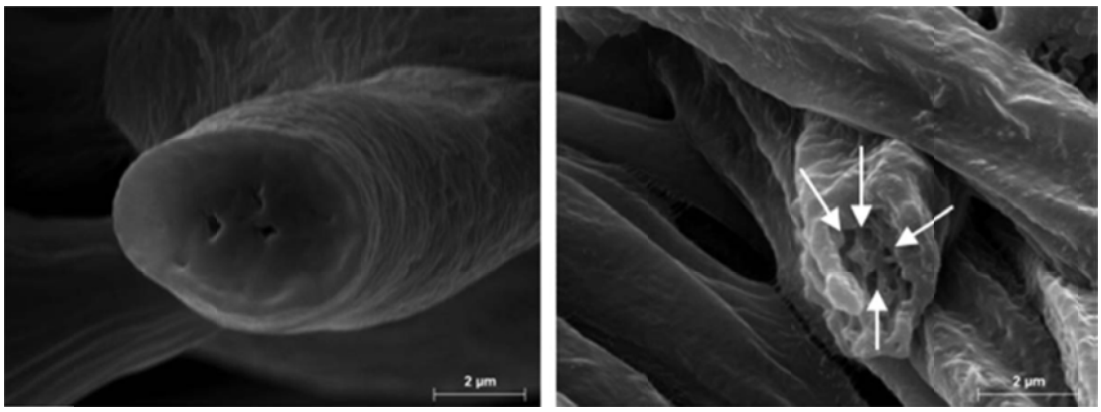

Figure 2. Cross-section SEM images of pure PCL (left) and PCL/PCM (right) fibers. Arrows indicate the channels where PCM is supposed to be located.

3.2. Thermal properties and molecular changes of electrospun structures

The thermal behavior of the electrospun structures as well as their associated molecular changes during dodecane phase transitions was analyzed by DSC and temperature-resolved ATR-FTIR spectroscopy, respectively. DSC analysis was also used to ascertain the degree of PCM incorporation.

Thermal properties (enthalpy values, melting and crystallization temperatures, and supercooling degree) of the pure dodecane and of the hybrid electrospun materials analyzed by DSC at 2 ºC/min are given in Table 2. From the DSC results, it was observed that pure dodecane melted at -9 ºC and crystallized at -11.9 ºC in a narrow temperature range, having an enthalpy of 196.9 J/g. This result is in accordance with other authors (Desai et al. 2008).

Table 2. Thermal properties of pure biopolyesters, PCM and biopolyester/PCM structures.

Samples	ΔHM (J/g dodecane)	Tm (ºC)	ΔHc (J/g dodecane)	Tc_1 (ºC)	Tc_2 (ºC)	Tc_3 (ºC)	Supercooling (ºC)
PCL	55.77 ± 5.0	55.55 ± 1.9	-51.05 ± 1.2	30.95 ± 1.9	-	-	-
PLA	28.52 ± 6.9	147.93 ± 5.1	-17.39 ± 2.3	91.87 ± 0.6*	-	-	-
PCM	196.88	-9	-199.03	-12	-	-	2.98
PCL/PCM	73.71 ± 2.2[a]	-8.31 ± 0.6[a]	-73.87 ± 2.8[a]	-13.53 ± 0.4[a]	-23.03 ± 0.4[a]	-	5.22 ± 1.09[a]
PLA/PCM	20.08 ± 4.1[b]	-9.71 ± 0.1[b]	-23.15 ± 4.3[b]	-23.36 ± 0.3[b]	-29.12 ± 2.3[b]	-38.98 ± 0.9[a]	13.65 ± 0.28[b]

ΔHm: melting enthalpy; Tm: melting temperature; ΔHc: crystallization enthalpy; Tc1, Tc2, Tc3: crystallization peaks temperatures. a-b: Different superscripts within a column indicate significant differences between byopolyester/PCM structures ($p < 0.05$). *This value refer to the cold crystallization transition of PLA

Figure 3 shows the ATR-FTIR spectra of the pure polymeric fibers, the pure dodecane, and the hybrid electrospun materials analysed at 20 ºC. At this temperature, the pure dodecane is characterized by the -CH2 and -CH3 stretching vibration bands at 2957, 2922, and 2852 cm^{-1}. These bands were also observed in the PLA and PCL hybrid structures even though they were overlapped with spectral bands from the biopolymeric structures, thus confirming the PCM encapsulation in both polymeric matrices.

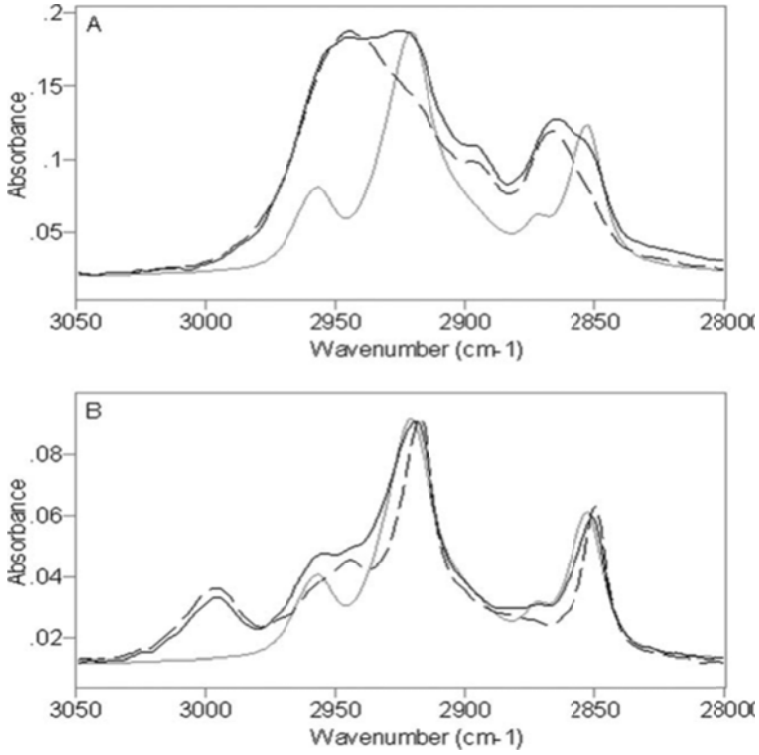

Figure 3. ATR-FTIR spectra of the pure polymers (black dashed line), pure dodecane (grey line) and hybrid electrospun materials (black solid line) for (A) PCL and (B) PLA structures.

Furthermore, melting and crystallization behavior of dodecane deposited as a liquid over the ATR crystal was also followed using ATR-FTIR spectroscopy since there are specific spectral changes which correlate with conformational changes of paraffins during their phase transition (Gnatyuk et al. 2007). Specifically, as observed in this study, the melting process of non-encapsulated dodecane was mainly characterized by the disappearance of the factor group splitting at 2960 and 2952 cm^{-1}, the displacement of the band at 2913 cm^{-1} towards higher wavenumbers and by the continuous drop of the band observed at 716 cm^{-1} until it disappeared. The factor group splitting is the splitting of bands in the vibrational spectra of crystals due to the presence of

more than one (interacting) equivalent molecular entity in the unit cell of certain symmetries and has been previously observed in other n-alkanes in other frequency regions (Sasaki et al. 2009; Makarenko et al. 2004). The existence of a unique band at 716 cm^{-1} in the solid state of dodecane indicates that when the crystal is formed, it presents the triclinic structure typical of even numbered n-paraffins with n≤26 (Gnatyuk et al. 2007).

Therefore, these conformational changes were analyzed through ATR-FTIR experiments as a function of temperature in the pure PCM and in the hybrid electrospun structures and the results were compared with the DSC data.

For pure dodecane, as observed in Figure 4(A), the spectral changes associated to the melting of the paraffin took place around -9 ºC in agreement with DSC results. In contrast, during the cooling scan, ATR-FTIR spectra [Figure 4(B)] showed that the splitting of the band at 2957 cm^{-1} into two components, at 2952 and 2959 cm^{-1} (factor group splitting), as well as the appearance of the band at 716 cm^{-1} occurred at -7 ºC. These changes suggest that there are conformational changes associated to molecular order taking place at this temperature during the ATR-FTIR run. In contrast, the onset temperature of crystallization as measured by DSC was -11.8 ºC. These results are in agreement with previous literature showing that the crystallization temperature detected by IR spectroscopy was higher than that obtained through DSC (Gnatyuk et al. 2007). The differences observed in the onset of crystallization determined by both characterization techniques could, perhaps, be explained by the fact that, in the case of the DSC, the experiment was carried out in nitrogen atmosphere in a closed chamber while the ATR accessory was exposed to the ambient humidity. During cooling in the vicinity of 0 ºC, ice crystals could form on the ATR surface, which may act as

heterogeneous nucleating sites that could promote early dodecane crystallization. The -OH stretching band at ca. 3580 cm^{-1} associated to water could be seen in the spectra of dodecane, thus adding strength to this hypothesis (results not shown). Additionally, it is also possible that the ATR crystal surface could promote additional nucleation sites for the PCM layer immediately in contact with the crystal.

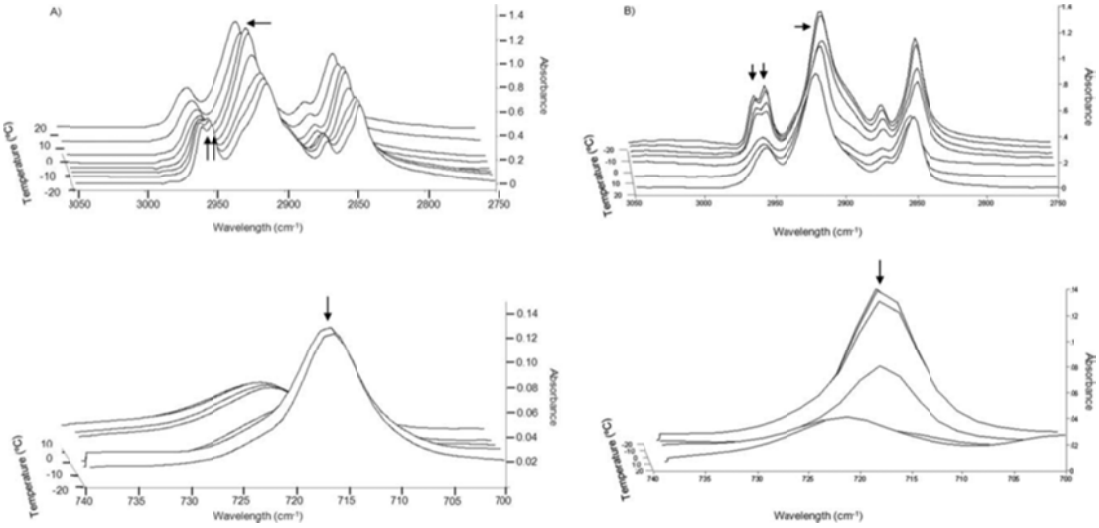

Figure 4. ATR-FTIR spectra of pure dodecane at different temperatures during (A) heating and (B) cooling. Arrows indicate the evolution of factor group splitting, the displacement of the band at 2916 cm^{-1} and the evolution of the band at 716 cm^{-1}.

Thermal properties of dodecane varied when this PCM was encapsulated in both biopolyester matrices. From Table 2, it can be seen that when dodecane was encapsulated in PLA, there was more variability among the enthalpy values of the different samples and the melting temperature was lower than that of non-encapsulated dodecane. This fact could be explained by the

reduced PLA fibers average diameter (Figure 1), leading to the formation of smaller or more defective dodecane crystals and, probably, to a heterogeneous distribution of the PCM along the fibers. In contrast, more homogeneous enthalpy values and no variation in the melting temperature (if compared with nonencapsulated dodecane) were obtained for the PCL/dodecane systems, which allowed an easier PCM encapsulation. Nevertheless, in both biopolyester-based encapsulation structures, the melting process occurred over a broader temperature range than in pure dodecane (peak width of ~3 ºC for the encapsulated dodecane vs. ~1 ºC for the bulk paraffin), probably because in the encapsulated systems there was a greater heterogeneity of crystals due to the different crystallization mechanisms, as it will be explained later, and also because the polymers themselves could be hindering heat transfer across the structures, thus prolonging the melting event (Mathot, 1994). In contrast with the similarities in the melting temperature between bulk and encapsulated dodecane, the crystallization event was considerably different. While pure dodecane crystallized at -11.98 ºC, a greater supercooling degree was observed in both PCL and PLA capsules. The supercooling effect was probably due to the reduction of the PCM particle size, since the number of nuclei needed to initiate the crystallization process decreased with reducing the diameter of the dodecane drops inside the fibers (Yamagishi et al. 1996). Moreover, a multiple crystallization profile was seen for encapsulated dodecane and, specifically, two and three crystallization temperatures were detected for the hybrid PCL and PLA structures, respectively. Multiple crystallization processes have been attributed to the rotator phase transition, which is observed in some n-alkanes when their particle size is reduced (Zhang et al. 2004). A rotator phase is defined as lamellar crystals, which exhibit long-range order in the molecular axis

orientation and center-of-mass position but lack rotational degrees of freedom of the molecules about their long axis (Kraack et al. 2000). In these cases, more than one peak is observed in the DSC analysis during the crystallization process due to the different kind of crystals attained depending on the crystallization mechanism followed. The first peak belongs to the heterogeneously nucleated liquid-rotator transition, the second one includes the rotator-crystal transition and the last one is attributed to the homogeneously nucleated liquid-crystal transition. Sometimes the second and third transitions appear as a single peak (Zhang et al. 2004), as was the case here for the hybrid PCL/dodecane structures.

In a similar way as with pure dodecane, the hybrid PCL and PLA structures were also analyzed by ATR-FTIR spectroscopy in order to better understand the conformational changes occurring during the phase transitions. It is of particular interest to realize that, in order to get a proper ATR signal, the samples had to be pressed against the ATR crystal, which was not a requirement for the case of the liquid neat PCM experiment described above. As with pure dodecane, the spectral changes associated with the melting event for both encapsulation structures occurred at the same temperatures observed through DSC, although they were observed over a broader temperature range (results not shown). This could be explained on the bases of infrared spectroscopy being able to pick up conformational changes beyond first order melting/crystallization transitions and may also be more sensitive to ill-defined lateral order phenomena compared to DSC (Desai et al. 2008).

Regarding the crystallization of dodecane within the electrospun biopolyesters, it was mainly followed through the increase in the FTIR band at 2950 cm^{-1} related to the factor group splitting [cf. arrows in Figures 5(A,B)] and

through the displacement of the band at 2922 cm^{-1}. Figure 5 displays the temperature-resolved crystallization spectra (from 3050 to 2970 cm^{-1}) and the wavenumber versus temperature plot for the band at 2922 cm^{-1} of PCL/PCM and PLA/PCM fibers.

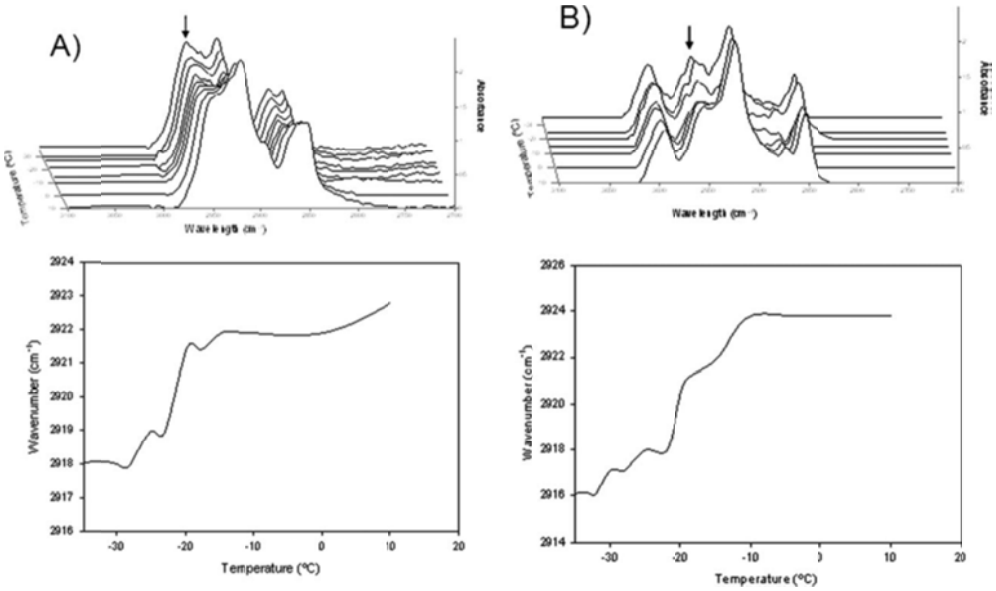

Figure 5. ATR-FTIR crystallization spectra of (A) PCL/PCM and (B) PLA/PCM structures at different temperatures and the wavenumber versus temperature plot for the band at 2922 cm21 of PCL/PCM (A) and PLA/PCM (B) fibers.

In the case of the PCL/PCM fibers, it was seen that a band at 2950 cm^{-1} appeared at -13 ºC and its intensity continuously increased during the cooling scan [Figure 5(A)]. The same event was observed in the PLA/PCM structures [Figure 5(B)], which became obvious at -10 ºC, when an increase in the band at 2951 cm^{-1} was observed. The band was not clearly seen until -15 ºC in agreement with the rise in band intensity observed for the pure component.

These results seem to indicate that some conformational changes of dodecane were taking place from -10 ºC. However, crystallization as such, required lower temperatures, probably as a result of the discussed reduction in drop size due to encapsulation. Regarding the displacement of the band at 2922 cm^{-1}, from Figure 5(A), it can be seen that for PCL hybrid structures there were three sharp changes during the shift of this band, taking place at -14, -20, and -25 ºC, approximately. These three jumps could be related with the corresponding rotator states defined earlier, although DSC was not able to detect separately the second and third one. For PLA/PCM fibers, Figure 5(B) shows that the abrupt changes along the displacement of the band at 2922 cm^{-1} were detected at -12, -25, and -30 ºC and these changes could also be related with the different rotator states. The fact that the crystallization temperatures detected with the spectroscopic technique were slightly higher than those obtained through DSC could be attributed, as previously mentioned, to a potentially greater nucleation effect promoted by ice crystals and/or by the ATR crystal itself. Moreover, these samples were pressed over the ATR crystal which could also affect the phase transition temperature, as it can be observed from a typical phase diagram. From phase diagrams, it can be observed that for a fixed temperature, the material state changes if pressure is modified, i.e., when increasing the pressure, the paraffins can be in solid state, even though the temperature is higher than their crystallization temperature. Although phase diagrams only describe ideal systems, the effect of pressure on the crystallization temperature of some alkanes in real systems has been already reported by some authors (Chan et al. 2000; Vieira et al. 2010).

3.3. Evaluation of the PCM encapsulation efficiency and loading

The PCM encapsulation efficiency and loading capacity of the polymeric fibers was evaluated from the enthalpy results obtained through DSC and also by NMR and TGA. The encapsulation efficiency through DSC was calculated by dividing the theoretical melting enthalpy of the hybrid materials by the experimental melting enthalpy obtained for these materials. The theoretical melting enthalpy was obtained considering the quantity of the PCM added to the electrospinning solution (45 or 20%) and multiplying this factor by the enthalpy of the pure dodecane. Table 3 shows the encapsulation yield derived from the DSC results of both biopolymeric matrices and the calculated total amount of dodecane encapsulated in these two fiber systems. According to DSC, PCL structures presented greater encapsulation efficiency than PLA fibers. Therefore, for PCL/dodecane structures, an encapsulation efficiency of 83% was achieved, which means that the capsules are composed by ~37 wt % of PCM (the core material) and ~63 wt % of the PCL shell material. Thus, the energy storage of the encapsulation system (considering both the PCM and the PCL) was around 72 J/g of material which is similar to some PCM products currently commercialized for dealing with room and human comfort range temperatures (http://energain.co.uk.; http://www.basf.com). On the other hand, according to DSC, only a 10 wt % of the PCM was providing energy storage capacity in the PLA structures, thus having a considerably lower energy storage capacity (~20 J/g).

Table 3. PCM Encapsulation Content and Efficiency as Inferred by DSC and of the Content as Determined by NMR and TGA

	DSC		NMR			TGA	
Samples	PCM (wt.%)	Efficiency (%)	Peaks ratio[a]	PCM (wt.%)	Efficiency (%)	PCM (wt.%)	Efficiency (%)
PCL/PCM	37.44 ± 1.1	~ 83	0.29 ± 0.2	39.12 ± 3.7	~ 87	35.86 ± 0.9	~ 80
PLA/PCM	10.20 ± 2.1	~ 51	0.67 ± 0.1	19.76 ± 2.3	~ 100	19.60 ± 1.0	~ 100

a: Ratio of the integration of resonance peaks from the biopolyesters (δ of 2.40–2.25 ppm of the adjacent protons to the carbonyl group for PCL and δ 5.30–5.00 ppm of the –CH groups for PLA) and dodecane (δ of 1.40–1.15 ppm of the –CH2 groups).

In order to confirm the encapsulation efficiency results obtained through DSC, the hybrid electrospun materials were subjected to NMR analyses using integration of resonance peaks from the polymer chains (at δ of 2.40–2.25 ppm of the adjacent protons to the carbonyl group for PCL and d of 5.30–5.00 ppm of the -CH groups for PLA) (Touhtouh et al. 2010; Espartero et al. 1996) and those from dodecane (δ of 1.40–1.15 ppm of the -CH2- groups of dodecane) (Silverstein et al. 2006). Although, the NMR technique does not provide accurate quantitative information, it can be useful to estimate a range of values for the PCM loading levels (Phadungphatthanakoon et al. 2011). The NMR assays were done in the liquid state favoring the release of the dodecane because of the complete dissolution of fibers and, thus, these results were expected to provide a more accurate data regarding dodecane loading than the indirect DSC data. The results are compiled in Table 3 and show that while the PCM loading level for the PCL/PCM fibers was closer to the results obtained through DSC (~39 wt % of dodecane encapsulated), in the case of the PLA/PCM electrospun materials the dodecane loading results were very different depending on the technique used. While NMR provided a PCM loading of around 20%, according to the enthalpy results from DSC the loading

inferred was just around 10%. This might be explained by the fact that the intrinsic morphology of the obtained PLA fibers, which were considerably thinner, could impede the complete crystallization of the encapsulated dodecane. In view of the results, it is hypothesized that a fraction of encapsulated dodecane does never crystallize, most likely because the undercooling required is larger than the one applied or because it interacts with the polymer in very small confined moieties. This also happened but to a much smaller degree for PCL since 45% of the PCM was theoretically encapsulated while only ca. 37% provided energy storage capacity.

To further estimate the loading content of the hybrid PCM/biopolyester fibers, TGA was used. The derivative curves from the pure polymers (PLA and PCL) and from the paraffin showed separate decomposition temperatures and, when the hybrid fibers were analyzed it was also possible to distinguish between the decomposition curves of the biopolyester and the PCM. Table 4 compiles the maximum of the weight loss first derivative (TD) and the corresponding peak onset and endset values for the pure compounds and hybrid fibers obtained from the TGA curves.

Table 4. TGA Maximum of the weight loss first derivate for the PCM dodecane (T_{D1}) and the biopolyesters (T_{D2}) and the corresponding peak onset and endset values for dodecane (T_1) and the biopolyesters (T_2)

Samples	Onset T_1 (ºC)	T_{D1} (ºC)	Endset T_1 (ºC)	Onset T_2 (ºC)	T_{D2} (ºC)	Endset T_2 (ºC)
Dodecane	40.5	197.1	210.5	-	-	-
PCL	-	-	-	322.9	410.8	472.1
PLA	-	-	-	265.9	340.8	370.7
PCL/PCM	77.9	189.2-209.4	272.9	319.4	409.2	471.6
PLA/PCM	75.7	152.9	226.1	247.9	334.5	367.4

From Table 4, it can be observed that both the onset and endset temperatures of dodecane degradation were displaced towards higher temperatures when the PCM was within the electrospun fibers. However, the effect of the paraffin in the thermal stability of the biopolyesters was different and, while a slight decrease in the thermal stability of PLA was observed in the hybrid fibers, no significant changes in the thermal degradation parameters were seen for PCL fibers. In any case, it was possible to clearly distinguish two different degradation curves (the first one corresponding to the PCM and the second one to the biopolyester) in the hybrid fibers. Through the integration of the areas of the corresponding peaks it was possible to estimate the PCM loading in the electrospun fibers (Table 3). When this method was used, the PCM content of the PLA and PCL fibers was calculated to be ~19.6 and ~35.9%, in agreement with the NMR data. These results confirm that, in the case of PLA, the encapsulation efficiency was greater than that calculated through DSC.

3.4. Diminishing the supercooling effect

In order to reduce the supercooling effect in the encapsulated structures, different nucleating agents were added to dodecane. Thus, a nanoclay,

tetracosane, and dodecanol were tested. All of these substances were solid at the crystallization temperature of dodecane and, thus, they were thought to act as first nuclei for the crystallization process. Figure 6 shows the reduction in supercooling of the nucleating agents assayed. From this figure, it is observed that dodecanol was seen to act as the most suitable nucleating agent, and thus it was selected for doing a more exhaustive study.

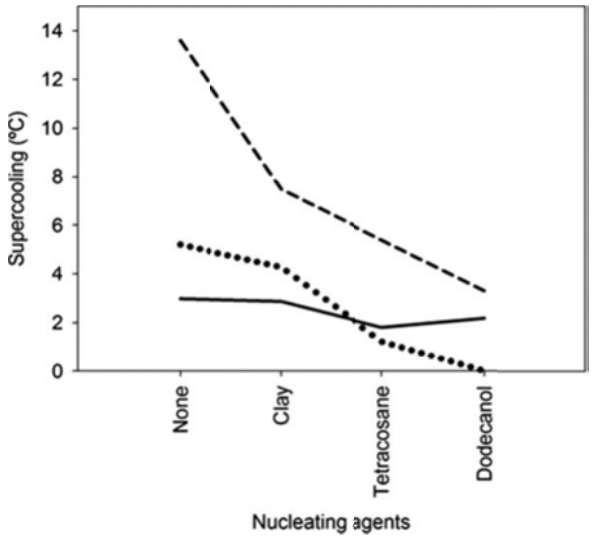

Figure 6. Effect of the nucleating agents in the supercooling for dodecane (solid line), PCL/dodecane (dotted line), and PLA/dodecane (dashed line).

Figure 7 shows the thermograms of (a) the pure PCM (b) the PCM with 10% of dodecanol and (c) the PCL/PCM fibers (d) and the PLA/PCM fibers with 5 and 10% of dodecanol, respectively. From Figure 7(a) and (b), it is seen that the melting process of the PCM with 10% of dodecanol occurred in a wider temperature range (from -9.6 to -0.7 ºC approximately) than for the pure PCM. This melting behavior is associated with the precipitation of redundant

dodecanol in dodecane near the melting point of dodecane, as it was reported before by Fan and coworkers with octadecane and octadecanol (Fan et al. 2004; Domanska & Rolinska, 1993). When the PCM with dodecanol was encapsulated inside the PCL structures [Figure 7(c)], two overlapping melting peaks were observed probably due to heterogeneous crystal formation as a consequence of dodecanol addition. However, this was not observed in PLA/PCM fibers additivated with 10% of dodecanol [Figure 7(d)] where only one melting peak was observed. Similarly to the result shown in the PCM/dodecanol mixture [Figure 7 (b)], the thermograms of PCL/PCM and PLA/PCM structures prepared with the nucleating agent also presented a melting shoulder expanding over a broad temperature range.

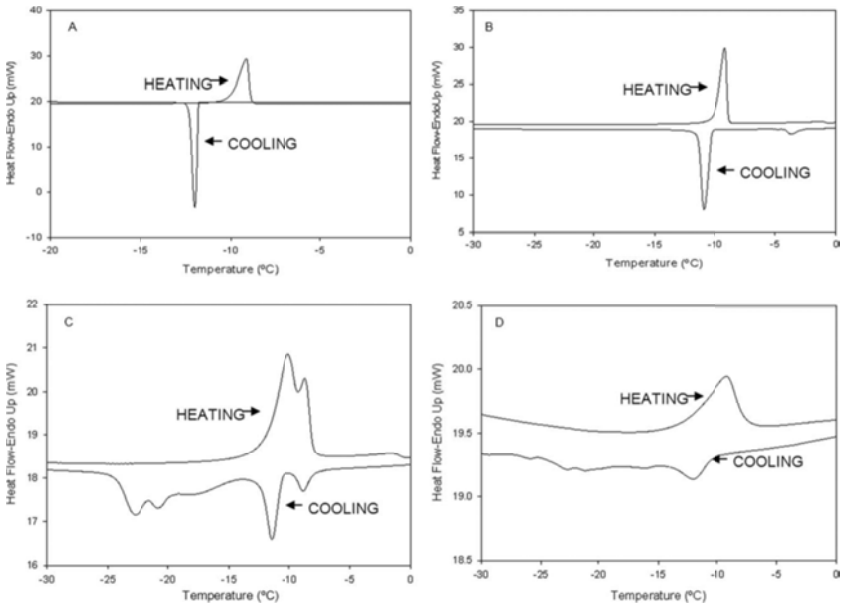

Figure 7. DSC thermograms of (a) pure PCM, (b) PCM with 10 wt % dodecanol, (c) PCL/PCM fibers with 5 wt.-% dodecanol, and (d) PLA/PCM fibers with 10 wt.- % dodecanol.

Table 5 shows crystallization temperatures obtained by DSC and the percentage of latent heat released at each temperature in both, PCL/PCM and PLA/PCM electrospun fibers prepared with different amounts of dodecanol (0, 5 and 10 wt %). The enthalpy results showed that addition of 5 and 10 wt % of dodecanol to PCL/PCM structures favored the release of 40% and 55% of the latent heat without supercooling, respectively. However, when the amount of nucleating agent was increased to 10 wt %, part of the heat was released close to 0 ºC, which is far from the target temperature expected for the application of these materials. For PLA/PCM structures, the effect of dodecanol was slightly different. Specifically, for this matrix, it was observed that addition of a 5 wt % of nucleating agent was not effective in reducing supercooling; however, when 10 wt.-% dodecanol was included within the fibers, a 35% of the PCM crystallized without supercooling. Therefore, these results further confirm that crystallization of dodecane was favored in thicker structures (such as the ones obtained with PCL), whereas in the thinner PLA structures it was necessary to add a greater amount of nucleating agent to facilitate the crystallization of the PCM.

Table 5. Thermal properties of the electrospun PCL/PCM and PLA/PCM fibers prepared with dodecanol.

Samples	% dodecanol	T_m (º C)	T_{c1} (º C)	ΔH_1 (%)	T_{c2} (º C)	ΔH_2 (%)	T_{c3} (º C)	ΔH_3 (%)	Supercooling (ºC)
PCL/PCM	0	-8.31 ± 0.6^{a}	-13.53 ± 0.4^{a}	65.23 ± 8.0	-23.03 ± 0.4^{a}	34.77 ± 8.01	-	-	5.22 ± 1.09
	5	-9.43 ± 0.30^{abc}	-7.94 ± 0.8^{b}	10.00 ± 3.3	-12.59 ± 2.2^{b}	29.12 ± 5.0	-22.43 ± 0.4^{a}	60.87 ± 8.3	1.49 ± 0.70
	10	-8.66 ± 0.46^{ab}	-2.11 ± 0.5^{c}	18.34 ± 0.6	-11.95 ± 0.1^{b}	55.44 ± 4.8	-22.48 ± 0.4^{a}	26.21 ± 4.2	0
PLA/PCM	0	-9.71 ± 0.10^{bc}	-23.36 ± 0.3^{d}	88.93 ± 5.93	-38.0 ± 4.23^{c}	11.07 ± 5.93	-	-	13.65 ± 0.28
	5	-10.25 ± 0.78^{c}	-22.11 ± 1.9^{d}	70.43 ± 1.6	-32.53 ± 2.3^{c}	28.42 ± 1.6	-37.01 ± 0.51^{b}	1.15 ± 0.3	11.86 ± 2.50
	10	-9.39 ± 0.25^{abc}	-12.73 ± 0.2^{a}	35.01 ± 2.1	-23.38 ± 0.05^{a}	37.17 ± 3.2	-31.16 ± 0.8^{c}	27.82 ± 5.3	3.34 ± 0.21

Tm: melting temperature; ΔH: % of latent heat release at each crystallization temperature. Tc1, Tc2, Tc3: crystallization temperatures.

a-dDifferent superscripts within a column indicate significant differences among samples ($P < 0.05$)

4. CONCLUSIONS

In this study, heat management materials were successfully developed based on the encapsulation of a PCM (dodecane) inside biodegradable polyesters (PCL and PLA) by means of the electrospinning technique. PCL/dodecane fibers were considerably thicker than the PLA/dodecane encapsulates obtained. The hybrid materials made from PCL were able to encapsulate a greater amount of dodecane than those obtained with PLA. Regarding the thermal properties, it was observed that the melting behavior of the encapsulated PCM was similar as for the pure PCM. However, the crystallization was affected by the encapsulation process because of the reduced size of the PCM pockets obtained and, generally, higher supercooling was observed in the developed electrospun structures. Nevertheless, the addition of a nucleating agent was able to minimize this effect. Regarding to the efficiency of the process, the PCM efficiency and loading in the fibers was measured by DSC, TGA, and NMR. Results showed that PCL fibers were able to encapsulate a heat storage capacity equivalent to ~37 wt % of the PCM. However, for the PLA materials, the dodecane loading results were different depending on the technique used. While NMR and TGA provided an encapsulation loading of around 20 wt %, according to the results from DSC, the heat storage capacity was equivalent to a loading of 10 wt % of the PCM. The differences in the latter case were ascribed to a fraction unable to crystallize inside the PLA matrix. Nevertheless, the structures developed presented improved properties with respect to the neat PCM, since in the encapsulated systems there was a fraction of the PCM which showed no supercoiling effect. Thus, these systems could be of significant interest in energy storage and thermal insulation

applications. In particular, the materials produced within this study could be applied as coatings for refrigeration machinery or for food/biomedical packaging where low temperatures are required to keep an optimum product quality.

5. REFERENCES

Alkan, C., Sari, A., & Karaipekli, A. (2011). Preparation, thermal properties and thermal reliability of microencapsulated n-eicosane as novel phase change material for thermal energy storage. Energy Conversion and Management, 52(1), 687-692.

Buschle-Diller, G.; Cooper, J.; Xie, Z.; Wu, Y.; Waldrup, J.; Ren, X. (2007). Release of antibiotics from electrospun bicomponent fibers. Cellulose. 14(6), 553-562.

Chan, A.K.C.; Hemmingsen, P.V.; Radosz, M. (2000). Fluid-liquid and fluid-solid transitions of tetracontane in propane. Journal of Chemical and Engineering Data. 45(2), 362-368.

Chen, Y.; Xinsong, L.; Tangying, S. (2007). Electrospinning and crosslinking of zein nanofiber mats Journal of Applied Polymer Science. 103(1), 380-385.

Cohn, D. and Hotovely Salomon, A. (2005). Designing biodegradable multiblock PCL/PLA thermoplastic elastomers Biomaterials. 26(15), 2297-2305.

Desai, K.; Kit, K.; Li, J.; Zivanovic, S. (2008). Morphological and surface properties of electrospun chitosan nanofibers. Biomacromolecules 9, 1000-1006.

Domanska, U. and Rolinska, J. (1993). Measurement and correlation of the solubility of n-alkanols (C18, C20) in n-alkanes (C7-C16) Fluid Phase Equilibria. 86(C), 233-250.

Espartero, J.L.; Rashkov, I.; Li, S.M.; Manlova, N.; Vert, M. (1996). NMR analysis of low molecular weight poly(lactic acid)s. Macromolecules. 29(10), 3535-3539.

Fan, Y.F.; Zhang, X.X.; Wang, X.C.; Li, J.; Zhu, Q.B. (2004). Super-cooling prevention of microencapsulated phase change materialThermochimica Acta. 413(1-2), 1-6.

Fernandez, A., Torres-Giner, S., & Lagaron, J.M. (2009). Novel route to stabilization of bioactive antioxidants by encapsulation in electrospun fibers of zein prolamine. Food Hydrocolloids 23, 1427-1432.

Garkhal, K.; Verma, S.; Jonnalagadda, S., Kumar, N. (2007). Fast degradable poly(L-lactide-co-ε-caprolactone) microspheres for tissue engineering: Synthesis, characterization, and degradation behavior Journal of Polymer Science, Part A: Polymer Chemistry 2007. 45(13), 2755-2764.

Gnatyuk, I. I., Platonova, N. V., Puchkovskaya, G. A., Kotelnikova, E. N., Filatov, S. K., Baran, J., & Drozd, M. (2007). Polymorphic transformations of C26H54 and C 28H58 n-paraffins as typical rotator substances. Journal of Structural Chemistry, 48(4), 654-665.

Haroosh, H.J.; Chaudhary, D.S. and Dong, Y. (2012). Electrospun PLA/PCL fibers with tubular nanoclay: Morphological and structural analysis Journal of Applied Polymer Science. 124(5), 3930-3939.

Huang, M.H.; Li, S.; Vert, M. (2004). Synthesis and degradation of PLA-PCL-PLA triblock copolymer prepared by successive polymerization of ε-caprolactone and DL-lactide Polymer. 45(26), 8675-8681.

http://energain.co.uk.

http://www.basf.com/group/corporate/en/brand/MICRONA_PCM.

Jiang, H.; Zhao, P.; Zhu, K. (2007). Fabrication and characterization of zein-based nanofibrous scaffolds by an electrospinning method Macromolecular Bioscience. 7(4), 517-525.

Kishimoto, A.; Setoguchi, T.; Yoshikawa, M.; Nakahira, T. (1995). In: Proceedings of 16th Japan Symposium on Thermophysical Properties (p. 233).

Kraack, H., Sirota, E. B., & Deutsch, M. (2000). Measurements of homogeneous nucleation in normal-alkanes. Journal of Chemical Physics, 112(15), 6873-6885.

Li, D., & Xia, Y. (2004). Electrospinning of nanofibres: Reinventing the wheel? Advanced Materials, 16(14), 1151-1170.

Makarenko, S.P., Puchkovska, G.A., Kotelnikova, E.N., Filatov, S.K. (2004). Spectroscopic study of rotation-crystalline modifications of mixtures of n-paraffins C22-C24 Journal of Molecular Structure. 704(1-3), 25-30.

Mathot, V.B.F. In Calorimetry and thermal analysis of polymers. Carl Hanser Verlag. Munnich, Vienna, New York, 1994. p 232-297.

Miyoshi, T.; Toyohara, K.; Minematsu, H. (2005). Preparation of ultrafine fibrous zein membranes via electrospinning Polymer International. 54(8), 1187-1190.

Pamula, E. and Menaszek, E. (2008). In vitro and in vivo degradation of poly(l-lactide-co-glycolide) films and scaffolds. Journal of Materials Science: Materials in Medicine. 19(5), 2063-2070.

Phadungphatthanakoon, S.; Poompradub, S.; Wanichwecharungruang, S.P. (2011). Increasing the thermal storage capacity of a phase change material by encapsulation: Preparation and application in natural rubber Applied Materials and Interfaces. 3(9), 3691-3696.

Perez-Masia, R.; Lopez-Rubio, A.; Lagaron, J.M. (2013). Development of zein-based heat-management structures for smart food packaging Food Hydrocolloids. 30(1), 182–191.

P201131063 Patent Application (2011). Procedimiento de encapsulación de PCMs. Inventors: Lagaron, J. M., Perez-Masia, R., & Lopez-Rubio, A. Holder entity: CSIC.

Sasaki, K., Inayoshi, N., Tashiro, K. (2009). In situ ftir-atr observation of phase transition behavior of n-alkane molecules induced by friction motion on a metal interface Journal of Physical Chemistry C. 113, 3287-3291.

Senador, A.E.; Shaw, M.T. and Mather, P.T. (2001). Electrospinning of polymeric nanofibers: Analysis of jet formation Materials Research Society Symposium Proceedings. 661, KK591-KK596.

Sharma, A., Tyagi, V. V., Chen, C. R., & Buddhi, D. (2009). Review on thermal energy storage with phase change materials and applications. Renewable and Sustainable Energy Reviews, 13(2), 318-345.

Silverstein, R.M.; Webster, F.X.; Kiemle, D. In Spectrometric identification of organic compounds. 7th ed. John Wiley and Sons Ltd, United States, 2006.

Torres-Giner, S., Gimenez, E., & Lagaron, J. M. (2008). Characterization of the morphology and thermal properties of Zein Prolamine nanostructures obtained by electrospinning. Food Hydrocolloids, 22(4), 601-614.

Torres-Giner, S.; Martínez-Abad, A.; Ocio, M.J.; Lagaron, J.M. (2010). Stabilization of a nutraceutical omega-3 fatty acid by encapsulation in ultrathin electrosprayed zein prolamine Journal of Food Science. 75(6), N69-N79.

Touhtouh, S.; Becquart, F.; Taha, M. (2012). Effect of Compatibilization on poly-ε-caprolactone grafting onto poly(ethylene-co-vinyl alcohol). Journal of Applied Polymer Science. 123(5), 3145-3153.

Vieira, L.C.; Buchuid, M.B.; Lucas, E.F. (2010). Effect of pressure on the crystallization of crude oil waxes. I. selection of test conditions by microcalorimetry Energy and Fuels. 24(4), 2208-2212.

Wang, B.Y.; Fu, S.Z.; Ni, P.Y.; Peng, J.R.; Zheng, L.; Luo, F.; Liu, H.; Qian, Z.Y. (2012). Electrospun polylactide/poly(ethylene glycol) hybrid fibrous scaffolds for tissue engineering Journal of Biomedical Materials Research - Part A. 100 A(2), 441-449.

Yamagishi, Y., Sugeno, T., Ishige, T., Takeuchi, H., & Pyatenko, A. T. (1996). An evaluation of microencapsulated PCM for use in cold energy transportation medium In Energy Conversion Engineering Conference. Proceedings of the 31st Intersociety (Vol. 3, pp. 2077-2083).

Zahedi, P.; Karami, Z.; Rezaeian, I.; Jafari, S.H.; Mahdaviani, P; Abdolghaffari, A.H.; Abdollahi, M. (2012). Preparation and performance evaluation of tetracycline hydrochloride loaded wound dressing mats based on electrospun nanofibrous poly(lactic acid)/poly(Ïμ-caprolactone) blends Journal of Applied Polymer Science. 124(5), 4174-4183.

Zhang, X. X., Fan, Y. F., Tao, X. M., & Yick, K. L. (2005). Crystallization and prevention of supercooling of microencapsulated n-alkanes. Journal of Colloid and Interface Science, 281(2), 299-306.

CHAPTER III

Use of electro-hydrodynamic processing to develop nanostructured materials for the preservation of the cold chain

CHAPTER III: Use of electro-hydrodynamic processing to develop nanostructured materials for the preservation of the cold chain

ABSTRACT

In this study Rubitherm-RT5®, a PCM with a phase transition temperature around 5ºC, was encapsulated inside PCL, PLA and PS by means of electro-hydrodynamic processing in order to develop thermal energy storage systems for refrigeration applications. The effect of the morphology of the encapsulation structures (fibrillar or spherical) on thermal properties and encapsulation efficiency was evaluated. The morphology of the structures played an important role on the energy storage capacity, since PCM was better encapsulated in fibrillar structures, providing higher energy storage capacity. The greater encapsulation efficiency was achieved for the fibers, which showed that ~80-90 wt.-% of the incorporated PCM, effectively remained within the polymeric matrices. These hybrid structures are of great interest for the development of smart packaging systems aimed at improving food quality preservation under refrigeration conditions.

Keywords: electrospinning, encapsulation, phase change material (PCM), polycaprolactone, polylactic acid, polystyrene.

1. INTRODUCTION

Conventional food packaging has been used to enable marketing of products and to provide passive protection against environmental contaminations or influences that affect the shelf life of foodstuffs (de Abreu, Cruz & Losada, 2012). However, consumers are claiming higher quality, safer and fresher products and, thus, new functions are demanded to the packaging structures. Therefore, over the last decade, there has been an increased research interest in the development of different active packaging systems, such as oxygen scavengers, moisture absorbers, flavor and odor absorbers/releasers or antimicrobials systems, which have an active role in food preservation, extending the shelf life or improving the conditions of packaged food through the retention or release of compounds from/to the food or package headspace. A more recent concept of packaging structure having an active role in food preservation is what is called “smart packaging”, able to detect changes in the packaging environment and react in order to counteract them. An example of these novel structures is packaging with heat management properties. It is well-known that temperature is a critical parameter which activates chemical reactions and microorganisms growth. In this sense, refrigeration temperatures have preservative effects on perishable products and thus, by controlling the temperature along the different stages of the food production, a great number of deteriorative processes could be avoided and the shelf life of products could be increased. However, temperature fluctuations during storage and commercialization of foods can result in a number of quality drawbacks, such as crystal ice growth in products like meat or ice-cream.

A possible approach to control thermal variations during storage and distribution of food, maintaining the preservation temperature constant and thus, preventing temperature fluctuations which can derive in food quality loss is through packaging structures with thermal energy storage capacity. This can be attained through the incorporation of phase change materials (PCMs) into the packaging structures. PCMs are able to absorb or release a great amount of energy during their melting/crystallization process and, as a consequence, they are able to buffer the thermal variations of the environment, and thus, they could provide thermal protection to the packaged food. The use of PCMs in energy storage systems has been recently applied in different fields such as building materials, air conditioning applications, solar energy storage systems, greenhouses, temperature regulating textiles, electronic devices and biomedical systems (Sarier, Onder, Ozay & Ozkilic, 2011). Specifically in the food packaging area, PCMs are replacing dry ice containers used during the transport and storage of perishable foodstuffs. Some of the advantages of using PCMs include the weight reduction of the containers in comparison with dry ice and, their reusability during many thermal cycles.

Among all the compounds available as phase change materials, paraffins are one of the most studied, since they are chemically stable and do not degrade after repeated cycling. Paraffins are highly compatible with a wide variety of materials and have a latent heat of fusion of around 200 kJ/kg depending on the particular paraffin selected (Ehid, & Fleischer, 2012). However, the use of paraffins for thermal energy storage applications also presents some drawbacks. On one hand, paraffins have

a low thermal conductivity, which limits the energy that can be extracted from them. Another problem is their handling, since they are liquid at ambient temperature and, what is more important, they need to undergo a phase change (i.e. from liquid to solid and viceversa) at the target temperature to exert the desired functionality. Some strategies to overcome these difficulties are the reduction of the PCMs particles' diameter in order to achieve a very high surface area to volume ratio, thus increasing their thermal conductivity (Alkan, Sari & Karaipekli, 2008). Furthermore, the encapsulation of these particles in a solid matrix can solve the handling problems of the PCMs. The most common paraffin encapsulation techniques are interfacial polymerization (Chu et al., 2003), emulsion polymerization (McDonald & Devon, 2002), in situ polymerization (Yang, Xu & Zhang, 2003), layer by layer deposition of polyelectrolytes (Sukhorukov et al., 2004), spray drying and coacervation (Hawlader, Uddin & Khin, 2003). However, only small amounts of PCM can be effectively encapsulated by some of these techniques, and they render too large particle sizes for some applications (Sánchez-Silva et al., 2010). Therefore, a rather novel route for PCMs encapsulation, based on the electrospinning process (Lagaron, Pérez-Masiá & López-Rubio, 2011), is proposed in this work. The electrospinning process uses high voltage electric fields to produce electrically charged jets from viscoelastic polymer solutions which on drying, by the evaporation of the solvent, produce ultrathin polymeric structures (Li & Xia, 2004). This technique has recently proven to encapsulate different materials with significant yielding and flexibility in design, obtaining submicron sized structures (Torres-Giner, Giménez & Lagaron, 2008; Fernández, Torres-Giner & Lagaron, 2009; López-Rubio & Lagaron, 2012). Although there

are a few works using electrospinning to develop PCM-containing materials, most of them deal with room and human comfort range temperatures (Chen, Wang & Huang, 2007; McCann, Marquez & Xia, 2006; Arecchi, Mannino & Weiss, 2010; Alay, Göde & Alkan, 2010; Cai, et al., 2012; Seifpoor, Nouri & Mokhtari, 2011).

The aim of this work was to use the electrospinning technology to obtain novel food packaging energy storage systems of interest in refrigeration applications. Two biopolyesters, polylactic acid (PLA) and polycaprolactone (PCL), were used as shell materials since they have attracted great interest amongst the existing biodegradable matrices because of their good physical properties (when compared to other biodegradable and renewable polymers), excellent biocompatibility and commercial availability (Pamula & Menaszek, 2008; Cohn & Hotovely Salomon, 2005; Huang, Günter, Doetsch & Mehling, 2010; Garkhal, Verma, Jonnalagadda & Kumar, 2007). Furthermore, the encapsulation systems based on these biodegradable materials were compared with others obtained with polystyrene (PS), since this petro-based polymer is currently used in refrigerating equipments and food packaging. Regarding the PCM, Rubitherm-RT5® (RT5) was encapsulated in the different polymers. RT5 is a commercial mixture of paraffins, specifically $C_{14}H_{30}$ (33%), $C_{15}H_{32}$ (47%), $C_{16}H_{34}$ (16%), $C_{17}H_{36}$ (3%) and $C_{18}H_{38}$ (1%), which presents a phase transition at around 5ºC. This temperature is commonly used to keep the refrigerating conditions of foodstuffs in retail and display cabinets at supermarkets or in household refrigerators. For each material, the effect of encapsulation morphology

(fibrillar or spherical) on the molecular organization and on the thermal properties of the capsules was evaluated.

2. MATERIALS AND METHODS

2.1 Materials

Rubitherm-RT5® (RT5) was purchased from Rubitherm (Germany). A semicrystalline extrusion grade of polylactide (PLA) (Natureworks) with a D-isomer content of approximately 2% was used. It had a weight-average molecular weight (Mw) of 150,000 g/mol and a number average molecular weight (Mn) of ca. 130,000 g/mol. The polycaprolactone (PCL) grade FB100 was kindly supplied in pellet form by Solvay Chemicals (Belgium). This grade had a density of 1.1 g/cm3 and a mean molecular weight of 100,000 g/mol. Polystyrene (PS) commercial grade foam and N,N-dimethylformamide (DMF) with 99% purity were purchased from Sigma-Aldrich (Spain). Trichloromethane was supplied by Panreac Quimica S.A. (Spain).

2.2. Preparation of polymer/RT5 solutions

Based on previous studies, the different polymers and RT5 were dissolved under magnetic stirring, in a solvent prepared with a mixture of trichloromethane:N,N-dimethylformamide (85:15 w/w) in order to produce fibrillar (fibers) or spherical (beads) capsules according to the conditions presented in Table 1:

Table 1. Composition of the different polymer solutions used and morphology of the electrospun structures obtained thereof.

Type of Polymer	Polymer concentration (%)	Polymer:PCM	Morphology
PCL	13	55:45	Fibres
PLA	5	80:20	Fibres
PS	10	55:45	Fibres
PCL	1.5	55:45	Beads
PLA	2.5	55:45	Beads
PS	2.5	55:45	Beads

2.3. Characterization of the solution properties

The viscosity and surface tension of the pure RT5, the solvent mixture used and all the biopolymeric solutions were characterized before the electrospinning process. The viscosity of the solutions was measured using a rotational viscosity meter Visco Basic Plus L from Fungilab S.A. (Spain) using a Low Viscosity Adapter (spindle LCP). The surface tension was measured using the Wilhemy plate method in an EasyDyne K20 tensiometer (Krüss GmbH, Germany). Both measurements were done, in triplicate, at 25ºC.

2.4. Preparation of the polymer-PCM fibers or beads through electrospinning

Fibers and beads were obtained using the electrospinning technique. The electrospinning apparatus, equipped with a variable high-voltage 0-30 kV power supply, was a FluidNatek® basic setup assembled and supplied by BioInicia S.L. (Spain). The polymer/PCM solutions were electrospun under a steady flow-rate using a stainless-steel needle situated toward a metallic grid used as collector. The needle was

connected through a PTFE wire to the polymer solution kept in a 5 mL plastic syringe which was disposed horizontally lying on a digitally controlled syringe pump. The electrospinning conditions were the following: 1 mL/h flow-rate, 12.5 kV voltage and 10 cm tip-to-collector distance for all the solutions.

2.5. Scanning Electron Microscopy (SEM)

The morphology of the electrospun structures was examined using scanning electron microscopy (SEM; Hitachi S-4100) after having been sputtered with a gold–palladium mixture under vacuum. All SEM experiments were carried out at 10kV. Fibers and beads diameters were measured by means of the Adobe Photoshop CS4 software from the SEM micrographs in their original magnification.

2.6. Attenuated total reflectance infrared spectroscopy (ATR-FTIR)

ATR-FTIR spectra were collected at 25ºC in a FTIR Tensor 37 equipment (Bruker, Germany). The spectra were collected in the different materials by averaging 20 scans at 4 cm-1 resolution. The experiments were repeated twice to verify that the spectra were consistent between individual samples.

2.7. Differential scanning calorimetry (DSC)

Thermal analyses of electrospun structures were carried out on a DSC analyzer (Perkin Elmer DSC 7, US) from -25 to 25ºC in a nitrogen atmosphere using a refrigerating cooling accessory (Intracooler 2, Perkin Elmer, US). The scanning rate was 2ºC/min in order to minimize the influence of this parameter in the thermal properties. The amount of

material used for the DSC experiments was adjusted so as to have a theoretical PCM content of 1-2 mg approximately. Measurements were done in triplicate.

2.8. Evaluation of the energy storage ability of the PCL/RT5 fibers

PCL fibers and PCL/RT5 fibers were stored at -18ºC overnight and then put in a controlled-temperature chamber at 15ºC. The temperature evolution of the material was registered with an infrared thermometer MS Plus (PCE Instruments, Spain).

2.9. Statistical analysis

Statistical analysis of data was performed through analysis of variance (ANOVA) using Statgraphics Plus for Windows 5.1 (Manugistics Corp., Rockville, MD). Homogeneous sample groups were obtained by using LSD test (95% significant level).

3. RESULTS AND DISCUSSION

3.1. Solution properties and morphology of the encapsulated materials

Based on previous knowledge about the parameters that affect the electrospinning process, different polymer/RT5 solutions were prepared in order to produce fibrillar or spherical structures for the encapsulation of the commercial PCM. It is well-known that the viscosity and the surface tension of polymeric solutions are very important to determine the range of concentrations from which continuous fibers or beads can be obtained (Fong, Chun, & Reneker, 1999). As previously reported by Fong et al. (Fong et al., (Fong et al., 1999), high viscosity values are generally achieved when increasing the polymer concentration in the electrospinning solution and this condition favors the formation of fibers without beads. This fact explains the different polymer concentrations used in this work (cf. Table 1) in which, the most concentrated solutions were used to obtain fibers, while lower polymer concentrations were selected for the production of beads. It may be noted that the polymer concentration and the maximum polymer/PCM ratio used, were based on screening studies on the electrospinning of the polyesters/PCM solutions. Table 2 shows the viscosity and surface tension values of the different polymer/PCM solutions, the pure PCM and the solvent mixture. As expected, the viscosity of all polymer/PCM solutions was greater than that of pure PCM due to the presence of the polymer which increased the total solids concentration. Furthermore, the viscosity of the polymer/PCM solutions was greater in the solutions used to obtain fibers than in those used to form beads, as the amount of polymer in the former was greater. However, the type and concentration of polymer

did not considerably affect the surface tension values, except in PCL/RT5 where a slight decrease in this parameter was observed as the polymer concentration increased. These results indicate that, for this study, the viscosity of the solutions was the main parameter that influenced the morphology of the encapsulation systems.

Table 2. Viscosity (μ) and surface tension (σ) of the different solutions used for electrospinning.

	Fibres			Beads		
	Polymer:RT5	η (cP)	σ (mN/m)	Polymer:RT5	η (cP)	σ (mN/m)
PCL/RT5	55:45	1148.11 ± 54.4^{1a}	28.00 ± 0.1^{1a}	55:45	11.07 ± 0.4^{2a}	28.87 ± 0.2^{2a}
PLA/RT5	80:20	45.27 ± 4.0^{1b}	28.50 ± 0.1^{1b}	55:45	7.07 ± 0.5^{2b}	28.53 ± 0.2^{1a}
PS/RT5	55:45	83.44 ± 5.0^{1c}	27.95 ± 0.2^{1a}	55:45	4.23 ± 0.1^{2c}	27.87 ± 0.2^{1b}
RT5	0:100	2.29 ± 0.1^{1d}	26.73 ± 0.2^{1c}	0:100	2.29 ± 0.1^{1d}	26.73 ± 0.2^{1c}
Solvent	-	1.00 ± 0.1^{1e}	28.34 ± 0.1^{1b}	-	1.00 ± 0.1^{1e}	28.34 ± 0.1^{1a}

a-e: Different superscripts within the same column indicate significant differences among biopolyester/PCM structures ($p < 0.05$)

1-2: Different superscripts within the same parameter indicate significant differences for a determined polymer/PCM due to the morphology reached (fibres or beads) ($p < 0.05$)

The morphology of the electrospun structures was analyzed through scanning electron microscopy (SEM). Figure 1 shows the SEM images of the different encapsulated systems and the corresponding size distribution of the fibers or beads. For the fibers, it was observed that PCL and PS led to fibers with an average diameter greater than 1 μm, although PS structures presented some beaded areas. In the case of PLA, this polymer produced very thin structures (with an average diameter of 214 nm) also with some beaded areas. The differences in average fiber diameters could be attributed to both the viscosity of the solutions and the solvent-polymer interactions. On the one hand, it is difficult for the

fluid to split into thin fibers when the solution viscosity is high (Li & Xia, 2004), which is in agreement with the thicker fibers observed for PCL/PCM systems. However, in spite of the great difference observed between the viscosity of PCL/PCM and PS/PCM solutions, the electrospun fibers obtained from both systems showed similar diameters as observed from the particle size distribution graphs (cf. Figure 1). In this case, the small differences observed in fiber diameter between these two systems can be related with polymer-solvent interactions as well as other factors intimately related with the electrospinning process such as the electrical conductivity of the polymer solution. The different fiber diameters could also explain the total amount of PCM that could be theoretically incorporated within the electrospun structures. Thus, only 20% of RT5 could be added to the thin PLA structures, while the thicker fibers obtained from the PCL and PS solutions favored the encapsulation of up to 45% of PCM. It is worth noting that the maximum ratios of the polymer/PCM tested were typically near 50/50. Greater PCM loadings tended to destabilize the encapsulation process for the selected polymer/PCM systems.

For the beaded structures, the average diameter of the capsules was around 2-3 μm regardless of the polymer used, although the size distribution was wider in the case of PCL/RT5 and PS/RT5 materials, where beads from 500 to 5000 nm were obtained. It is worth noting that the decrease of the polymer concentration in the case of the beads, together with the addition of the PCM, complicated the intermolecular entanglements of the polymers during the capsule's formation. This fact resulted in the collapse of the spherical structure and the production of

wrinkled particles as observed in Figure 1 for PLA and PS bead structures, which seemed to be empty (Hong, Li, Yin, Li & Zou, 2008). Moreover, it has also been reported that oil evaporates from the structures during the vacuum conditions used during the SEM experiments, which also explains the collapsed appearance of the capsules shown in Figure 1 (Angeles, Chenk & Velankar, 2008). In the case of PCL/RT5 solutions it was difficult to obtain only beads and, even when the polymer concentration was reduced to 1.5%, a large amount of thin fibers were also observed. However, PCL concentrations below 1.5% were not suitable for electrospinning because of a continuous dripping of the solution. The PS/RT5 diluted solution provided beads with a wider diameter size range together with some thin fibers. In contrast, beads with a homogeneous size distribution were achieved for the solutions of PLA/RT5. The fact that PLA formed micrometric beads, with an average diameter of ~3.2 μm could explain the greater capacity of these structures for encapsulating the PCM when compared to PLA fibers, since the latters presented an average diameter of only ~0.2 μm. The morphological differences among the studied polymer/PCM systems were again attributed to the viscosity of the solutions and the solvent-polymer interactions. When the polymer concentration was reduced, less polymer entanglements were obtained and thus beads or beaded fibers were obtained. Nevertheless, the spinnability of a polymer is also related to the intermolecular interactions between the polymer chain and the solvent molecules which could contribute to the formation of fibers instead of beads. In fact, when the polymer-solvent interaction is favored, higher molecular chain entanglements can be achieved and the formation of beads is hindered (Luo, Stride &

Edirisinghe, 2012). This fact could explain the greater viscosity of the PCL solutions, even with a lower polymer concentration, and the difficulty in producing bead structures with this polymer.

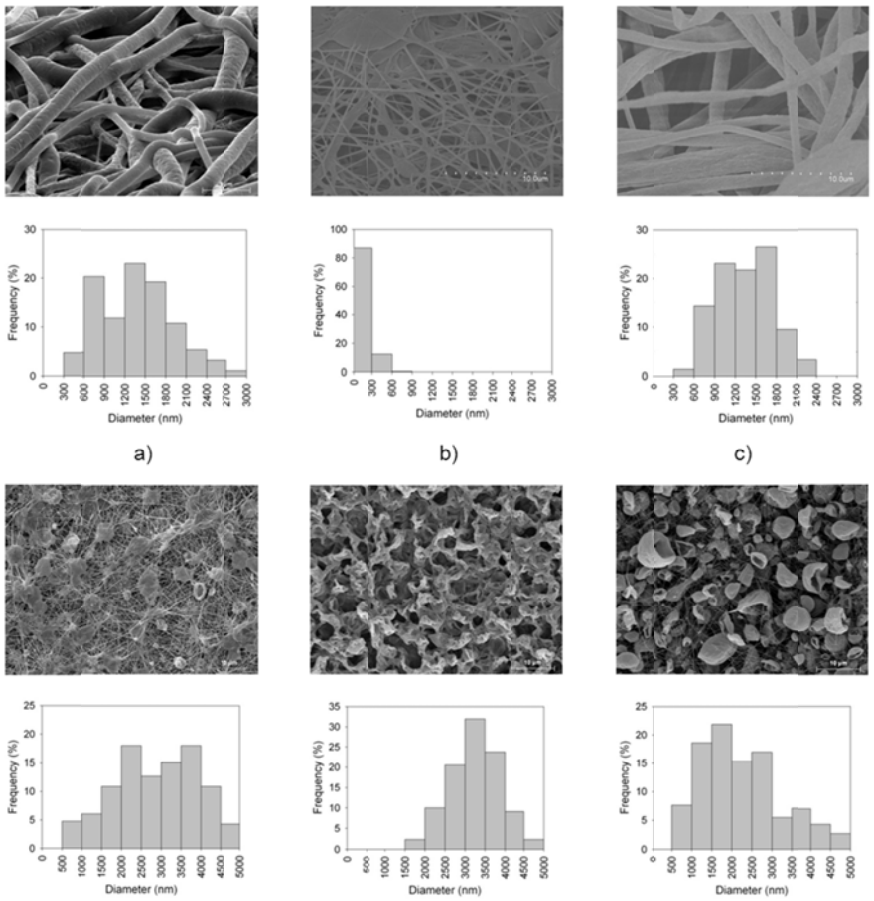

Figure 1. Selected SEM images and size distribution of fibers (up) and beads (down) of: a) PCL/RT5; b) PLA/RT5; c) PS/RT5.

3.2. ATR-FTIR analysis

ATR-FTIR analyses were carried out in order to corroborate the presence of RT5 in the capsules, as well as to study the molecular organization of the materials. The experiments were done at room temperature (25ºC), at which RT5 was in liquid state, and at -25ºC, at which RT5 was crystallized. Figure 2a shows the ATR-FTIR spectra of the pure RT5 at 25ºC (black line) and at -25ºC (grey line) from 2800 to 3000 cm^{-1}, where the most characteristic bands of the PCM can be found. This region is associated to the stretching vibrations of methyl groups, characteristics of alkane compounds. From this figure it can be observed that while the liquid RT5 presented spectral bands at 2957 cm^{-1}, 2922 cm^{-1} and 2853 cm^{-1}, when the PCM was crystallized, these bands were shifted toward lower wavenumbers due to an increase in intermolecular attractive forces in the solid state, which decreased the intramolecular vibrational transition energies (Porter, Jeffries & Hanson, 2009). Moreover, in the crystalline state the bands arose sharper and more intense mainly because of the higher degree of homogeneity of the intermolecular interactions. This leads to less dispersion of vibrational levels related to a higher molecular order (Wolkers, Oliver, Tablin & Crowe, 2004). From Figure 2b it is observed that the spectral band at 722 cm^{-1} attributed to the methyl rocking vibration present in the liquid RT5, splitted in two upon paraffin crystallization. This doublet is typical of odd alkanes with orthorhombic structure (MacPhail, Strauss, Snyder & Eilger, 1984).

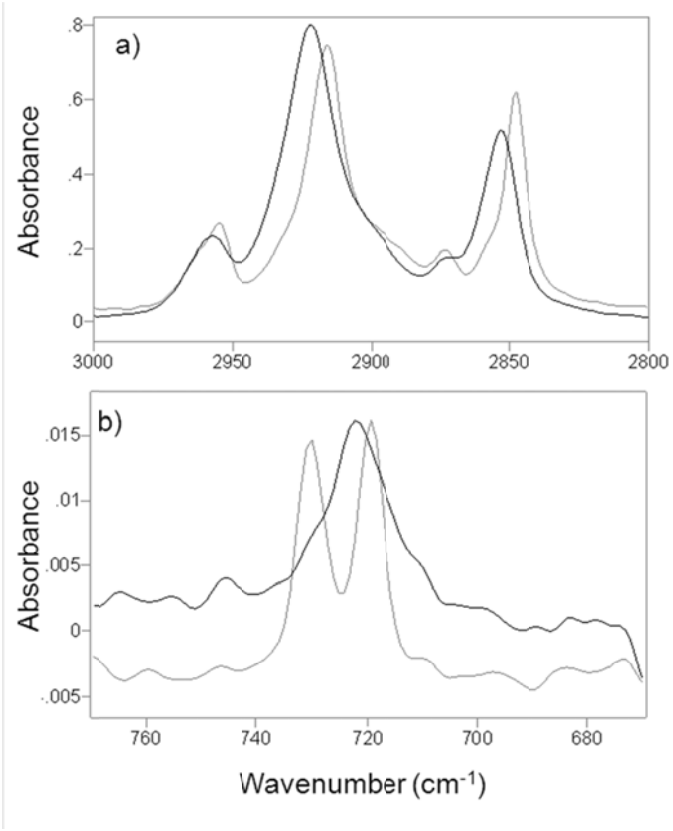

Figure 2. ATR-FTIR spectra of the pure RT5 at 25ºC (black line) and at -25ºC (grey line) from 2800 to 3000 cm^{-1} (a) and from 750 to 670 cm^{-1} (b).

The encapsulated systems were also analyzed using ATR-FTIR at 25 and -25ºC. Figure 3 shows the ATR-FTIR spectra from 2800 to 3000 cm^{-1} at 25ºC of the pure RT5, the pure polymers, the hybrid fibers and the hybrid beads. This figure shows that in this specific spectral region, the polymers also presented some characteristic bands. Nevertheless, they were not completely overlapped with those of the PCM and, thus, it was possible to identify the RT5 bands in the hybrid systems. From this figure

it was also observed that the PCM was effectively encapsulated in all the polymeric matrices (both fibers and beads), since the RT5 bands were evident in all the structures. At 25ºC the rocking vibration band (722 cm^{-1}) of the PCM was difficult to see due to the contribution of other spectral bands from the polymers in this region (data not shown).

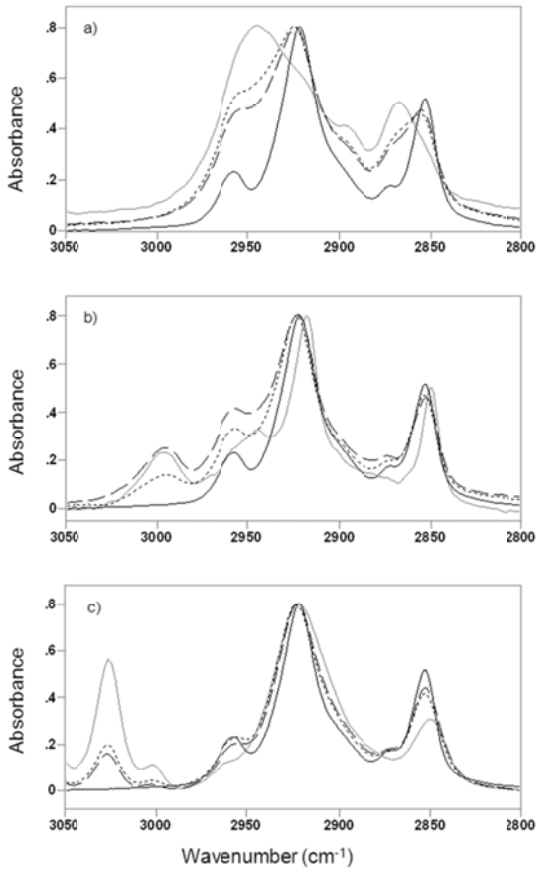

Figure 3. ATR-FTIR spectra of polymer (grey), RT5 (black), hybrid fibers (dashed) and beads (dotted) at 25ºC: a) PCL-RT5; b) PLA-RT5; c) PS-RT5.

The hybrid materials were also analyzed at -25ºC in order to study the molecular organization of the encapsulated PCM upon crystallization. Figure 4 shows the ATR-FTIR spectra of RT5 and the capsules at -25ºC in the regions of 2800-3000 cm^{-1} and 670-750 cm^{-1}. For PCL/RT5 fibers it was observed that the bands attributed to the PCM arose at the same wavenumbers as those of pure RT5, which suggested that there were no interactions between the PCL fibers and the PCM and, thus, RT5 could crystallize inside the fibers. However, it was seen that the methyl stretching vibration bands arose broader than those of the pure PCM, probably because of a lower molecular order of the PCM molecules inside the capsules, as well as to the contribution of PCL, which also presented a spectral band nearby this region. On the contrary, when studying this region in the PCL/RT5 beads, it was seen that the bands were slightly displaced towards higher wavenumbers than in the spectrum of pure RT5. Moreover, the intensity of the doublet band at 722 cm^{-1} was significantly lower than that of the pure PCM. This result suggested that a lower amount of PCM was encapsulated in PCL beaded capsules, probably because of the heterogeneous structures (thin fibers with beaded areas) obtained from this biopolymeric solutions. For PLA/RT5 and PS/RT5 materials, it was seen that in the 2800-3000 cm^{-1} area, the PCM bands arose at higher wavenumbers and slightly broader than the pure RT5. This fact indicates lower molecular order of the PCM molecules probably due to the presence of the polymers which could be hindering or modifying the crystallization of the PCM. It was also observed that the doublet at 722 cm^{-1} was present in PLA/RT5 beads and PS/RT5 fibers, while it did not arose in PLA/RT5 fibers and PS/RT5 beads. This result could be related to the PCM amount finally

encapsulated in these hybrid structures, i.e. the low amount of PCM present in the latter structures cannot be detected in this spectral range, as it will be confirmed below.

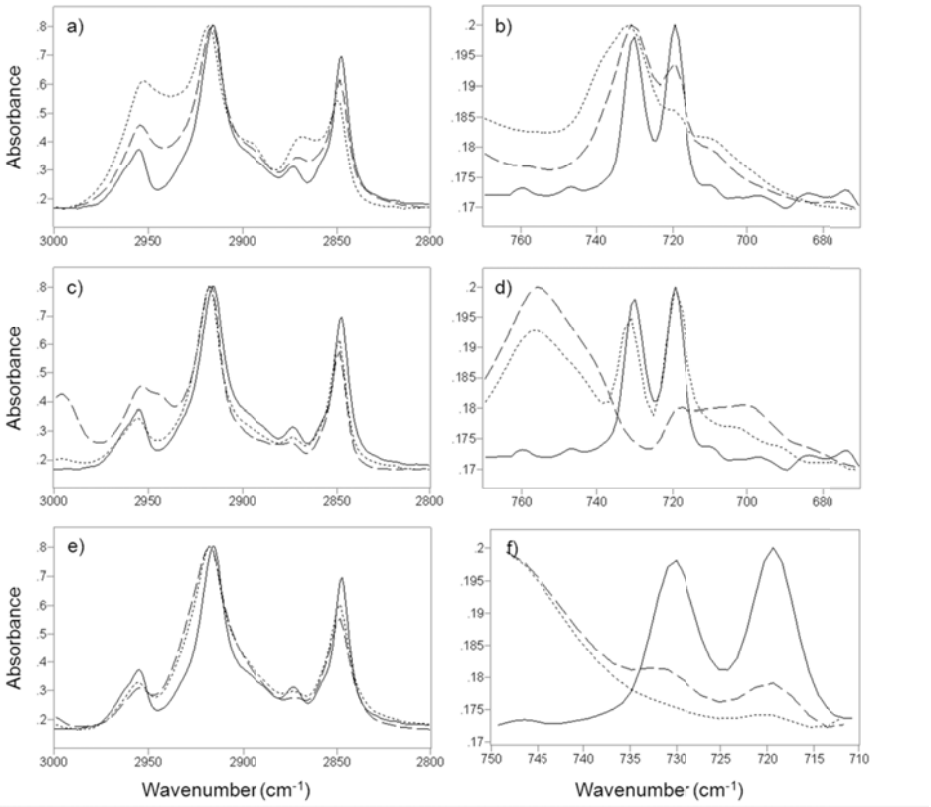

Figure 4. ATR-FTIR of RT5 (black), fibers (dashed) and beads (dotted) from 2800 to 3000 cm^{-1} and from 750 to 670 cm^{-1} at -25ºC of PCL-RT5 (a and b); PLA-RT5 (c and d); PS-RT5 (e and f).

3.3. Thermal properties

Thermal properties (enthalpy values, melting and crystallization temperatures and supercooling degree) of the hybrid electrospun materials analyzed by DSC at 2ºC/min are given in Table 3 (fibers) and Table 4 (beads). The supercooling degree is the lag between the melting and crystallization temperatures, calculated as the difference between the last melting and the first crystallization peaks detected. From these data it was observed that pure RT5 melted at 6.52ºC and crystallized at 5.26ºC, having a melting enthalpy of 142.2 J/g. It was observed that the onset temperature of the melting process for all the fibers did not significantly differ from that of pure RT5, but the maximum of melting increased when RT5 was encapsulated within these structures. This result indicates that the melting process occurred over a broader temperature range in the hybrid structures than in the pure PCM, as it can be observed from the peak width. This fact probably occurred because in the encapsulated systems there was a greater heterogeneity of crystals due to the different fibers diameters and also because the polymers themselves could be hindering heat transfer across the structures (Mathot, 1994). Moreover, while in the PCL/RT5 fibers, a single melting peak of the PCM was observed at 7.4ºC, for the PLA/RT5 and PS/RT5 hybrid structures, two different melting peaks of the PCM were observed. This fact could be attributed to the formation of two different crystal populations as a consequence of the confined state of the paraffins. This might be related to a greater stability of the rotator phase transitions occurring in paraffins as it will be further described below.

Regarding the crystallization, the thermal behavior of the PCL/RT5 fibers was similar to that of the non-encapsulated PCM, i.e. in both cases the beginning of the process was around 6ºC and the PCM crystallized in only one peak. Nevertheless, in the PCL/RT5 fibers the crystallization peak was broader, probably due to the greater heterogeneity of crystals and also because PCL could be impeding the heat transfer, as it was commented before. In contrast, for PLA and PS hybrid fibers the crystallization occurred in multiple stages. This behavior could be attributed to the different crystallization mechanisms, as well as to the different populations of crystals found along the fibers. It has been reported that when some paraffins are microencapsulated, they can undergo what is called a rotator phase transition (Zhang, Fan, Tao & Yick, 2005). A rotator phase is defined as lamellar crystals which exhibit long-range order in the molecular axis orientation and center-of-mass position, but lack rotational degrees of freedom of the molecules about their long axis (Kraack, Sirota & Deutsch, 2000). When this transition takes place, various crystallization temperatures can be detected through DSC, corresponding to the heterogeneusly liquid-rotator transition, the rotator-crystal transition and the homogeneously liquid-crystal transition, although sometimes the first and the second mechanisms could happen together (Zhang et al., 2005). Therefore, the thinner fibers obtained for PLA/RT5 and PS/RT5 fibers could be fauvoring these crystallization mechanisms. Moreover, as it was commented before, it has been observed that, in the confined state, rotator phases which are unstable in bulk, became metastable (Fu, Liu, Liu, Su, & Wang, 2011), fact that would explain the presence of two melting peaks in these developed materials.

Concerning the supercooling effect, it was greater in the PCL/RT5 fibers than in the pure RT5, probably due to a delayed heat transfer through the biopolyester matrix. However, for PLA and PS hybrid fibers, it was seen that the last melting peak temperature and the first crystallization peak temperatures almost matched, so the supercooling effect was reduced in these structures.

Table 3. Thermal properties of the various polymer/RT5 fibers developed

	Melting					Crystallization						
System	Onset (ºC)	Tm_1 (ºC)	Tm_2 (ºC)	Width (ºC)	ΔH_{meas} (J/g)	Onset (ºC)	Tc_1 (ºC)	Tc_2 (ºC)	Tc_3 (ºC)	Width (ºC)	ΔH_{meas} (J/g)	Supercooling (ºC)
RT5	2.83 ± 0.3^{a}	6.52 ± 0.4^{a}	-	3.92 ± 0.6^{a}	142.23 ± 9.7^{a}	5.83 ± 0.5^{a}	5.26 ± 0.3^{a}	-	-	1.08 ± 0.2^{a}	-144.62 ± 6.8^{a}	1.3 ± 0.4^{a}
PCL/RT5	2.92 ± 0.2^{a}	7.37 ± 0.1^{b}	-	5.78 ± 1.0^{b}	61.35 ± 8.5^{b}	6.27 ± 0.3^{a}	4.11 ± 0.5^{b}	-	-	6.98 ± 1.4^{b}	-61.948 ± 7.1^{b}	3.26 ± 0.5^{b}
PLA/RT5	3.22 ± 0.4^{a}	7.46 ± 0.5^{b}	10.73 ± 0.2^{a}	5.59 ± 0.2^{b}	24.94 ± 3.5^{c}	10.15 ± 0.1^{b}	9.37 ± 0.1^{c}	4.07 ± 0.4^{a}	-5.28 ± 0.3^{a}	17.39 ± 1.0^{c}	-25.21 ± 3.8^{c}	1.36 ± 0.3^{a}
PS/RT5	3.46 ± 0.3^{a}	7.97 ± 0.3^{b}	10.78 ± 0.3^{a}	7.90 ± 0.1^{c}	50.75 ± 7.3^{b}	9.24 ± 0.5^{c}	8.72 ± 0.1^{d}	3.61 ± 0.4^{a}	-9.32 ± 0.4^{b}	22.35 ± 1.9^{d}	-56.68 ± 5.3^{d}	2.06 ± 0.2^{c}

Tm1 and Tm2: first and second peak temperatures respectively; Tc1, Tc2, Tc3: first, second and third crystallization peaks temperatures respectively.

a-d: Different superscripts within a column indicate significant differences between biopolyester/PCM fibers ($p < 0.05$)

With regard to the thermal properties of the beaded or spherical morphologies, it was seen that the melting process was delayed and the peak temperature increased for all the polymeric matrices. This again seems to be related to the thermal lag associated to the presence of polymer shells, as well as to potential interactions between the PCM and the polymers as suggested by spectral band shifts (cf. Figure 4 and Section 3.2). However, this complex thermal behaviour, which could also be a consequence of different crystal morphologies, needs a more thorough study which is out of the scope of the present work.

The crystallization of the PCM in the hybrid PLA/RT5 and PS/RT5 beads was also characterized by several transition events which again could be attributed to the different crystallization mechanisms (rotator phase, heterogenous and homogeneous). Regarding the supercooling, it increased when compared to the the non-encapsulated RT5. It is well-known that the undercooling required to obtain crystallization significantly increases when reducing the droplet size in comparison to the bulk material as each droplet must be nucleated separately and the nucleation mechanism shifts from heterogeneous to homogeneous nucleation (Montenegro, Antonietti, Mastai & Landfester, 2003). Therefore, from the data obtained, it can be concluded that the use of these hybrid beads as encapsulation morphologies would not be suitable for refrigeration applications, since the phase transition temperatures obtained for these structures did not match the temperature required in the refrigeration systems.

Table 4. Thermal properties of the various polymer/RT5 beads developed

	Melting					Crystallization						
System	Onset (ºC)	Tm_1 (ºC)	Tm_2 (ºC)	Width (ºC)	ΔH_{meas} (J/g)	Onset (ºC)	Tc_1 (ºC)	Tc_2 (ºC)	Tc_3 (ºC)	Width (ºC)	ΔH_{meas} (J/g)	Supercooling (ºC)
RT5	2.83 ± 0.3[a]	6.52 ± 0.4[a]	-	3.92 ± 0.6[a]	142.23 ± 9.7[a]	5.83 ± 0.5[a]	5.26 ± 0.3[a]	-	-	1.08 ± 0.2[a]	-144.62 ± 6.8[a]	1.3 ± 0.4[a]
PCL/RT5	8.85 ± 1.3[b]	13.20 ± 0.8[b]	-	5.50 ± 1.0[b]	21.01 ± 1.5[b]	12.09 ± 0.4[b]	11.20 ± 0.9[b]	-	-	4.86 ± 1.0[b]	-19.81 ± 0.9[b]	2.00 ± 0.1[a]
PLA/RT5	5.36 ± 1.0[c]	10.81 ± 1.0[c]	-	6.52 ± 0.4[b]	42.89 ± 6.8[c]	9.67 ± 0.3[c]	8.66 ± 0.3[c]	5.52 ± 0.5[a]	-	8.58 ± 1.9[c]	-42.95 ± 6.9[c]	2.15 ± 0.9[a]
PS/RT5	6.54 ± 1.6[c]	11.78 ± 1.9[c]	15.02 ± 1.7	9.63 ± 0.8[c]	24.96 ± 3.5[b]	12.91 ± 1.5[b]	12.03± 1.6[b]	6.95 ± 1.3[a]	-4.87 ± 1.6	21.05 ± 0.8[d]	-26.44 ± 2.8[d]	3.00 ± 0.5[b]

Tm1 and Tm2: first and second peak temperatures respectively; Tc1, Tc2, Tc3: first, second and third crystallization peaks temperatures respectively.

a-d: Different superscripts within a column indicate significant differences between biopolyester/PCM beads ($p < 0.05$)

3.4. Evaluation of the PCM loading and thermal energy storage capability

The encapsulation efficiency was calculated by dividing the experimental melting enthalpy obtained for the hybrid materials by the experimental melting enthalpy obtained for pure RT5, considering the quantity of the PCM added to the electrospinning solutions. Table 5 shows the encapsulation yield derived from the DSC results of the hybrid structures (both fibers and beads), the initial amount of PCM added to the solutions and the calculated total amount of RT5 effectively encapsulated in the systems. Results showed that fiber structures presented greater encapsulation efficiency than beads, which may be ascribed to the fact that continuous fiber structures contributed to retain greater amounts of PCM than discontinuous beads. When comparing among the various polymers used as encapsulating matrices, PCL and PS fibers demonstrated a greater ability to retain PCM than PLA fibers, probably due to the diameter of the structures obtained thereof. From Figure 1 it was seen that PCL and PS formed fibers with an average size higher than 1 μm, while PLA fiber mean diameter was around 200 nm and, thus, it is expected that the PCM was more easily encapsulated in the thicker PCL and PS structures. The greatest encapsulation efficiency was achieved for PCL/RT5 fibers (□96%), meaning that around 43 wt.-% of the material obtained was able to provide energy storage capacity. On the contrary, only 36 wt.-% and 18 wt.-% of the hybrid PS/RT5 and PLA/RT5 fiber structures, respectively, had energy storage capacity.

In contrast, for the compositions that gave rise to beaded structures, PLA was the most efficient matrix, being ≈30 wt.-% of the material able to provide energy storage capacity. However, changing from fiber to bead morphology significantly reduced the encapsulation efficiency of PCL and PS structures, showing that only an 18-19 wt.-% of the capsules provided energy storage capacity. This could be explained by the different bead morphology reached depending on the matrix used, since PLA led to a continuous mat of beads, while PCL and PS formed bead structures together with very thin fibers, which probably were not able to fully encapsulate the PCM.

Table 5. Encapsulation efficiency and PCM loading of the various polymer/RT5 capsules developed

	System	Efficiency (%)	Initial PCM (%)	PCM loaded (%)
	RT5	100	100	100
Fibres	PCL/RT5	95.85 ± 13.3	45	43.13 ± 6.0
	PLA/RT5	87.67 ± 12.2	20	17.53 ± 2.4
	PS/RT5	79.29 ± 11.3	45	35.68 ± 5.1
Beads	PCL/RT5	42.62 ± 12.9	45	19.18 ± 5.8
	PLA/RT5	61.45 ± 6.5	45	27.7 ± 2.9
	PS/RT5	38.0 ± 6.2	45	17.1 ± 2.8

3.5. Evaluation of the energy storage ability of the PCL/RT5 fibers

From Table 5 it was observed that PCL/RT5 fibers were the most efficient energy storage material providing ~60 J/g. Therefore, this system was selected for the evaluation of the energy storage ability of the material developed. For this aim, a piece of 0.5 g of the hybrid PCL/RT5 fibers mat and the same amount of pure PCL fibers for

comparison purposes were stored at -18ºC and then they were exposed to 15ºC. Figure 5 shows the temperature evolution of pure PCL fibers and PCL/RT5 fibers. From this figure it can be seen that the PCL fibers without PCM reached the room temperature in 80 s. However, the hybrid fibers were able to keep the temperature at around 4-6ºC during 1.5 min and room temperature was reached after 3.5 min, i.e. incorporation of the PCM within the polymer fibers almost tripled the time needed to reach room temperature, thus demonstrating the heat management capacity of this type of structures. Additional experimental and modelling information of this material is presented in Annexe 1.

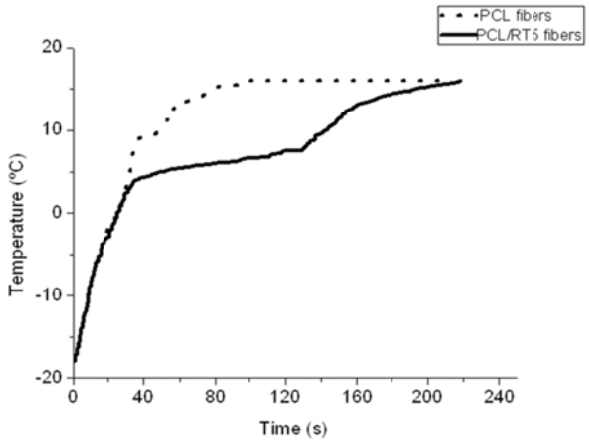

Figure 5. Temperature evolution of PCL and PCL/RT5 fibers.

4. CONCLUSIONS

In this work different polymeric capsules containing Rubitherm-RT5®, a phase change material (PCM) with a phase transition at around 5ºC, were developed by means of the electro-hydrodynamic processing. Different encapsulation morphologies, fibrillar (fibers) and spherical (beads) were attained depending on the properties of the polymer/PCM solutions. ATR-FTIR results showed that the PCM could be encapsulated in both types of morphologies, although fibers seemed to be more suitable for energy storage applications since the thermal properties of the PCM retained in the fiber structures were not as modified as within the beads. Furthermore, the encapsulating efficiency and the energy storage capacity of fibers were also greater than in the beads. Thus, it can be concluded that materials comprising electrospun fibers are a promising alternative to develop smart packaging materials for foods stored under refrigeration conditions. Besides, among all the polymers tested, PCL was the most efficient matrix with ~43% of RT5 encapsulated. Moreover, these fibers showed the ability of temperature buffering at the phase transition temperature of the PCM for some time. Thus, the incorporation of these hybrid fibers in the food packaging materials or in the walls of refrigeration equipment can be a suitable strategy to buffer the thermal fluctuations with the aim of improving the quality and safety of foodstuffs.

5. REFERENCES

Alay, S., Göde, F., & Alkan, C. (2010). Preparation and characterization of poly(methylmethacrylate-coglycidyl methacrylate)/n-hexadecane nanocapsules as a fiber additive for thermal energy storage. Fibers and Polymers, 11(8), 1089-1093.

Alkan, C., Sari, A., & Karaipekli, A. (2011). Preparation, thermal properties and thermal reliability of microencapsulated n-eicosane as novel phase change material for thermal energy storage. Energy Conversion and Management, 52(1), 687-692.

Angeles, M., Cheng, H.-L., & Velankar, S.S. (2008). Emulsion electrospinning: composite fibers from drop breakup during electrospinning. Polymers for Advanced Technologies, 19, 728-733.

Arecchi, A., Mannino, S., & Weiss, J. (2010). Electrospinning of poly(vinyl alcohol) nanofibers loaded with hexadecane nanodroplets. Journal of Food Science, 75(6), N80-N88.

Cai, Y., Gao, C., Xu, X., Fu, Z., Fei, X., Zhao, Y., Chen, Q., Liu, X., Wei, Q., He, G., & Fong, H. (2012). Electrospun ultrafine composite fibers consisting of lauric acid and polyamide 6 as form-stable phase change materials for storage and retrieval of solar thermal energy. Solar Energy Materials and Solar Cells, 103, 53-61.

Chen, C., Wang, L., & Huang, Y. (2007). Electrospinning of thermo-regulating ultrafine fibers based on polyethylene glycol/cellulose acetate composite. Polymer, 48(18), 5202-5207.

Chu, L. Y., Xie, R., Zhu, J. H., Chen, W. M., Yamaguchi, T., & Nakao, S. I. (2003). Study of SPG membrane emulsification processes for the preparation of monodisperse core-shell microcapsules. Journal of Colloid and Interface Science, 265(1), 187-196.

Cohn, D., & Hotovely Salomon, A. (2005). Designing biodegradable multiblock PCL/PLA thermoplastic elastomers. Biomaterials, 26(15), 2297-2305.

de Abreu, D.A.P., J.M. Cruz, and P.P. Losada. (2012). Active and Intelligent Packaging for the Food Industry. Food Reviews International. 28(2), 146-187.

Ehid, R., & Fleischer, A. S. (2012). Development and characterization of paraffin-based shape stabilized energy storage materials. Energy Conversion and Management, 53(1), 84-91.

Fernandez, A., Torres-Giner, S., & Lagaron, J. M. (2009). Novel route to stabilization of bioactive antioxidants by encapsulation in electrospun fibers of zein prolamine. Food Hydrocolloids, 23(5), 1427-1432.

Fong, H., Chun, I., & Reneker, D. H. (1999). Beaded nanofibers formed during electrospinning. Polymer, 40(16), 4585-4592.

Fu, D., Liu, Y., Liu, G., Su, Y., & Wang, D. (2011). Confined crystallization of binary n-alkane mixtures: stabilization of a new rotator phase by enhanced surface freezing and weakened intermolecular interactions. Physical Chemistry Chemical Physics, 13, 15031-15036.

Garkhal, K., Verma, S., Jonnalagadda, S., & Kumar, N. (2007). Fast degradable poly(L-lactide-co-ε-caprolactone) microspheres for tissue engineering: Synthesis, characterization, and degradation behavior. Journal of Polymer Science, Part A: Polymer Chemistry, 45(13), 2755-2764.

Hawlader, M. N. A., Uddin, M. S., & Khin, M. M. (2003). Microencapsulated PCM thermal-energy storage system. Applied Energy, 74(1-2), 195-202.

Huang, L., Günther, E., Doetsch, C., & Mehling, H. (2010). Subcooling in PCM emulsions-Part 1: Experimental. Thermochimica Acta, 509(1-2), 93-99.

Hong YL, Li YY, Yin YZ, Li DM, Zou GT. (2008). Electro-hydrodynamic atomization of quasi-monodisperse drug-loaded spherical/wrinkled microparticles. Journal of Aerosol Science 39 (6), pp. 525-536

Kraack, H., Sirota, E. B., & Deutsch, M. (2000). Measurements of homogeneous nucleation in normal-alkanes. Journal of Chemical Physics, 112(15), 6873-6885.

Lagaron, J. M., Perez-Masia, R., & Lopez-Rubio, A. (2011). Procedimiento de encapsulación de PCMs. In (Vol. ES_201131063). Spain.

Li, D., & Xia, Y. (2004). Electrospinning of nanofibers: Reinventing the wheel? Advanced Materials, 16(14), 1151-1170.

López-Rubio, A., & Lagaron, J. M. Whey protein capsules obtained through electrospraying for the encapsulation of bioactives. Innovative Food Science and Emerging Technologies, 13 (JANUARY) , pp. 200-206

Luo, C. J., Stride, E., & Edirisinghe, M. (2012). Mapping the influence of solubility and dielectric constant on electrospinning polycaprolactone solutions. Macromolecules, 45(11), 4669-4680.

MacPhail, R. A., Strauss, H. L., Snyder, R. G., & Eiliger, C. A. (1984). C-H stretching modes and the structure of n-alkyl chains. 2. Long, all-trans chains. Journal of Physical Chemistry, 88(3), 334-341.

Mathot, V. B. F. (1994). Calorimetry and thermal analysis of polymers: Carl Hanser Verlag.

McCann, J. T., Marquez, M., & Xia, Y. (2006). Melt coaxial electrospinning: A versatile method for the encapsulation of solid materials and fabrication of phase change nanofibers. Nano Letters, 6(12), 2868-2872.

McDonald, C. J., & Devon, M. J. (2002). Hollow latex particles: Synthesis and applications. Advances in Colloid and Interface Science, 99(3), 181-213.

Montenegro, R., Antonietti, M., Mastai, Y., & Landfester, K. (2003). Crystallization in miniemulsion droplets. Journal of Physical Chemistry B, 107, 5088-5094.

Pamula, E., & Menaszek, E. (2008). In vitro and in vivo degradation of poly(l-lactide-co-glycolide) films and scaffolds. Journal of Materials Science: Materials in Medicine, 19(5), 2063-2070.

Porter, J.M., Jeffries, J.B., Hanson, R.K. (2009). Mid-infrared absorption measurements of liquid hydrocarbon fuels near 3.4 μ m. Journal of Quantitative Spectroscopy and Radiative Transfer 110 (18) ,2135-2147

Sánchez-Silva, L., Rodríguez, J. F., Romero, A., Borreguero, A. M., Carmona, M., & Sánchez, P. (2010). Microencapsulation of PCMs with a styrene-methyl methacrylate copolymer shell by suspension-like polymerisation. Chemical Engineering Journal, 157(1), 216-222.

Sarier, N., Onder, E., Ozay, S., & Ozkilic, Y. (2011). Preparation of phase change material-montmorillonite composites suitable for thermal energy storage. Thermochimica Acta, 524(1-2), 39-46.

Seifpoor, M., Nouri, M., & Mokhtari, J. (2011). Thermo-regulating nanofibers based on nylon 6,6/polyethylene glycol blend. Fibers and Polymers, 12(6), 706-714.

Sukhorukov, G. B., Shchukin, D. G., Dong, W. F., Möhwald, H., Lulevich, V. V., & Vinogradova, O. I. (2004). Comparative analysis of hollow and filled polyelectrolyte microcapsules templated on melamine formaldehyde and carbonate cores. Macromolecular Chemistry and Physics, 205(4), 530-535.

Torres-Giner, S., Gimenez, E., & Lagaron, J. M. (2008). Characterization of the morphology and thermal properties of Zein Prolamine nanostructures obtained by electrospinning. Food Hydrocolloids, 22(4), 601-614.

Yang, R., Xu, H., & Zhang, Y. (2003). Preparation, physical property and thermal physical property of phase change microcapsule slurry and phase change emulsion. Solar Energy Materials and Solar Cells, 80(4), 405-416.

Wolkers, W.F., Oliver, A.E., Tablin, F. & Crowe, J.H. (2004). A Fourier-transform infrared spectroscopy study of sugar glasses. Carbohydrate Research 339 (6), 1077-1085

Zhang, X. X., Fan, Y. F., Tao, X. M., & Yick, K. L. (2005). Crystallization and prevention of supercooling of microencapsulated n-alkanes. Journal of Colloid and Interface Science, 281(2), 299-306.

CHAPTER IV

Surfactant-aided electrospraying of low molecular weight carbohydrate polymers from aqueous solutions

CHAPTER IV: Surfactant-aided electrospraying of low molecular weight carbohydrate polymers from aqueous solutions

ABSTRACT

In this work it is demonstrated, for the first time, that it is feasible to develop, using the electrospraying technique, low molecular weight carbohydrate-based capsule morphologies from aqueous solutions through the rational use of surfactants. Two different low molecular weight carbohydrate polymers were used, a maltodextrin and a commercial resistant starch. The solution properties and subsequent high voltage sprayability was evaluated upon addition of non-ionic (Tween-20, and Span-20) and zwitterionic (lecithin) surfactants. The morphology and molecular organization of the structures obtained was characterized and related to the solution properties. Results showed that, while unstable jetting and dropping occurred from the pure carbohydrate solutions without surfactant, the addition of some surface active molecules above their critical micelle concentration facilitated capsule formation. Higher surfactant concentrations led to smaller and more homogeneous capsule morphologies, related to lower surface tension and higher conductivity of the solutions.

Keywords: Electrospraying, electrospinning, encapsulation, surfactant, aqueous solution, carbohydrate

1. INTRODUCTION

The development of micro-, submicro- and nanostructures from biopolymers for functional food applications is an emerging area of interest. Apart from the conventional microencapsulation techniques, such as spray drying or coarcervation, electrospinning has been recently suggested to be a simple and straightforward method to generate submicron encapsulation structures for a variety of bioactive molecules (Xie et al. 2008; Lopez-Rubio & Lagaron, 2012; Bock et al. 2012). Electrospinning is a process that produces continuous polymer fibers with diameters in the submicrometer range through the action of an external electric field imposed on a polymer solution or melt. The electrospun nanostructures morphology is affected by the solution properties (mainly by the viscosity, surface tension and conductivity of the polymer solution) and by the process parameters (voltage, flow rate of the solution, tip-to-collector distance). For certain materials, size-reduced capsules can be obtained when lowering the polymer concentration and/or increasing the tip-to-collector distance. In this case, the electrospinning process is normally referred to as "electrospraying" due to the non-continuous nature of the structures obtained. To date, a wide variety of polymers and polymer blends have been electrospun, with synthetic polymers yielding the best results in terms of physical properties and uniformity. On the other hand, electrospinning of biopolymer solutions has been proven to be difficult due to several factors such as the polycationic nature of many biopolymers, the low chain flexibility which complicates chain entanglements (essential for fiber formation) and their generally poor

solubility in organic solvents (Kriegel et al. 2009). Moreover, unlike synthetic polymers, a natural polymer derived from different sources presents widely varying properties and it has been observed that the viscosity of the solutions may vary with time due to, for instance, aqueous hydrolysis of the biopolymer (Bhattarai & Zhang, 2007).

Electrospinning from aqueous solutions is beneficial from an environmental point of view. Furthermore, the use of water does not generate toxicity problems. On the contrary, organic solvents may be even prohibited for certain applications, such as in the case of food products (Kriegel et al. 2010). That issue further complicates the electrospinning process due to the ionization of water molecules at high voltages in an air environment, which may cause corona discharge. Besides, aqueous solutions present high surface tension values which hinder the formation of stable jets during the electrospinning. Moreover, polymers that have low aqueous solubility, low Mw polymers and polymers with rigid or globular structures that do not generate sufficient viscosity are not easily electrospun when they are in an aqueous solution (Nagarajan et al. 2007; Stijnman et al. 2011).

Different surfactants have been added to the electrospinning solutions for various purposes, like enzyme stabilization (Herricks et al., 2005), creation of mesoporous structures (Hong et al. 2009; Hou et al., 2009), or to make compatible hydrophilic fillers with hydrophobic matrices (Kim et al. 2006). However, more importantly, surfactants have been seen to improve the spinnability of polymer solutions, which is normally a consequence of the reduction in their surface tension (Bonino et al., 2011). To the best of our knowledge, all the studies carried out to date

in this area, relate to fiber formation and it has been demonstrated that addition of surfactants reduce fiber defects, but do not promote fiber formation for solutions which are not readily spinnable (Aceituno-Medina et al. 2013). However, the effect of surfactant addition on the sprayability or capsule formation from biopolymer solutions is unknown.

In this study, we hypothesize that addition of surfactants to aqueous biopolymer solutions may prove to be a convenient method to produce encapsulation structures by modulating the electrospraying conditions. To test this hypothesis, various surfactants (a zwitterionic and two nonionic surfactants) were added to two different low molecular weight carbohydrate polymer solutions. Solutions were subjected to electrospraying and the influence of surfactant type and charge on solution properties and on the morphology of the submicron structures generated were evaluated.

2. MATERIALS AND METHODS

2.1 Materials

A maltodextrin with a DE value of 16.5-19.5 was purchased from Sigma Aldrich. A commercial resistant starch (derived from corn starch) was Fibersol® (www.fibersol.com) commercial grade. The non-ionic surfactants, polyoxyethylene sorbitan monolaureate (Tween-20) and sorbitan monolaureate (Span-20), and the zwitterionic surfactant, L-α-phosphatidylcholine (lecithin) were supplied by Sigma-Aldrich. All products were used as received without further purification.

2.2 Determination of the critical micelle concentrations (CMC) for each surfactant by plate tensiometry

The CMC of surfactants in the absence and presence of the low molecular weight carbohydrate polymers was determined by measuring the surface tension as a function of surfactant concentration through a digital tensiometer (model EasyDyne K20, Krüss GmbH, Hamburg, Germany) using the Wilhemy plate method. An amount of 30 g of each test solution was poured into an 80 mm diameter glass beaker. The glass had been previously rinsed with absolute ethanol and deionized and distilled water and then dried at 70ºC to remove any surface-active material. All measurements were done in triplicate after equilibrating the solutions at 25ºC.

2.3 Preparation of carbohydrate-based solutions

Carbohydrate-based solutions were prepared by dissolving a 20 wt.-% of the materials in distilled water through gentle stirring at room

temperature. Different concentrations of the various surfactants (0, 5, and 30 wt.-% with respect to the biopolymer weight) were added to the solutions.

2.4 Characterization of the carbohydrate-based solutions

The apparent viscosity (ηa) of the polymeric solutions at 100 s^{-1} was determined using a rotational viscosity meter Visco Basic Plus L from Fungilab S.A. (San Feliu de Llobregat, Spain) using a Low Viscosity Adapter (LCP). The surface tension of the biopolymer solutions was measured using the Wilhemy plate method in an EasyDyne K20 tensiometer (Krüss GmbH, Hamburg, Germany). Both tests were carried out in triplicate. The conductivity of the solutions was measured using a conductivity meter XS Con6 (Labbox, Barcelona, Spain). All measurements were made at 25 ºC.

2.5 Preparation of carbohydrate-based capsules through electrospraying

The electrospinning apparatus, equipped with a variable high-voltage 0-30 kV power supply, was a single needle Fluidnatek® basic setup from Bioinicia S.L. (Valencia, Spain). The syringe containing the carbohydrate solutions was placed horizontally to the collector. The distance between the needle and the collector was set at 10 cm. The experimental setup was housed in a laminar flow safety cabinet. The electrosprayed capsules were obtained using a voltage of 9 kV and a flow rate of 0.15 mL/h.

2.6 Infrared spectroscopy

Attenuated total reflectance infrared spectroscopy (ATR-FTIR) experiments were performed in a controlled chamber at 21 ºC and 40% RH coupling the ATR accessory GoldenGate of Specac Ltd. (Orpington, UK) to a Bruker (Rheinstetten, Germany) FTIR Tensor 37 equipment. All the spectra were collected within the wavenumber range of 4000–600 cm^{-1} by averaging 15 scans at 4 cm^{-1} resolution. Analysis of the spectral data was performed by using Grams/AI 7.02 (Galactic Industries, Salem, NH, USA) software.

2.7 Scanning electron microscopy (SEM)

SEM was conducted on a Hitachi microscope (Hitachi S-4100) at an accelerating voltage of 10 KV and a working distance of 15 mm. The electrosprayed capsules were sputtered with a gold-palladium mixture under vacuum before their morphology was examined using SEM. Capsule diameters of the electrosprayed materials were measured by means of the Adobe Photoshop CS3 extended software from the SEM micrographs in their original magnification.

3. RESULTS AND DISCUSSION

3.1. Critical micelle concentration (CMC) of the different surfactants

Surfactants are amphiphilic molecules that readily absorb at surfaces, thereby lowering surface or interfacial tension of the medium in which they are dissolved. Moreover, above a critical concentration, the so-called critical micelle concentration, surfactants self-assemble to form a variety of colloidal structures, which have different properties from those of the dissolved surfactant monomers, e.g., solubility, surface hydrophilicity, charge density. Previous studies have demonstrated that addition of non-ionic and ionic surfactants above their critical micelle concentration to polymer solutions, significantly improved the electrospinning process generating defect-free fibers (Kriegel et al., 2009). Therefore, in this study, the first intention was to add different surfactants above their CMC to study their influence on the sprayability of low Mw carbohydrates. The CMC informs about the concentration of surfactant necessary to form a monolayer of molecules oriented about the air-water interface (Lin et al. 2004; Chou et al. 2005). On the other hand, the concentration needed for the polymer-surfactant association is the critical aggregation concentration (CAC) and it is usually lower than the CMC by a factor between 1 and 10. Both the surfactant concentration and the polymer-surfactant interactions may result in changes in the rheology and conductivity of the solutions, factors which greatly affect the electrospinning/ electrospraying process (Lin et al. 2004).

Initially, the surface tension for different surfactant concentrations in aqueous solution in the absence and presence of the low molecular weight carbohydrates was measured and CMC values were determined when the plateau in surface tension was obtained. Table 1 shows the CMC values for the different surfactants assayed and the concentration added in the solutions. For all the solutions tested it was observed that very low concentrations of the surfactants were needed to reach the CMC, regardless of whether the carbohydrates were present. It was also observed that CMC increased with the addition of the biopolymers probably because the surfactants were also interacting with the biopolymers in solution. It is possible that in the presence of carbohydrates, the concentration of the surfactants in the surface decreased, as part of the surfactant was bound to the carbohydrates. As a result, the amount of surfactant needed to reach the CMC increased (Chou et al., 2005). Knowing this plateau value, two different concentrations of each surfactant (5 and 30 wt.%) were added to the carbohydrate solutions, which corresponded to 28.9 mM of Span-20, 8.2 mM of Tween-20 and 13.2 mM of lecithin when 5% of surfactant with respect to the biopolymer weight was added; and 173.2 mM of Span 20, 49.0 mM of Tween 20 and 79.0 mM of lecithin when 30% of surfactant with respect to the biopolymer weight was incorporated. Please note that both concentrations were well higher than the CMC of the surfactants.

Table 1. Critical micelle concentration (CMC) of the different surfactants in aqueous solution in absence and presence of the carbohydrates.

	CMC surfactant (mM)		
Carbohydrate (wt-%)	Span-20	Tween-20	Lecithin
Aqueous solution	0.04	0.01	0.12
Resistant starch 20%	0.1	0.03	0.16
Maltodextrin 20%	0.1	0.05	0.16

3.2. Solution properties

The physical properties of the carbohydrate-surfactant solutions are critical in the successful preparation of the electrosprayed structures. Therefore, the conductivity, viscosity and surface tension of the different solutions were measured and the results are summarized in Table 2. From these data it is observed that the addition of resistant starch to water did not considerably increase the conductivity of the solvent because this material did not present any electrical charge. On the contrary, the maltodextrin-based solutions presented enhanced conductivity values. This fact could be due to maltodextrin forming charged ions when dissolved in water. From Table 2, it is also observed that addition of non-ionic surfactants to the resistant starch solutions produced a slight increase in the conductivity, probably due to the existence of polar groups in this molecule (Lin et al. 2004). However, when Span-20 and Tween-20 were incorporated to the maltodextrin solutions, they did not affect the conductivity, showing that the effect of these surfactants in the solution conductivity is very limited and it is only

relevant when the solution presents very low conductivity. In contrast, addition of lecithin led to higher conductivity in both carbohydrate solutions. This fact was related to the zwitterionic nature of the lecithin which presents asymmetric positive and negative electric charges. These charges were dissociated in aqueous solution and thus, led to an increase of the electrical conductivity (Hunley et al. 2010). Concerning the viscosity, it was seen that very low values were obtained regardless the absence or presence of the surfactants. These results were expected, since the low molecular weight carbohydrates used in this study would require greater concentrations to achieve comparable solution viscosities to high molecular weight polymers. In particular, the addition of Span-20 and Tween-20 hardly increased the viscosity values. However, addition of lecithin increased the solutions viscosity from ca. 2 to 5 cP, probably because the interactions between the carbohydrates and the ionic surfactant were stronger than those with the non-ionic surfactants. Nevertheless, low viscosity values are needed for electrospraying, since higher viscosity favors the formation of fibers instead of spherical capsules (beads) (Fong et al. 1999). Finally, Table 2 shows the surface tension of the different solutions assayed. It was observed that surface tension values of surfactant-free solutions were over 50 mN/m, due to the high surface tension of water, which was the solvent used in the solutions. Addition of the different surfactants led to a decrease in surface tension, reaching the plateau values obtained for the CMC of the different surfactants. In general, it can be stated that increasing the surfactant concentration led to greater conductivity and viscosity values.

Table 2. Conductivity, viscosity and surface tension of the carbohydrate-surfactant solutions.

Matrix	Surfactant	Surfactant concentration (%)	Conductivity (μS)	Viscosity (cP)	Surface Tension (mN/m)
Resistant starch	-	0	16.85	2	56.00
	Span 20	5	33	2.37	26.07
		30	73	2.31	25.87
	Tween 20	5	35	2.16	31.03
		30	136.3	2.82	35.43
	Lecithin	5	208	2.15	30.00
		30	862	5.4	27.50
Maltodextrin	-	0	798	2.23	52.67
	Span 20	5	790	2.22	25.27
		30	786	2.42	24.7
	Tween 20	5	802	2.24	35.10
		30	843	2.31	35.00
	Lecithin	5	928	2.83	32.50
		30	1776	5.3	26.2

3.3. Morphology of the electrosprayed carbohydrates

The electrospraying of all the solutions was performed under the same processing conditions (cf. section 2.5). Initially, the carbohydrate-aqueous solutions without surfactants were electrosprayed and it was observed that although the commercial resistant starch formed spherical capsules with sizes ranging from a few nm to ~2 μm with an average size of 0.6 ± 0.3 μm (image not shown), extensive dropping occurred due to unstable electrospraying. On the other hand, it was not possible to obtain any electrosprayed structure from the maltodextrin aqueous solution. These results can be explained by the physical properties of the solutions. As it was commented before, both

carbohydrate solutions presented high surface tension and low viscosity values; however, resistant starch did not greatly increase the conductivity of the solution, while the addition of maltodextrin produced very high conductivity values. Stable electrospraying or electrospinning is known to be attained when the electrostatic forces inside the droplets (the coulomb repulsions), which are achieved due to electrical conductivity and the electric field applied, are strong enough to overcome the surface tension effect (Zhang & Kawakami, 2010). In this case, the interface of the droplets can be deformed and the Taylor cone and the subsequent electrospraying process can be achieved. Thus, in the case of the resistant starch solution, the dropping probably occurred due to the combination of high surface tension and low conductivity. In contrast, when the coulombic repulsions are too high and overcome the viscoelastic forces, less chain entanglements take place during electrospraying and thus, very small particles or non-defined structures are obtained (Bock et al., 2012). Therefore, the addition of maltodextrin produced an excessive increase of the conductivity which completely hindered the electrospraying process.

The addition of surfactants to the carbohydrate aqueous solutions produced a decrease in surface tension which favored the formation of electrosprayed structures. Figure 1 shows the SEM images and corresponding size distribution of the materials obtained from the electrospraying of the different resistant starch solutions. From Figures 1A and 1B it was seen that, regardless of concentration, when Span-20 was added to the resistant starch solution, three different capsule size populations were found, although the structures were smaller and more

homogeneous in size when 30% of the surfactant was added. Figures 1C and 1D show that the addition of 5% of Tween-20 also generated three populations with respect to the capsules diameter. However, when the concentration was increased to 30%, only two different size distributions and smaller capsules were attained. On the other hand, when lecithin was included in the solutions, only one population with respect to the capsule's diameters was seen (Figures 1E and 1F). Moreover, the particle size was greatly reduced when compared to capsules obtained from the carbohydrate without surfactant. Thus, the average size in this case was 0.3 ± 0.1 µm and 0.2 ± 0.1 µm when 5% and 30% of lecithin was added respectively. The variations observed between the different structures can be mainly attributed to the electrical conductivity of the solutions. It is known that higher conductivity leads to a decrease in size because Coulombic repulsion forces compete with the viscoelastic forces of the solution and disentangle more easily the polymer network formed during electrospraying. In other words, increasing conductivity makes it easier for the solution to be broken up into smaller droplets (Gañan-Calvo et al. 1997; Bock et al., 2012).

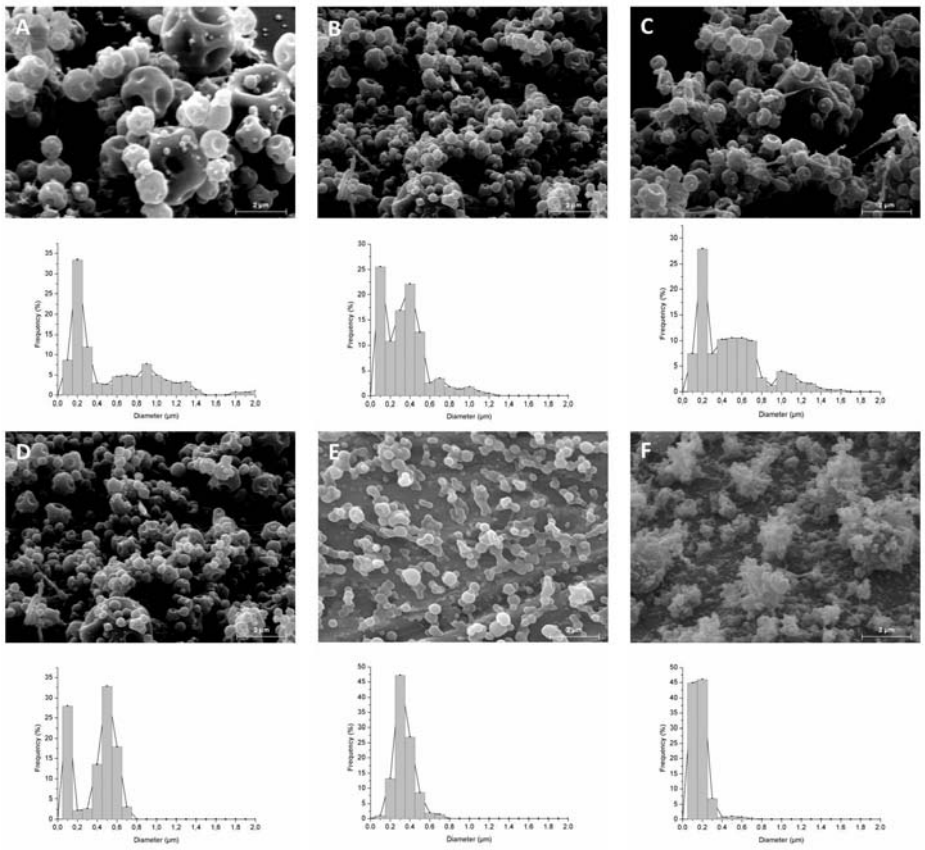

Figure 1. Selected SEM images (up) and their corresponding capsule size distribution (down) of resistant starch-based structures with the different surfactants: (A) 5% Span-20; (B) 30% Span-20; (C) 5% Tween-20; (D) 30% Tween-20; (E) 5% lecithin and (F) 30% lecithin.

Regarding the maltodextrin structures, Figure 2 shows the SEM images and corresponding size distribution of the materials obtained. It is observed that the addition of non-ionic surfactants allowed the formation of almost mono-disperse particles from a few nm to 500 nm (Figures 2A to 2D). This fact was explained from the surface tension decrease produced by the surfactants. Viscoelastic and electrical forces

must overcome the surface tension effect in order to obtain a defined structure. When surfactants were not added to the maltodextrin solution, the droplets formed on the needle tip grew until its mass was large enough to escape and electrospraying could not occur (Xu & Hanna, 2006). However, the addition of the non-ionic surfactants reduced the surface tension and thus, a conical meniscus was formed on the needle tip. The meniscus further deformed and broke into droplets with small particle sizes and narrow size distribution due to the electrostatic force introduced by the maltodextrin. Nevertheless, when 30% of Tween-20 was added to the solution, the electrical conductivity increased and different capsule morphologies were obtained, probably because the high electrical forces favored weak entanglements in the polymer (Bock et al., 2012). The addition of lecithin produced an excessive increase in the conductivity which completely hindered capsule formation.

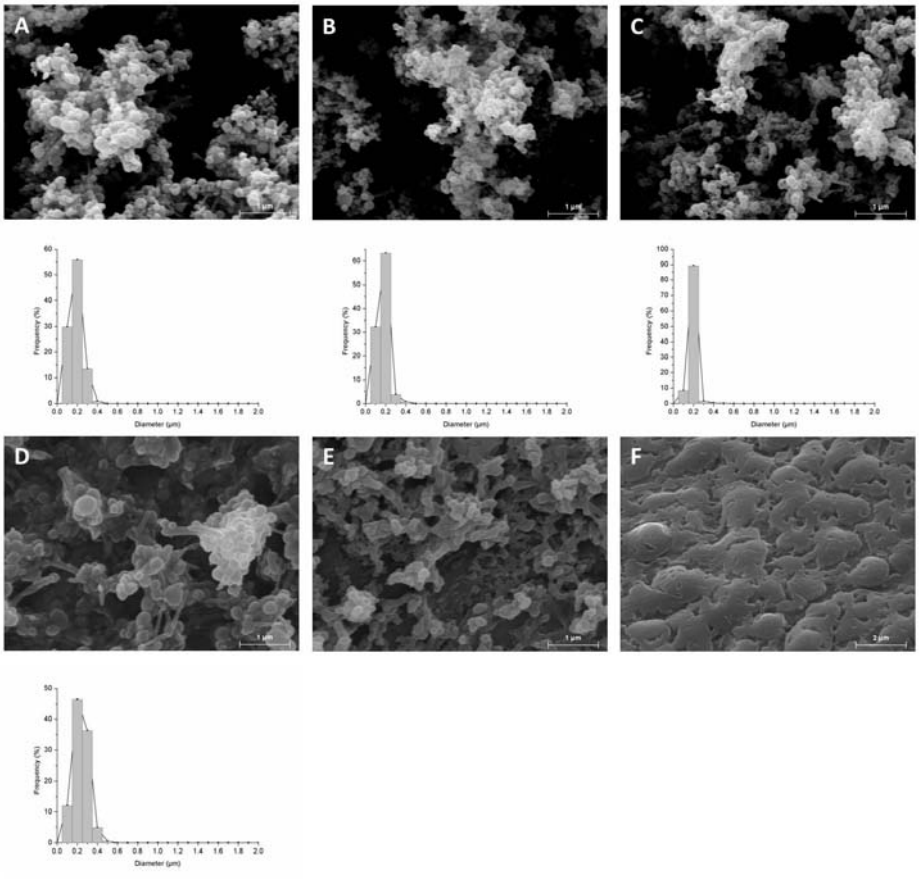

Figure 2. Selected SEM images and their corresponding capsule size distribution of maltodextrin-based structures with different surfactants: (A) 5% Span-20; (B) 30% Span-20; (C) 5% Tween-20; (D) 30% Tween-20; (E) 5% lecithin and (F) 30% lecithin.

It is interesting to note that, apart from the capsular morphology generated, addition of surfactants also led to needle-like morphologies in both carbohydrate matrices, thus confirming that addition of these amphiphilic molecules, which decreased the surface tension of the aqueous solutions, considerably enhanced chain entanglements.

In general, from the morphology of the structures obtained, it can be stated that non-ionic surfactants are more suitable for generating encapsulation structures from low molecular weight carbohydrate polymers, and that the size and size distribution can be modified by the type and amount of surfactant added.

3.4 Infrared spectra of the encapsulates

ATR-FTIR analyses were done in order to characterize the molecular organization of the structures attained, as well as to confirm the presence of the surfactants in the carbohydrate structures. In first place, the region from 800 to 1200 cm^{-1} was analyzed for all the materials obtained. This area presents the characteristic vibrational bands of the carbohydrates, corresponding to the stretching vibrations of C-O and C-C groups, and the bending vibration of C-O-H (Wolkers et al. 2004; Kacurakova & Mathlouthi, 1996). From Figure 3 it was observed that when surfactants were added to the resistant starch, these bands were shifted by approximately 2-6 cm^{-1} suggesting that there was a chemical interaction between the carbohydrate and the surfactants. Specifically, the most noted shift was observed for the band which arose at 1006 cm^{-1} in the resistant starch (Figures 3A to 3C). This band was shifted towards higher wavenumbers in the surfactant/polymer capsules, which could mean stronger hydrogen bonding due to the interaction of the carbohydrate with the surfactants (Wolkers et al. 2004). It is interesting to note that greater band shifts were related to smaller capsule mean diameters, which may be probably explained by the greater specific surface present in the material containing smaller capsules. Moreover, in this specific carbohydrate polymer, i.e. the resistant starch, a clear

change in band shape was also observed in the spectral range 950-1050 cm^{-1}, which also resulted in narrower bands in the encapsulates containing the surfactants, indicating that surfactant addition led to greater molecular order. On the contrary, for the maltodextrin structures (Figures 3E to 3F), the characteristic carbohydrate bands hardly shifted with the incorporation of the surfactants, indicating that their interaction with the polymer may be less intense than in the previous case. Nevertheless, it was seen that lecithin produced the greatest band displacements for both polymer matrices probably because it is a zwitterionic surfactant which presented a stronger interaction with the polymers (Lin et al. 2004).

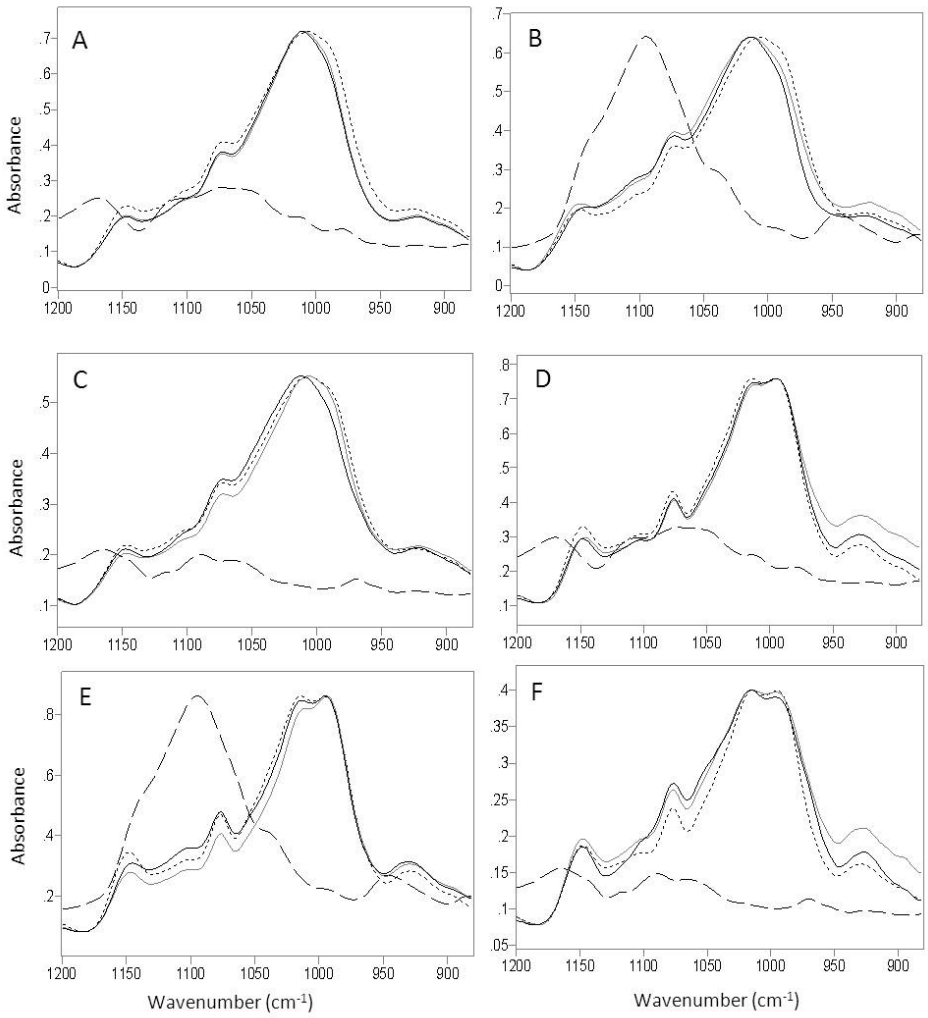

Figure 3. ATR-FTIR spectra from 1200 to 880 cm^{-1} for the pure carbohydrate (dotted line), the surfactants (dashed line), the carbohydrate with 5% of surfactant (gray line) and with 30% of surfactant (black line) for: (A) resistant starch/Span-20; (B) resistant starch/Tween-20; (C) resistant starch/lecithin; (D) maltodextrin/Span-20; (E) maltodextrin/Tween-20; and (F) maltodextrin/lecithin.

Furthermore, the most characteristic band of the surfactants which was not overlapped with the carbohydrate bands was considered to determine the effect of the concentration of the surfactants in the electrosprayed material. Figure 4 shows the capsule's spectra from 1800 to 1600 cm^{-1} where the band corresponding to the carbonyl group, at around 1740 cm^{-1}, attributed to the surfactants was located. From the spectra, it was observed that the surfactants were incorporated in all the structures, since this peak appeared in all the materials. It is worth noting that the lecithin band showed the greatest shift when it was combined with the polymers, thus confirming the stronger interaction between the ionic surfactants with the polymers. Moreover, this peak could also reveal the amount of surfactant included in the initial solutions, since it was more intense with the increasing concentration of the surfactant.

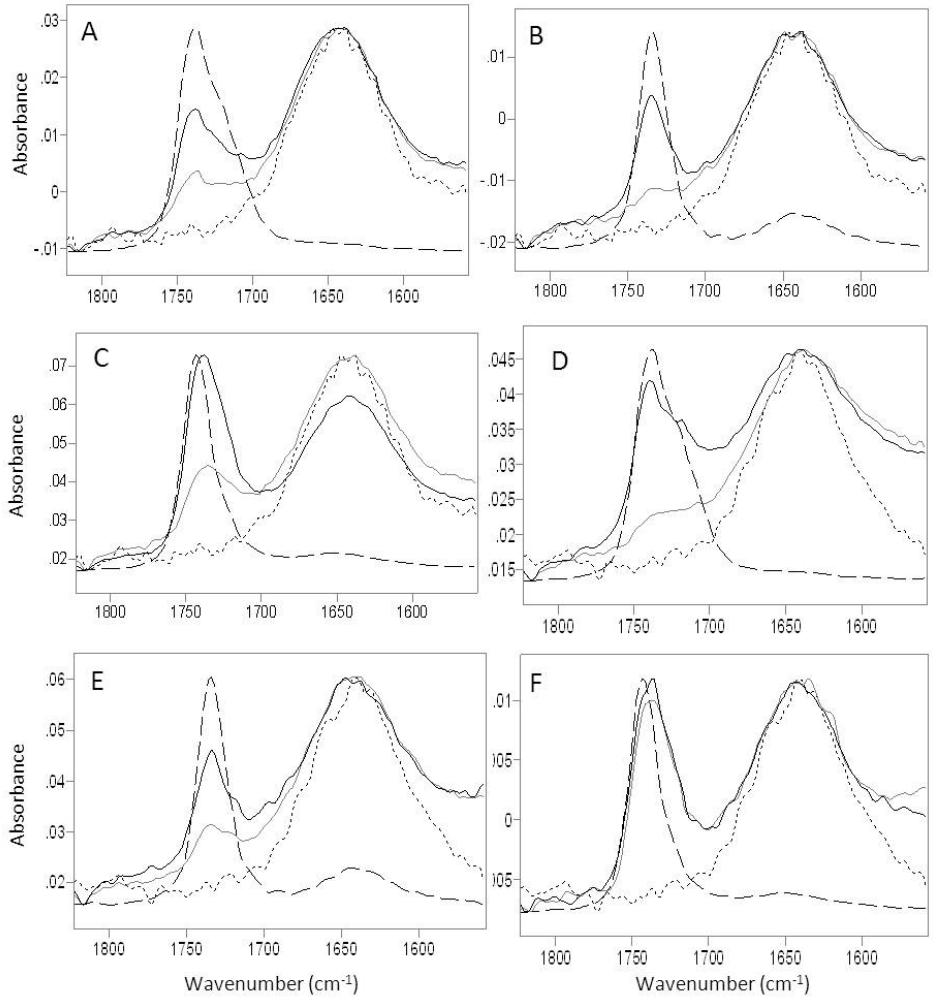

Figure 4. ATR-FTIR spectra from 1600 to 1800 cm^{-1} for the pure carbohydrate (dotted line), the surfactants (dashed line), the carbohydrate with 5% of surfactant (gray line) and with 30% of surfactant (black line) for: (A) resistant starch/Span-20; (B) resistant starch/Tween-20; (C) resistant starch/lecithin; (D) maltodextrin/Span-20; (E) maltodextrin/Tween-20; and (F) maltodextrin/lecithin (F).

4. CONCLUSIONS

In this work it is demonstrated that addition of surfactants considerably improves the electrospraying of low Mw carbohydrate aqueous polymer solutions. Specifically, ultrathin capsules made from a commercial resistant starch and a maltodextrin with Span-20, Tween-20 or lecithin were developed. This was mainly due to a reduction in the surface tension caused by surfactant addition, which stabilized the electrospraying process. However, it has also been shown that the type and amount of surfactant greatly influenced the morphology and size distribution of the encapsulation structures generated. In general, it can be stated that non-ionic surfactants were more suitable for the electrospraying of low Mw carbohydrate solutions, as electrically charged surfactants gave rise to fused and too small structures. FTIR results showed that the surfactants were effectively incorporated in the carbohydrate polymers and while greater molecular order and different capsule sizes were obtained from resistant starch solutions by changing the type and concentration of surfactant, only very small structures were formed from maltodextrin solutions, due to their high electrical conductivity. These results are highly interesting for the development of encapsulation structures for food-related applications where the use of aqueous solutions is mandatory.

5. REFERENCES

Aceituno-Medina, M., Lopez-Rubio, A., Mendoza, S., & Lagaron, J.M. (2013). Development of novel ultrathin structures based in amaranth (Amaranthus hypochondriacus) protein isolate through electrospinning. Food Hydrocolloids 31, 289-298.

Bhattarai, N., & Zhang, M. (2007). Controlled synthesis and structural stability of alginate-based nanofibers. Nanotechnology 18, 455601.

Bock, N., Dargaville, T.R. & Woodruff, M.A. (2012). Electrospraying of polymers with therapeutic molecules: State of the art. Progress in Polymer Science 37, 1510-1551

Bonino, C.A., Krebs, M.D., Saquing, C.D., Jeong, S.I., Shearer, K.L., Alsberg, E., Khan, S.A. (2011). Electrospinning alginate-based nanofibers: From blends to crosslinked low molecular weight alginate-only systems. Carbohydrate Polymers 85, 111-119.

Chou, D.K., Krishnamurthy, R., Randolph, T.W., Carpenter, J.F., Manning, M.C. (2005). Effects of Tween 20 and Tween 80 on the stability of albutropin during agitation. Journal of Pharmaceutical Sciences 94, 1368-1381.

Fong, H. Chun, I. & Reneker, D. H. (1999). Beaded nanofibers formed during electrospinning. Polymer 40, 4585-4592.

Herricks, T.E., Kim, S.-H., Kim, J., Li, D., Kwak, J.H., Grate, J.W., Kim, S.H., & Xia, Y. (2005). Direct fabrication of enzyme-carrying polymer nanofibers by electrospinning. Journal of Materials Chemistry 15, 3241-3245.

Hong, Y., Fan, H., & Zhang, X. (2009). Synthesis and protein adsorption of hierarchical nanoporous ultrathin fibers. Journal of Physical Chemistry B 113, 5837-3842.

Hou, Z., Yang, P., Lian, H., Wang, L., Zhang, C., Li, C., Chai, R., Cheng, Z., & Lin, J. (2009). Multifunctional hydroxyapatite nanofibers and microbelts as drug carriers. Chemistry - A European Journal 15, 6973-6982.

Hunley, M.T., England, J.P. & Long, T.E. (2010). Influence of counteranion on the thermal and solution behavior of Poly(2-(dimethylamino)ethyl methacrylate)-Based Polyelectrolytes. Macromolecules 43, 9998-10005.

Kacurakova, M. & Mathlouthi, M. (1996). FTIR and laser-Raman spectra of oligosaccharides in water: characterization of the glycosidic bond. Carbohydrate Research, 284, 145–157.

Kim, H.-W., Lee, H.-H., & Knowles, J.C. (2006). Electrospinning biomedical nanocomposite fibers of hydroxyapatite/poly(lactic acid) for bone regeneration. Journal of Biomedical Materials Research Part A, 79A, 643-649.

Kriegel, C., Kit, K.M., McClements, D.J., & Weiss, J. (2009). Influence of surfactant type and concentration on electrospinning of chitosan-poly(ethylene oxide) blend nanofibers. Food Biophysics 4, 213-228.

Kriegel, C., Kit, K.M., McClements, D.J., & Weiss, J. (2010). Nanofibers as carrier systems for antimicrobial microemulsions. II. Release characteristics and antimicrobial activity. Journal of Applied Polymer Science 118, 2859-2868.

Lin, T., Wang, H.X., Wang, H.M.,& Wang, X.G. (2004). The charge effect of cationic surfactants on the elimination of fibre beads in the electrospinning of polystyrene. Nanotechnology 15, 1375–1381.

Lopez-Rubio, A. & Lagaron, J.M. (2012). Whey protein capsules obtained through electrospraying for the encapsulation of bioactives. Innovative Food Science and Emerging Technologies 13, 200-206.

Nagarajan, R., Drew, C., & Mello, C.M. (2007). Polymer-micelle complex as an aid to electrospinning nanofibers from aqueous solutions. The Journal of Physical Chemistry C 111, 16105-16108.

Stijnman, A.C., Bodnar, I. & Hans Tromp, R. (2011). Electrospinning of food-grade polysaccharides. Food Hydrocolloids 25, 1393-1398.

Wolkers, W.F., Oliver, A.E., Tablin, F. & Crowe, J.H. (2004). A Fourier-transform infrared spectroscopy study of sugar glasses. Carbohydrate Research 339, 1077-1085.

Xie, J., Li, X. & Xia, Y (2008). Putting electrospun nanofibers to work for biomedical research. Macromolecular Rapid Communications 29, 1775-1792.

Xu, Y. & Hanna, M.A. (2006). Electrospray encapsulation of water-soluble protein with polylactide. Effects of formulations on morphology, encapsulation efficiency and release profile of particles. International Journal of Pharmaceutics 320, 30-36.

Zhang, S.L. & Kawakami, K. (2010). One-step preparation of chitosan solid nanoparticles by electrospray deposition. International Journal of Pharmaceutics. 397, 211-217.

CHAPTER V

Development and optimization of novel encapsulation structures of interest in functional foods through electrospraying

CHAPTER V: Development and optimization of novel encapsulation structures of interest in functional foods through electrospraying

ABSTRACT

The aim of this work was to establish strategies for the development of electrosprayed encapsulation structures, of interest in food applications, based on aqueous hydrocolloid solutions. Specifically, various polysaccharides and two different proteins were evaluated for capsules formation. To this aim, the hydrocolloid solution properties were analysed and compared with the solution properties of two polymers readily spinnable in water (PVOH and PEO). Increasing the hydrocolloid concentration to promote chain entanglements resulted in a valid strategy only for a few matrices (related to their greater Mw). As alternative strategies to improve the physical properties and, thus, the sprayability of the solutions, addition of gums and surfactants to modify the viscosity and surface tension of the solutions, respectively, was evaluated. Moreover, denaturation of proteins was also carried out in order to investigate the effect of this treatment on the electrospraying process and on capsules formation. Results showed that the incorporation of some of these molecules, as well as protein denaturation, significantly changed the solution properties, allowing the development of encapsulation structures from all the hydrocolloids assayed. The morphology of the structures obtained was characterized and the molecular organization of some of the capsules was studied and related to the electrosprayability and capsules morphology.

Keywords: electrospinning, electrospraying, encapsulation, hydrocolloids, bioactives

1. INTRODUCTION

The encapsulation of food and nutraceutical ingredients is an emerging area of interest due to the instability of some of these compounds at ambient and digestive conditions (Ezhilarasi et al. 2013). In general, encapsulation seeks to protect these products and, thus, assure their health-promoting properties, although it can also be used to improve sensorial properties of food products containing ingredients that inherently have undesirable flavours and/or odours (Nasirullah et al. 2011).

Apart from the conventional microencapsulation techniques, such as spray drying or coarcervation, electro-hydrodynamic processes have been recently suggested to be simple and straightforward methods to generate submicron encapsulation structures for a variety of bioactive molecules (Xie et al. 2008; Lopez-Rubio and Lagaron 2012; Bock et al. 2012; Pérez-Masiá et al. 2013, Bakhshi et al. 2013). These techniques use electrostatic forces to produce electrically charged jets from viscoelastic polymer solutions which on drying, by the evaporation of the solvent, produce ultrathin structures (Li and Xia 2004). When ultrathin continuous fibres are obtained, the process is called “electrospinning”. When size-reduced capsules are attained, the process is normally referred to as “electrospraying” due to the non-continuous nature of the structures obtained. For food and nutraceutical applications, capsules are generally preferred, since apart from facilitating handling and subsequent incorporation into different products, they also present greater surface/volume ratio and, thus, are expected to have better release profiles than fibres (Hong et al. 2008). The morphology and composition of micro/nanostructures attained can be modulated through controlling the process parameters, mainly the operational conditions (the high voltage

applied, the distance between the spinneret and the collector and the feeding rate), the solution properties (the viscosity, the surface tension and the electrical conductivity), and the material of choice. Specifically, for food and nutraceutical applications, the encapsulating material should be suitable for human consumption. Moreover, although during the electrospraying process the solvent should be completely evaporated, it may be convenient to only make use of allowed food contact solvents in order to avoid toxicity problems, as it has been proven that a certain amount of solvent can remain in the electrospun structures (Aceituno-Medina et al. 2013).

Electrospraying from aqueous solutions, apart from not generating toxicity problems, has the advantage of being beneficial from an environmental point of view. However, the use of water further complicates electrospraying due to the ionization of water molecules at high voltages in an air environment, which may cause corona discharge. Besides, aqueous solutions present high surface tension values which hinder the formation of stable jets during the process. Nevertheless, it is possible to obtain micro- and nanocapsules through electrospraying from aqueous solutions using some biopolymers such as polyvinyl alcohol (PVOH) or polyethylene oxide (PEO). These biopolymers have been already used for capsules formation through electro-hydrodynamic processes, mainly for pharmaceutical and medical applications (Sridhar et al. 2011; Zamani et al. 2013). However, for the incorporation of the micro/nanocapsules within food matrices, the use of food hydrocolloids as encapsulating matrices is highly preferred, not only for achieving a better integration of the capsules in the foodstuffs, but also to improve assimilation of the capsules from the consumers. The use of food hydrocolloids further complicates the electrospraying process, since these materials are usually low

molecular weight polymers which do not generate sufficient viscosity and that generally have strong inter- and intramolecular forces, which need to be somehow counteracted to promote capsule formation (Nagarajan et al. 2007; Stijnman et al. 2011).

In this work, a thorough study about the electrospraying of different food hydrocolloids from aqueous solutions has been carried out. Specifically, various polysaccharides, such as dextran, maltodextrin, a resistant starch, pullulan and fructooligosaccharides (FOS), and two proteins (a whey protein concentrate from milk and a soy protein isolate) were evaluated as matrix materials. To this aim, different hydrocolloid aqueous solutions were prepared, characterized and compared with the physical properties of aqueous solutions made from spinnable polymers in water (specifically, PVOH and PEO). Specifically, the viscosity, surface tension and electrical conductivity of the solutions were evaluated. Afterwards, the physical properties of the solutions were optimized for the electrospraying process through the incorporation of different substances. Particularly, the influence of gums on the solution viscosity and the effect of surfactant addition on the surface tension values were studied when capsules could not be attained from the neat hydrocolloidal solutions. Moreover, denaturation of the proteins was also carried out in order to understand how this change in molecular conformation affected capsules formation. The morphology of the structures attained was analysed through scanning electron microscopy (SEM) and the molecular organization of the capsules was studied through attenuated total reflectance infrared spectroscopy (ATR-FTIR).

2. MATERIALS AND METHODS

2.1. Materials

PVOH was kindly donated by Plásticos Hidrosolubles (Spain). The commercial resistant starch was Fibersol® (www.fibersol.com) commercial grade, manufactured by ADM/Matsutani (Iowa, USA). This material is considered to be a fraction of starch that can resist digestion. The fructooligosaccharides (FOS) used were Fibruline Instant (FI) and Fibrulose F97, which were kindly donated by InnovaFood S.L (Spain). Whey protein concentrate (WPC) was kindly donated by ARLA (ARLA Food Ingredients, Viby, Denmark). Under the commercial name Lacprodan® DI-8090, the composition per 100 g of product consisted of ~80 g of protein, ~9 g of lactose, and ~8 g of lipids, the rest being water and minerals like sodium and potassium. Soy protein isolate (SPI) was donated by The Solae Company (Switzerland). Guar gum was purchased at Capers Community Markets (Canada). PEO, dextran, maltodextrin (DE 16.5-19.5), pullulan, Xanthan gum, Span-20 and folic acid were supplied by Sigma-Aldrich (Spain) and they were used as received, without further purification.

2.2. Preparation of the solutions

The biopolymers (PVOH and PEO) and the SPI solutions were prepared by dissolving 5, 10 or 20% (w/v) of the polymers in distilled water. When higher concentrations of these materials were used, very dense solutions were obtained, which were difficult to characterize. The rest of the food hydrocolloid solutions (dextran, resistant starch, FOS, maltodextrin, pullulan and WPC) were prepared by dissolving 10, 20 or 40% (w/v) of the hydrocolloids in distilled water. 1% (w/w) of gums and/or 5% (w/w) of surfactant respect to the polymer weight were added when needed.

2.3. Characterization of the solutions

The apparent viscosity (ηa) of the polymeric solutions was determined using a rotational viscosity meter Visco Basic Plus L from Fungilab S.A. (San Feliu de Llobregat, Spain) using the Low Viscosity Adapter (LCP) spindle. The surface tension of the solutions was measured using the Wilhemy plate method in an EasyDyne K20 tensiometer (Krüss GmbH, Hamburg, Germany). The conductivity of the solutions was measured using a conductivity meter XS Con6 (Labbox, Barcelona, Spain). All measurements were made in triplicate at 25ºC.

2.4. Electrospraying process

The electrospraying apparatus, equipped with a variable high-voltage 0-30 kV power supply, was a Fluidnatek® basic setup assembled and supplied by BioInicia S.L. (Valencia, Spain). Details of the basic electrospraying setup can be found elsewhere (Torres-Giner et al. 2010).Solutions were introduced in a 5 mL plastic syringe and were electrosprayed under a steady flow-rate using a stainless-steel needle with internal diameter 0.9 mm. The needle was connected through a PTFE wire to the syringe. The syringe was lying on a digitally controlled syringe pump while the needle was in horizontal towards a stainless-steel plate attached to a copper grid used as collector. The experiment was carried out at ambient conditions (20 ºC and 40% RH). The conditions for obtaining the capsules were modified depending on the polymer used. Basically, the flow rate was set from 0.1 to 0.15 mL/h. Specifically, it was 0.1 for FOS solutions and 0.15 mL for the rest of the hydrocolloid solutions. The voltage varied from 9 to 16 kV and the distance between the tip and the collector varied from 9-20 cm.

2.5. Scanning electron microscopy (SEM)

SEM was conducted on a Hitachi microscope (Hitachi S-4100) at an accelerating voltage of 10 KV and a working distance of 12-16 mm. The capsules were sputtered with a gold-palladium mixture under vacuum before their morphology was examined using SEM. Capsule diameters were measured by means of the Adobe Photoshop CS3 extended software from the SEM micrographs in their original magnification.

2.6. Attenuated total reflectance infrared spectroscopy (ATR-FTIR)

ATR-FTIR spectra were collected at 25ºC in a FTIR Tensor 37 equipment (Bruker, Germany). The spectra were collected in the different materials by averaging 20 scans at 4 cm-1 resolution. The experiments were repeated twice to verify that the spectra were consistent between individual samples.

2.7. Statistical analysis

Statistical analysis of data was performed through analysis of variance (ANOVA) using Statgraphics Centurion XV (Manugistics Corp., Rockville, MD). Homogeneous sample groups were obtained by using LSD test (95% significant level).

3. RESULTS AND DISCUSSION

3.1. Characterization and comparison of PVOH and PEO vs. food hydrocolloids solution porperties and evaluation of their electrosprayability

The success of the electro-hydrodynamic process strongly depends on the solution properties. Thus, the physical properties of the PVOH and PEO polymers and food hydrocolloidal solutions were analysed and related to their electrospinnability/electrosprayability. The morphology of the structures obtained was also investigated. Table 1 shows the viscosity, the surface tension, the electrical conductivity and the electrospinnability of the different solutions prepared. This table also shows the capsule's morphology and the capsule's average size in the cases where it was possible to electrospun/electrospray the solutions. Generally, it was observed that the solutions containing the high molecular weight polymers (PVOH and PEO) had higher viscosities and lower surface tension values than the hydrocolloid-based solutions and both conditions favoured the electrospinning process. This physical properties of the solutions made that either capsules or fibres were attained from the different polymer solutions assayed. Regarding the hydrocolloidal solutions, it was seen that only a few aqueous hydrocolloidal solutions had the capacity of forming encapsulation structures through electrospraying. Specifically, only the hydrocolloids which presented a higher molecular weight and, thus, led to a significant viscosity increase when increasing the hydrocolloid concentration in the solution, were able to form capsules. These results can be explained on the basis of solution properties in relation with the electrospinning/electrospraying process. On one hand, it is well-known that electrospinning/electrospraying is only achieved when the solution viscosity is high enough to produce the necessary polymer

entanglements to form the fibres/capsules. On the other hand, the surface tension is also a crucial parameter for the process, since high surface tension values could overcome the electrostatic forces generated by the high voltage applied and the electrical conductivity of the solution and, thus, hinder the Taylor cone formation and the subsequent electrospinning/electrospraying process (Bock et al. 2012; Fong et al. 1999). Regarding the electrical conductivity, it was seen that this parameter did not considerably affect the process and, for similar viscosity and surface tension values, electrosprayability was not modified at different conductivity values. Nevertheless, it is worth noting that, if electrical conductivity is too high, there is too much charge carried by the electrospraying jet, fact that can destabilize the jet and complicate the process (Bock et al. 2012; Ding et al. 2005).

Regarding the capsules morphology it was seen that for PVOH and PEO at low polymer concentrations, beads were formed, while increasing the polymer concentration and, thus, the viscosity, fibres were obtained. This can be explained by an increase in the polymer chain entanglements when the viscosity was higher, which led to the formation of fibres. It is important to note that the chain entanglements also depend on the molecular weight of the polymers and, as a result, for similar viscosity values, different morphologies can be attained depending on the polymer used (Bock et al. 2012). Concerning the size of the structures developed, it was observed that a greater size distribution was obtained for the hydrocolloid-based capsules. This fact was probably due to the more unfavourable solution properties of these solutions, which destabilize the electrospraying jet and led to more heterogeneous structures.

Therefore, from Table 1 it was concluded that in order to carry out a stable electrospraying process, it was necessary to modify the viscosity and the surface tension of the food hydrocolloid solutions. Specifically, higher viscosities and lower surface tension values should be attained. Nevertheless, an exception was observed for the SPI solutions. In this case, it was seen that although the solution properties seemed to be appropriate for capsule development through electrospraying, unstable jetting occurred and encapsulation structures could not be developed from the SPI solutions. This fact could be related to the globular structure of the soy protein, with strong inter- and intramolecular forces which impeded chain entanglements between adjacent molecules needed for capsules formation (Vega-Lugo and Lim 2008). Therefore, protein thermal denaturation could improve the electrospraying process of SPI solutions since unfolding the protein chains could favour the formation of polymer entanglements.

Table 1. Solution properties and electrospinnability of the different matrices.

Matrix (%)		Viscosity (cP)	Surface Tension (mN/m)	Electrical Conductivity (μS)	Spinnability	Morphology	Average capsule's size (μm)
PVOH	5	9.1 ± 0.7^{a}	40.6 ± 0.6^{a}	181.3 ± 4.1^{a}	YES	Capsules + thin fibers	0.7 ± 0.2^{a}*
	10	28.2 ± 2.3^{b}	42.1 ± 0.1^{b}	300.0 ± 7.0^{b}	YES	Fibers	0.1 ± 0.1^{b}
	20	884.9 ± 14.1^{c}	43.7 ± 0.4^{c}	391.7 ± 2.1^{c}	YES	Fibers	0.2 ± 0.1^{b}
PEO ($M_w \sim 200000$)	5	58.1 ± 1.4^{a}	55.9 ± 1.5^{a}	144.6 ± 1.3^{a}	YES	Capsules + thin fibers	0.5 ± 0.1^{a}*
	10	374.1 ± 7.8^{b}	53.5 ± 0.2^{b}	144.4 ± 4.1^{a}	YES	Capsules + thin fibers	0.5 ± 0.1^{a}*
	20	18738.0 ± 106.2^{c}	50.1 ± 1.8^{c}	159.2 ± 2.0^{b}	YES	Fibers	0.3 ± 0.1^{b}
Dextran ($M_w \sim 70000$)	10	10.9 ± 0.5^{a}	57.3 ± 0.1^{a}	50.4 ± 2.3^{a}	NO	---	---
	20	28.8 ± 0.1^{b}	54.2 ± 0.3^{b}	28.9 ± 0.8^{b}	NO	---	---
	40	94.2 ± 2.9^{c}	59.3 ± 0.3^{c}	23.5 ± 0.5^{c}	YES	Capsules	0.9 ± 0.5^{a}
Resistant Starch ($M_w \sim 1700\text{-}2700$)	10	4.4 ± 0.5^{a}	59.2 ± 0.4^{a}	28.8 ± 2.2^{a}	NO	---	---
	20	5.5 ± 0.5^{a}	57.1 ± 1.6^{b}	18.0 ± 1.1^{b}	NO	---	---
	40	9.1 ± 0.9^{b}	57.9 ± 0.8^{ab}	18.9 ± 0.6^{b}	NO	---	---
Maltodextrin ($M_w \sim 1300$)	10	4.8 ± 0.5^{a}	52.0 ± 0.7^{a}	503.0 ± 1.4^{a}	NO	---	---
	20	5.2 ± 0.2^{a}	52.7 ± 0.1^{a}	677.5 ± 0.7^{b}	NO	---	---
	40	5.3 ± 0.5^{a}	51.6 ± 0.4^{a}	896.7 ± 1.2^{c}	NO	---	---

Pullulan (M_w ~ 100000)	10	18.9 ± 0.1[a]	58.7 ± 0.1[a]	19. 7 ± 0.5 [a]	NO	---	---
	20	133.3 ± 0.7[b]	53.2 ± 0.2[b]	17.3 ± 0.4[b]	YES	Capsules + thin fibers	1.0 ± 0.7 [a]*
	40	1690.6 ± 9.1[c]	58.5 ± 1.4[a]	16.8 ± 0.1[b]	YES	Fibers	0.1 ± 0.1[b]
FOS-F97	10	4.8 ± 0.2[a]	61.6 ± 0.8[a]	51.1 ± 1.5 [a]	NO	---	---
	20	5.2 ± 0.6[a]	63.6 ± 0.9[b]	49.9 ± 0.7 [a]	NO	---	---
	40	7.2 ± 1.2[b]	64.3 ± 0.1[b]	44.7 ± 0.1[b]	NO	---	---
FOS-FI	10	5.4 ± 0.4[a]	59.9 ± 0.4[a]	72.0 ± 3.6 [a]	NO	---	---
	20	5.6 ± 0.3 [a]	58.6 ± 1.0[b]	69.1 ± 1.6 [a]	NO	---	---
	40	8.29 ± 0.5[b]	58.1 ±0.2[b]	79.9 ± 3.1 [b]	NO	---	---
WPC (M_w ~ 20000-70000)	10	5.4 ± 0.3[a]	46.7 ± 1.0[a]	1643.0 ± 25.5 [a]	NO	---	---
	20	10.8 ± 0.5[b]	46.5 ± 0.7 [a]	2280.0 ± 10.1 [b]	YES	Multiple particles	---
	40	49.0 ± 1.3[c]	41.9 ± 0.2[b]	2753.3 ± 20.8[c]	YES	Capsules	1.0 ± 0.6 [a]
SPI (M_w ~ 30000-350000)	5	10.6 ± 0.4[a]	44.4 ± 0.6 [a]	1689.7 ± 11.0 [a]	NO	---	---
	10	70.5 ± 3.4[b]	44.4 ± 0.5 [a]	2723.3 ± 23.1 [b]	NO	---	---
	20	---	---	---	NO	---	---

a-c: Different superscripts within the same column and the same matrix indicate significant differences among each concentration ($p < 0.05$).

*Data from capsules

3.2. Improvement of aqueous hydrocolloidal solutions for electrospraying

From Table 1 it can be seen that most of the aqueous hydrocolloidal solutions were not suitable for electrospraying and, thus, it was not possible to develop encapsulation structures from them at the various concentrations assayed. In contrast, the different PVOH and PEO solutions and those hydrocolloid-based solutions obtained from the higher molecular weight hydrocolloids (dextran, pullulan and WPC) were spinnable giving raise to either capsules or fibres depending on the solution properties. As it was commented before, the main reasons of the sprayability differences were the low viscosity together with too high surface tension values that presented most of the hydrocolloid solutions. Various strategies were established in order to improve these physical properties and, thus, be able to electrospray the hydrocolloid-based solutions which were not possible to form capsules with the previous conditions assayed. For increasing the viscosity, different methodologies were followed depending on the hydrocolloid type. For the polysaccharide solutions (resistant starch, maltodextrin, F97 and FI) some thickening agents were added. Specifically, 1% (w/w) with respect to the polymer of guar gum (GG) and xanthan gum (XG) were incorporated in the solutions. Concerning the SPI solution greater viscosity values were sought by the denaturation of the protein through a thermal treatment. Denaturation leads to protein unfolding and exposure of the functional groups which could improve intermolecular interactions, both between the different protein chains and with the

solvent, resulting in increased viscosity. For the reduction of the surface tension, a 5% (w/w) with respect to the polymer weight of surfactant was incorporated in both, the polysaccharide and the protein solutions. Specifically a non-ionic surfactant (Span-20) was added, since it has been previously reported that electrically charged surfactants give rise to more instability in the electrospraying jet, thus, hampering capsule development (Pérez-Masiá et al. 2014). Moreover, both strategies were carried out together in order to ascertain if electrosprayability and capsule morphology were significantly affected when viscosity and surface tension were simultaneously modified. Specifically, Span-20 and guar gum were added to the solutions to reduce surface tension and increase the viscosity of the solutions, respectively. In the case of the SPI solution, the combined effect of the thermal denaturation and the surfactant addition was also studied. The different strategies were investigated using the aqueous solutions with 20% (w/v) of hydrocolloids, except for SPI, where 10% (w/v) solutions were used. Table 2 compiles the solution properties, electrosprayability, morphology and average size of the capsules obtained from the hydrocolloid solutions containing the different additives. From this table, it can be observed that the incorporation of the different substances effectively modified the solution properties, allowing stable electrospraying from almost all the hydrocolloid solutions studied. The specific effects derived from the incorporation of the different additives on solution properties and capsule morphology are further described and discussed below.

Table 2. Solution properties, electrosprayability and morphology of the different hydrocolloid solutions with different additives: guar gum (GG), xanthan gum (XG) and span-20.

Matrix (%)	Additive (%)	Viscosity (cP)	Surface Tension (mN/m)	Electrical Conductivity (µS)	Electrospraying	Morphology	Average capsule's size (µm)
Resistant Starch (20%)	---	5.5 ± 0.5 [a]	57.1 ± 1.6[a]	18.0 ± 1.1[a]	NO	---	---
	GG (1%)	11.6 ± 0.3 [b]	55.3 ± 0.6[b]	24.3 ± 0.2[b]	YES	Capsules + Films	0.8 ± 0.6[a]
	XG (1%)	177.7 ± 0.6[c]	58.5 ± 0.3[c]	147.5 ± 1.0[c]	YES	Capsules + Films	0.4 ± 0.3[b]
	Span-20 (5%)	5.6 ± 0.3 [a]	25.6 ± 0.1[d]	25.3 ± 0.5[bd]	YES	Capsules	0.5 ± 0.4[b]
	GG (1%)/Span-20 (5%)	11.4 ± 0.3 [b]	25.9 ± 0.1[d]	26.7 ± 1.7[d]	YES	Capsules + Films	0.7 ± 0.3[a]
Maltodextrin (20%)	---	5.2 ± 0.2 [a]	52.7 ± 0.1[a]	677.5 ± 0.7[a]	NO	---	---
	GG (1%)	11.2 ± 0.2 [b]	50.0 ± 0.5[b]	697.0 ± 4.6[b]	YES	Capsules + Films	0.7 ± 0.6[a]
	XG (1%)	58.6 ± 0.8[c]	50.1 ± 2.1[b]	822.0 ± 12.2[c]	YES	Capsules + Films	0.3 ± 0.2[b]
	Span-20 (5%)	5.8 ± 0.1 [a]	25.1 ± 0.6[c]	681.0 ± 7.1[a]	YES	Capsules	0.1 ± 0.1[c]
	GG (1%)+ Span-20 (5%)	11.6 ± 0.3 [b]	25.4 ± 0.2[c]	694.3 ± 5.3[b]	YES	Capsules + Films	0.6 ± 0.5[a]
FOS-F97 (20%)	---	5.2 ± 0.6 [a]	63.6 ± 0.9[a]	49.9 ± 0.7[a]	NO	---	---
	GG (1%)	16.9 ± 0.8 [b]	39.1 ± 0.8[b]	47.9 ± 0.6[a]	YES	Capsules + Films	0.6 ± 0.8[a]
	XG (1%)	192.0 ± 5.2[c]	48.4 ± 0.2[c]	168.4 ± 2.2[b]	YES	Capsules + Films	0.3 ± 0.5[b]
	Span-20 (5%)	5.3 ± 0.3 [a]	26.0 ± 0.6[d]	55.1 ± 0.4[c]	YES	Capsules (Aggregates)	0.6 ± 0.3[a]

	GG (1%)+ Span-20 (5%)	16.5 ± 1.1 [b]	25.8 ± 0.2[d]	71.1 ± 1.8[d]	YES	Capsules + Films	1.7 ± 1.2[c]
FOS-FI (20%)	---	5.6 ± 0.3 [a]	58.6 ± 1.0[a]	69.1 ± 1.6[a]	NO	---	---
	GG (1%)	18.1 ± 1.3 [b]	49.9 ± 1.7[b]	80.5 ± 3.5[b]	YES	Capsules	0.6 ± 0.8[a]
	XG (1%)	542.6 ± 10.5[c]	58.1 ± 2.0[a]	227.7 ± 2.5[c]	YES	Capsules + Films	0.1 ± 0.1[b]
	Span-20 (5%)	5.5 ± 0.2 [a]	26.0 ± 0.2[c]	62.9 ± 0.2[d]	YES	Capsules (Aggregates)	0.5 ± 0.3[a]
	GG (1%)+ Span-20 (5%)	45.4 ± 2.8[d]	25.5 ± 0.1[c]	80.0 ± 1.5[b]	YES	Capsules + Films	0.3 ± 0.3[c]
SPI (10%)	---	70.5 ± 3.4 [a]	44.4 ± 0.5[a]	2723.3 ± 23.1[a]	NO	---	---
	Denaturation	26.6 ± 4.1[b]	42.6 ± 0.7[b]	2810.0 ± 40.0[b]	YES	Capsules /Multiple particles	0.2 ± 0.1[a]
	Span-20 (5%)	59.0 ± 0.8[c]	32.3 ± 0.3[c]	2643.3 ± 15.3[c]	YES	Capsules /Multiple particles	0.3 ± 0.2[b]
	Denat + Span-20 (5%)	56.3 ± 2.0 [c]	32.0 ± 0.3[c]	2493.3 ± 35.1[d]	YES	Capsules /Multiple particles	0.2 ± 0.1[c]

a-d: Different superscripts within the same column and the same matrix indicate significant differences among each concentration ($p < 0.05$).

3.2.1. Addition of gums

From Table 2 it can be observed that, as expected, the incorporation of gums to the polysaccharide solutions increased their viscosity. However, it was seen that xanthan gum led to a considerably greater increase than guar gum, due to the ability of xanthan molecules, in solution, to form a highly ordered network of entangled, stiff molecules through its charged trisaccharide side-chains (Norton et al. 1984). Furthermore, xanthan gum also produced greater surface tension and electrical conductivity values than guar gum, which destabilized the electrospraying jet. This fact explained the continuous dripping during electrospraying in all the solutions containing xanthan gum. Another interesting observation was that, upon addition of the gums, a continuous film was formed together with the capsules in most of the materials assayed. This was probably because of the ability of gums to retain water, causing an incomplete drying of the electrospraying jet and leading to the collapse of the humid structures in the collector which formed a continuous hydrocolloid film. This effect could not be avoided even modifying the processing parameters, such as lowering the feeding rate, increasing the tip to collector distance or increasing the hydrocolloid concentration so as to facilitate the elimination of the solvent. It is also important to note that FOS also presented a greater ability to retain water than other hydrocolloids. Thus, FOS capsules were obtained by increasing the tip-to-collector distance with respect to the other hydrocolloids in order to avoid water drops on the collector. From the average capsules sizes obtained it was seen that addition of xanthan gum led to the formation of smaller structures, probably because of the higher electrical

conductivity of the solutions. Figure 1 shows the polysaccharide capsules obtained with gums. From this figure it is clearly observed that addition of xanthan gum led to the formation of smaller capsules. It was also seen that a continuous film was formed in most of the materials.

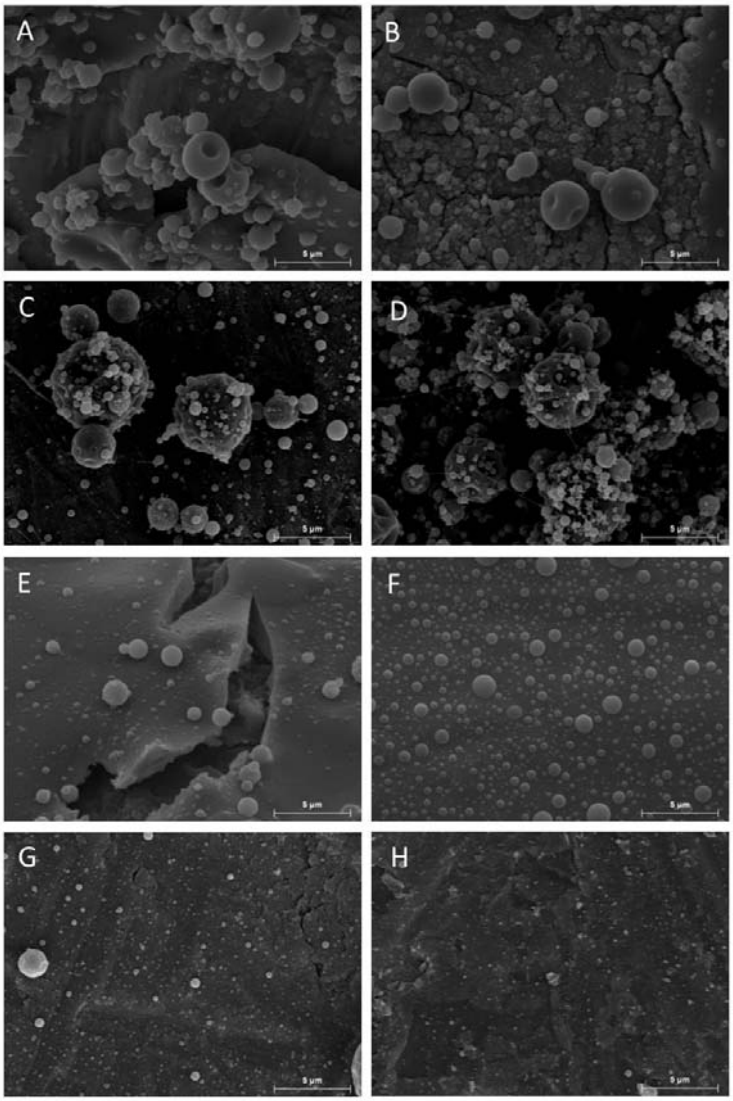

Figure 1. SEM images of different hydrocolloid capsules with 1% (w/w) of gum: (A) Resistant Starch/GG; (B) Maltodextrin/GG; (C) FOS-F97/GG; (D) FOS-FI/GG; (E) Resistant Starch/XG; (F) Maltodextrin/XG; (G) FOS-F97/XG; and (H) FOS-FI/XG. Scale mark of all images is 5 µm.

3.2.2. SPI denaturation

As commented above, the strategy to increase the viscosity of the SPI solution was to apply a thermal treatment to induce denaturation, to both unfold the protein chains and expose their functional groups to facilitate entanglements. However, from Table 2, it can be observed that denaturation led to a viscosity decrease of the SPI solution. This fact could be related to the protein extraction process carried out by the suppliers. According to Vega-Lugo and Lim (2008), as-received SPI used in this work was highly hydrolysed during the extraction process, which may have contributed to poor intermolecular interactions and thus, to its lower viscosity after the thermal treatment. Nevertheless, denaturation of SPI improved the electrospraying of this hydrocolloid, probably because of the destruction of the globular structure of the native protein, which led to greater chain entanglements. Figure 2 shows the SEM image of the SPI capsules obtained after denaturation. It was seen that multiple particles and very small capsules were obtained, probably because of the lower viscosity and the higher conductivity values of SPI. For high electrical conductivity values, the columbic repulsion forces are greater and compete with the viscoelastic forces of the solution, disentangling more easily the polymer network which is being formed during electrospraying. Therefore, increasing conductivity makes it easier for the solution to be broken up into smaller droplets, giving rise to different morphologies (Bock et al. 2012).

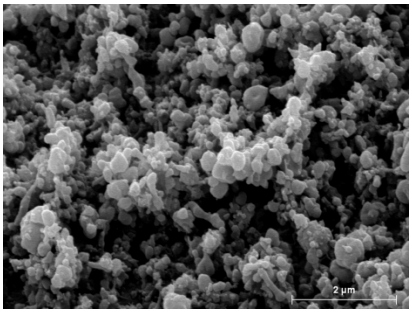

Figure 2. SEM image of capsules obtained from 10% (w/v) SPI solutions after denaturation

3.2.3. Addition of surfactant

From Table 2 it can be observed that the incorporation of Span-20 effectively dropped the surface tension of all the solutions assayed. It was seen that for all the hydrocolloids, similar surface tension values were attained when adding the surfactant, regardless the presence or absence of gum. This fact was due to the surfactant concentration added. It is well-known that surfactants absorb at solution surfaces, thereby lowering the surface tension of the medium in which they are dissolved. Furthermore, above a critical concentration, the so-called critical micelle concentration (CMC), the surface tension of the solutions reaches an equilibrium value. The CMC of Span-20 and its respective equilibrium surface tension values in various solutions were previously studied (Pérez-Masiá et al. 2014) and it was seen to be 0.1 mM. In this work, Span-20 was added above its CMC, so the plateau surface tension was reached in all the solutions assayed. Figure 3 shows the SEM images of the capsules obtained from the hydrocolloid/surfactant solutions. It was seen that addition of Span-20 to the resistant starch solution led to the formation of very homogenous capsules. In the case of FOS, capsules

aggregation and a partial collapse of the structures were observed when Span-20 was added. This fact could be due to the greater ability of water retention of FOS, which hindered the electrospraying jet drying. In fact, tip-to-collector distance had to be increased in this case with respect to the other hydrocolloids, as it was commented before. Therefore, although the collected material was apparently dried, humid structures could be reaching the collector and causing the capsules collapse. Very small capsules with multiple morphologies were attained from maltodextrin and SPI due to the higher electrical conductivity of these solutions. It is worth noting that addition of Span-20 enabled the electrospraying of SPI, even when it was not subjected to thermal treatment. This was probably because of an interaction between the surfactant and the protein. From Table 2 it was seen that the incorporation of Span-20 produced a significant viscosity change on the SPI solution, which suggested an interaction between both components. This interaction probably favoured chain entanglements during the electrospraying process and led to the capsules formation.

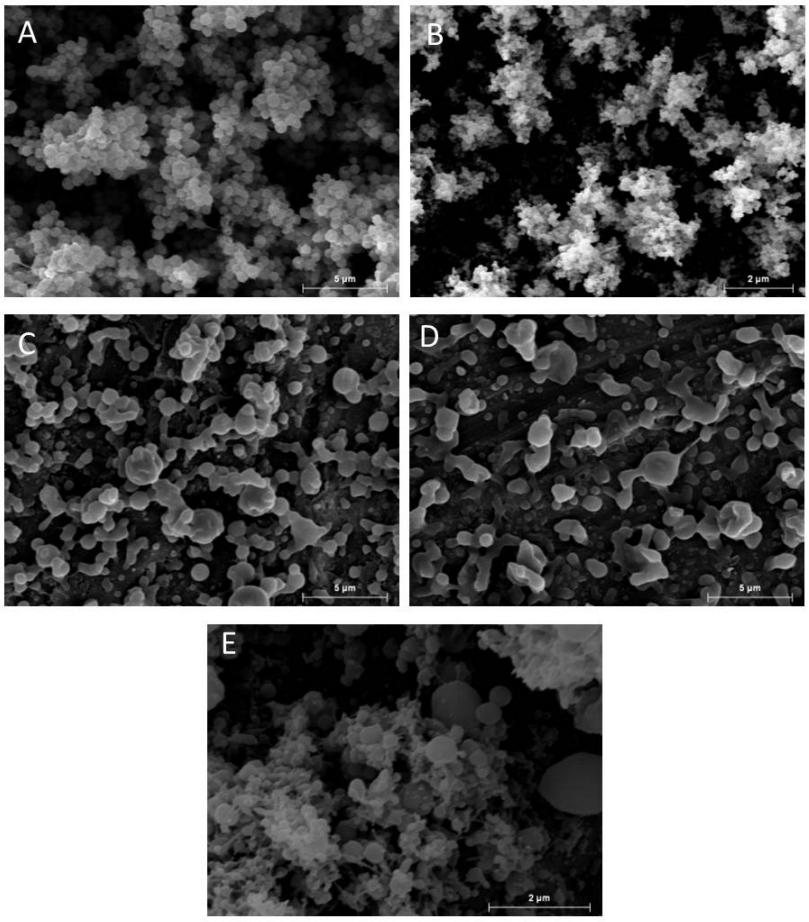

Figure 3. SEM images of the different hydrocolloid capsules with 5% (w/w) of Span-20 obtained from: (A) Resistant starch; (B) Maltodextrin; (C) FOS-F97; (D) FOS-FI; and (E) SPI. Scale mark is 5 µm for images A, C and D and 2 µm for images B and E.

3.2.4. Effect of combined addition of gums, surfactant and/or denaturation

From Table 2 it can be seen that, when the strategies to improve solution properties for electrospraying were carried out together, the viscosity and surface tension values of the different solutions were brought to suitable values for capsule formation using this electro-hydrodynamic process. Figure 4 shows the SEM images of the capsules obtained combining the strategies to increase the viscosity and reduce the surface tension of the hydrocolloid solutions. It was observed that, the presence of the gum in the case of the polysaccharide solutions, hindered solvent evaporation and, thus, a continuous film was also generated during the electrospraying process. This fact was mainly seen in FOS, since in this case, both the gum and the surfactant may be contributing to the water retention. In the case of SPI, when the surfactant was incorporated to the denatured protein solutions, small, wrinkled and aggregated particles were obtained probably because of the high electrical conductivity of this solution.

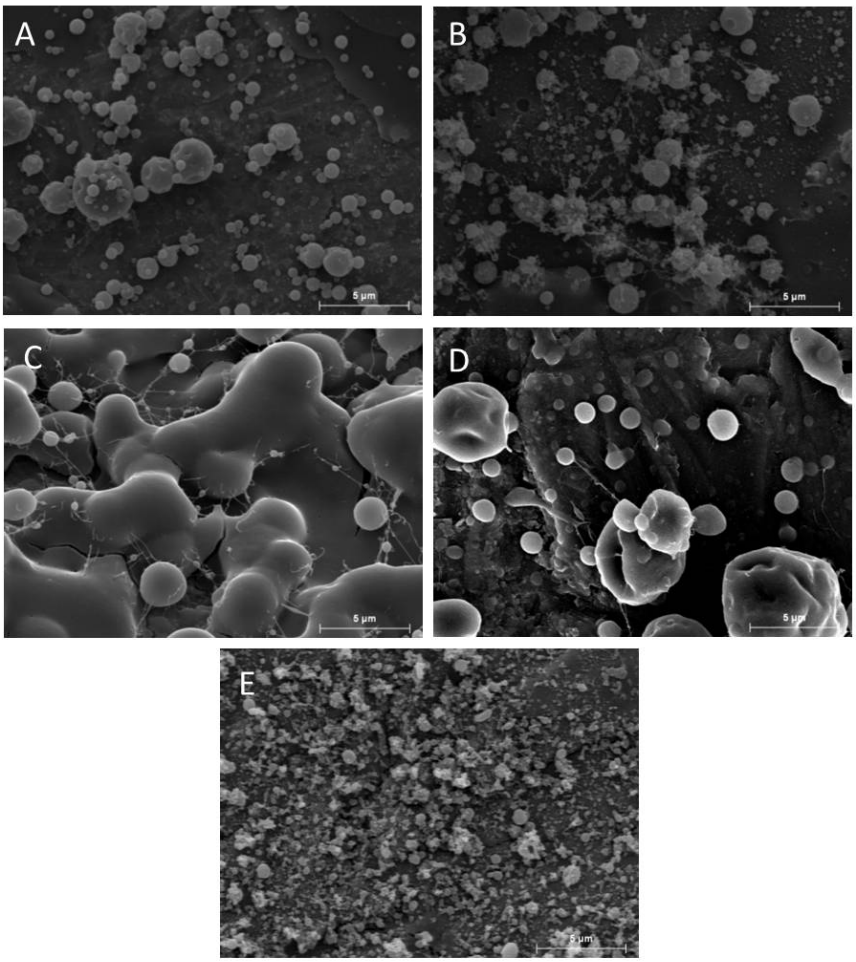

Figure 4. SEM images of the different hydrocolloid capsules with 1% (w/w) of guar gum (GG) and 5% (w/w) of Span-20 obtained from: (A) Resistant Starch/GG/Span-20; (B) Maltodextrin/GG/Span-20, (C) FOS-F97/GG/Span-20 and (D) FOS-FI/GG/Span-20; and (E) denatured SPI/Span20. Scale mark of all images is 5 µm.

3.3. Molecular organization of the capsules

ATR-FTIR experiments were carried out in order to figure out the effect of the addition of gums and surfactants and the effect of denaturation on the molecular organization of the hydrocolloid matrices and, thus, to better understand the capsules morphologies attained. Figure 5 shows the ATR-FTIR spectra of some of the hydrocolloids assayed. Initially, resistant starch and FOS-FI capsules were analyzed as an example of the polysaccharide capsules behavior when incorporating the gums and the surfactant. Moreover, SPI capsules were also studied to better understand the influence of the thermal treatment and of the surfactant incorporation on these capsules. Figures 5A and 5B show the ATR-FTIR spectra of resistant starch and FI capsules, respectively, from 1200 to 700 cm^{-1}. This region includes the most characteristic vibrational bands of the carbohydrates. From these figures it was observed that all the electrosprayed structures presented narrower and better defined bands than the pure components, which indicated that the formation of capsules led to a greater molecular order when comparing to the bulk materials. Specifically, for the resistant starch, this area shows the C-O stretching and C-OH bending vibrations at around 1148, 1072 and 1010 cm^{-1}. Further bands were also found at around 924, 850 and 766 cm-1 which were attributed to skeletal vibrations of the pyranose ring, specifically to C-H stretching vibration and the α(1-6) and α(1-4) glycosidic bonds (Smrčková et al. 2013; Siddiqui et al. 2014). Concerning the spectra of the FI capsules, Figure 5B shows the C-O-C stretching vibration at ~1110 cm^{-1}, the C-OH stretching vibration at ~1018 and 990 cm^{-1}, and the C-H stretching vibration at ~930 cm^{-1} (Tewari and Malik

2007). Another remarkable observation was that the OH stretching band which appeared at around 3300 cm^{-1} arose at lower wavenumber in FI structures than in the resistant starch ones (data not shown). Moreover, this band was also moved towards lower wavenumbers when xanthan gum was added (data not shown). The lower wavenumber indicated the presence of more bonded OH groups, probably because of greater water retention of these structures (those with FOS and with xanthan gum) as it was commented before (D'Souza et al. 2008).

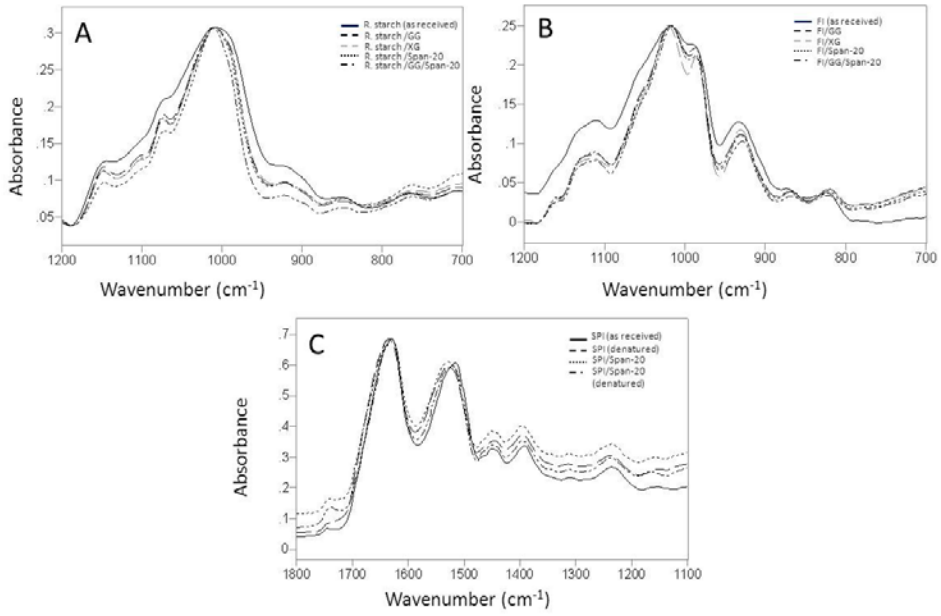

Figure 5. ATR-FTIR spectra of: (A) resistant starch capsules; (B) FOS-FI capsules; and (C) SPI capsules.

Finally, the molecular organization of the SPI capsules was also studied, to better understand the electrosprayability differences and the capsules morphology in this case. Figure 5C shows the ATR-FTIR spectra of the protein materials from 1800 to 1100 cm^{-1}, where the most characteristic protein bands are found. Specifically, the amide I and amide II bands arose at around 1630 and 1530 cm^{-1} respectively. It was observed that denaturation led to a band broadening and a shift towards higher wavenumbers of both amide bands. The broadening could be related to a greater molecular disorder due to the protein unfolding. Regarding the amide bands shift, it could be due to a protein structure variation. Specifically, the amide I shift was attributed to a secondary structure variation, since during thermal treatment the hydrogen bonds stabilizing the native structure of the proteins are disrupted, causing loss of the α-helix and β-sheets structures and creating new β-sheets arrangements (Eissa et al. 2006). The amide II band variations were related to in plane N-H and C-N vibrations (Kong and Yu 2007). Nevertheless, these changes may have favoured the protein entanglements during electrospraying and, thus, enable capsules formation.

4. CONCLUSIONS

From this study, it has been demonstrated that the addition of gums and surfactants effectively modified the aqueous hydrocolloid dispersion properties allowing capsule formation through electrospraying. Results showed that, generally, addition of surfactants, and especially non-ionic surfactants, was the most interesting strategy for improving the sprayability of these materials, since gums retained too much solvent and protein denaturation that led to aggregated and wrinkled particles. These results are very interesting for food-related applications, since addition of gums and surfactants allowed structure formation through electrospraying, avoiding the use of organic solvents, which are not allowed in the food industry. Moreover, the use of food hydrocolloids as matrix materials also favors the application of these capsules in foodstuffs. Particularly, these capsules could be used to protect different bioactive ingredients, such as vitamins, antioxidants, enzymes or probiotics, which are extremely sensitive to ambient and food processing conditions. Nevertheless, it is worth noting that matrix materials are water dispersible and, thus, their protective ability should be evaluated when incorporated to aqueous food products.

5. REFERENCES

Aceituno-Medina, M., Lopez-Rubio, A., Mendoza, S., Lagaron, J.M. (2013). Development of novel ultrathin structures based in amaranth (Amaranthus hypochondriacus) protein isolate through electrospinning. Food Hydrocolloids 31, 289-298.

Bakhshi, P.K., Nangrejo, M.R., Stride, E., Edirisinghe, M. (2013). Application of Electro-hydrodynamic Technology for Folic Acid Encapsulation. Food and Bioprocess Technology 6 (7), pp. 1837-1846.

Bock, N., Dargaville, T.R. & Woodruff, M.A. (2012). Electrospraying of polymers with therapeutic molecules: State of the art. Progress in Polymer Science 37, 1510-1551.

Ding, L., Lee, T., Wang, C.-H. (2005). Fabrication of monodispersed Taxol-loaded particles using electro-hydrodynamic atomization. Journal of Controlled Release 102 (2), pp. 395-413.

D'Souza, L., Devi, P., Divya Shridhar, M.P., Naik, C.G. (2008). Use of Fourier Transform Infrared (FTIR) spectroscopy to study cadmium-induced changes in Padina tetrastromatica (Hauck). Analytical Chemistry Insights 2008 (3), pp. 135-143

Eissa, A.S., Puhl, C., Kadla, J.F., Khan, S.A. (2006). Enzymatic cross-linking of β-lactoglobulin: Conformational properties using FTIR spectroscopy. Biomacromolecules 7 (6) , pp. 1707-1713

Ezhilarasi, P.N., Karthik, P., Chhanwal, N., Anandharamakrishnan, C. (2013). Nanoencapsulation Techniques for Food Bioactive Components: A Review. Food and Bioprocess Technology 6(3), pp. 628-647.

Fong, H., Chun, I., Reneker, D.H. (1999). Beaded nanofibers formed during electrospinning. Polymer 40 (16), pp. 4585-4592.

Hong YL, Li YY, Yin YZ, Li DM, Zou GT. (2008). Electro-hydrodynamic atomization of quasi-monodisperse drug-loaded spherical/wrinkled microparticles. Journal of Aerosol Science 39 (6), pp. 525-536.

Kong, J., Yu, S. (2007). Fourier transform infrared spectroscopic analysis of protein secondary structures. Acta Biochimica et Biophysica Sinica 39 (8), pp. 549-559

Li, D. & Xia, Y. (2004). Electrospinning of nanofibers: Reinventing the wheel? Advanced Materials, 16(14), 1151-1170.

Lopez-Rubio, A. & Lagaron, J.M. (2012). Whey protein capsules obtained through electrospraying for the encapsulation of bioactives. Innovative Food Science and Emerging Technologies 13, 200-206.

Nagarajan, R., Drew, C., & Mello, C.M. (2007). Polymer-micelle complex as an aid to electrospinning nanofibers from aqueous solutions. The Journal of Physical Chemistry C 111, 16105-16108.

Nasirullah, Pravin Kumar, Rizwan Shariff, (2011). Development of nutraceutical carriers for functional food applications. Nutrition & Food Science, Vol. 41 Iss: 1, pp.34 – 43.

Norton, I.T., Goodall, D.M., Frangou, S.A., Morris, E.R., Rees, D.A. (1984). Mechanism and dynamics of conformational ordering in xanthan polysaccharide. Journal of Molecular Biology 175, 371-394.

Pérez-Masiá, R., Fabra, M.J., Lagaron, J.M., López-Rubio, A. (2013). Use of electrospinning for encapsulation. In Mittal, V (Editor), Encapsulation Technologies. (pp. 107-136). Chemical Engineering Department, The Petroleum Institute, Abu Dhabi, United Arab Emirates.

Pérez-Masiá, R., Lagarón, J.M., López-Rubio. (2014). A Surfactant-aided electrospraying of low molecular weight carbohydrate polymers from aqueous solutions. Carbohydrate polymers (2014), 101, pp. 249-255.

Siddiqui, N.N., Aman, A., Silipo, A., Qader, S.A.U., Molinaro, A. (2014). Structural analysis and characterization of dextran produced by wild and mutant strains of Leuconostoc mesenteroides. Carbohydrate Polymers 99 , pp. 331-338.

Smrčková, P., Horský, J., Šárka, E., Koláček, J., Netopilík, M., Walterová, Z., Kruliš, Z., (...), Hrušková, K. (2013). Hydrolysis of wheat B-starch and characterisation of acetylated maltodextrin. Carbohydrate Polymers 98 (1), pp. 43-49

Sridhar, R., Venugopal, J.R., Sundarrajan, S., Ravichandran, R., Ramalingam, B., Ramakrishna, S. (2011). Electrospun nanofibers for pharmaceutical and medical applications. Journal of Drug Delivery Science and Technology 21 (6), pp. 451-468.

Stijnman, A.C., Bodnar, I. & Hans Tromp, R. (2011). Electrospinning of food-grade polysaccharides. Food Hydrocolloids 25, 1393-1398.

Tewari, J.C., Malik, K. (2007). In situ laboratory analysis of sucrose in sugarcane bagasse using attenuated total reflectance spectroscopy and chemometrics. International Journal of Food Science and Technology 42 (2) , pp. 200-207.

Torres-Giner, S., Martinez-Abad, A., Ocio, M. J., & Lagaron, J. M. (2010). Stabilization of a

nutraceutical omega-3 fatty acid by encapsulation in ultrathin electrosprayed zein

prolamine. Journal of Food Science, 75, N69–N79.

Vega-Lugo, A.-C., Lim, L.-T. (2008). Electrospinning of soy protein isolate nanofibers. Journal of Biobased Materials and Bioenergy 2 (3), pp. 223-230

Xie, J., Li, X. & Xia, Y (2008). Putting electrospun nanofibers to work for biomedical research. Macromolecular Rapid Communications 29, 1775-1792.

Zamani, M., Prabhakaran, M.P., Ramakrishna, S. (2013). Advances in drug delivery via electrospun and electrosprayed nanomaterials. International Journal of Nanomedicine 8, pp. 2997-3017.

CHAPTER VI

Encapsulation of folic acid in food hydrocolloids through nanospray drying and electrospraying for nutraceutical applications

CHAPTER VI: Encapsulation of folic acid in food hydrocolloids through nanospray drying and electrospraying for nutraceutical applications

ABSTRACT

In this work, two different technologies (electrospraying and nanospray drying) were evaluated for the encapsulation of folic acid using both a whey protein concentrate (WPC) matrix and a commercial resistant starch. The morphology of the capsules, molecular organization of the matrices upon encapsulation, encapsulation efficiency, and stability of the folic acid within the capsules under different storage conditions and upon thermal exposure were studied. Results showed that spherical nano-, submicro- and microcapsules were obtained through both techniques, although electrospraying led to smaller capsule sizes and to an enhanced control over their size distribution. Greater encapsulation efficiency was observed using WPC as encapsulating matrix, probably related to interactions between the protein and folic acid which favoured the incorporation of the bioactive. The best results in terms of bioactive stabilization in the different conditions assayed were also obtained for the WPC capsules, although both materials and encapsulation techniques led to improved folic acid stability, especially under dry conditions.

Keywords: encapsulation, electrospraying, spray drying, food hydrocolloids, folic acid

1. INTRODUCTION

The encapsulation of nutraceutical and functional ingredients is an area of increased interest over the last years which seek to protect these products from adverse environmental conditions and, thus, increase their shelf-life and assure their health-promoting properties. Moreover, the encapsulation of these components also enables their incorporation into different food matrices which results in novel functional food products with potential health benefits.

A variety of techniques have been used to encapsulate functional components, such as nanoemulsions (Silva, Cerqueira & Vicente, 2012), coacervation (de Conto, Grosso & Gonçalves, 2013; Tamjidi, Nasirpour & Shahedi, 2012), extrusion methods (Li, Chen, Sun, Park & Cha, 2011), fluidized bed coating (Zuidam & Simoni, 2010), spray cooling (Gibbs, Selm, Catherine & Mulligan, 1999) or spray drying (Murugesan & Orsat, 2012). Among these methods, spray drying is nowadays the most common and cheapest technology in the food industry to produce microencapsulated additives for food applications (Gharsallaoui, Roudaut, Chambin, Voilley & Saurel, 2007). The active material to be encapsulated through the spray drying technique is dispersed in a carrier polymer solution which is atomized into small droplets. The solvent is evaporated using a warmed gas and the resulting solid capsules are collected as dry powder (Gibbs et al., 1999; Gharsallaoui et al., 2007). It is worth noting that this technology can be used with aqueous solutions, thus avoiding the use of organic solvents which could generate toxicity problems in contact with food. Nevertheless, it needs relatively high temperatures to eliminate the water from the

polymeric/biopolymeric solutions, fact that could affect the stability of the bioactive ingredient. Apart from these well-known encapsulation techniques, electrospinning has recently arisen as an alternative technology that can also be used for encapsulation (Torres-Giner, Martínez-Abad, Ocio & Lagaron, 2009; Lopez-Rubio & Lagaron, 2012). Besides being a very simple technique, some advantages of electrospinning for encapsulation include that neither temperature nor organic solvents are needed, thus, being an ideal method for protecting sensitive encapsulated ingredients. Electrospinning makes use of high voltage electric fields to produce electrically charged jets from viscoelastic polymer solutions which on drying, by the evaporation of the solvent, produce ultrathin polymeric structures (Li & Xia, 2004). The electrospun nanostructures morphology and diameter are affected by the solution properties and by the process parameters and, for certain materials, reduced size capsules can be obtained when adjusting both. In this case, the electrospinning process is normally referred to as "electrospraying" due to the non-continuous nature of the structures obtained (Lopez-Rubio & Lagaron, 2012). Capsules and, thus, electrospraying, are generally preferred for food and nutraceutical applications, since apart from facilitating handling and subsequent incorporation into different products, they also present greater surface to volume ratio and, thus, are expected to have better release profiles than fibers (Hong, Li, Yin, Li, & Zou, 2008).

An essential micronutrient which cannot be synthesized by humans and, thus, it must be ingested through the diet is folic acid (Lopera, Guzman, Cataño & Gallardo, 2009). Folic acid is the synthetic form of folates, a

broad group of compounds with vitamin functionality (Bakhshi, Nangrejo, Stride & Edirisinghe, 2013). Specifically, folic acid is a water-soluble vitamin which is vital for a variety of physiological functions in humans. It plays an important role in the prevention of neural tube defects in infants and might decrease the likelihood of developing vascular diseases and some cancers (Liang, Zhang, Zhou & Subirade, 2013). According to these beneficial effects, the European Regulations (Regulations 1924/2006; 1925/2006) allow the addition of folic acid in food an when its content provides more than 15% of the recommended daily amount, eight different health claims related to the beneficial effects of this vitamin are allowed in the food label (Regulation 432/2012). However, folic acid undergoes degradation reactions when it is exposed to light, temperature, moisture, acid or alkaline medium and oxygen atmosphere (Lopera et al., 2009). Therefore, the encapsulation of this bioactive ingredient is a plausible option to improve its stability and to assure its bioactivity within the food product during commercialization.

Regarding the matrix materials employed for encapsulation, food hydrocolloids are very convenient for nutraceutical and food applications, since many of them are soluble in aqueous solutions, thus, avoiding toxicity problems. Specifically, in the case of folic acid, there are some works which have shown the feasibility of spray drying for the encapsulation of this bioactive molecule within food hydrocolloids obtaining proper encapsulation efficiencies (Lopera et al., 2009). However, electrospinning from hydrocolloidal aqueous solutions has proven difficult due to several factors such as the polycationic nature or

the low chain flexibility of these materials which complicates chain entanglements (essential for fiber formation) (Kriegel, Kit, McClements & Weiss, 2009). Moreover, the high surface tension of water, as well as, the ionization of water molecules at high voltages in an air environment, also complicates the electrospinning process. Therefore, synthetic polymers such as polyethylene oxide (PEO) (Alborzi, Lim & Kakuda, 2013) or multiple stages processes (Bakhshi et al., 2013) have been employed to date for the folic acid encapsulation through the electrospinning technology. Recent works have demonstrated that it is possible to obtain hydrocolloid-based encapsulation structures using electrospraying through the proper adjustment of the aqueous solution properties (mainly surface tension and viscosity) upon addition of several additives (surfactants and gums) (Pérez-Masiá, Lagaron & Lopez-Rubio, 2014a and 2014b).

The aim of this work was to compare the more traditional spray drying technique (but using a novel nanospray drying device able to obtain smaller encapsulation structures) with the electrospraying methodology for folic acid encapsulation using two different food hydrocolloid matrices (a whey protein concentrate and a commercial resistant starch). Initially, whey protein concentrate (WPC) was used since it has excellent functional characteristics, it is a low cost ingredient and it has proven useful for the encapsulation of several functional ingredients through electrospinning (Lopez-Rubio & Lagaron, 2011 and 2012). Additionally, a commercial resistant starch (derived from corn starch) with trade name Fibersol was also employed for folic acid encapsulation. Both materials are dispersable in aqueous solutions and, thus, they are

very convenient for nutraceutical applications. The encapsulation structures obtained through the two methodologies were characterized, and a comparative evaluation of the encapsulation efficiency and folic acid stability, under different storage conditions, and after applying a heating process were ascertained.

2. MATERIALS AND METHODS

2.1. Materials

Whey protein concentrate (WPC) was kindly donated by ARLA (ARLA Food Ingredients, Viby, Denmark). Under the commercial name Lacprodan® DI-8090, the composition per 100 g of product consisted of ~80 g of protein, ~9 g of lactose, and ~8 g of lipids, being the rest water and minerals like sodium and potassium. The commercial resistant starch was Fibersol® (www.fibersol.com) commercial grade, manufactured by ADM/Matsutani (Iowa, USA). Guar Gum was purchased at Capers Community Markets (Vancouver, Canada). Folic acid (>97% purity) and the surfactant Span 20 were supplied by Sigma-Aldrich (Spain). All products were used as received without further purification.

2.2. Preparation of the solutions

The solutions were prepared depending on the encapsulation technology by dissolving 0.4 or 20% w/v of the matrix hydrocolloids in water for the spray drying or the electrospraying technique, respectively. Additionally, 0.5% w/w of Guar gum with respect to the biopolymer matrix was incorporated in the resistant starch solutions. Span 20 was added to the solutions to attain 5 wt.% with respect to the hydrocolloids weight. When folic acid was incorporated, 1.5 wt.% of the bioactive with respect to the polymers weight was added. The solutions were stirred at room temperature until homogeneous dispersions of all the components were obtained.

2.3. Encapsulation through spray drying

The solutions with and without folic acid were spray-dried using a Nanospray-dryer B-90 (Büchi, Switzerland) with a 0.7 µm membrane cap. The solutions were introduced into the equipment through a silicone wire, which was connected to the spraying head of the equipment. The air flow was ~140 L/h with an inlet and outlet temperatures of 90ºC and 45ºC, respectively.

2.4. Encapsulation through electrospraying

The electrospinning apparatus, equipped with a variable high-voltage 0-30 kV power supply, was a Fluidnatek® LE-10 purchased from BioInicia S.L. (Valencia, Spain). Solutions with and without folic acid were introduced in a 5 mL plastic syringe and were electrospun under a steady flow-rate using a stainless-steel needle. The needle was connected through a PTFE wire to the syringe. The syringe was lying on a digitally controlled syringe pump while the needle was in horizontal towards a copper grid used as collector. The electrospraying conditions for obtaining the capsules were optimized and fixed at 0.15 mL/h of flow-rate, 10 kV of voltage and a tip-to-collector distance of 9-11 cm.

2.5. Characterization of the hydrocolloid/folic acid solutions

The apparent viscosity (ηa) of the hydrocolloid solutions was determined using a rotational viscosity meter Visco Basic Plus L from Fungilab S.A. (San Feliu de Llobregat, Spain) using a Low Viscosity Adapter (LCP). The surface tension of the biopolymer solutions was measured using the Wilhemy plate method in an EasyDyne K20

tensiometer (Krüss GmbH, Hamburg, Germany). The conductivity of the solutions was measured using a conductivity meter XS Con6 (Labbox, Barcelona, Spain). All measurements were made at 25ºC.

2.6. Optical microscopy

Optical microscopy images were taken using a digital microscopy system (Nikon Eclipse 90i) fitted with a 12 V, 100W halogen lamp and equipped with a digital imaging head which integrates an epifluorescence illuminator. A digital camera head (Nikon DS-5Mc) with a 5 megapixel CCD cooled with a Peltier mechanism was attached to the microscope. Nis Elements software (Nikon Instruments Inc., USA) was used for image capturing.

2.7. Scanning Electron Microscopy (SEM)

The morphology of the encapsulation structures was examined using SEM on a Hitachi microscope (Hitachi S-4100) after having been sputtered with a gold-palladium mixture under vacuum. All SEM experiments were carried out at 10 kV. Capsule diameters were measured by means of the Adobe Photoshop CS3 software from the SEM micrographs in their original magnification.

2.8. Attenuated total reflectance infrared spectroscopy (ATR-FTIR)

Attenuated total reflectance infrared spectroscopy (ATR-FTIR) was used to analyze the molecular organization of the capsules. The experiments were recorded in a controlled chamber at 21ºC and 40% RH coupling the ATR accessory GoldenGate of Specac Ltd. (Orpington, UK) to a Bruker (Rheinstetten, Germany) FTIR Tensor 37 equipment. All the spectra were

collected within the wavenumber range of 4000–600 cm-1 by averaging 15 scans at 4 cm-1 resolution. Analysis of the spectral data was performed by using Grams/AI 7.02 (Galactic Industries, Salem, NH, USA) software.

2.9. Folic acid encapsulation efficiency and stability assay

To assess the encapsulation yield, the amount of folic acid was determined by HPLC following the methodology described by Konings (1999) using a Merck-Hitachi 7000 (Merck, Darmstadt, Germany) HPLC equipped with an ultraviolet detector (LaChrom, Merck-Hitachi, model 7400), a LiChrosphere® 100 RP-18 (5 µm) column (Merck, Darmstadt, Germany) protected with a guard column (LiChroCART® 4-4, Merck, Darmstadt, Germany). The column was first eluted with a gradient of acetonitrile and 30 mmol/L phosphate buffer (potassium phosphate and ortho-phosphoric acid 85%, pH 2.2) at a flow rate of 0.9 mL/min. The gradient started at 6% acetonitrile, which was maintained isocritically for the first 6 min, and then the acetonitrile concentration was increased to 25% over 24 min and decreased back to 6% after 5 min. The injection volume was 40 µL. The running time was 40 min, and the time between injections was 20 min. Peak identification and quantification was based on the retention time compared with non-encapsulated folic acid measuring the UV absorbance at 290 nm. All samples were analysed in quadruplicate and data were expressed as µg/ml and the losses percentage of folic acid along the storage and heating were also calculated.

The stability of encapsulated folic acid was carried out taking into consideration three different situations that can be found in the food industry: dissolution in aqueous media, storage in dryness and temperature exposure. It is important to note that the heat treatment was applied after storage in dryness during 2 months. Aqueous solutions were prepared weighing 1 mg of capsules and dissolving them in 1 mL of deionised water. Immediately, the amount of folic acid was determined by HPLC, as explained above, and the solutions were stored at room conditions (23ºC and 65% relative humidity). Samples were tightly closed to avoid water losses though evaporation, and folic acid content was analysed every 15 days (up to 60 days). In addition, the folic acid capsules were stored in dryness in the same room conditions (temperature, humidity), in the presence and absence of light and, in a similar way, the content of this bioactive was analysed every 15 days (up to 60 days). To evaluate the stability when exposed to high temperature, the samples stored during 2 months were placed in a heating oven at 120ºC during 20 minutes. Every 5 minutes during the heating process, samples were taken out of the oven and re-suspended in distilled water (1 mg/mL w/v) before being injected in the HPLC to determine the amount of folic acid. In parallel a solution of 1 mg/ml of pure folic acid was assayed to evaluate the effect of encapsulation process in the stability of this bioactive.

2.10. Statistical analysis

A statistical analysis of data was performed through analysis of variance (ANOVA) using Statgraphics Plus for Windows 5.1 (Manugistics Corp., Rockville, MD). Homogeneous sample groups were obtained by using

LSD test (95% significant level). In the stability study ANOVA was applied taking into consideration the sample type and storage time, and a post-hoc test was used to establish the differences among mean values at significant level of 95%.

3. RESULTS AND DISCUSION

3.1. Solution properties

Before encapsulation, optimum solution parameters were set for both technologies. In the case of spray drying, much diluted solutions were produced in order to avoid the spraying head membrane blockage. Therefore, very low apparent viscosity values were obtained (< 2cP; data not shown).

In the case of electrospraying, the successful development of encapsulation structures using this technology strongly depends on the solution properties and, hence, an initial optimization of solution composition was carried out. From a screening study, it was seen that resistant starch solutions led to very low apparent viscosity values, which resulted in unstable jetting and no structures were formed from these solutions. Therefore, a thickening agent, specifically guar gum, was added to this solution in order to increase the viscosity and facilitate molecular entanglements between the carbohydrate chains. Moreover, guar gum also helped to avoid folic acid precipitation in the syringe during the electrospraying encapsulation process. It was also observed that, even though high protein and carbohydrate concentrations were used, the surface tension values of the aqueous solutions were still too high to allow capsule's formation. Hence, the surfactant Span-20 was incorporated in the solutions, since it has been previously seen that this compound effectively reduces solution surface tension, favouring the electrospraying process and, thus, capsules formation (Pérez-Masiá et al., 2014a and 2014b). The gum and the

surfactant were also included in the spray-drying solutions in order to obtain the same shell materials in both cases. Table 1 shows the apparent viscosity, the surface tension and the electrical conductivity of the final hydrocolloid-based electrospraying solutions with and without folic acid. It can be observed that low apparent viscosity values were obtained for both biopolymeric solutions in the absence of folic acid. This fact was mainly due to the low molecular weight of both hydrocolloids and, also to the concentration of these biopolymers in the solutions. This parameter was kept low in order to limit the chain entanglements of the biopolymers and, thus, obtain discontinuous particles instead of continuous fibers. In the presence of folic acid it was observed that the apparent viscosity of the resistant starch solution was not significantly modified. In contrast, the WPC solution presented an enhanced apparent viscosity suggesting that the folic acid was interacting with the protein. With regard to the surface tension, it was seen that the incorporation of the surfactant (Span 20) in all the solutions decreased this parameter to suitable values for stable electrospraying. From Table 1 it can also be observed that the electrical conductivity of the WPC solutions was much higher than that of the resistant starch ones, due to the ionic nature of the protein in solution.

Table 1. Solution properties of the electrospraying solutions

	Viscosity (cP)	Surface tension (mN/m)	Conductivity (μS)
WPC	5.56 ± 0.4[a]	31.74 ± 0.7[a]	1750 ± 12.1[a]
WPC/Folic acid	198.11 ± 0.4[b]	29.50 ± 0.3[b]	1690.67 ± 6.7[b]
Resistant starch	5.52 ± 0.5[a]	25.16 ± 0.8[c]	37.25 ± 0.5[c]
Resistant starch/Folic acid	5.86 ± 0.1[a]	25.83 ± 0.2[c]	39.37 ± 0.2[d]

[a-d] Different letters in the same column show statistical significant differences ($p<0.05$).

3.2. Morphology of the capsules

Initially, optical microscopy using a fluorescence source was used to confirm capsules formation, as well as to confirm the proper encapsulation of folic acid, since this vitamin presents fluorescence in the UV range, while the matrix materials did not presented this feature. Figure 1 shows the optical micrographs of the hydrocolloids/folic acid capsules developed and it was observed that both matrices led to the formation of spherical capsules, although some agglomerations were seen in the starch-based materials. Moreover, from the fluorescence images it was also seen that folic acid was properly encapsulated in both matrices regardless the encapsulation technique employed.

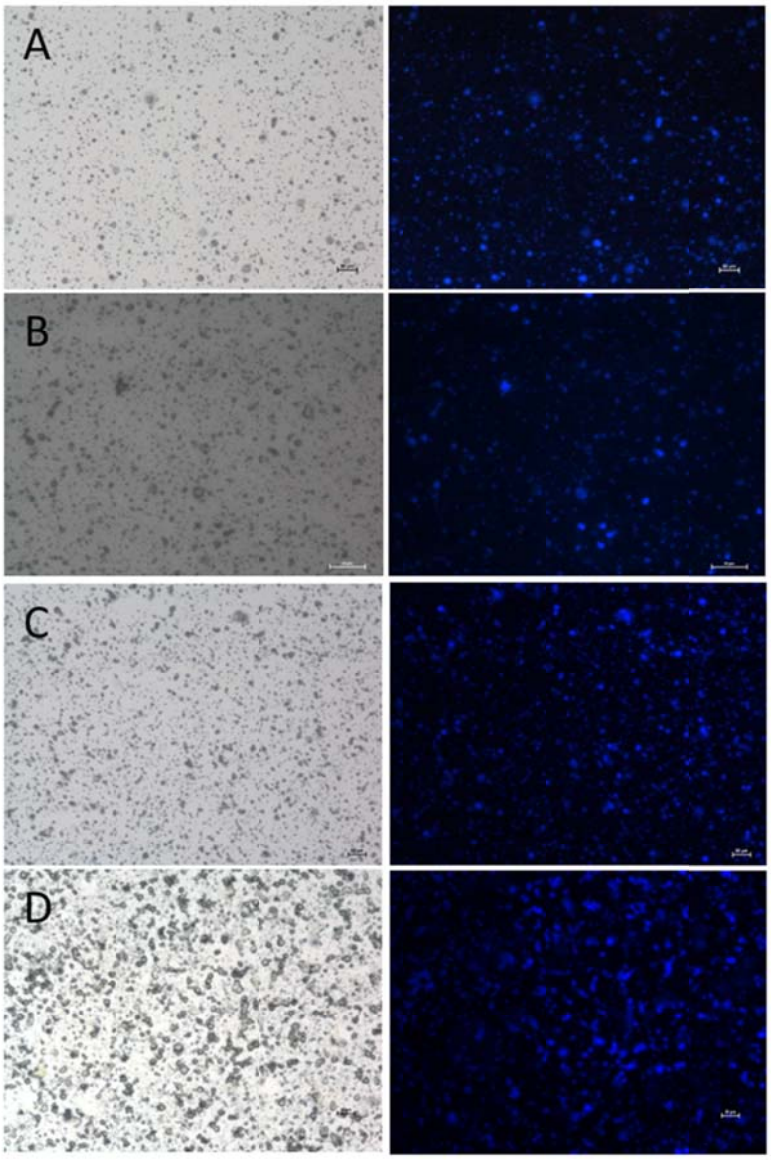

Figure 1. Optical micrographs (under normal illumination and using a fluorescence source to distinguish encapsulated folic acid) of WPC/Folic acid (A,B) and Resistant Starch/Folic acid (C,D) capsules obtained through nanospray drying (A, C) and electrospraying (B, D). Scale bar corresponds to 10 µm.

The capsules obtained were also observed through scanning electron microscopy (SEM) in order to better characterize their size and morphology. Figure 2 shows the SEM images and the corresponding size distribution of the resulting capsules attained through nanospray-drying and electrospraying. It was observed that spherical submicron and micron capsules were obtained through both techniques, although spray-drying generally led to bigger average diameters and broader size distribution of the capsules, since it is more difficult to control the morphology and size of the particles with this technology. On the contrary, electrospraying led to an enhanced control over the size of the capsules and generally, narrower size distributions were found when using this technique. Moreover, smaller structures were attained when using this technique, which could favour the incorporation and dispersion of the capsules within food products without affecting their textural characteristics. However, it was seen that when resistant starch was used as encapsulating matrix, some big structures were obtained even through electrospraying, which could be due to the presence of guar gum in the solutions. A previous study showed that gums retained water causing an incomplete drying of the electrospraying jet and leading to more unstable electrospraying process, fact that could result in more heterogeneous capsule sizes (Pérez-Masiá et al., 2014b). Nevertheless, it was observed that the incorporation of guar gum was essential, not only for capsule formation, but also in order to avoid a premature folic acid precipitation during the experiments, keeping the folic acid in suspension with resistant starch within the plastic syringe. It was also seen that the incorporation of the folic acid did not considerably affect the morphology of the capsules.

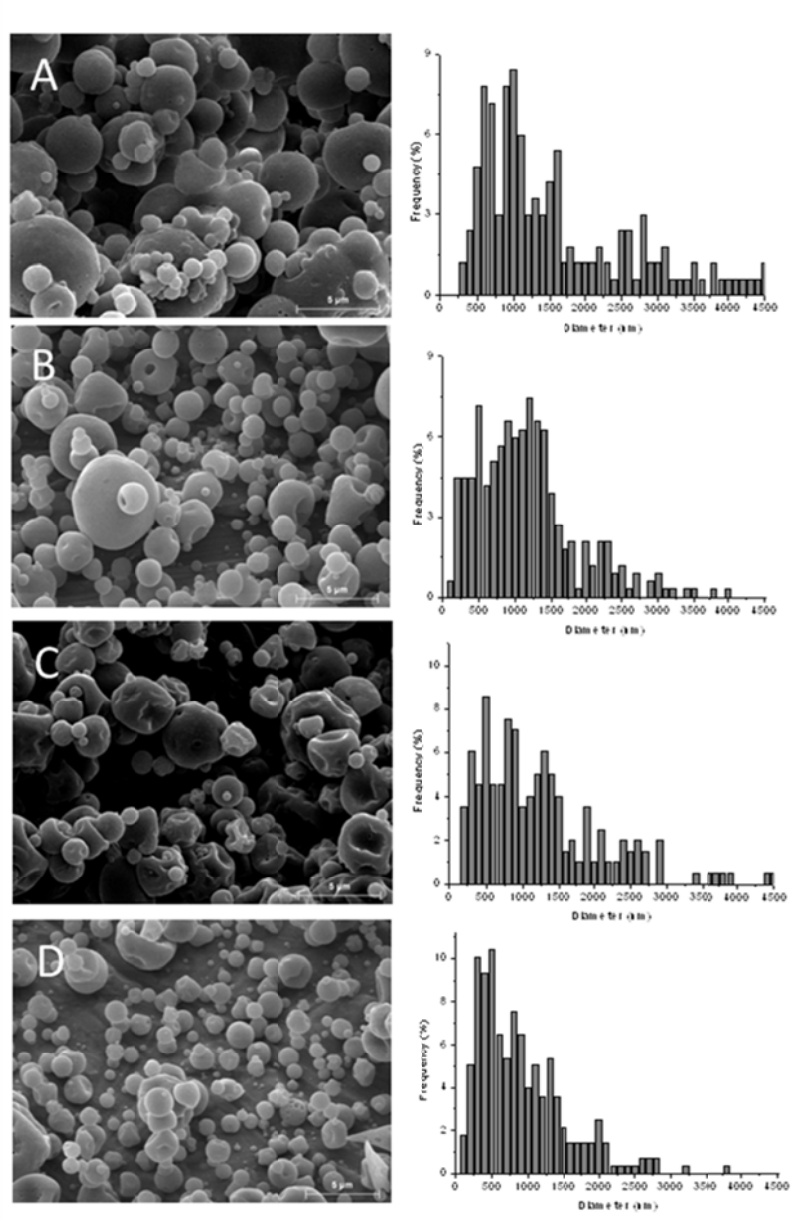

Figure 2.1. Selected SEM images and size distribution of WPC (A), WPC/folic acid (B), resistant starch (C) and resistant starch /folic acid (D) capsules developed through nanospray drying.

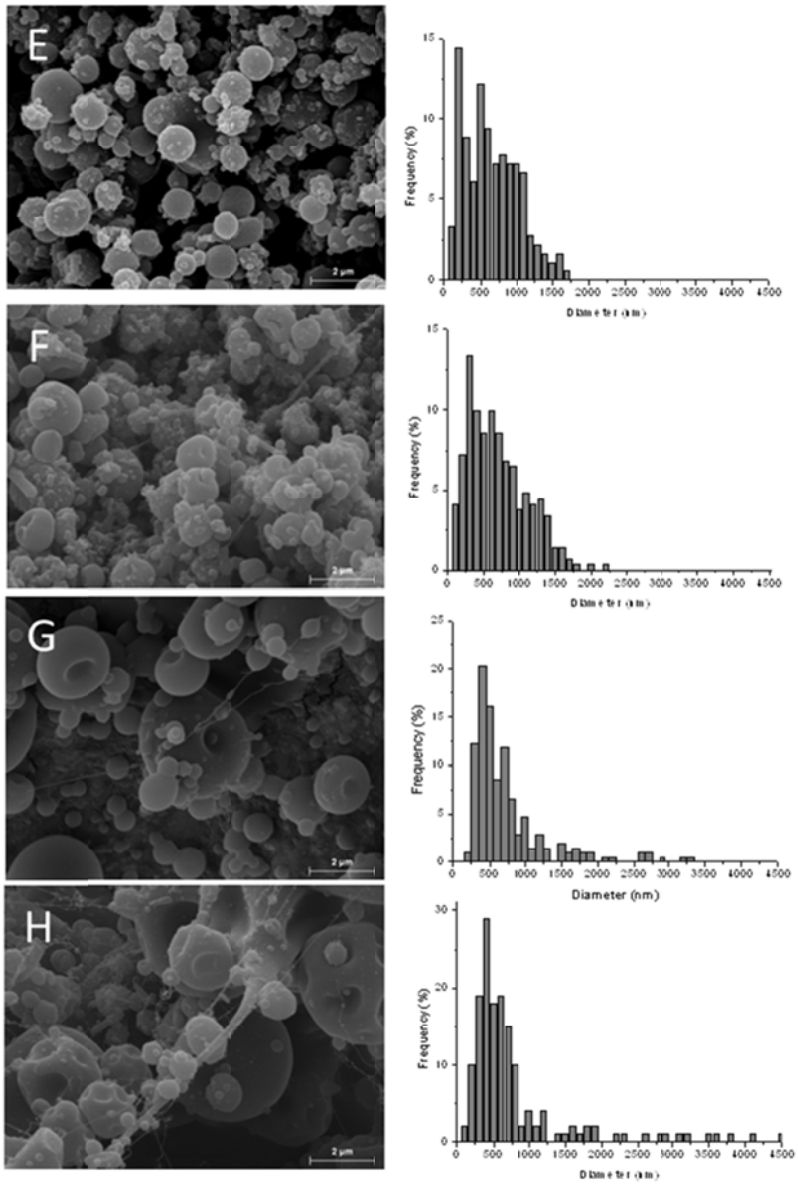

Figure 2.2. Selected SEM images and size distribution of WPC (E), WPC/folic acid (F), resistant starch (G) and resistant starch /folic acid (H) capsules developed through electrospraying.

3.3. Changes in molecular organization

Attenuated total reflectance infrared spectroscopy (ATR-FTIR) experiments were carried out in order to identify molecular changes in the hydrocolloids due to the encapsulation processes, as well as to detect interactions between the hydrocolloid matrices and the folic acid. Figure 3 shows the spectra from 4000 to 600 cm^{-1} of the capsules' individual components. It was observed that folic acid was mainly characterized by the O-H (~3545 cm^{-1}), N-H (~3418 and ~3323 cm^{-1}) and the C=O stretching vibrations (~1695 cm^{-1}), the bending mode of the N-H group (~1606 cm^{-1}) and the absorption of the phenyl ring (~1485 cm^{-1}) (Hammud et al., 2013; Bakhshi et al., 2012). The IR spectrum from WPC is mainly characterized by the amide I and II bands at around 1633 and 1516 cm^{-1}, respectively (Xiaozhan et al., 2009). Regarding the IR spectrum of the resistant starch, it presented the characteristic carbohydrate overlapped bands from 800 to 1200 cm^{-1} related to the stretching vibrations of C-O and C-C groups, and the bending vibration of C-O-H group (Wolkers, Oliver, Tablin, & Crowe, 2004; Kacurakova & Mathlouthi, 1996). In this region, a characteristic band from resistant starch which was not overlapped with the vibrational bands from folic acid was seen at around 1008 cm^{-1}, although guar gum also presented a similar band nearby this wavenumber. Therefore, the amide bands of the WPC and the starch band at 1008 cm^{-1} were studied to analyze the effect of the encapsulation techniques and the incorporation of folic acid on the molecular organization of the capsules.

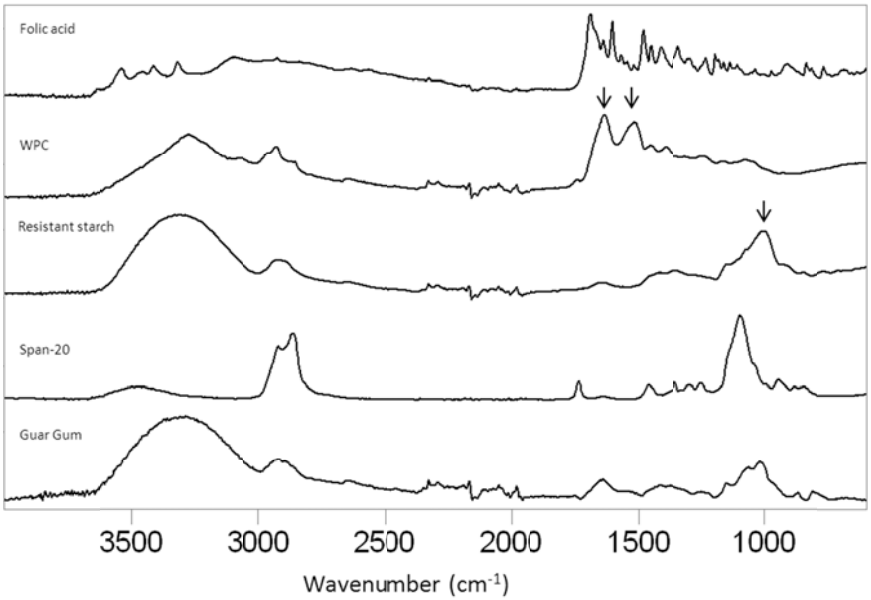

Figure 3. ATR-FTIR spectra of the capsules' individual components. Arrows show the most characteristic bands of the hydrocolloids which were considered for the analysis of the hybrid encapsulation structures.

Figure 4 displays the selected characteristic bands of the unprocessed encapsulating matrices and those from the capsules with and without folic acid. It was seen that, probably due to the low concentration of the bioactive within the capsules, the folic acid signal was not apparent in the infrared spectra. Nevertheless, the presence of the vitamin produced some variations in the spectra of the capsules. From Figures 4A and 4B it was seen that amide I and II bands were shifted towards higher wavenumbers in the spectra from the capsules, suggesting that some molecular changes occurred in the whey protein as a consequence of capsule formation using both technologies. Specifically, the spray drying technique led to a greater displacement of the spectral bands than the electrospraying method probably because the former used high

temperatures that could affect more strongly the molecular bonding of the WPC chains. It was also seen that the capsules which contained the folic acid presented narrower bands than those without the bioactive, which suggested that the incorporation of folic acid led to a greater molecular order. The incorporation of the vitamin also produced a greater displacement of the amide II band when compared to those without the bioactive, suggesting some kind of interaction between the proteins and the folic acid (as also inferred by the previously described increase in solution apparent viscosity). In fact, it has been already reported that the main proteins found in whey obtained from bovine milk have the ability to interact with folic acid through different mechanisms (Liang et al., 2013). It has also been seen that folic acid is able to conjugate to different polymers via an amide linkage through the carboxylic group of the bioactive, which is evident at around 1695 cm^{-1} (Sudimack & Lee, 2000; Teng, Luo, Wang, Zhang & Wang, 2013). Thus, the shifts toward higher wavenumber of the amide II band could be ascribed to the interaction between the protein matrix and the folic acid. Regarding the resistant starch infrared spectra, it was observed that the band at 1008 cm^{-1} located in the characteristic carbohydrate region, was also shifted towards higher wavenumbers when the starch was processed through both encapsulation techniques (Figures 4C and 4D). However, in this case, the shift could also be due to the presence of guar gum, which presented a band nearby this wavenumber. Nevertheless, it is worth noting that the band displacement was greater for the spray dried structures. Again, this result could be explained by the higher temperature applied during this encapsulation process, as well as to a greater amount of guar gum in the spray dried capsules due

to a better incorporation of capsules components through this technique. The differences in incorporation of the various compounds in the capsules could be explained by the different processing conditions during encapsulation, i.e., while during the nanospray drying process the solutions were continuously stirred, during electrospraying the solutions were left static within the syringes and, thus, partial precipitation of some compounds took place during the electrospraying process. From Figures 4C and 4D it was also observed that in this case the incorporation of the folic acid also produced narrower bands, suggesting a greater molecular order of the structures. Nevertheless, the incorporation of the bioactive did not considerably affect the molecular organization of the resistant starch capsules. Thus, it could be concluded that these materials did not interact with each other, but the folic acid was physically confined within the starch capsules.

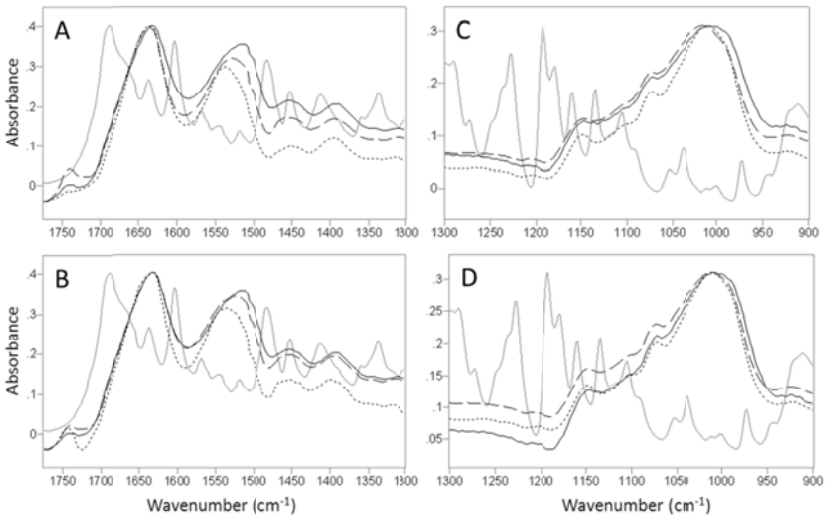

Figure 4. ATR-FTIR spectra of folic acid (grey lines), neat hydrocolloids (black lines), capsules without folic acid (dashed lines) and of the capsules with folic acid (dotted lines) for the WPC nanospray dried (A) and electrosprayed materials (B) and the resistant starch nanospray dried (C) and electrosprayed (D) materials.

3.4. Encapsulation efficiency and folic acid stability

HPLC chromatograms from encapsulated and non-encapsulated folic acid and from the encapsulation matrices at the beginning of the stability study and immediately after they were dissolved in water (0 days) are displayed in Figure 5. Although both the encapsulation matrices and the folic acid absorb at 290 nm, it was observed that the peaks were effectively separated in the chromatograms, with an elution time around 27-30 minutes for folic acid and 35 minutes for the matrices. This separation could probably be achieved by the buffer with a pH 2.2, since at this pH a decrease on the interactions between folic

acid and the different encapsulation matrices has been previously reported (Liang & Subirade, 2012). The peak area of the folic acid also showed differences between samples, indicating that the different biopolymers and encapsulating technologies could induce variability of results in the amount of encapsulated folic acid.

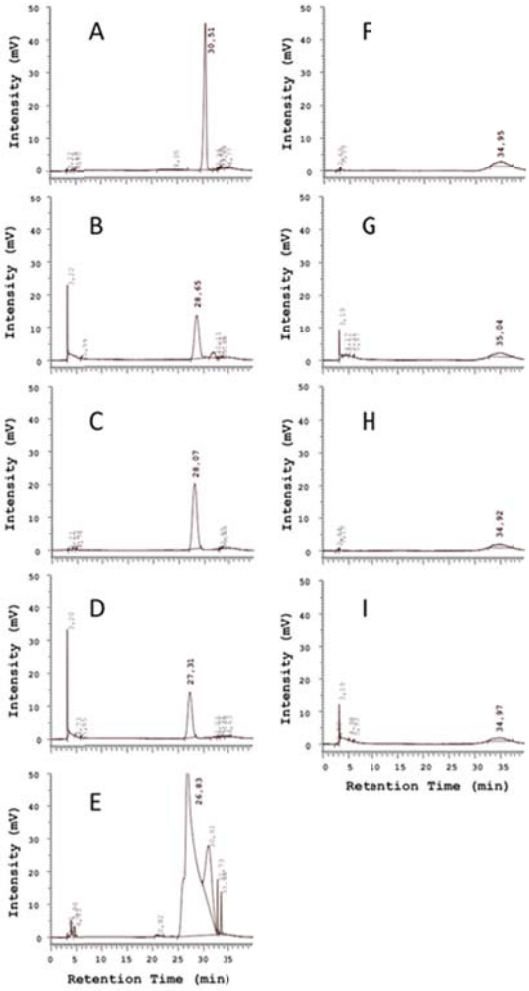

Figure 5. HPLC chromatograms of: WPC/folic acid capsules obtained through nanospray drying (A) and electrospraying (D) and the same structures without folic acid (F and H, respectively); Resistant starch/folic acid capsules obtained through nanospray drying (B) and electrospraying (D) and the same structures without folic acid (G and I, respectively); and non-encapsulated folic acid.

Table 2 shows the amount of folic acid in the different encapsulation structures as a function of storage time under different conditions (after dissolving the capsules in water and dry capsules in the presence or absence of light). Taking into consideration that the initial amount of folic acid was 1.5% (15 μg/mg), from the initial data it was seen that the encapsulation efficiency was higher for WPC matrix than for the resistant starch. This result was probably related to the interactions taking place between the protein matrix and the bioactive, which would facilitate the incorporation of the folic acid within the protein capsules. From these data it was also observed that there were not significant differences in encapsulation efficiency when using nanospray drying or electrospraying. When comparing the encapsulation yield with other works, it was seen that similar loadings were found when using food hydrocolloids as encapsulation matrices (Madziva, Kailasapathy & Phillips, 2004).

Table 2. Amounts of folic acid expressed as µg/mg of different capsules assayed after the storage in water solution and the storage in dry conditions under light and darkness during 60 days[1].

	Encapsulation efficiency (%)	0 days	15 days	30 days	45 days	60 days
			Water solution			
WPC/Folic acid (nd)	83.9 ± 7.8^{a}	12.59 ± 0.83^{a}	7.07 ±0.14^{a*}	7.47 ± 1.09^{a*†}	6.60 ± 1.03^{a*†}	4.03 ± 1.91^{a†}
WPC/Folic Acid (e-sp)	80.8 ± 12.9^{a}	12.12 ± 1.37^{a}	2.00 ± 0.11^{b*}	1.41 ± 0.14^{b*}	2.02 ± 0.18^{b*}	0.59 ± 0.03^{b†}
Resistant starch/Folic acid (nd)	52.5 7.6^{b}	7.87 ± 0.81^{b}	0.51 ± 0.03^{c*}	0.38 ± 0.09^{c*†}	0.20 ± 0.14^{c†}	0.18 ± 0.17^{c†}
Resistant starch/Folic acid (e-sp)	44.0 5.5^{b}	6.75 ± 0.43^{b}	0.17 ± 0.07^{d*}	0.06 ± 0.03^{d*†}	0.05 ± 0.01^{d†}	0.09 ± 0.05^{d*†}
			Dry/Natural light			
WPC/Folic acid (nd)	83.9 ± 7.8^{a}	12.59 ± 0.83^{a}	11.40 ± 0.24^{a*}	11.46 ± 0.26^{a*}	10.19 ± 0.87^{a*†}	9.19 ± 0.16^{a†}
WPC/Folic Acid (e-sp)	80.8 ± 12.9^{a}	12.12 ± 1.37^{a}	9.27 ± 1.73^{b*}	8.77 ± 0.14^{b*}	7.46 ± 0.17 ^{b†}	7.13 ± 0.25^{b†}
Resistant starch/Folic acid (nd)	52.5 ± 7.6^{b}	7.87 ± 0.81^{b}	7.86 ± 0.26^{c*}	5.54 ± 0.05^{c†}	3.10 ± 2.17$^{c\dagger **}$	1.38 ± 0.68c**
Resistant starch/Folic acid (e-sp)	44.0 ± 5.5^{b}	6.75 ± 0.43^{b}	5.54 ± 0.19^{d*}	4.34 ± 0.28^{d†}	1.98 ± 0.63^{c**}	0.80 ± 0.11d***
			Dry/Darkness			
WPC/Folic acid (nd)	83.9 ± 7.8^{a}	12.59 ± 0.83^{a}	12.26 ± 0.13^{a*}	11.74 ± 0.23^{a*}	11.47 ± 0.22^{a*}	10.79 ± 0.54^{a*}
WPC/Folic Acid (e-sp)	80.8 ± 12.9^{a}	12.12 ± 1.37^{a}	12.88 ± 0.22^{a*}	12.70 ± 0.16^{a*}	11.92 ± 0.10^{a†}	11.08 ± 0.15^{a**}
Resistant starch/Folic acid (nd)	52.5 ± 7.6^{b}	7.87 ± 0.81^{b}	8.60 ± 0.47^{a*}	6.98 ± 0.26^{b†}	6.22 ± 0.18^{b†}	4.71 ± 0.62^{b**}
Resistant starch/Folic acid (e-sp)	44.0 ± 5.5^{b}	6.75 ± 0.43^{b}	5.84 ± 0.12^{c*}	5.88 ± 0.11^{c*}	4.38 ± 0.18^{c†}	4.23 ± 0.37^{b†}

1Values are expressed as mean ± standard deviation.

a-d Different letters in the same column for each storage condition (water solution, dry/natural light or dry/darkness) show statistical significant differences ($p<0.05$).

*, † Different symbol in the same row show statistical significant differences ($p<0.05$) along the storage time.

Regarding the stability of folic acid within the capsules, a different behaviour was observed depending on the storage conditions, i.e. aqueous solution or dryness. Figure 6 shows the stability of folic acid, expressed as percentage of the initial amount of bioactive found in the capsules, in the different structures assayed during 60 days for capsules in aqueous solutions (Figure 6A) and for capsules in dry conditions under natural light (Figure 6B) and darkness (Figure 6C). It was seen that for capsules in aqueous solution, the amount of folic acid significantly decreased after 15 days in all cases except in the WPC capsules obtained through nanospray drying. In these samples, the losses of the synthetic folate were around 60%, remaining quite stable along time until 45 days. On the other hand, the folic acid degradation was extremely marked in the resistant starch capsules, in which losses were higher than 90% of the initial amount. This result can be explained by the high solubility of this polysaccharide in water, which led to a very quick release of the bioactive which was, thus, no longer protected. From Figure 6A it was also observed that the capsules obtained through spray drying displayed better protection ability than those obtained through electrospraying. As it was seen from ATR-FTIR results, the two encapsulation techniques led to different matrix conformations and, from the results it appeared that spray drying could provide more compact structures which would consequently had improved moisture resistance. Nevertheless, it is worth noting that non-encapsulated folic acid drastically reduced its content, only remaining 1% after 15 days of storage and, hence, even the highly soluble resistant starch capsules provided improved folic acid stability.

In contrast with the slight improvements observed when the storage experiments were carried out with the capsules immersed in aqueous solutions, from Figures 6B and 6C it was observed that under dry conditions, encapsulation effectively provided a great folic acid stability during storage time, especially when the encapsulating matrix was WPC independently of the encapsulation technology. The WPC capsules were able to almost keep the bioactive stability at 100% in darkness conditions, while 40% of non-encapsulated folic acid was degraded. From these figures it can also be seen that resistant starch capsules did not provide a great protective effect when compared with non-encapsulated folic acid. However it should be noted that the relative humidity of the storage room in dry conditions was around 65% and, thus, starch capsules could be at least partially dissolved, leaving the folic acid exposed to the ambient conditions.

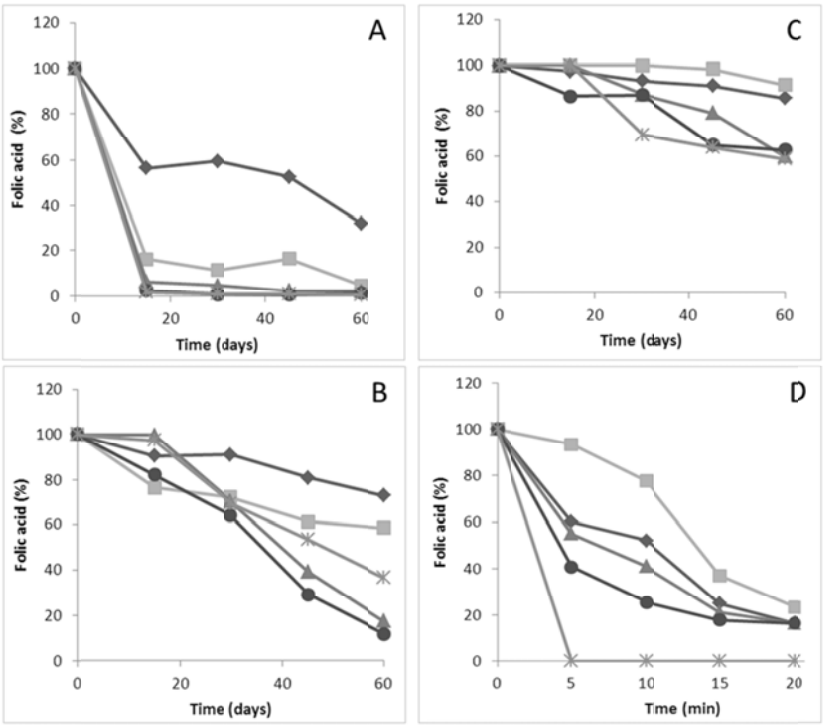

Figure 6. Stability of folic acid, expressed as percentage of the initial amount, in the different capsules assayed along storage: non encapsulated folic acid (cross); WPC/Folic acid capsules obtained through nanospray drying (rhombus) and electrospraying (square); and Resistant starch/folic acid capsules obtained through nanospray drying (triangle) and electrospraying (circle). Figure A represents the aqueous solutions of encapsulated folic acid, and Figures B and C represent the stability of folic acid in the capsules stored in dry conditions both under natural light and in darkness respectively. Figure D represents the stability of folic acid along the thermal assay during 20min.

Regarding the folic acid stability upon high temperature exposure, it is important to note that this study was carried out after the stability assay in dryness conditions, and thus, the capsules were not freshly prepared, but they were studied after 2 months of storage. Figure 4D shows the

stability of the different samples after thermal treatment at 120ºC for different times.

It was seen that non-encapsulated folic acid was completely degraded after only 5 minutes at 120ºC, as no peaks were detected through HPLC. In contrast, the encapsulation structures were able to keep part of the bioactive in good conditions during the experiment. In general, it was observed that the percentage of losses of folic acid were directly proportional to the time of treatment, providing higher stability WPC than resistant starch capsules. This fact could be due to the interaction between folic acid and whey proteins, since it has been previously reported that this interaction could act as a protective factor. Specifically, Liang & Subirade (2012) observed that this biopolymer induce a thermal stabilization of synthetic folate until 85ºC. Nevertheless, it is worth noting that this study was done with stored samples, rather than fresh capsules as the rest of the stability studies. Therefore, folic acid could be already partially degraded, and further studies should be carried out in order to better assess the protective effect of capsules during heating conditions.

4. CONCLUSIONS

In this work, folic acid was encapsulated using two different matrices (WPC and a commercial resistant starch) and two different encapsulation techniques (spray drying and electrospraying). This study showed that electrospraying can be used as a promising technology in the food industry for encapsulation applications, since the capsules obtained presented similar morphological characteristics than those obtained through spray drying. Furthermore, it does not require heating or the use of organic agents which could destroy some sensitive encapsulated nutrients or cause toxicity problems. Specifically, results showed that spherical submicron and micron capsules were obtained for all the compositions assayed, although electrospraying generally allowed an enhanced control over the size distribution of the capsules and smaller capsules. Concerning the encapsulation efficiency, it was observed that there were not significant differences between both encapsulation technologies. However, WPC led to higher encapsulation yields than resistant starch, probably because of the interaction between the protein matrix and the folic acid which facilitated the incorporation of the bioactive within the capsules. With regard to the biopolymers used, it was observed that WPC protected the folic acid against the degradation during storage in both situations (aqueous solution and dryness). On the contrary, resistant starch capsules provided lower stability to folic acid when capsules were suspended in aqueous solution. Nevertheless, protection was greater in dryness conditions; hence these capsules might be better applied in dry foods. Regarding the folic acid stability under thermal exposure, even though

promising results were obtained, further studies should be carried out in order to determine the potential applications.

5. REFERENCES

Alborzi, S., Lim, L.-T., Kakuda, Y. (2013). Encapsulation of folic acid and its stability in sodium alginate-pectin-poly(ethylene oxide) electrospun fibres. Journal of Microencapsulation 30 (1), pp. 64-71.

Bakhshi, P.K., Nangrejo, M.R., Stride, E., Edirisinghe, M. (2013). Application of Electro-hydrodynamic Technology for Folic Acid Encapsulation. Food and Bioprocess Technology 6 (7), pp. 1837-1846.

de Conto, L.C., Grosso, C.R.F., Gonçalves, L.A.G. (2013). Chemometry as applied to the production of omega-3 microcapsules by complex coacervation with soy protein isolate and gum Arabic. LWT - Food Science and Technology 53 (1), pp. 218-224.

Gharsallaoui, A., Roudaut, G., Chambin, O., Voilley, A., Saurel, R. (2007). Applications of spray-drying in microencapsulation of food ingredients: An overview. Food Research International 40 (9), pp. 1107-1121.

Gibbs, F., Selim, A., Catherine, N., & Mulligan, B. (1999). Encapsulation in the food industry: a review. International Journal of Food Sciences and Nutrition, 50 (3), 213-224.

Hammud, K.K., Mohammed, J.M., Radif, M.M., Raouf, A.L.M., Mahmmood, S.S., Neama, R.R., Znad, D.E., Abbas, S.J. (2013). Thermodynamic parameters for phenanthrene interaction with a biological π- acceptor (folic acid) by spectroscopic measurements. Journal of Chemical and Pharmaceutical Research 5 (2), pp. 24-28.

Hong YL, Li YY, Yin YZ, Li DM, Zou GT. (2008). Electro-hydrodynamic atomization of quasi-monodisperse drug-loaded spherical/wrinkled microparticles. Journal of Aerosol Science 39 (6), pp. 525-536.

Kacurakova, M. & Mathlouthi, M. (1996). FTIR and laser-Raman spectra of oligosaccharides in water: characterization of the glycosidic bond. Carbohydrate Research, 284, 145–157.

Konings, E.J.M. (1999). A validated liquid chromatographic method for determining folates in vegetables, milk powder, liver and flour. Journal of AOAC International, 82, 119–127.

Kriegel, C., Kit, K.M., McClements, D.J., & Weiss, J. (2009). Influence of surfactant type and concentration on electrospinning of chitosan-poly(ethylene oxide) blend nanofibers. Food Biophysics 4, 213-228.

Li, D. & Xia, Y. (2004). Electrospinning of nanofibers: Reinventing the wheel? Advanced Materials, 16(14), 1151-1170.

Li, X.Y., Chen, X.G., Sun, Z.W., Park, H.J., Cha, D.-S. (2011). Preparation of alginate/chitosan/carboxymethyl chitosan complex microcapsules and application in Lactobacillus casei ATCC 393. Carbohydrate Polymers 83 (4), pp. 1479-1485.

Liang, L. & Subirade, M. (2012). Study of the acid and thermal stability of β-lactoglobulin-ligand complexes using fluorescence quenching. Food Chemistry 132 (4), pp. 2023-2029

Liang, L., Zhang, J., Zhou, P., Subirade, M. (2013). Protective effect of ligand-binding proteins against folic acid loss due to photodecomposition. Food Chemistry 141 (2), pp. 754-761.

Lopera, S.M.C., Guzmán, C.O., Cataño, C.R., Gallardo, C.C. (2009). Development and characterization of folic acid microparticles formed by spray-drying with gum arabic and maltodextrin. Vitae 16 (1), pp. 55-65.

Lopez-Rubio, A. & Lagaron, J.M. (2011). Procedimiento de obtención de micro-, submicro- y nanocápsulas basado en proteínas del suero de la leche. Spanish Patent No. P201131048.

Lopez-Rubio, A. & Lagaron, J.M. (2012). Whey protein capsules obtained through electrospraying for the encapsulation of bioactives. Innovative Food Science and Emerging Technologies 13, pp. 200-206.

Madziva, H., Kailasapathy, K., Phillips, M. (2005). Alginate-pectin microcapsules as a potential for folic acid delivery in foods. Journal of Microencapsulation, 22(4), pp. 343-351.

Murugesan, R. & Orsat, V. (2012). Spray Drying for the Production of Nutraceutical Ingredients-A Review. Food and Bioprocess Technology 5 (1), pp. 3-14.

Pérez-Masiá, R., Lagaron, J.M., Lopez-Rubio, A. (2014a). Surfactant-aided electrospraying of low molecular weight carbohydrate polymers from aqueous solutions. Carbohydrate Polymers, 101 (1), pp. 249-255.

Pérez-Masiá, R., Lagaron, J.M., Lopez-Rubio, A. (2014b). Development and Optimization of Novel Encapsulation Structures of Interest in Functional Foods Through Electrospraying. Food and Biopocess Technology. DOI: 10.1007/s11947-014-1304-z

Regulation 1924/2006 of the European Parliament and of the Council of 20 December 2006 on nutrition and health claims made on foods. Official Journal of the European Union. Published 18/01/2007.

Regulation 1925/2006 of the European Parliament and of the Council of 20 December 2006 on the addition of vitamins and minerals and of certain other substances to foods. Official Journal of the European Union. Published 30/12/2006.

Regulation 432/2012. Commission regulation (EU) No 432/2012 of 16 May 2012 establishing a list of permitted health claims made on foods, other than those referring to the reduction of disease risk and to children's development and health. Official Journal of the European Union. Published 25/05/2012.

Silva, H.D., Cerqueira, M.A., Vicente, A.A. (2012). Nanoemulsions for Food Applications: Development and Characterization. Food and Bioprocess Technology 5 (3), pp. 854-867.

Sudimack, J. & Lee, R.J. (2000). Targeted drug delivery via the folate receptor. Advanced Drug Delivery Reviews 41 (2), pp. 147-162.

Tamjidi, F., Nasirpour, A., Shahedi, M. (2012). Physicochemical and sensory properties of yogurt enriched with microencapsulated fish oil. Food Science and Technology International 18 (4), pp. 381-390.

Teng, Z., Luo, Y., Wang, T., Zhang, B., Wang, Q. (2013). Development and application of nanoparticles synthesized with folic acid conjugated soy protein. Journal of Agricultural and Food Chemistry 61 (10), pp. 2556-2564.

Torres-Giner, S., Martinez-Abad, A., Ocio, M.J., Lagaron, J.M. (2010). Stabilization of a nutraceutical omega-3 fatty acid by encapsulation in

ultrathin electrosprayed zein prolamine. Journal of Food Science 75 (6), pp. N69-N79.

Wolkers, W.F., Oliver, A.E., Tablin, F. & Crowe, J.H. (2004). A Fourier-transform infrared spectroscopy study of sugar glasses. Carbohydrate Research 339 (6), 1077-1085.

Xiaozhan, Y., Dacheng, W., Zongliang, D., Ruixia, L., Xulong, C., Xiaohui, L. (2009). Spectroscopy study on the interaction of quercetin with collagen. Journal of Agricultural and Food Chemistry 57 (9), pp. 3431-3435.

Zuidam, N. J. & Shimoni, E. (2010). Overview of microencapsulates for use in food products or processes and methods to make them. In: Encapsulation Technologies for Active Food Ingredients and Food Processing. Springer Science Business Media LLC.

CHAPTER VII

Morphology and stability of edible lycopene-containing micro- and nanocapsules produced through electrospraying and spray drying

CHAPTER VII: Morphology and stability of edible lycopene capsules produced through electrospraying and spray drying

ABSTRACT

In this work, lycopene was encapsulated through electrospraying and spray drying (using a microporous membrane cap) within different edible biopolymeric matrices. Specifically, dextran, a whey protein concentrate (WPC) and chitosan were used as matrix materials. As a strategy to incorporate the hydrophobic bioactive within the hydrophilic matrices, emulsion electropraying and spray drying from emulsion were carried out. Moreover and, for comparison purposes, coaxial electrospraying was also performed. The electrospraying solutions properties were studied, since they do not only affect the success of the electrohydrodynamic process, but also influence the morphology of the capsules. Apart from characterizing the morphology and molecular organization of the developed capsules, the encapsulation efficiency and the lycopene stability under moisture and heating conditions were also evaluated. Results showed that even though encapsulation structures were obtained from all the matrices assayed through both processing technologies, spray drying, as a consequence of the high temperatures needed in this process, affected lycopene stability. It was also seen that WPC presented the greatest encapsulation efficiency, probably ascribed to the interactions between the biopolymer and the lycopene. Furthermore, WPC capsules were able to better protect lycopene against moisture and thermal degradation.

Keywords: lycopene, encapsulation, electrospraying, electrospinning, spray drying

1. INTRODUCTION

Carotenoids are some of the most common pigments in nature, the most abundant being β-carotene, lycopene, lutein and zeaxanthin. These compounds are incorporated into foods, not only due to their colorant properties, but also to their nutraceutical uses. Specifically, lycopene is a natural red pigment mainly found in tomato and other red fruits, like watermelon or papaya, and it is one of the main responsible of the antioxidant capacity of these products. It has received great interest in recent years because of its activity in the prevention of chronic diseases such as atherosclerosis, skin cancer, and prostate cancer (Rao and Agarwal, 1999; Xue et al. 2013). However, lycopene presents several unsaturated bonds in its molecular structure, which makes it very susceptible to oxidants, light and heat. This fact makes that lycopene could lose its beneficial properties during processing and storage of foodstuffs. Moreover, it has a very low water solubility, which limits its industrial applicability in aqueous-based systems. A possible approach to overcome these limitations is the micro/nanoencapsulation of lycopene. Some technologies have been already used to prepare lycopene microcapsules. For instance, many authors have prepared lycopene microcapsules through the spray drying methodology. However, the resulted capsules did not present an optimum stability at room temperature (Matioli and Rodriguez-Amaya 2002; Shu et al. 2006; Rocha et al. 2012). Blanch et al. (2007) prepared lycopene microcapsules by supercritical fluid extraction method. The use of supercritical fluids in food is recommended, because it avoids the employment of large amounts of organic solvents. However, the costs of equipment and

operation are too high and the technological parameters need further optimization (Guo et al. 2012). Other techniques such as complex coacervation have been used, (Rocha-Selmi et al. 2013; Silva et al. 2012) but in this case either organic solvents (not convenient for food applications), high temperature or acid conditions are needed, which could affect lycopene stability.

In this study, the use of electro-hydrodynamic processing for obtaining micro/nanocapsules of lycopene was proposed as a novel encapsulation technology. This technique was compared to the spray drying methodology, since it is the most common encapsulation technology used in the food industry nowadays. Nevertheless, in this work, a novel spray drying device able to obtain smaller encapsulation structures (nanospray dryier) was used. The electro-hydrodynamic process uses electrostatic forces to produce electrically charged jets from viscoelastic polymer solutions which on drying, by the evaporation of the solvent, produce ultrathin structures (Li and Xia 2004). In particular, the technique is referred to as electrospinning when ultrathin continuous fibers are obtained. When size-reduced capsules are obtained, the technique is called electrospraying. For food and nutraceutical applications, capsules are generally preferred rather than fibers, since apart from facilitating handling and subsequent incorporation into different products, they usually present greater surface/volume ratio and, thus, are expected to have better release profiles than fibers (Hong et al. 2008). It is important to note that electrospraying does not require the use of high temperatures and, thus, temperature-sensitive ingredients, such as the carotenoids, may be encapsulated using this

processing technique without suffering from any activity loss. Moreover, electrosprayed capsules can be produced from some biopolymers using aqueous solutions, mainly by changing the solution properties through the addition of proper additives (Pérez-Masiá et al. 2014). This issue has special interest in food applications, where the use of organic solvents could lead to toxic effects due to the presence of remaining solvents in the structures. However, lycopene presented very low water solubility, thus electrospraying and subsequent encapsulation of this compound from water-based solutions is not simple. Nevertheless, emulsion electrospraying, as well as coaxial electrospraying can be used for the encapsulation of immiscible compounds. In the emulsion electrospraying, an immiscible liquid phase is dispersed into a polymer solution until both components form a stable emulsion. As a result, the immiscible phase forms the core material and the polymer constitutes the shell of the capsules (Angeles et al. 2007). In the coaxial methodology, the polymer and the core material are introduced into the electrospraying equipment from separated solutions, thus the immiscibility problem is solved.

In this work, lycopene was encapsulated through electrospraying and spray drying in various food hydrocolloid matrices for potential food applications. Specifically, a whey protein concentrate from milk (WPC), and two polysaccharides (dextran and chitosan) were evaluated. It is worth noting that WPC and dextran are water dispersible polymers, thus, emulsion and coaxial electrospraying were used in these cases. In the case of the spray drying methodology, an emulsion was also formed with these materials. For chitosan, an acetic acid solution was used,

where lycopene could be easily dissolved and, thus, uniaxial electrospraying or spray drying from the acid solution were carried out. Acetic acid is allowed for food contact applications and would not generate toxicity problems in case some solvent remained within the capsules. The morphology and the molecular organization of the capsules obtained were evaluated. Moreover, the stability of encapsulated lycopene was carried out taking into account different situations that can be found in the food industry, such as the incorporation of the capsules into aqueous-based foods and exposure to thermal treatments.

2. MATERIALS AND METHODS

2.1. Materials

Whey protein concentrate (WPC) was kindly donated by ARLA (ARLA Food Ingredients, Viby, Denmark). Under the commercial name Lacprodan® DI-8090, the composition per 100 g of product consisted of ~80 g of protein, ~9 g of lactose, and ~8 g of lipids, being the rest water and minerals like sodium and potassium. Dextran (Mw ~70000), low molecular weight chitosan (~50000-190000), lycopene, Tween-20 and soybean oil were supplied by Sigma-Aldrich (Spain) and they were used as received, without further purification.

2.2. Preparation of the encapsulation solutions

For the uniaxial electrospraying, 2% (w/v) of chitosan and 1.5% (w/w) of lycopene with respect to the chitosan weight were dissolved in a 90% (v/v) aqueous/acetic solution. For the coaxial electrospraying, the shell solutions were prepared by dissolving 30% (w/v) of WPC or 20% (w/v) of dextran and 5% (w/v) of Tween-20 in distilled water. The core solution was prepared by dissolving 1.25% (w/v) of lycopene in soybean oil. For the emulsion electrospraying, an aqueous surfactant solution was prepared by dissolving 10% (w/v) of Tween-20 in water. Afterwards, 16% (v/v) of lycopene/soybean oil solution [1.25 %(w/v)] was added to the surfactant solution to prepare an emulsion premix. The premix was ultrasonicated at 10% of amplitude and 20 kHz of process frequency for 120s using an ultrasonic homogenizer (Bandelin electronic, Germany). Finally, 30% (w/v) of WPC or 20% (w/v) of dextran were added to the

emulsion and they were mechanically stirred until homogeneous emulsions were obtained.

For the spray solutions, 0.04 % (w/v) of chitosan and 1.5% (w/w) of lycopene with respect to the chitosan weight were dissolved in a 0.4% (v/v) aqueous/acetic solution. For the preparation of the water dispersible biopolymer solutions, Tween-20 was dissolved in distilled water and afterwards, 0.3% (v/v) of lycopene/soybean oil solution [1.25 %(w/v)] was added to the surfactant solution to prepare an emulsion premix. The premix was ultrasonicated at 10% of amplitude and 20 kHz of process frequency for 120 s using an ultrasonic homogenizer (Bandelin electronic, Germany). Finally, 0.4% (w/v) of dextran or WPC was added to the emulsion and they were mechanically stirred until homogeneous emulsions were obtained.

2.3. Emulsion particle size characterization

The mean particle size and size distribution of the O/W emulsion attained were determined via dynamic light scattering (DLS) with a Zetasizer Nano-ZS 90 (Malvern Instruments Corp., UK). All measurements were performed a 25ºC in triplicate and intensity-weighted results were reported.

2.4. Characterization of the electrospraying solutions

The apparent viscosity (ηa) of the polymeric solutions at 100 s-1 was determined using a rotational viscosity meter Visco Basic Plus L from Fungilab S.A. (San Feliu de Llobregat, Spain). The surface tension of the solutions was measured using the Wilhemy plate method in an

EasyDyne K20 tensiometer (Krüss GmbH, Hamburg, Germany). The conductivity of the solutions was measured using a conductivity meter XS Con6 (Labbox, Barcelona, Spain). All measurements were made in triplicate at 25ºC.

2.5. Encapsulation through electrospraying

The electrospraying apparatus, equipped with a variable high-voltage 0-30 kV power supply, was a Fluidnatek® basic setup assembled and supplied by BioInicia S.L. (Valencia, Spain). Solutions were introduced in a 5 mL plastic syringe and were electrosprayed under a steady flow-rate using a stainless-steel needle. For the coaxial electrospraying, two concentrical needles were used. The inner one was used for the core material and the outer one for the shell solution. The needle was connected through a PTFE wire to the syringe. The syringe was lying on a digitally controlled syringe pump while the needle was in horizontal towards a stainless-steel plate attached to a copper grid used as collector. The flow rate was 0.15 mL/h, the voltage varied from 12 to 18 kV and the distance between the tip and the collector varied from 9-20 cm.

2.6. Encapsulation through spray drying

The solutions with and without lycopene were spray-dried using a Nanopray-dryer B-90 (Büchi, Switzerland) with a 7.0 µm spray cap. The solutions were introduced into the equipment through a silicone wire, which was connected to the spraying head of the equipment. The air flow was ~140 L/h with an inlet and outlet temperatures of 90ºC and 45ºC, respectively.

2.7. Scanning electron microscopy (SEM)

SEM was conducted on a Hitachi microscope (Hitachi S-4100) at an accelerating voltage of 10 KV and a working distance of 12-16 mm. The capsules were sputtered with a gold-palladium mixture under vacuum before their morphology was examined using SEM. Capsule diameters were measured by means of the Adobe Photoshop CS3 extended software from the SEM micrographs in their original magnification.

2.8. Attenuated total reflectance infrared spectroscopy (ATR-FTIR)

ATR-FTIR spectra were recorded in a controlled chamber at 24°C and 40% RH using a Bruker FT-IR Tensor 37 equipment (Rheinstetten, Germany) coupled with the ATR accessory GoldenGate of Specac Ltd. (Orpington, UK) in the 4000–600 cm^{-1} range. The spectra were collected in the different materials by averaging 20 scans at 4 cm-1 resolution. The experiments were repeated twice to verify that the spectra were consistent between individual samples.

2.9. Encapsulation efficiency

The lycopene encapsulation efficiency was calculated by dividing the lycopene concentration found in the capsules by the initial lycopene concentration added to the different solutions. Lycopene was extracted from the capsules by dissolving the capsules in water and afterwards, adding dodecane to the solution in order to separate the lycopene from the rest of the components. The capsules' concentration was evaluated from the UV absorbance of the capsules using a SP-2000UV spectrophotometer (Spectrum, Shanghai, China). As lycopene has an

absorption maximum at a wavelength of 476 nm, the bioactive concentration in the capsules was calculated according to a calibration curve obtained for different known lycopene concentrations and the corresponding absorbance at this wavenumber:

$y = 0.0187x – 0.0008$ ($R^2 = 0.99$) (Equation 1)

Where "y" was the lycopene concentration and "x" was the UV absorbance at 476 nm.

2.10. Water sorption analysis

Water sorption of different capsules was evaluated at 70%RH in the outer atmosphere. To this aim, a controlled amount of capsules was put over a plate and the weight gain vs. time curves at 24ºC was studied until constant weight. Afterwards, lycopene was again extracted from capsules and the bioactive concentration was studied through the UV absorbance of lycopene at 476 nm using the previously obtained calibration curve (cf. Equation 1).

2.11. Thermal stability of lycopene

Thermal stability of lycopene in WPC capsules was studied through the exposure of the structures and the raw lycopene to heating conditions and the evaluation of the antioxidant activity of the samples before and after the heating experiment. Specifically, samples were stored at 70ºC in darkness during 4 h, since it was observed that degradation of non-encapsulated lycopene occurred in these conditions. Antioxidant activity of lycopene was evaluated according to the ABTS radical cation ($ABTS^{\bullet+}$) methodology developed by Re et al. (1999). To this aim, $ABTS^{\bullet+}$ was

produced by reacting ABTS solution with potassium persulfate and allowing the mixture to stand in the dark at room temperature for 12–16 h before use. For the study of the antioxidant activity of different samples, the $ABTS^{\bullet+}$ solution was diluted with ethanol to an absorbance of 0.70 (±0.02) at 734 nm. Afterwards, capsules and raw lycopene were dissolved in dichloromethane and an aliquot of these solutions was added into the $ABTS^{\bullet+}$ solution in order to inhibit the $ABTS^{\bullet+}$ absorbance. The percentage inhibition of absorbance at 734 nm after 4 minutes was calculated for each sample, since it was previously observed that reaction between carotenoids and $ABTS^{\bullet+}$ was totally complete after this time (Re et al. 1999). A Trolox curve in the same solvent was used as reference (Equation 2) and results were reported as a function of equivalent Trolox concentration.

$y = 6.7579x + 2.0433 (R^2 = 0.99)$ (Equation 2)

Where "y" was the percentage inhibition of $ABTS^{\bullet+}$ absorbance at 734 nm and "x" was the corresponding Trolox concentration (μM).

2.12. Statistical analysis

Statistical analysis of data was performed through analysis of variance (ANOVA) using Statgraphics Centurion XV (Manugistics Corp., Rockville, MD). Homogeneous sample groups were obtained by using LSD test (95% significant level).

3. RESULTS AND DISCUSSION

3.1. Emulsion particle size characterization and electrospraying solution properties

Initially, the emulsions obtained were characterized. Figure 1 shows the particle size distribution of the O/W emulsion attained before adding the biopolymers. From this figure it was observed that only one curve was seen with the maximum peak at ~150 nm. This result indicated that there was only one population of particles with an average size of ~150 nm. It was not possible to measure the particle size distribution of the emulsion containing the biopolymers, as upon their incorporation at the concentration used for electrospraying, the turbidity of the solution became too high for a correct characterization.

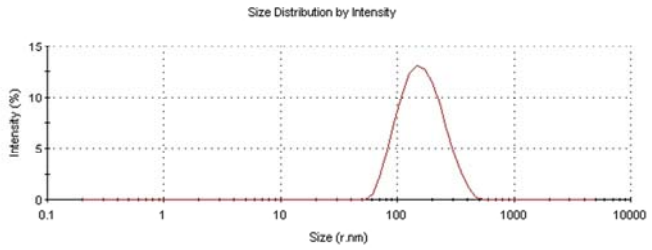

Figure 1. Particle size distribution of the O/W emulsion without the biopolymers.

Regarding the physical properties of the electrospraying solutions, they strongly affect the stability of the process and the successful development of structures through this technology. Moreover, capsules morphology is also influenced by solution properties. Table 1 compiles the viscosity, surface tension and electrical conductivity of the

electrospraying solutions assayed. These final compositions were obtained after a previous optimization process in which the concentration of the various compounds was adjusted until stable emulsions and electrospraying jets were obtained. Nevertheless, it was seen that a phase separation always occurred in dextran emulsions after a few hours. On the contrary, lycopene-containing WPC emulsions were stable during days. From Table 1 it can be observed that the incorporation of lycopene to the dextran and WPC solutions through the emulsion process, significantly affected the solution properties. Specifically, it was seen that viscosity considerably increased for both solutions because, in this case, lycopene was incorporated through soybean oil which was rather viscous. It is worth noting that the viscosity increase was greater for the WPC solution, which could indicate some kind of interaction between the protein and the lycopene in solution. Regarding the surface tension and electrical conductivity, it was observed that for the dextran solution these parameters slightly increased when compared to the solution without lycopene. However, in the case of WPC, the presence of the soybean oil/lycopene in the solution significantly decreased the electrical conductivity. This again could be ascribed to the interaction between the protein and the lycopene, thus, resulting in the neutralization of some of the protein charges. In contrast with the previous results, the chitosan solution properties were not modified upon lycopene incorporation. It is important to highlight that, in this case, lycopene was not incorporated through soybean oil, but it was directly added to the acid chitosan solution. Nevertheless, these data suggested that there were no interactions between chitosan and lycopene.

Table 1. Solution properties of the different electrospraying solutions

	Viscosity (cP)	Surface Tension (mN/m)	Electrical conductivity (μS)
Dextran	29.6 ± 0.2[a]	35.6 ± 0.2[a]	91.7 ± 0.8[a]
WPC	19.0 ± 0.9[b]	35.2 ± 0.2[a]	2056.7 ± 35.1[b]
Chitosan	49.0 ± 2.0[c]	39.9 ± 0.8[b]	392 ± 4.7[c]
Soybean Oil/lycopene	58.9 ± 0.7[d]	33.8 ± 0.1[c]	0.2 ± 0.1[d]
Dextran/lycopene	73.4 ± 1.1[e]	36.7 ± 0.5[d]	103.2 ± 1.0[e]
WPC/lycopene	110.7 ± 1.3[f]	36.7 ± 0.2[d]	1578.3 ± 11.2[f]
Chitosan/lycopene	49.3 ± 2.3[c]	39.1 ± 1.3[b]	398 ± 7.1[c]

a-f: Different superscripts within the same column indicate significant differences among different solutions ($p < 0.05$)

3.2. Morphology of the lycopene-containing capsules

SEM was used in order to analyse capsules' size and morphology. Figure 2 shows the SEM images of the different biopolymer/lycopene capsules obtained. Emulsion electrospraying of the dextran-based solution led to very homogeneous capsule sizes, while coaxial electrospraying produced more aggregated particles. This fact could be due to a worse entrapment of the soybean oil/lycopene solution when coaxial electrospraying was used, probably because of the non-continuous nature of the capsules, which complicated the incorporation of the antioxidant into the structures. In this case, part of the oil could leak from the dextran matrix, thus, causing capsules aggregation. It was also observed that spray drying gave rise to bigger structures with a broader capsule size distribution. In contrast, when WPC was used as encapsulating matrix, more heterogeneous structures were obtained through electrospraying, while smoother and more regular size capsules

were produced through spray drying. This result might be explained by the greater electrical conductivity of the protein solutions, which could destabilize the electrospraying jet, thus producing different particle sizes. In this case, aggregated particles were also seen when coaxial electrospraying was used, probably because oil leakages. Regarding the structures made up of chitosan, from Figure 1 it can be observed that very small capsules were obtained through electrospraying or spray drying. This fact was attributed to the use of the acid solvent, which generated strong electrostatic repulsions along the chitosan chains. These repulsive interactions hindered the formation of chain entanglements and, thus, small capsules were attained with this polymer (Torres-Giner et al. 2008).

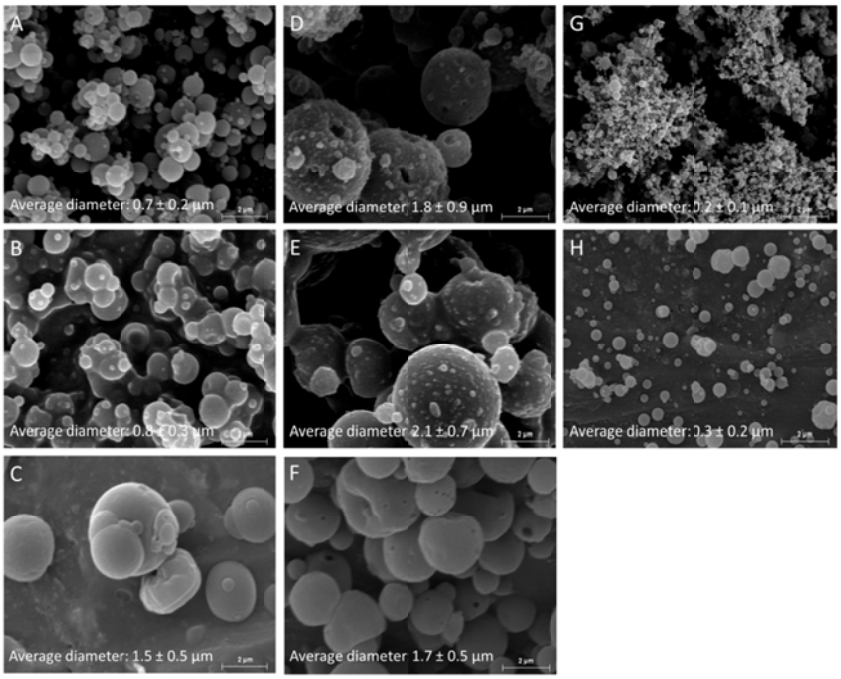

Figure 2. Selected SEM images of dextran/lycopene capsules obtained through emulsion electrospraying (A), coaxial electrospraying (B) and spray drying (C); WPC/lycopene capsules obtained through emulsion electrospraying (D), coaxial electrospraying (E) and spray drying (F); chitosan/lycopene capsules obtained through uniaxial electrospraying (G) and spray drying (H). Scale bars correspond to 2µm.

3.3. Infrared spectra of the bioactive capsules

ATR-FTIR analyses were done in order to confirm the presence of the antioxidant in the different structures, as well as to characterize the molecular organization of the capsules and detect interactions between the matrix and the core material. Figure 3 shows the ATR-FTIR spectra of the different materials assayed. From Figure 3A it was seen that FTIR

spectra of dextran encapsulation structures showed some bands attributed to both soybean oil (SBO) and lycopene (cf. arrows in Figure 3A). Specifically, it was seen that the C-H stretching vibration bands, centered around 2930 cm^{-1}, which appeared as a single broad spectral band for the as-received dextran, became narrower and better defined in the dextran capsules. These could be related to a greater molecular order due to the formation of the capsules, as well as to the presence of the SBO and lycopene in these capsules, since it was seen that both components presented sharp bands in this area. Moreover, the C=O group of the triglycerides of SBO found at 1743 cm^{-1} (Vlachos et al. 2005) and the lycopene band attributed to the C=C trans bond found at 957 cm^{-1} (Rubio-Diaz, Francis & Rodriguez-Saona, 2011) also appeared in the dextran capsules, especially in those obtained through spray drying. Therefore, FTIR results suggested that lycopene was incorporated in all the structures, but spray drying seemed to produce a greater encapsulation yield. It is also important to note that spectral bands of dextran were shifted depending on the encapsulation technology used. This shift was attributed to the process conditions, i.e. the solution preparation and subsequent drying of the carbohydrate, which could led to a rearrangement of the molecules, which was also probably influenced by the presence of surfactant. Figure 3A shows the details of the spectral region from 800 to 1200 cm^{-1}, in which the characteristic vibrational bands from carbohydrates arise), and it shows that the maximum of the most intense carbohydrate band at around 1005 cm^{-1} varied depending on the encapsulation technology used, i.e. this band arose at ~1006 cm^{-1}, ~1004 cm^{-1} and ~1012 cm^{-1} in the capsules obtained through emulsion electrospraying, coaxial electrospraying and spray

drying, respectively. The shift towards higher wavenumbers has been normally related to shorter and more attractive bonds (Wolkers et al. 2004). Therefore, this result suggested that the molecular conformation of capsules was affected by the encapsulation technology and spray drying, probably as a consequence of the high temperatures used in this process, produced more compact structures.

Regarding the WPC capsules, Figure 3B shows that the C=O band of SBO at 1743 cm^{-1} and the lycopene band at 957 cm^{-1} also appeared in the spectra from all the capsules, thus confirming the encapsulation of the lycopene through all the techniques used. Moreover, it was observed that both amide bands of the WPC/lycopene capsules were shifted in comparison to the pure protein. In this case the shifts could be attributed not only to the process conditions, but also to chemical or physico-chemical interactions between the protein and the bioactive, since the previous results showed related to the viscosity and the emulsion stabilization suggested that some kind of interaction occurred between the protein and the lycopene, as already reported in previous works (Zhang and Zhong, 2013; Mensi et al. 2013). Specifically, it was seen that amide I band (~1630 cm^{-1}) was displaced towards lower wavenumbers, indicating new β-sheets arrangements (Eissa et al. 2006) and the amide II band (~1530 cm^{-1}) of WPC/lyc capsules was displaced towards greater wavenumbers when compared to the as-received WPC powder. This latter shift was related to changes in the in-plane N-H and C-N vibrations (Kong and Yu 2007). Again, it is interesting to highlight that these shifts were different depending on the kind of encapsulation

technique, being the sprayed capsules those which again presented the most noticeable shifts.

Concerning the chitosan materials, from Figure 3C it was observed that the chitosan spectra completely changed after both encapsulation processes. This fact was attributed to the acetylation of chitosan due to the dissolution of the biopolymer in acetic acid media. Specifically, the main changes in the chitosan spectra occurred in the amide I and II regions (from 1700 to 1500 cm^{-1} aprox.). In this area the as-received chitosan shows the amide I and amide II bands at around 1650 and 1590 cm^{-1} respectively. However, after processing, the capsules presented two dominant bands centered at around 1546 and 1405 cm^{-1} associated to carboxylate ions (NH_3^+ and $COOH^-$). The amine groups in this chemical form are referred to as protonated or activated amine groups. These results suggested that capsules could exhibit antimicrobial performance (Fernández-Saiz, Ocio & Lagaron, 2006), even though the free acetic acid band at ~1706 cm^{-1} was not evident in the capsules spectra, indicating that solvent was completely evaporated during the encapsulation process. However, lycopene signal was not apparent in these capsules, suggesting that the bioactive could be degraded in the presence of the concentrated acetic acid or that it was not properly encapsulated in this case (maybe as a consequence of the smaller size of these structures). As with the other encapsulation matrices, it is interesting to note that, depending on the encapsulation technology used, the characteristic spectral bands arose slightly at different wavenumbers, thus confirming different molecular conformations depending on the technology used.

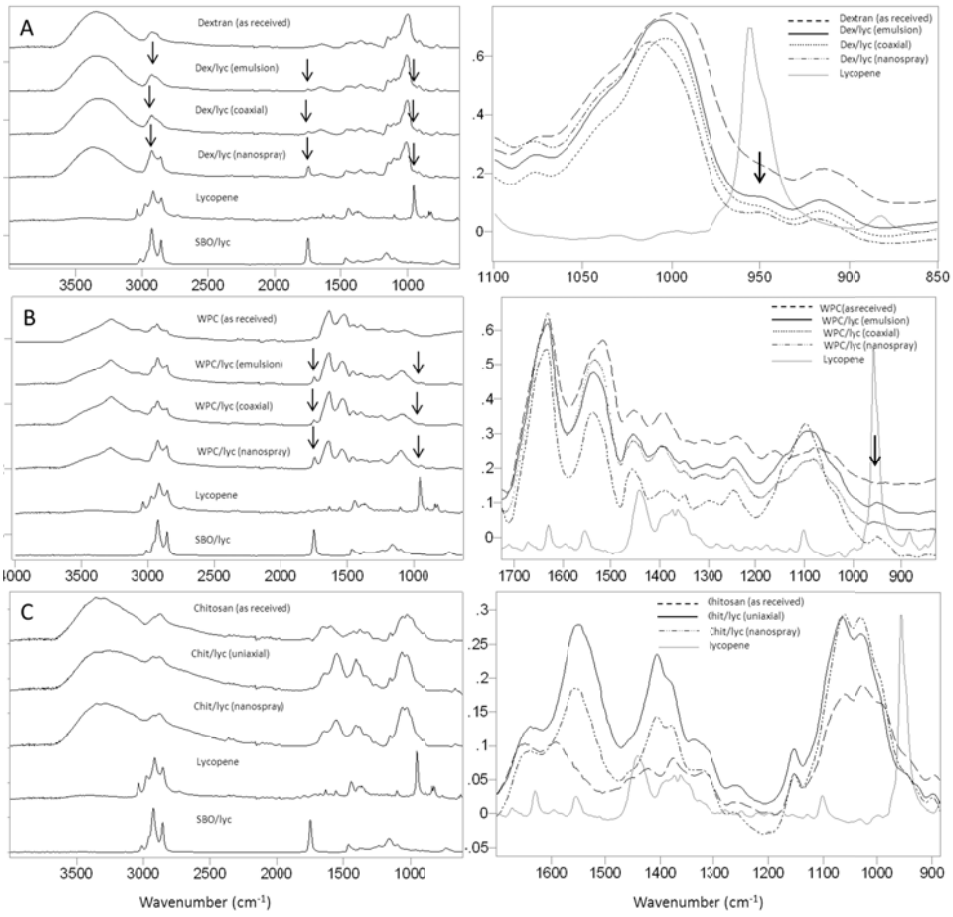

Figure 3. ATR-FTIR spectra of the different materials assayed: (A) dextran-based materials, (B) WPC-based materials and (C) chitosan-based materials. Arrows point out the most remarkable spectral changes as a consequence of lycopene incorporation. Images on the left side show the complete spectra of the materials from 4000 to 600 cm-1. Images on the right side show the lycopene contribution in the spectra of the different materials.

3.4. Encapsulation efficiency

The encapsulation efficiency of the different structures developed was evaluated through UV spectroscopy. Figure 4 shows the UV spectra from 350 to 650 nm of the raw lycopene, as well as of the lycopene extracted from the capsules. It was observed that lycopene presented 3 characteristic bands at 449, 476 and 509 nm, being the band at 476 nm the most intense one. Therefore, the intensity of the band at 476 nm was used to evaluate lycopene concentration according to Equation 1 (cf. materials and methods, section 2.8). From Figure 4 it can be observed that lycopene extracted from the capsules presented a similar spectrum than that from raw lycopene. However, lycopene extracted from chitosan capsules presented very low absorbance values probably because of a greater degradation of the carotenoid in this case due to the acid conditions used in the formation of these capsules. From this figure it is also seen that the high temperature employed during spray drying also affected to the stability of the bioactive. Indeed, if comparing the spectra of extracted lycopene from the electrosprayed and spray dried capsules (cf. Figure 4A vs. 4B), it is clear that the high temperature involved in the spray drying technique led to a certain degradation of the bioactive, as reflected by the lower spectral intensity.

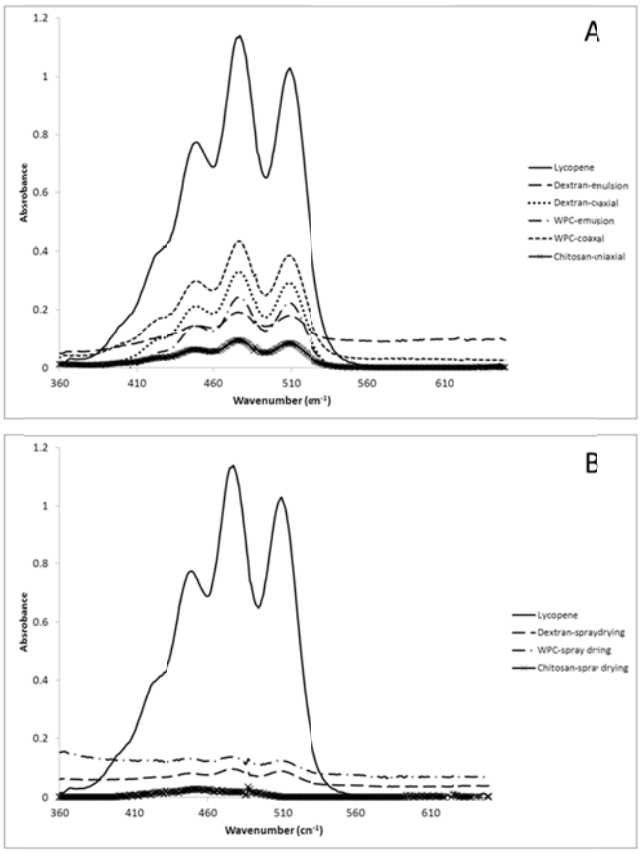

Figure 4. UV spectra from 350 to 650 nm of lycopene extracted from electrosprayed capsules (A) and sprayed capsules (B).

Table 2 shows the initial lycopene concentration added to the solutions and the lycopene concentration remaining in the capsules obtained through Equation 1, expressed as the percentage of lycopene with respect to the total solids in the capsules. The encapsulation efficiency is also included in this table and it was calculated by dividing the initial lycopene concentration by the lycopene concentration found in the

capsules. From this table it was seen that capsules obtained through spray drying presented very low encapsulation efficiencies for all the matrices, probably because the high temperature needed for solvent evaporation during capsule formation affected lycopene stability. This data seems to be in disagreement with FTIR results, which suggested that spray drying led to higher encapsulation yield. However, FTIR spectra showed the soybean oil (SBO) signal which was not affected by temperature. Thus, although higher amount of SBO/lycopene solution was probably encapsulated through spray drying, lycopene was possibly degraded due to heat exposure and, thus, the bioactive signal could not be detected through UV spectroscopy. This result is in accordance with previous works which have studied lycopene loss during heating or drying of tomato products (Rocha et al. 2012; Goula and Adamopoulos, 2005). Table 2 also shows that for dextran, emulsion electrospraying also led to low encapsulation efficiency, due to the unstable emulsion formed with this polymer. Therefore, for this material it was better to use the coaxial methodology, which led to an encapsulation yield around 55-60%. For WPC capsules it was seen that emulsion electrospraying led to proper encapsulation efficiency, since WPC and SBO/lycopene solution produced a stable emulsion which did not separate during the electrospraying experiment. Regarding the coaxial electrospraying very high variability was found, probably because this technique led to a worse encapsulation process with oil leakages, which made that some capsules presented very high lycopene contents, while other structures presented very low encapsulation yields. Finally, it was observed that lycopene was poorly encapsulated in chitosan capsules through uniaxial

electrospraying. Moreover, the lycopene found in these capsules was probably partially degraded due to the acid conditions used in this case, as it was previously seen from the UV spectra.

Table 2. Lycopene concentration and encapsulation efficiency of different capsules assayed

		Lycopene concentration		
		Solution concentration (%)	Capsules concentration (%)	Encapsulation efficiency (%)
Dextran/lycopene	Emulsion e-sp.	0.5	0.13 ± 0.04^{a}	26.0 ± 8.7^{a}
	Coaxial e-sp.	0.4	0.23 ± 0.07^{b}	57.5 ± 17.7^{b}
	Spray-Drying	0.5	0.08 ± 0.02^{a}	16.0 ± 4.3^{a}
WPC/lycopene	Emulsion e-sp.	0.4	0.29 ± 0.03^{b}	72.5 ± 7.1^{b}
	Coaxial e-sp.	0.3	0.23 ± 0.06^{b}	75.2 ± 33.5^{b}
	Spray-Drying	0.4	0.11 ± 0.01^{a}	27.5 ± 2.1^{a}
Chitosan/lycopene	Uniaxial e-sp.	1.5	0.41 ± 0.02^{c}	27.3 ± 4.2^{a}
	Spray-Drying	1.5	0.04 ± 0.01^{d}	2.7 ± 2.3^{c}

a-d: Different superscripts within the same column indicate significant differences among lycopene capsules ($p < 0.05$)

3.5. Water sorption analysis

If considering the developed structures for food applications, and taking into account that most food products have high water activity, it is important to know the water sorption behavior of the different capsules and, what is more important, the bioactive stability in the presence of moisture. To this aim, water sorption was evaluated through the exposure of the capsules and also of the raw lycopene (for comparison purposes) at ambient temperature (T = 21 ºC) and high relative humidity (~70%). Their weight gain was evaluated until a constant value was reached. Afterwards, lycopene was extracted from the capsules and evaluated through UV spectroscopy in order to study the efficiency of

the capsules for stabilizing the antioxidant compound under moisture conditions. Table 3 shows the weight gain of all the capsules developed, the initial lycopene concentration in the capsules previously obtained (cf. Table 2), the lycopene concentration after moisture exposure obtained through Eq. 1 and the total lycopene loss. From this table it can be clearly seen that after moisture exposure, in all cases, lycopene absorbance decreased. This effect was attributed to spatial rearrangements of the double bonds and partial degradation of the bioactive (Tan and Soderstrom, 1989). Specifically, it was seen that ~65% of non-encapsulated lycopene was degraded, even when the raw lycopene hardly increased its weight after moisture exposure. Nevertheless, the oxygen presence and ambient temperature (21ºC) in the moisture chambers could also alter the molecular structure of the lycopene. Regarding the capsules it was seen that water uptake of capsules was generally greater than those of raw lycopene, probably because capsules' matrices were hydrophilic materials which favored the water sorption. Specifically, it was seen that dextran capsules absorbed a greater amount of water than WPC and chitosan, ascribed to its higher water solubility. This fact affected lycopene stability, since dextran capsules were partially dissolved and lycopene was thus exposed to moisture, oxygen and temperature conditions. Thus, it was seen that the lycopene absorbance decreased in these capsules after the moisture exposure, probably because of the degradation of part of the antioxidant. On the contrary, WPC is not water soluble, but it is water dispersible, thus water sorption was lower for these capsules than for dextran capsules. In this case, it was seen that WPC capsules obtained through emulsion electrospraying and spray drying were able to better

protect the bioactive, which was not considerably affected after moisture exposure. However, a considerable decrease of the lycopene content was seen for the WPC capsules obtained through coaxial electrospraying. This was probably because, as it was commented before, non-continuous capsules hindered the proper incorporation of the bioactive through the coaxial methodology and, thus, there was some leakage from these capsules. Therefore, part of the lycopene could be on the surface of the structures exposed to humidity and, thus, more prone to degradation. Regarding chitosan, it is important to highlight that it was partially acetylated due to the solution preparation procedure with acetic acid as the solvent. This fact resulted in increased water solubility of chitosan, affecting the water uptake of these capsules (Pillai et al. 2009). Even though water uptake was limited in the chitosan matrices, in comparison with the other encapsulating materials, lycopene was completely degraded in these capsules, not only due to moisture exposure, but also probably because of the acid conditions needed for capsules formation, which led to a rapid degradation of the antioxidant. From Table 3 it can also be observed that water uptake was greater for electrosprayed capsules than for capsules obtained through spray drying. As it was previously seen from ATR-FTIR results, molecular organization of matrices was different in electrosprayed than in sprayed capsules. Particularly, it was seen that sprayed capsules presented more attractive bonds and thus more compact structures than electrosprayed capsules. This fact could be hindering water uptake in the sprayed capsules. Moreover, the greater specific surface of the electrosprayed materials could be also favoring water sorption.

Table 3. Weight increase of raw lycopene and capsules after moisture exposure, lycopene concentration found before (initial) and after (final) the water sorption and total lycopene loss after the water sorption.

			Lycopene concentration		
		Weight gain (%)	Initial (%)	Final (%)	Lycopene loss
Lycopene	raw material	2.5 ± 0.7^{a}	100 ± 0.0^{a}	36.2 ± 10.6^{a}	63.8 ± 10.6^{a}
Dextran/lycopene	emulsion e-sp.	10.6 ± 1.4^{b}	0.13 ± 0.04^{b}	0^{b}	100^{b}
	coaxial e-sp.	15.1 ± 0.8^{c}	0.23 ± 0.07^{bc}	0.09 ± 0.02^{c}	56.6 ± 13.6^{a}
	spray-drying	6.0 ± 1.8^{d}	0.08 ± 0.02^{b}	0.06 ± 0.01^{c}	19.8 ± 15.2^{c}
WPC/lycopene	emulsion e-sp.	6.1 ± 1.0^{d}	0.29 ± 0.03^{c}	0.26 ± 0.01^{d}	11.6 ± 7.3^{c}
	coaxial e-sp.	5.2 ± 0.9^{d}	0.23 ± 0.06^{c}	0.11 ± 0.06^{c}	52.1 ± 23.6^{ac}
	spray-dring	2.3 ± 0.6^{a}	0.11 ± 0.01^{b}	0.10 ± 0.02^{c}	16.7 ± 23.3^{cd}
chitosan/lycopene	uniaxial e-sp.	3.3 ± 1.2^{a}	0.41 ± 0.02^{d}	0^{b}	100^{b}
	spray-drying	4.8 ± 0.2^{d}	0.04 ± 0.01^{e}	0^{b}	100^{b}

a-d: Different superscripts within the same column indicate significant differences among different lycopene capsules ($p < 0.05$)

3.6. Thermal stability

Thermal treatments are commonly employed for food processing and, thus, lycopene stability under heating conditions is an important attribute to evaluate. Specifically in this work, the stability of non-encapsulated lycopene and lycopene encapsulated in WPC capsules obtained through emulsion electrospraying was studied, since it was previously seen that these structures provided the best encapsulation efficiency and protection under moisture conditions. To this end, the antioxidant activity of lycopene was evaluated according to the ABTS methodology. It is important to note that WPC capsules also contained SBO and, thus, the antioxidant activity of the solution lycopene/SBO was taken as the control value. Table 4 shows the antioxidant activity of

lycopene before and after the thermal treatment (70ºC during 4h). From this data it was observed that initially, both systems presented similar antioxidant activity, which confirmed that lycopene was not degraded after encapsulation in the WPC matrix. However, after the thermal treatment it was seen that the ABTS inhibition percentage of the non-encapsulated lycopene/SBO solution considerably decreased, when compared to the lycopene/SBO extracted from the WPC capsules. This data indicated that lycopene lost its antioxidant activity and, thus, its beneficial effects when it was exposed to heating conditions. In contrast, WPC capsules were able to significantly reduce the bioactive degradation and, thus, while the antioxidant activity of non-encapsulated lycopene was reduced by ~80%, more than 60% of the antioxidant activity was retained when encapsulated in WPC. These promising results seem to indicate that encapsulation using adequate matrices and encapsulation technologies would effectively have an impact in the commercial life of the antioxidant.

Table 4. Antioxidant activity, according to ABTS methodology, of non-encapsulated lycopene/SBO and encapsulated lycopene/SBO before and after the thermal treatment (70 ºC during 4 hours).

		% inhibition/µg antioxidant	µM Trolox/µg antioxidant
Lycopene/SBO	Before thermal exposure	25.6 ± 6.2^{a}	3.5 ± 0.9^{a}
	After thermal exposure	5.2 ± 0.6^{b}	0.5 ± 0.1^{b}
Lycopene/SBO from WPC capsules	Before thermal exposure	24.1 ± 1.8^{a}	3.3 ± 0.3^{a}
	After thermal exposure	14.6 ± 1.8^{c}	1.9 ± 0.3^{c}

a-c: Different superscripts within the same column indicate significant differences among antioxidant activity ($p < 0.05$)

4. CONCLUSIONS

In this work it has been demonstrated, for the first time, that lycopene can be properly encapsulated through electrospraying using aqueous biopolymer solutions. These results are very interesting for food-related applications in which organic solvents could lead to toxicity problems. The antioxidant-containing electrosprayed capsules were compared with those obtained through spray drying and results showed that poor encapsulation efficiencies were obtained through the latter technique, probably because of the high temperature required in this case which led to a partial degradation of the antioxidant. On the contrary, emulsion electrospraying could be used for lycopene encapsulation, especially when using protein matrices which create more stable emulsions which do not phase separate during the encapsulation process. Coaxial electrospraying could also be used for lycopene encapsulation, although some leakages were found in this case probably because of the non-continuous nature of the structures developed which resulted in a worse entrapment of the core material. Chitosan was also used as a matrix to encapsulate lycopene through both techniques. However, the acid conditions needed in this case in order to dissolve the polymer affected lycopene stability. Nevertheless, other bioactive ingredients with higher acid resistance could be potentially encapsulated using this matrix. Finally, it was seen that WPC-based capsules were able to protect lycopene from both moisture and heating conditions and, thus, this kind of capsules could be used to increase lycopene shelf life when incorporated in different food products.

5. REFERENCES

Angeles, M., Cheng, H.-L., & Velankar, S.S. (2008). Emulsion electrospinning: composite fibers from drop breakup during electrospinning. Polymers for Advanced Technologies, 19, 728-733.

Blanch GP, Castillo MLR, Mar Caja M, Pérez-Méndez M, Sánchez-Cortés S. (2007) Stabilization of all-trans-lycopene from tomato by encapsulation using cyclodextrins. Food Chemistry 105, 1335-1341.

Eissa, A.S., Puhl, C., Kadla, J.F., Khan, S.A. (2006). Enzymatic cross-linking of β-lactoglobulin: Conformational properties using FTIR spectroscopy. Biomacromolecules 7 (6) , pp. 1707-1713.

Fernandez-Saiz, P., Ocio, M.J., Lagaron, J.M. (2006). Film-forming process and biocide assessment of high-molecular-weight chitosan as determined by combined ATR-FTIR spectroscopy and antimicrobial assays. Biopolymers 83, 577-583.

Goula, A.M. & Adamopoulos, K.G. (2005). Stability of lycopene during spray drying of tomato pulp. LWT - Food Science and Technology 38 (5), 479-487.

Guo, H., Huang, Y., Qian, J.-q., Gong, Q.-y., Tang, Y. (2012). Optimization of technological parameters for preparation of lycopene microcapsules. Journal of Food Science and Technology, DOI 10.1007/s13197-011-0600-0.

Hong Y.L, Li Y.Y, Yin Y.Z, Li D.M, Zou G.T. (2008). Electro-hydrodynamic atomization of quasi-monodisperse drug-loaded spherical/wrinkled microparticles. Journal of Aerosol Science 39 (6), pp. 525-536.

Kong, J., Yu, S. (2007). Fourier transform infrared spectroscopic analysis of protein secondary structures. Acta Biochimica et Biophysica Sinica 39 (8), pp. 549-559.

Li, D. & Xia, Y. (2004). Electrospinning of nanofibers: Reinventing the wheel? Advanced Materials, 16(14), 1151-1170.

Matioli, G. & Rodriguez-amaya, D.B. (2002). Licopeno encapsulado em goma arábica e maltodextrina: Estudo da estabilidade. Brazilian Journal of Food Technology. 5, 197–203.

Mensi, A., Choiset, Y., Rabesona, H., Haertlé, T., Borel, P., Chobert, J.-M. (2013). Interactions of β-lactoglobulin variants A and B with vitamin A. Competitive binding of retinoids and carotenoids. Journal of Agricultural and Food Chemistry 6 (17), 4114-4119.

Pérez-Masiá, R., Lagarón, J.M., López-Rubio, A. (2014). Development and optimization of novel encapsulation structures of interest in functional foods through electrospraying. Food and Bioprocess Technology. DOI 10.1007/s11947-014-1304-z

Pillai, C.K.S., Paul, W., Sharma, C.P. (2009). Chitin and chitosan polymers: Chemistry, solubility and fiber formation. Progress in Polymer Science (Oxford), 34 (7), 641-678.

Rao, A.V. & Agarwal, S. (1999). Role of lycopene as antioxidant carotenoid in the prevention of chronic disease: a review. Nutrition Research 19, 305–323.

Re, R., Pellegrini, N., Proteggente, A., Pannala, A., Yang, M., Rice-Evans, C. (1999). Antioxidant activity applying an improved ABTS radical cation decolorization assay. Free Radical Biology and Medicine 26 (9-10), 1231-1237.

Rocha, G.A., Fávaro-Trindade, C.S., Grosso, C.R.F.(2012). Microencapsulation of lycopene by spray drying: Characterization, stability and application of microcapsules. Food and Bioproducts Processing 90, 37-42.

Rocha-Selmi, G.A., Favaro-Trindade, C.S., Grosso, C.R.F. (2013). Morphology, stability, and application of lycopene microcapsules produced by complex coacervation. Journal of Chemistry, DOI 10.1155/2013/982603.

Rubio-Diaz, D.E., Francis, D.M., Rodriguez-Saona, L.E. (2011). External calibration models for the measurement of tomato carotenoids by infrared spectroscopy. Journal of Food Composition and Analysis, 24 (1), 121-126.

Shu, B., Yu, W., Zhao, Y., Liu, X. (2006). Study on microencapsulation of lycopene by spray-drying. Journal of Food Engineering 76, 664–669.

Silva, D.F., Favaro-Trindade, C.S., Rocha, G.A., Thomazini, M. (2012). Microencapsulation of lycopene by gelatin-pectin complex coacervation. Journal of Food Processing and Preservation 36 (2), 185-190.

Tan, B. & Soderstrom, D.N. (1989). Qualitative aspects of UV-vis spectrophotometry of β-carotene and lycopene. Journal of Chemical Education 66 (3), 258-260.

Torres-Giner, S., Ocio, M.J., Lagaron, J.M. (2008). Development of active antimicrobial fiber-based chitosan polysaccharide nanostructures using electrospinning. Engineering in Life Sciences 8 (3), 303-314.

Vlachos, N., Skopelitis, Y., Psaroudaki, M., Konstantinidou, V., Chatzilazarou, A., Tegou, E. (2006). Applications of Fourier transform-infrared spectroscopy to edible oils. Analytica Chimica Acta 573-574, pp. 459-465.

Wolkers, W.F., Oliver, A.E., Tablin, F. & Crowe, J.H. (2004). A Fourier-transform infrared spectroscopy study of sugar glasses. Carbohydrate Research 339, 1077-1085.

Xue, F., Li, C., Liu, Y., Zhu, X., Pan, S., Wang, L. (2013). Encapsulation of tomato oleoresin with zein prepared from corn gluten meal. Journal of Food Engineering 119, 439-445.

Zhang, Y. & Zhong, Q. (2013). Probing the binding between norbixin and dairy proteins by spectroscopy methods. Food Chemistry 139 (1-4), 611-616.

IV. GENERAL DISCUSSION

Micro- and nanoencapsulation have generated great interest over the last years in multiple fields. Particularly in the food industry, this technology presents potential applications for the development of smart packaging structures, as well as for the production of novel healthy foods. Therefore, in this thesis, the development of different encapsulation structures of interest in the food area was carried out. To this aim, the electro-hydrodynamic processing was used for the production of the micro- and nanocapsules, since this technique leads to the formation of ultrathin structures and allows the control of the morphology and size of the capsules. Furthermore, it does not require the use of high temperatures, organic solvents can be avoided and there is no limitation in terms of the substance to encapsulate, independently of the chemical nature of the encapsulating matrix and the core material.

Thus, on the one hand, encapsulation structures were produced through electro-hydrodynamic processing for smart packaging applications. In this field, phase change materials (PCMs) were encapsulated into different matrices in order to obtain heat management packaging structures. Specifically, PCMs with phase transitions in the food preservation temperature range were sought (from -18 ºC to 5 ºC).

Initially, zein was studied as the matrix material and dodecane was selected as the PCM. In this study, dodecane was encapsulated in both, fibers and capsules, and it was observed that fibers seemed to be more appropriate for PCM encapsulation, since the encapsulation efficiency, as well as the total amount of PCM encapsulated in fibers, were higher than for the capsule-like morphologies. Thermal properties of the

materials were studied through DSC and FTIR and it was seen that the melting temperature was very similar for the non-encapsulated and the encapsulated dodecane. However, encapsulation through uniaxial methodology led to multiple crystallization temperatures of the PCM, probably because the confinement of the PCM in a very small capsule, which make more stable different rotator phases during crystallization. Nevertheless, coaxial electrospinning produced materials with only one crystallization temperature. This fact was attributed to the sizes of the coaxial fibers, which were bigger than those of the uniaxial electrospun fibres and moreover, in the coaxial methodology, the PCM was not incorporated in an emulsion, but it was introduced from the bulk product, so that the crystallization behavior was more similar to that of pure dodecane. Nevertheless, all the structures attained in this study presented the supercooling effect, i.e. a delay in the crystallization temperature of the material, causing a difference between the melting and the crystallization temperatures. Thus, different nucleating agents were also introduced in the capsules in order to advance the crystallization temperature. The main conclusion of this study was that coaxial configuration and nucleating agents were needed for obtaining proper heat management materials based on zein through electro-hydrodynamic processing.

In the smart packaging area, polyesters were also investigated as encapsulating matrices, since these polymers present suitable properties for packaging applications. Specifically, they present good physical properties (when compared to other biodegradable and renewable polymers), processability, water resistance, excellent

biocompatibility and commercial availability. Moreover, biopolyesters present similar solubility properties than organic PCMs, thus allowing the production of PCM capsules through uniaxial processing. Therefore, a second study was carried out using PCL and PLA as matrix materials and dodecane as the core material. In this work only fibers were produced and it was seen that PCL/dodecane fibers were considerably thicker than the PLA/dodecane structures obtained. Thus, the hybrid materials made from PCL were able to encapsulate a higher amount of dodecane than those obtained with PLA. Thermal properties were evaluated through DSC and FTIR and results showed that the melting was similar for the pure PCM and for the encapsulated PCM. However, the crystallization was affected by the encapsulation process because of the reduced size of the particles obtained and, generally, higher supercooling was observed in the developed electrospun structures. Therefore, nucleating agents were needed in order to avoid this effect. Regarding the encapsulation efficiency, different techniques were used in order to detect the PCM amount obtained in the fibers. DSC was initially used, since this technique provides the useful values for the energy storage application of the materials. However, DSC could provide wrong data about the loading of the fibers, since it could be that the PCM stay in the fibers but it do not crystallize due to the encapsulation effect, thus the PCM was not taken into account. Thus, NMR and TGA were also used to measure the PCM loading, since these assays favored the release of dodecane due to the complete dissolution or degradation of the matrix materials. These results showed that PCL fibers were able to encapsulate ~37 wt-% of the PCM. However, for the PLA materials, the dodecane loading results were different depending on the technique

used. While NMR and TGA provided an encapsulation loading of around 20 wt-%, according to the results from DSC, the heat storage capacity was equivalent to a loading of 10 wt % of the PCM. The differences in the latter case were ascribed to a fraction unable to crystallize inside the PLA matrix. Therefore, from this study it was concluded that PCL was more suitable than PLA for PCM encapsulation through electrospinning.

Finally, a PCM with a phase transition with most practical applications was encapsulated into different matrices. Specifically, Rubitherm RT5, a PCM with a phase transition around 5 ºC, was encapsulated into PCL, PLA and PS fibers and beads. This temperature is commonly used to keep the refrigerating conditions of foodstuffs in retail and display cabinets at supermarkets or in household refrigerators. Moreover, RT5 is a commercial PCM composed of different paraffins which theoretically do not present supercooling effect. In this work it was confirmed that fibers seemed to be more suitable for energy storage applications than beads, since the thermal properties of the PCM retained in the fiber structures were not as modified as within the beads. Furthermore, the encapsulating efficiency and the energy storage capacity of fibers were also greater than in beads. It was also observed that among all the polymers tested, PCL was the most efficient matrix with ~43% of RT5 encapsulated. Moreover, these fibers showed the ability of temperature buffering at the phase transition temperature of the PCM for some time. Thus, the incorporation of these hybrid fibers in the food packaging materials or in the walls of refrigeration equipment can be a suitable strategy to buffer the thermal fluctuations with the aim of improving the quality and safety of foodstuffs.

As it was commented before, micro- and nanoencapsulation also present a great interest in the development of novel healthy foods through the encapsulation of functional ingredients and its incorporation in foodstuffs. Therefore, in this thesis novel micro/nanoencapsulation structures were developed from food hydrocolloids through electrospraying. Thus, different food hydrocolloids were evaluated for capsules formation and different strategies were studied in order to optimize the electrospraying process. Initially, the effect of the variation of the surface tension of different carbohydrates solutions on the electrospraying process and capsules morphology was studied. In this work different surfactants were incorporated in the solutions and it was observed that it considerably improves the electrospraying process due to the surface tension reduction. However, non-ionic surfactants were more suitable for the capsules formation, as electrically charged surfactants gave rise to fused and too small structures due to the high electrical conductivity attained in this case.

Afterwards, a more thorough study was carried out for the development of electrosprayed encapsulation structures based on aqueous hydrocolloid solutions. In this work the solution properties of different polysaccharides and proteins were analysed and compared with the solution properties of two polymers readily spinnable in water (PVOH and PEO). From this study it was concluded that viscosity and surface tension were the most significant parameters affecting the electrosprayability of the solutions. Specifically, the hydrocolloid solutions generally led to low viscosity and high surface tension values,

which complicate the electrospraying process. Thus, alternative strategies to improve these physical properties were established. On the one hand, addition of gums and protein denaturation were carried out in order to increase the viscosity solution. On the other hand, lower surface tension values were achieved through the addition of non-ionic surfactant into the solutions. Moreover, both strategies were carried out together. It was seen that generally, addition of non-ionic surfactants, was the most interesting strategy for improving the sprayability of these hydrocolloid-based solutions, since gums retained too much solvent and protein denaturation led to aggregated and wrinkled particles.

Finally, different bioactives were incorporated into the hydrocolloid capsules. Initially, folic acid was encapsulated into resistant starch and whey protein capsules through electrospraying and spray drying. From this work, it was observed that there were not significant differences of encapsulation efficiencies between both encapsulation technologies. However, the protein led to higher encapsulation yields than resistant starch and it also better protected the folic acid against degradation during storage in different conditions. Lycopene was also encapsulated into dextran, chitosan and whey protein through electrospraying and spray drying. From this study it was seen that the bioactive was considerably affected by the heating conditions during the spray drying encapsulation, thus, very low encapsulation efficiencies were obtained with this technology. On the contrary, emulsion and coaxial electrospraying could be used for lycopene encapsulation, especially when using the WPC matrix, which led to higher encapsulation yields and better protected the bioactive under moisture and thermal

conditions. Therefore, it can be concluded that electrospraying is a useful technique to generate capsules for food applications and protect sensitive ingredients from adverse conditions.

V. CONCLUSIONS

- Novel heat management materials were produced by the encapsulation of different PCMs within different biopolymer matrices.

- Fibers were seen to be more appropriate for PCM encapsulation, since the encapsulation efficiency and the energy storage capacity of fibers was higher than for the capsule-like morphologies. Moreover thermal properties were more similar to pure PCM in fibers than in capsules.

- Encapsulation through uniaxial electrospinning led to multiple crystallization temperatures of the PCM. On the contrary coaxial electrospinning produced materials with only one crystallization temperature. Nevertheless, uniaxial electrospinning usually led to higher encapsulation yields and more homogenous structures.

- PCL was the most efficient matrix for PCM encapsulation among all the polymers studied. PCL/PCM fibers showed the ability of temperature buffering at the phase transition temperature of the PCM for some time.

- Encapsulation structures based on aqueous hydrocolloid solutions were obtained through the electrospraying technology.

- Addition of non-ionic surfactants was the most interesting strategy for improving the sprayability of the hydrocolloid-based solutions.

- Different bioactive ingredients were incorporated into hydrocolloid capsules trough electrospraying and spray drying. It was seen that for sensitive substances, such as lycopene, spray drying affected to the stability of the bioactive. On the contrary electrospraying was able to encapsulate this substance without any activity loss.

- WPC led to higher encapsulation efficiencies than other polysaccharide matrices. It also showed better protection to the encapsulated bioactives under adverse conditions, such as moisture or heating.

VI. ANNEXES

ANNEX 1. Heat transfer study of micro-encapsulated PCM plates*.

From previous results it was observed that heat management materials obtained from PCL/RT5 fibers obtained through electro-hydrodynamic processing were the most efficient PCMs when compared with other polymer/RT5 fibers (cf. Chapter III). Therefore, these fibers were selected to obtain 0.5 to 1 cm thickness PCM plates. Figure 1 shows the plates obtained.

Figure 1. PCM plate obtained from PCL/RT5 fibers.

The heat transfer behaviour in the surface and the center of these plates was experimentally studied inside a temperature simulator. During the heating and cooling experiments, the air temperature inside the simulator was maintained constant. Maximum attention was taken to obtain a homogeneous initial temperature for the tested product. For heating experiment (plate initial temperature -10°C, air temperature in the simulator 20°C), the plates were kept inside a home freezer at -10°C for at least 12h. For cooling experiment (plate initial temperature 17°C,

air temperature in the simulator -10°C), the plates were kept at ambient temperature. When the product was moved to the simulator, it was packed inside an insulated box. Therefore, the initial center and surface temperatures were almost the same (<0.5°C of difference). Figure 2 shows the temperature evolution of the plate during various repetitions and no significant difference was observed. Thus, it was confirmed the stability of the material properties during heating and cooling cycles.

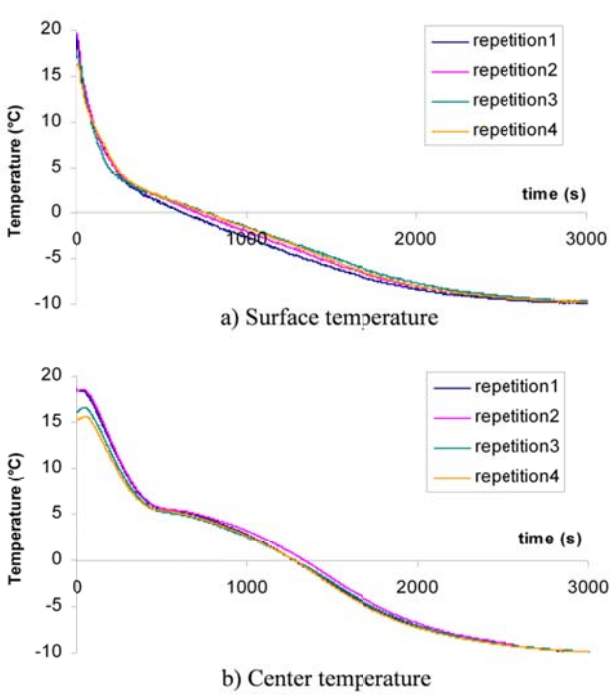

Figure 2. Temperature evolution of the PCM plate during various repetitions in the cooling experiment

The theoretical behavior of the plates was modelled by the enthalpy method (Zhou et al., 2010). Figure 3 shows a comparison between experimental and numerical results for the PCM plate during heating and cooling processes. It was observed that the model could correctly predict the temperature of the plates for both heating and cooling processes, especially for the plate center temperature. Slight differences could be related to the precision of the model input parameters (thermal properties, heat transfer coefficient…). Figures 3c and 3d confirmed a good agreement between the simulation and experience.

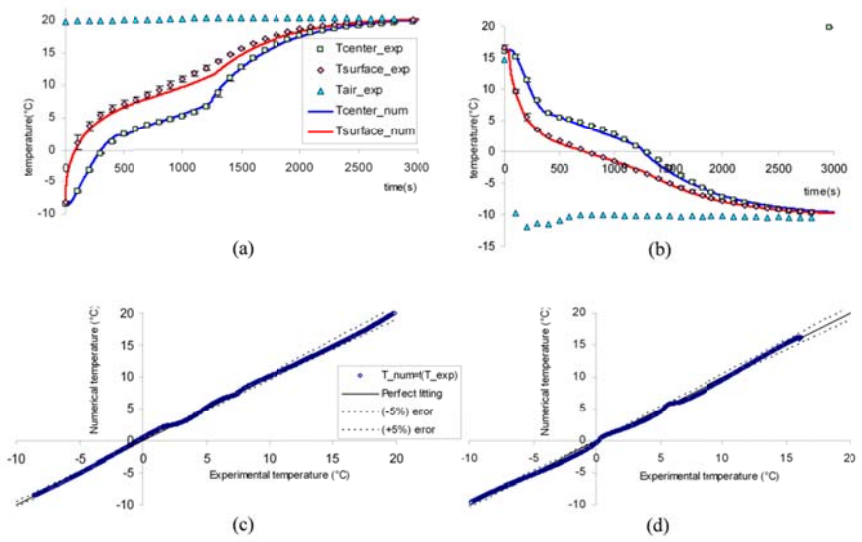

Figure 3. Comparison between experimental and numerical temperature for PCM plate: (a) Temperature evolution during heating process; (b) Temperature evolution during cooling process; (c) Correlation between experimental and numerical temperature at plate center - heating process; (d) Correlation between experimental and numerical temperature at plate center - cooling process.

References

Zhou G., Yang Y., Wang X., Cheng J., 2010. Thermal characteristics of shape-stabilized phase change material wallboard with periodical outside temperature waves. Applied Energy, 87,(8), 2666-2672.

(*) This annex is an an extract from a joint work by IRSTEA (France), IATA (Spain) and National Technical University of Athens (Greece). Hoang, H.M et al. 2014. Conference Proceedings 3rd IIR International Conference on Sustainability and the Cold Chain (ICCC2014).

ANNEX 2. List of publications.

This thesis compiles information from the following papers, patents and book chapters:

- Perez-Masia, R., Lopez-Rubio, A., Lagaron, J.M. Development of zein-based heat-management structures for smart food packaging. Food Hydrocolloids (2013), 30 (1), pp. 182-191.

- Perez-Masia, R., Lopez-Rubio, A., Fabra, M.J., Lagaron, J.M. Biodegradable polyester-based heat management materials of interest in refrigeration and smart packaging coatings. Journal of Applied Polymer Science (2013), 130 (5), pp. 3251-3262.

- Perez-Masia, R., Lagaron, J.M., Lopez-Rubio, A. Surfactant-aided electrospraying of low molecular weight carbohydrate polymers from aqueous solutions. Carbohydrate polymers (2014), 101, pp. 249-255.

- Perez-Masia, R., Lopez-Rubio, A., Fabra, M.J., Lagaron, J.M. Use of electro-hydrodynamic processing to develop nanostructured materials for the preservation of the cold chain. Innovative Food Science and Emerging Technologies (2014). Article under review.

- Perez-Masia, R., Lagaron, J.M., Lopez-Rubio, A. Development and Optimization of Novel Encapsulation Structures of Interest in Functional Foods through Electrospraying. Food & Bioprocess Technology (2014). DOI: 10.1007/s11947-014-1304-z.

- Perez-Masia, R., Lopez-Nicolas, R., Periago, M.J., Ros, G., Lagaron, J.M., Lopez-Rubio, A. Encapsulation of folic acid in food hydrocolloids through nanospray drying and electrospraying for nutraceutical applications. Food Chemistry, Article submitted April 2014.

- Perez-Masia, R., Lagaron, J.M., Lopez-Rubio, A. Morphology and stability of edible lycopene capsules produced through electrospraying and spray drying. Food & Bioprocess Technology (2014). Article submitted May 2014.

- Pérez-Masiá, R., Fabra, M.J., Lagaron, J.M., Lopez-Rubio, A. Use of electrospinning foe encapsulation in "Encapsulation Nanotechnologies" (Chapter 4). Scrivener Publishing (WILEY). ISBN: 978-1-118-34455-2.

- Lagaron, J.M., Lopez-Rubio, A., Fabra, M.J., Pérez-Masiá, R. Microencapsulation and Packaging-Value Added Solutions to Product Development in "The Art and Science of Microencapsulation: an Application Handbook for Food Industry" (Chapter 32). Elsevier.

- P201131063 Patent Application (2011). Procedimiento de encapsulación de PCMs. Inventors: Lagaron, J. M., Perez-Masia, R., & Lopez-Rubio, A. Holder entity: CSIC.

Food Hydrocolloids 30 (2013) 182–191

Contents lists available at SciVerse ScienceDirect

Food Hydrocolloids

journal homepage: www.elsevier.com/locate/foodhyd

Development of zein-based heat-management structures for smart food packaging

Rocío Pérez-Masiá, Amparo López-Rubio, Jose Maria Lagarón*

Novel Materials and Nanotechnology Group, IATA-CSIC, Apdo. Correos 73, 46100 Burjassot, Spain

ARTICLE INFO

Article history:
Received 3 April 2012
Accepted 10 May 2012

Keywords:
Phase changing material (PCM)
Electrospinning
Encapsulation
Zein
Paraffins
Dodecane

ABSTRACT

In this work, novel materials with heat management properties have been developed by means of the encapsulation of a phase changing material (PCM) in a biopolymeric matrix using the electrospinning technique. This study optimizes the methodology to obtain micro-, submicro- and nanoencapsulation structures based on zein (a maize protein) and dodecane (a PCM paraffin which has a transition temperature at −10 °C). The results demonstrate that dodecane can be properly encapsulated in the zein matrix under different conditions, although the efficiency and, thus, the heat management properties of the structures developed, change according to the encapsulation morphology and the electrospinning parameters/configuration employed. These encapsulation technologies can be of interest in the food industry in order to develop new smart packaging materials with the ability to maintain temperature control, e.g. to preserve the cold chain.

© 2012 Elsevier Ltd. All rights reserved.

1. Introduction

Nowadays, food industries market many products under refrigerating, chilling or freezing conditions, since low temperatures improve quality and microbial safety of foodstuffs. The preservation of the cold chain along the whole marketing period is vital to prevent the spoilage of the food products and to extend their shelf-life. Despite the efforts made by manufacturers and logistic providers, unwanted expositions to warm temperatures of the products often occur during their storage and transport from the industry to the consumers. These alterations in the cold chain can lead to detrimental changes in the food products such as crystal ice growth, acceleration of chemical reactions and/or microorganism growth. The development of energy storage systems in general and, specifically, phase changing materials (PCM's) included in the food packaging materials, could be a solution to buffer the temperature variations of the environment. PCM's are able to absorb or release energy during their melting/crystallization process and, as a consequence, they are able to increase the thermal energy storage capacity of the containers (Rentas, Macdonald, Houchens, Hmel, & Reid, 2004).

A large number of organic and inorganic materials can be identified as PCM's from their melting temperature. However, they should also present suitable physical, chemical and kinetic properties. Paraffin compounds fulfil most of the requirements for being used as PCM's, as they are reliable, predictable, non-toxic, chemically inert and stable below 500 °C. They also show little volume changes on melting and have low vapour pressure in the melt form (Sharma, Tyagi, Chen, & Buddhi, 2009). Nevertheless, PCM's, in general, present a number of drawbacks for direct practical applications, such as weak thermal stability, low thermal conductivity and the fact that some of them are liquid at ambient temperature and, thus, are not easy to handle or to be directly incorporated into packaging structures (Fang, Li, Yang, Liu, & Wu, 2009). The encapsulation of the PCM in a shell material is a plausible solution to avoid all these problems. By means of encapsulation, the PCM is protected against the influences of the outside environment by a shell that increases the heat-transfer area and withstands changes in volume when phase change occurs (Alkan, Sari, & Karaipekli, 2011), thus increasing the potential applications of these materials. Moreover, micro-, ultrathin- (submicro-) and nanoencapsulation enhance the efficiency of this technique because these methods prevent volatile losses, allow a greater dispersion and minimize the amount of non-encapsulated product (Abhat, 1982; Jafari, Assadpoor, He, & Bhandari, 2008; Soottitantawat et al., 2005). Furthermore, due to their very high surface-to-volume ratio, ultrathin and nanoencapsulation structures have less impact in texture, morphology, viscosity and other physical properties of the material where they are included (Shefer & Shefer, 2003).

The electrospinning technique has proven to be a very suitable method for encapsulation and various compounds, including biomedical substances or functional food ingredients have been

* Corresponding author. Tel.: +34 963900022; fax: +34 963636301.
E-mail address: lagaron@iata.csic.es (J.M. Lagarón).

0268-005X/$ – see front matter © 2012 Elsevier Ltd. All rights reserved.
doi:10.1016/j.foodhyd.2012.05.010

Applied Polymer SCIENCE

Biodegradable Polyester-Based Heat Management Materials of Interest in Refrigeration and Smart Packaging Coatings

Rocio Perez-Masia, Amparo Lopez-Rubio, Maria Jose Fabra, Jose Maria Lagaron
Novel Materials and Nanotechnology Group, IATA-CSIC, Avda. Agustin Escardino 7, 46980 Paterna, Valencia, Spain
Correspondence to: J. M. Lagaron (E-mail: lagaron@iata.csic.es)

ABSTRACT: In this study, two biodegradable matrices, polycaprolactone (PCL) and polylactide (PLA) were used to encapsulate for the first time a phase changing material (PCM), specifically dodecane (a paraffin which has a transition temperature at −10°C), through the use of the electrospinning technique with the aim of developing coating materials with energy storage capacity for thermal insulation applications. The encapsulation efficiency obtained using both matrices has been studied and the different morphology, thermal properties, and molecular structure of the materials developed were characterized. Results showed that dodecane can be properly encapsulated inside both biopolymers with a submicron drop size, albeit PCL provides better encapsulation performance. A temperature mismatch between melting and crystallization phenomena (the so-called supercooling effect) was observed in the encapsulated paraffin, mainly ascribed to the reduced PCM drop size inside the fibers. Addition of dodecanol was seen to best act as a nucleating agent for the PCL/PCM and PLA/PCM structures, allowing a significant amount of heat storage capacity for these systems without supercooling. These innovative ultrathin structured biomaterials are of interest as energy storage systems to advantageously coat or wrap temperature sensitive products in refrigeration equipment and constitute smart food or medical/pharmaceutical packaging.
© 2013 Wiley Periodicals, Inc. J. Appl. Polym. Sci. 000: 000–000, 2013

KEYWORDS: biopolymers and renewable polymers; differential scanning calorimetry; electrospinning; properties and characterization; structure-property relations

Received 5 November 2012; accepted 16 May 2013; Published online
DOI: 10.1002/app.39555

INTRODUCTION

The development of sustainable energy technologies has been intensified over the last years due to the continuous environmental and economic problems related to the energy sources used nowadays. In this field, phase changing materials (PCMs) can be used as energy storage materials, since they are able to absorb or release energy during their melting/crystallization processes. A large number of organic and inorganic materials can be identified as PCMs from their melting temperature. However, they should also present suitable physical, chemical, and kinetic properties. Paraffin compounds fulfill most of these requirements, as they are reliable, predictable, and chemically inert and stable below 500°C. They also show little volume changes on melting and have low vapor pressure in the melt form.[1] Nevertheless, the latent thermal energy storage systems based on PCMs present some drawbacks such as their low thermal conductivity, which limits the energy that can be extracted from them. Another hurdle is their handling, since some PCMs are liquid at ambient temperature and, what is more important; they need to undergo a phase change (i.e., from liquid to solid and vice versa) at the target temperature to exert the desired functionality. Nevertheless, there are some strategies to overcome these difficulties. On the one hand, the PCMs particles' diameter can be reduced to achieve a very high ratio of surface area to volume and, hence, to increase their thermal conductivity.[2] On the other hand, the encapsulation of these particles in a solid matrix allows the easy handling of liquid PCMs.

One innovative approach to encapsulate PCMs, reducing their drop size and controlling the morphology to a submicron scale is by the electrospinning process. This technique uses high voltage electric fields to produce electrically charged jets from viscoelastic polymer solutions. The solutions are dried, by the rapid evaporation of the solvent, producing ultrathin droplets of solid or liquid particles (core material, i.e., the PCM) which are packed into a polymeric matrix (shell material).[3] Thus, ultrathin structures of polymers containing PCMs can be developed to obtain novel thermal storage materials with suitable thermal performances.

Another important parameter which must be controlled during PCMs performance is the so-called supercooling effect, i.e., the lag between the melting and crystallization of the PCM. Generally, supercooling involves a reduction in the crystallization

© 2013 Wiley Periodicals, Inc.

Carbohydrate Polymers 101 (2014) 249–255

Contents lists available at ScienceDirect

Carbohydrate Polymers

journal homepage: www.elsevier.com/locate/carbpol

Surfactant-aided electrospraying of low molecular weight carbohydrate polymers from aqueous solutions

Rocío Pérez-Masiá, Jose M. Lagaron, Amparo López-Rubio*

Novel Materials and Nanotechnology Group, Institute of Agrochemistry and Food Technology (IATA-CSIC), Avda. Agustin Escardino 7, 46980 Paterna (Valencia), Spain

ARTICLE INFO

Article history:
Received 26 July 2013
Received in revised form
11 September 2013
Accepted 13 September 2013
Available online 21 September 2013

Keywords:
Electrospraying
Electrospinning
Encapsulation
Surfactant
Aqueous solution
Carbohydrate

ABSTRACT

In this work it is demonstrated, for the first time, that it is feasible to develop, using the electrospraying technique, low molecular weight carbohydrate-based capsule morphologies from aqueous solutions through the rational use of surfactants. Two different low molecular weight carbohydrate polymers were used, a maltodextrin and a commercial resistant starch. The solution properties and subsequent high voltage sprayability was evaluated upon addition of non-ionic (Tween20, and Span20) and zwitterionic (lecithin) surfactants. The morphology and molecular organization of the structures obtained was characterized and related to the solution properties. Results showed that, while unstable jetting and dropping occurred from the pure carbohydrate solutions without surfactant, the addition of some surface active molecules above their critical micelle concentration facilitated capsule formation. Higher surfactant concentrations led to smaller and more homogeneous capsule morphologies, related to lower surface tension and higher conductivity of the solutions.

© 2013 Elsevier Ltd. All rights reserved.

1. Introduction

The development of micro-, submicro- and nanostructures from biopolymers for functional food applications is an emerging area of interest. Apart from the conventional microencapsulation techniques, such as spray drying or coarcervation, electrospinning has been recently suggested to be a simple and straightforward method to generate submicron encapsulation structures for a variety of bioactive molecules (Bock, Dargaville, & Woodruff, 2012; Lopez-Rubio & Lagaron, 2012; Xie, Li, & Xia, 2008). Electrospinning is a process that produces continuous polymer fibers with diameters in the submicrometer range through the action of an external electric field imposed on a polymer solution or melt. The electrospun nanostructures morphology is affected by the solution properties (mainly by the viscosity, surface tension and conductivity of the polymer solution) and by the process parameters (voltage, flow rate of the solution, tip-to-collector distance). For certain materials, size-reduced capsules can be obtained when lowering the polymer concentration and/or increasing the tip-to-collector distance. In this case, the electrospinning process is normally referred to as "electrospraying" due to the non-continuous nature of the structures obtained. To date, a wide variety of polymers and polymer blends have been electrospun, with synthetic polymers yielding the best results in terms of physical properties and uniformity. On the other hand, electrospinning of biopolymer solutions has been proven to be difficult due to several factors such as the polycationic nature of many biopolymers, the low chain flexibility which complicates chain entanglements (essential for fiber formation) and their generally poor solubility in organic solvents (Kriegel, Kit, McClements, & Weiss, 2009). Moreover, unlike synthetic polymers, a natural polymer derived from different sources presents widely varying properties and it has been observed that the viscosity of the solutions may vary with time due to, for instance, aqueous hydrolysis of the biopolymer (Bhattarai & Zhang, 2007).

Electrospinning from aqueous solutions is beneficial from an environmental point of view. Furthermore, the use of water does not generate toxicity problems. On the contrary, organic solvents may be even prohibited for certain applications, such as in the case of food products (Kriegel, Kit, McClements, & Weiss, 2010). That issue further complicates the electrospinning process due to the ionization of water molecules at high voltages in an air environment, which may cause corona discharge. Besides, aqueous solutions present high surface tension values which hinder the formation of stable jets during the electrospinning. Moreover, polymers that have low aqueous solubility, low M_w polymers and polymers with rigid or globular structures that do not generate sufficient viscosity are not easily electrospun when they are in

* Corresponding author. Tel.: +34 963900022; fax: +34 963636301.
E-mail addresses: amparo.lopez@iata.csic.es, maloru1@hotmail.com (A. López-Rubio).

0144-8617/$ – see front matter © 2013 Elsevier Ltd. All rights reserved.
http://dx.doi.org/10.1016/j.carbpol.2013.09.032

Food Bioprocess Technol
DOI 10.1007/s11947-014-1304-z

ORIGINAL PAPER

Development and Optimization of Novel Encapsulation Structures of Interest in Functional Foods Through Electrospraying

Rocio Pérez-Masiá · Jose M. Lagaron · Amparo López-Rubio

Received: 27 January 2014 / Accepted: 16 March 2014
© Springer Science+Business Media New York 2014

Abstract The aim of this work was to establish strategies for the development of electrosprayed encapsulation structures, of interest in food applications, based on aqueous hydrocolloid dispersions. Specifically, various polysaccharides and two different proteins were evaluated for capsule formation. To this aim, the hydrocolloid dispersion properties were analysed and compared with the solution properties of two polymers readily spinnable in water (polyvinyl alcohol (PVOH) and polyethylene oxide (PEO)). Increasing the hydrocolloid concentration to promote chain entanglements resulted in a valid strategy only for a few matrices (related to their greater Mw). As alternative strategies to improve the physical properties and, thus, the sprayability of the dispersions, addition of gums and surfactants to modify their viscosity and surface tension, respectively, was evaluated. Moreover, denaturation of proteins was also carried out in order to investigate the effect of this treatment on the electrospraying process and on capsule formation. Results showed that the incorporation of some of these molecules, as well as protein denaturation, significantly changed the physical properties, allowing the development of encapsulation structures from all the hydrocolloids assayed. The morphology of the structures obtained was characterized, and the molecular organization of some of the capsules was studied and related to the electrosprayability and capsules morphology.

R. Pérez-Masiá · J. M. Lagaron · A. López-Rubio (✉)
Novel Materials and Nanotechnology Group, Institute of Agrochemistry and Food Technology (IATA-CSIC), Avda. Agustin Escardino 7, Paterna, Valencia 46980, Spain
e-mail: amparo.lopez@iata.csic.es

R. Pérez-Masiá
e-mail: rocio.perez@iata.csic.es

J. M. Lagaron
e-mail: lagaron@iata.csic.es

Published online: 28 March 2014

Keywords Electrospinning · Electrospraying · Encapsulation · Hydrocolloids · Bioactives

Introduction

The encapsulation of food and nutraceutical ingredients is an emerging area of interest due to the instability of some of these compounds at ambient and digestive conditions (Ezhilarasi et al. 2013). In general, encapsulation seeks to protect these products and, thus, assure their health-promoting properties, although it can also be used to improve sensorial properties of food products containing ingredients that inherently have undesirable flavours and/or odours (Nasirullah et al. 2011).

Apart from the conventional microencapsulation techniques, such as spray drying or coarcervation, electrohydrodynamic processes have been recently suggested to be simple and straightforward methods to generate submicron encapsulation structures for a variety of bioactive molecules (Xie et al. 2008; Lopez-Rubio and Lagaron 2012; Bock et al. 2012; Pérez-Masiá et al. 2013; Bakhshi et al. 2013). These techniques use electrostatic forces to produce electrically charged jets from viscoelastic polymer solutions which on drying, by the evaporation of the solvent, produce ultrathin structures (Li and Xia 2004). When ultrathin continuous fibres are obtained, the process is called 'electrospinning'. When size-reduced capsules are attained, the process is normally referred to as 'electrospraying' due to the non-continuous nature of the structures obtained. For food and nutraceutical applications, capsules are generally preferred, since apart from facilitating, handling and subsequent incorporation into different products, they also present greater surface/volume ratio and, thus, are expected to have better release profiles than fibres (Hong et al. 2008). The morphology and composition of microstructures/nanostructures attained can be modulated